

Calculating Conical Diffraction Coefficients

submitted by

Bradley David Bonner

for the degree of PhD

of the

University of Bath

2003

COPYRIGHT

Attention is drawn to the fact that copyright of this thesis rests with its author. This copy of the thesis has been supplied on the condition that anyone who consults it is understood to recognise that its copyright rests with its author and that no quotation from the thesis and no information derived from it may be published without the prior written consent of the author.

This thesis may be made available for consultation within the University Library and may be photocopied or lent to other libraries for the purposes of consultation.

Signature of Author

Bradley David Bonner

Summary

The computation of diffraction coefficients for the scattering of high-frequency waves by a conical obstacle can be reduced to the solution of a family of homogeneous boundary value problems for the Laplace-Beltrami-Helmholtz equation on a portion of the unit sphere bounded by a simple closed contour (in fact the intersection of the sphere with the conical scatterer). Distance on the contour is geodesic distance on the sphere. The diffraction coefficient may be determined by then integrating the resulting solutions with respect to the wave number (Babich et al, ‘On evaluation of the diffraction coefficients for arbitrary “nonsingular” directions of a smooth convex cone’, *SIAM J. Appl. Math.*, 60:536–373, 2000).

In this thesis we discuss the numerical computation of the diffraction coefficients using the boundary integral method, with the classical single/double layer potential approach. The kernels of the spherical integral operators which arise from this application have a diagonal singularity of the same type as the corresponding operators for the planar Helmholtz and planar Laplace equations. This allows us to prove stability and convergence for appropriate discrete collocation spaces in the case of smooth cones. Moreover, a question of key practical interest in this field of diffraction theory is the computation of diffraction coefficients when the scatterer has edges and corners. Here we adapt well-known methods for handling boundary integral equations on planar corner domains (J. Elschner and I.G. Graham, ‘Numerical methods for integral equations of Mellin type’, *J. Comp. Appl. Math.*, 125:423-437, 2000) to the current problem.

Acknowledgements

I would like to take this opportunity to thank my supervisors Ivan Graham and Valery Smyshlyaev whose assistance and advice have been invaluable. I would also like to thank my mum and dad, Jason and Toll for their support and encouragement throughout my years of study. Finally, I would like to acknowledge EPSRC for their financial support and the Department of Mathematical Sciences at the University of Bath for their excellent facilities.

Contents

1	Introduction	6
2	The High-frequency Scattering Problem and the Diffraction Coefficients	14
2.1	The acoustic scattering problem	15
2.1.1	The point source and planar incidence problem	20
2.1.2	High-frequency asymptotics and the stationary phase method	31
2.2	The electromagnetic diffraction problem	38
3	The Boundary Integral Method	44
3.1	Preliminary results	48
3.2	Relation to the planar Laplace case	56
4	Numerical Method for the Integral Equation	68
4.1	The collocation method	69
4.2	Smooth contour ℓ	71
4.3	Nonsmooth contour ℓ	73
4.3.1	The h -refinement method	74
4.3.2	The hp -refinement method	87
4.4	The discrete collocation method	90
5	Quadrature	96
5.1	Case 1 : Smooth integrands	98
5.1.1	Gauss-Legendre quadrature	103
5.2	Case 2 : Nearly singular integrands	104
5.3	Case 3 : Weakly singular integrands	107
5.4	Numerical results	110
6	Practical Computation of Diffraction Coefficients	118
6.1	Domains of observation	120

6.1.1	Deforming the contour in the acoustic case	121
6.1.2	Deforming the contour in the electromagnetic case	122
6.2	Calculating Legendre functions	125
6.3	Calculating the single and double layer potentials	127
6.3.1	Numerical results	129
6.4	Calculating the integral with respect to τ	133
6.4.1	Results	134
7	Conclusions and Further Work	146
7.1	Conclusions	146
7.2	Further work	147
A	Derivation of the Formulae for the Electromagnetic Diffraction	
	Coefficients	148
A.1	Debye potentials	150
A.2	Finding the Debye potentials	153
A.3	High frequency asymptotics	158

List of Figures

1-1	The tangent cone Ξ	7
1-2	Geometry of the cone	8
2-1	Contour of integration γ_1	24
2-2	Contour of integration \mathcal{W} , $\text{Im}(\mathcal{W}_2) < -\delta$, $\delta > 0$	31
2-3	Contour of integration \mathcal{W}'	33
2-4	Singular directions	36
2-5	Contour of integration γ_2	42
3-1	$\boldsymbol{\omega}$, \mathbf{m} and \mathbf{t}	45
3-2	Wedge w and contour ℓ	57
5-1	The ellipse $\mathcal{E}_{a,b}$	104
5-2	The contour ℓ associated with a trihedral cone	113
5-3	The “exact” solution to the integral equation (Dirichlet boundary conditions)	117
5-4	The “exact” solution to the integral equation (Neumann boundary conditions)	117
6-1	Contours of integration γ_3 and γ_4	123
6-2	Convergence of errors for the hp -method	132
6-3	Diffraction coefficients for circular cones (acoustic)	140
6-4	Diffraction coefficients for elliptic cones (acoustic)	141
6-5	Diffraction coefficients for trihedral cones (acoustic)	142
6-6	Radar cross section for circular cones (electromagnetic)	143
6-7	Radar cross section for elliptic cones (electromagnetic)	144
6-8	Radar cross sections for trihedral cones (electromagnetic)	145
A-1	Propagation of the electromagnetic incident wave	149
A-2	Contour of integration γ_2	154

Chapter 1

Introduction

This thesis is concerned with the construction and detailed analysis of a numerical method to calculate conical diffraction coefficients. Diffraction coefficients are fundamental objects determining principal amplitudes in the asymptotic expansion of high frequency acoustic, electromagnetic or other (e.g. elastic) wave fields exterior to a scattering obstacle and are determined from an associated canonical problem.

In this thesis we will only concern ourselves with the acoustic and electromagnetic cases. In the acoustic setting we will be concerned with the solution to the Helmholtz equation for a scalar field U

$$(\Delta + k^2)U(\mathbf{x}) = 0,$$

in \mathbb{R}^3 exterior to some obstacle D , where Δ is the usual Laplace operator and k is the wavenumber (proportional to the frequency ω). In the electromagnetic setting we will be interested in solving time-harmonic Maxwell's equations

$$\begin{aligned}\operatorname{curl} \mathbf{E}(\mathbf{x}) &= ik\mathbf{H}(\mathbf{x}), \\ \operatorname{curl} \mathbf{H}(\mathbf{x}) &= -ik\mathbf{E}(\mathbf{x}),\end{aligned}$$

also exterior to some scatterer D . Here \mathbf{E} is the electric field and \mathbf{H} is related to the magnetic field. Appropriate “ideal” boundary conditions are prescribed on the surface of the scatterer, the Dirichlet or Neumann conditions for the Helmholtz equation and the perfectly conducting condition for Maxwell's equations.

Applying a direct numerical method (e.g. a finite element or a boundary element method) to either of these problems would be computationally expensive since smaller elements would be required as frequencies get higher, to achieve

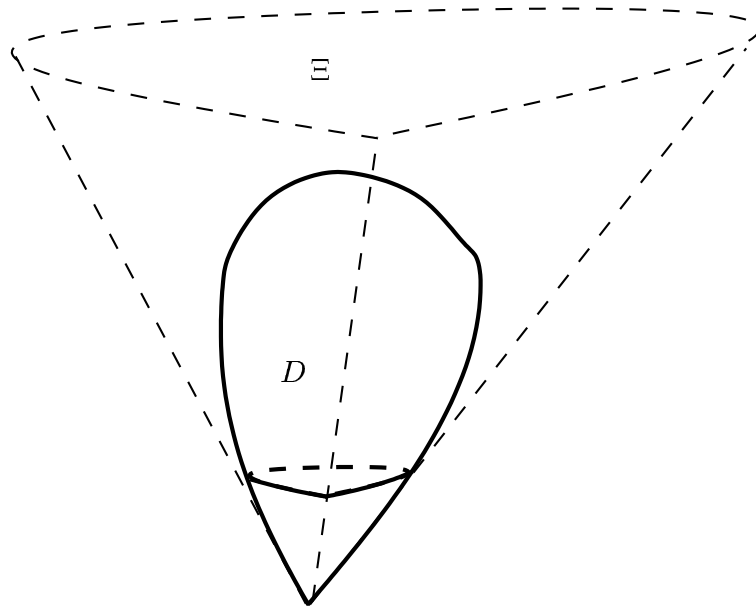


Figure 1-1: The tangent cone Ξ

accurate solutions. These numerical schemes would also require the construction of complicated meshes with further element refinement if singularities are present, e.g. due to surface irregularity of the scatterer, thus increasing the computational cost even further. In an effort to reduce these costs, asymptotic techniques can be utilised to capture the behaviour of U , \mathbf{E} and \mathbf{H} as $k \rightarrow \infty$. The asymptotic theory of high-frequency scattering (the Geometric Theory of Diffraction (GTD)) proposes that for a fixed observation point the asymptotics of the solutions to the scattering problems is made up of different types of scattered wave which depend on the local geometry of particular parts of the obstacle. Of particular interest is the wave diffracted by a singular (conical) point. According to the recipes of GTD, the first step is to use the “*principle of localisation*” to identify the principal asymptotics of the diffracted wave for the bounded scatterer, D , with those of the (semi-infinite) cone Ξ whose surface is tangent to D at the singular point (see Fig. 1-1). Taking the singular point to be the origin O , a portion of the cone Ξ is indicated with dotted lines in Fig 1-2. (The cone Ξ may have a rather arbitrary “cross-section” which may be specified by a domain M on S^2 , the unit sphere in \mathbb{R}^3 centred at the origin.)

It is well known from the GTD that the knowledge of diffraction coefficients for related canonical problems leads to the possibility of constructing the high frequency asymptotics in generic situations. Early investigations concerning the conical canonical problems considered the case when the cross-section of the

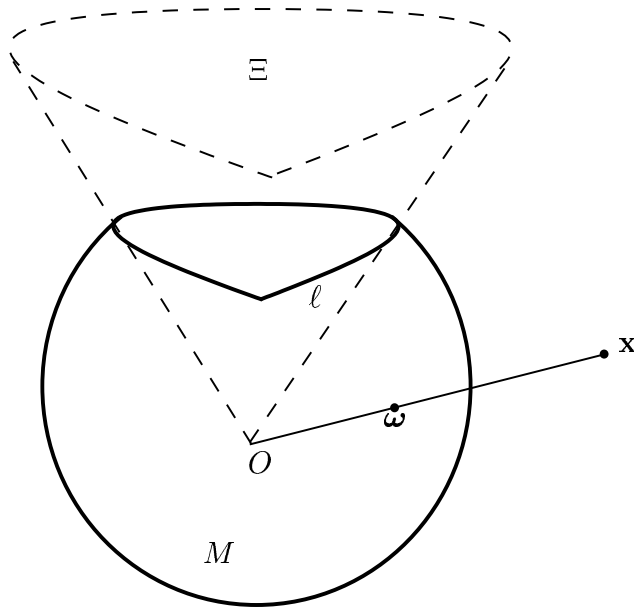


Figure 1-2: Geometry of the cone

cone was circular. More recently solutions for other cross-sections have been presented. In fact for circular cones a great deal of progress has been made with an asymptotic treatment using methods of eigenfunction expansions based on separation of variables to find an exact analytic expression for the diffraction coefficient in both the acoustic and electromagnetic cases (see e.g. [55] [18]). Similar approaches have been used for diffraction by an elliptic cone (including the degenerate case of a plane angular sector) by using separation of variables in sphero-conal coordinates to obtain explicit formulae (see e.g. [62]).

However these techniques, which provide analytic formulae for special geometries, do not extend to the case of diffraction by more general conical scatterers. The handling of arbitrary cones has been a particular challenge in diffraction theory for many years. In [16] the diffraction coefficients are expressed in terms of a solution to a boundary value problem for the Laplace operator on a part of the unit ball. In [23] an advanced Laplace operator calculus is developed on conical domains and this is used to express “singularity coefficients” near the “diffracted” wave front in terms of certain spectral characteristics of the Laplace-Beltrami operator. (The singularity coefficients are equivalent to the diffraction coefficients via a simple transformation.) However, neither of the approaches in [16], [23] provide a constructive formula which can be used.

Following ideas in [23] and using techniques based on Sommerfeld’s classical solution for the two-dimensional diffraction by a wedge [71] it is shown in [67],

[68] and [69] that the diffraction coefficient can be represented in the form of a contour integral in the complex plane. The integrand contains a Green's function for the Laplace-Beltrami operator (with a complex parameter) on a part of the unit sphere (centred at the vertex of the cone) exterior to the cone.

For example, consider the scalar (acoustic) case, with an incident plane wave on D , $U_{inc}(\mathbf{x}) = \exp(-ik\boldsymbol{\omega}_0 \cdot \mathbf{x})$, with the point $\boldsymbol{\omega}_0 \in S^2$ describing the direction of incidence. Then, seeking a time-harmonic solution, both the scattered wave U_{sc} and the total wave $U := U_{inc} + U_{sc}$ satisfy the 3D Helmholtz equation, $(\Delta + k^2)U = 0$, in the domain of propagation, and U_{sc} satisfies appropriate radiation and tip/edge conditions. The theory in [68] (see [8] and [9] also) describes the behaviour of the “tip-diffracted” component $U_{diff}(\mathbf{x})$ of $U_{sc}(\mathbf{x})$ at any point \mathbf{x} in the domain of propagation. Using spherical coordinates centred at the conical point: $\mathbf{x} = r\boldsymbol{\omega}$ with $\boldsymbol{\omega} \in S^2$ and $r > 0$ denoting the distance of \mathbf{x} from the conical point, it is predicted by the general recipes of the GTD that (with either Dirichlet or Neumann conditions imposed on the surface of the scatterer), U_{diff} has the asymptotic representation

$$U_{diff}(\mathbf{x}, k, \boldsymbol{\omega}_0) = 2\pi \frac{e^{ikr}}{kr} f(\boldsymbol{\omega}, \boldsymbol{\omega}_0) + O((kr)^{-2}), \quad k \rightarrow \infty. \quad (1.0.1)$$

Here the distribution $f(\boldsymbol{\omega}, \boldsymbol{\omega}_0)$, which is infinitely smooth everywhere except at the so-called “*singular directions*”, is the important diffraction coefficient.

A formula for f is given in [67], [68] and [9]. To explain how it works, let M denote the portion of the unit sphere S^2 which is exterior to Ξ . M is a sub-manifold of S^2 with boundary which we denote ℓ (see Fig 1-2). Let Δ^* denote the Laplace-Beltrami operator which is related to the 3D Laplace operator via

$$\Delta = r^{-2} \frac{\partial}{\partial r} \left(r^2 \frac{\partial}{\partial r} \right) + r^{-2} \Delta^*.$$

We introduce the function $g^{sc}(\boldsymbol{\omega}, \boldsymbol{\omega}_0, \nu)$ on M (the so-called “spectral function”), satisfying:

$$(\Delta^* + \nu^2 - 1/4)g^{sc}(\boldsymbol{\omega}, \boldsymbol{\omega}_0, \nu) = 0, \quad \boldsymbol{\omega}, \boldsymbol{\omega}_0 \in M \quad \text{and} \quad \nu \in \mathbb{C}, \quad (1.0.2)$$

along with zero Dirichlet or Neumann boundary condition on ℓ (whichever is given in the original scattering problem) for $g = g^{sc} + g_0$, with an explicit “incident” part g_0 . Once g^{sc} is known, the diffraction coefficient in (1.0.1) is then given by

the formula:

$$f(\boldsymbol{\omega}, \boldsymbol{\omega}_0) = \lim_{\epsilon \rightarrow 0^+} \frac{i}{\pi} \int_{\gamma_1} e^{-i\nu\pi - \epsilon\nu} g^{sc}(\boldsymbol{\omega}, \boldsymbol{\omega}_0, \nu) \nu d\nu. \quad (1.0.3)$$

The integration contour γ_1 in (1.0.3) is an analytic curve in the complex plane chosen as follows. Let $\nu_j > 0$, $j = 1, 2, \dots$ be such that ν_j^2 , $j = 1, 2, \dots$ are the eigenvalues of the problem $(-\Delta^* + 1/4)\Phi_j = \nu_j^2\Phi_j$, subject to the appropriate boundary conditions on ℓ (Dirichlet or Neumann) as given in the original problem. Then γ_1 has to be chosen so that ν_j lie on its right (see Fig. 2-1). We assume that $\text{Re}(\nu) \rightarrow \infty$ and $\text{Im}(\nu) \rightarrow \pm a$ for some constant $a > 0$ along the contour γ_1 . (It will be shown that the problem of computing the diffraction coefficients for the electromagnetic case also reduces to the problem of solving boundary value problems similar to (1.0.2). The boundary conditions will differ slightly from those for the acoustic case.)

Thus the computational procedure for realising the asymptotic formula (1.0.1) requires: (i) the computation of the Green's function $g^{sc}(\boldsymbol{\omega}, \boldsymbol{\omega}_0, \nu)$ for all required incidence directions $\boldsymbol{\omega}_0$ and observation directions $\boldsymbol{\omega} \in M$ and (ii) the computation of the integral in (1.0.3), by quadrature (most generally, for sufficiently small ϵ , when it becomes slowly convergent). Note that (ii) in turn implies that $g^{sc}(\boldsymbol{\omega}, \boldsymbol{\omega}_0, \nu)$ must be evaluated for sufficiently many $\nu \in \gamma_1$ to ensure an accurate answer.

As with most linear elliptic partial differential equations with constant coefficients, the boundary value problem (1.0.2) can be reformulated as an equivalent integral equation over the boundary ℓ . This is a non-standard application of classical potential theory since the boundary value problem is defined on a manifold on the surface of the sphere S^2 .

By seeking the solution to (1.0.2) in the form of a double layer potential (for Dirichlet boundary conditions) or single layer potential (for Neumann boundary conditions) we reformulate (1.0.2) into an integral equation of the form,

$$\frac{1}{2}u(\boldsymbol{\omega}, \nu) + \int_{\ell} L(\boldsymbol{\omega}, \boldsymbol{\omega}')u(\boldsymbol{\omega}', \nu)d\boldsymbol{\omega}' = b(\boldsymbol{\omega}), \quad (1.0.4)$$

for some kernel $L(\boldsymbol{\omega}, \boldsymbol{\omega}')$ defined on $\ell \times \ell$ (expressible in terms of the Legendre functions) and some smooth function b dependent on the boundary conditions. There are several numerical methods which one can use to solve equations of this form (see e.g. [3], [50]). We consider in this thesis the collocation method. Although the theory for the collocation method is incomplete (compared with

Galerkin methods for instance) it is cheaper to implement and therefore a practically popular choice.

When the contour ℓ is smooth then standard stability and convergence proofs for the collocation method apply. In contrast to this, if the boundary ℓ contains corners (i.e. when the conical scatterer has lateral edges) the integral operator is no longer compact and the solution in general will not be smooth near non-smooth points on ℓ . Hence, difficulties arise in proving the stability result that the resulting linear system of equations is nonsingular. We will show that the integral equation (1.0.4) is related to the integral equation corresponding to Laplace's equation on a domain with corners which has been studied extensively, see e.g. [5], [45]. It is also related to the planar Helmholtz equation, see e.g. [24], [26]. One major task in the implementation of the collocation method is the assembly of the stiffness matrix. This requires the calculation of integrals with “weakly singular”, “nearly singular” and “smooth” integrands. In general these integrals need to be computed numerically.

In [8], [9] and [12] a numerical method was implemented for the computation of (1.0.3) (and its electromagnetic analogue). The boundary integral method was used to compute g^{sc} . This was implemented in [8], [9] and [12] for the case when Ξ is a smooth cone, using “in effect” a simple low-order trapezoidal-Nyström type for the boundary integral equations and the trapezoidal rule for the contour integration with respect to ν in (1.0.3). However the papers [8], [9] and [12] contained no convergence analysis of the method and moreover, they dealt only with the case of a smooth cone Ξ . The case of a cone with lateral edges is of fundamental importance in both the high-frequency theory of diffraction (where it is one of the unsolved canonical problems [60]) and in practice, where high frequency scattering by e.g. antennae or corners of buildings is a key problem in microwave engineering.

Although the integral equation method reduces the problem of computing of $g^{sc}(\boldsymbol{\omega}, \boldsymbol{\omega}_0, \nu)$ to a computation on the (1D) contour ℓ on the surface of the unit sphere S^2 , this equation has to be solved many times for different values of ν (and also more times if different $\boldsymbol{\omega}_0$ are to be considered). Moreover, as we shall see, the evaluation of the kernel in the integral equation arising from the spherical PDE (1.0.2) is much more costly than for typical boundary integral equations in planar scattering theory. Thus there is strong practical demand for the development of an efficient algorithm, in particular one which solves the integral equation with the highest accuracy and the minimal number of kernel evaluations. Thus the aims of this thesis are:

- (i) To present a detailed review of the asymptotic techniques used to derive the formulae for the conical diffraction coefficients;
- (ii) To propose an efficient (variable order) method for computing the conical diffraction coefficients which is robust even when the cone Ξ has lateral edges;
- (iii) To minimise the number of kernel evaluations required in the implementation;
- (iv) To analyse the convergence of the method;
- (v) To demonstrate its use in the computation of diffraction coefficients in several sample cases.

This thesis is organised as follows. In Chapter 2 we give a detailed account of the asymptotic techniques developed by a group of authors in [67], [69], [8], [12], [9], [11] and [57]. We first formulate the diffraction problem and then concentrate on deriving the formulae for the diffraction coefficients in both the acoustic and electromagnetic settings. (We only give a brief discussion for the electromagnetic case but we present the technical details in Appendix A.) In Chapter 3 we describe the boundary integral method for computing g^{sc} . This leads to non-standard integral equations posed on the spherical contour ℓ . We present a detailed analysis of the resulting integral operator and investigate the well-posedness of the integral equation for both the case when the contour is smooth and when ℓ contains corners. In Chapter 4 we describe a flexible numerical method based on collocation with piecewise polynomials. We concentrate mainly on the h -version of collocation but we will briefly discuss the hp -version. We also describe the discrete collocation method and give (general) sufficient conditions to preserve stability and optimal convergence properties which are known when the integrals in the matrix are computed exactly. In Chapter 5 we use results proved in Chapter 4 to devise efficient quadrature rules to calculate the matrix entries in the discrete collocation method. We treat the integrals with weakly singular, nearly weakly singular and smooth integrands separately. Also we provide some computations of numerical solutions to the integral equation for various test cases. In Chapter 6 we address the following practical aspects of the method for computing diffraction coefficients: We describe the procedure for computing the contour integral in (1.0.3) (and for the electromagnetic analogue). We give a numerical algorithm for computing Legendre functions with a complex index (necessary for the computation of the kernel of the integral operator in

(1.0.4)). Finally we describe how to calculate the double/single layer potential once the density (u in (1.0.4)) satisfying the integral equation has been computed approximately. We also provide computations of diffraction coefficients for several sample problems. Finally in Chapter 7 some conclusions and possible further research avenues for the future are presented.

Chapter 2

The High-frequency Scattering Problem and the Diffraction Coefficients

In this chapter we will describe the problem of scattering of a high-frequency planar incident wave by an arbitrarily shaped bounded impenetrable obstacle with non-smooth *singular points* on its surface. (Examples of singular points are sharp conical points or edges.) Direct numerical methods to evaluate the scattered wave are computationally expensive and the situation is made worse by the presence of the non-smooth singular points. However when the frequency of the incident wave is high *asymptotic methods* can be employed to reduce the computational costs. The asymptotics of the scattered wave is expected to be composed of a number of different “components” corresponding to different types of wave field. In particular we are interested in the component corresponding to the wave diffracted by a singular point. The main idea behind the asymptotic method of calculating the diffracted wave is the principle of localisation (see e.g. [60]). We describe briefly in §2.1 how this allows us to consider the canonical problem of diffraction by a semi-infinite cone. We review the derivation of the so called *diffraction coefficients* which determine the principal amplitudes in the asymptotic expansion of the diffracted field.

The aim of this chapter is to review the general theory developed by a group of authors for the procedure of finding the conical diffraction coefficients (e.g. [67], [69], [8], [12], [9], [11] and [57]). The chapter is written in two sections. In §2.1 we discuss the problem of scattering of an incident planar acoustic wave by an obstacle with a conical point. We formulate the acoustic scattering problem and give a formula for the conical diffraction coefficient in Lemma 2.15 which is

subsequently simplified in equation (2.1.56). In §2.2 we turn our attention to the problem of diffraction by an electromagnetic incident wave from a conical obstacle. We briefly discuss the strategy for computing the electromagnetic diffraction coefficients. We give formulae for the electromagnetic diffraction coefficients in terms of scalar potentials which are somewhat analogous to the acoustic diffraction coefficients.

2.1 The acoustic scattering problem

We are interested in finding the wave scattered by a bounded impenetrable obstacle, D . A classical mathematical formulation of the associated scattering problem as a boundary value problem is as follows. We are concerned in general with the solution to the wave equation,

$$\Delta U(\mathbf{x}, t) - \frac{1}{c^2} \frac{\partial^2 U}{\partial t^2}(\mathbf{x}, t) = 0, \quad \mathbf{x} \in \Omega := \mathbb{R}^3 \setminus D, \quad (2.1.1)$$

exterior to the obstacle D with Dirichlet or Neumann boundary conditions prescribed on its boundary ∂D ,

$$\begin{aligned} \text{either} \quad & U(\mathbf{x}, t) = 0, \quad \text{for } \mathbf{x} \in \partial D, \\ \text{or} \quad & (\partial U / \partial \mathbf{n})(\mathbf{x}, t) = 0, \quad \text{for } \mathbf{x} \in \partial D, \end{aligned} \quad (2.1.2)$$

where \mathbf{n} is the unit normal to ∂D at \mathbf{x} exterior to Ω and c is the wave velocity. We consider the “time harmonic” solutions to (2.1.1) : $U(\mathbf{x}, t) = U(\mathbf{x}) \exp(-i\omega t)$ where ω is the frequency. Then $U(\mathbf{x})$ satisfies the Helmholtz equation

$$(\Delta + k^2)U(\mathbf{x}) = 0, \quad \mathbf{x} \in \Omega, \quad (2.1.3)$$

where $k = \omega/c$ is the wave number, along with the boundary conditions (2.1.2) with $U(\mathbf{x}, t)$ replaced by $U(\mathbf{x})$. The solution U is assumed to be twice continuously differentiable in the closure, $\bar{\Omega}$, of Ω with the singular points (i.e. “tip” and “edge” points of ∂D) removed. We split the solution U into the “incident part” and “scattered part”,

$$U = U_{inc} + U_{sc}, \quad (2.1.4)$$

the incident part is given by a solution to (2.1.3) in the absence of any obstacle. We also require that U_{sc} satisfies radiation conditions. Then by writing $r = |\mathbf{x}|$

we can formulate the radiation condition as follows:

$$U_{sc}(\mathbf{x}) = O(r^{-1}), \quad \left(\frac{\partial}{\partial r} - ik \right) U_{sc}(\mathbf{x}) = o(r^{-1}) \quad \text{as } r \rightarrow \infty, \quad (2.1.5)$$

uniformly in $\boldsymbol{\omega} = \mathbf{x}/|\mathbf{x}|$. These radiation conditions ensure that for a fixed wave number k , $U(\mathbf{x})$ exists and is unique for smooth boundaries ∂D (see e.g. [15, §6.4]). For boundaries with singular points x_0 the solution $U(\mathbf{x})$ can develop a “singularity” near x_0 , and so in addition U has to satisfy a certain “tip” condition and, if they exist, “edge” condition. To define this condition we introduce a subdomain of the domain of propagation, Ω , defining for every $R > 0$,

$$\Omega_R = \{\mathbf{x} \in \Omega : |\mathbf{x}| \leq R\}. \quad (2.1.6)$$

Then we seek a solution U that satisfies the Meixner condition:

$$\int_{\Omega_R} (|U(\mathbf{x})|^2 + |\nabla U(\mathbf{x})|^2) dV(\mathbf{x}) < \infty, \quad (2.1.7)$$

for every $R > 0$, i.e. $U \in H_{loc}^1(\Omega)$. The tip and edge condition corresponds physically to the requirement of the absence of “sources” at the singular points and mathematically ensure uniqueness of the solution.

We will consider in this thesis the case when the incident wave is a plane wave,

$$U_{inc}(\mathbf{x}) = e^{-ik\boldsymbol{\omega}_0 \cdot \mathbf{x}}. \quad (2.1.8)$$

Here $-\boldsymbol{\omega}_0$ is a unit vector defining the direction of the incidence. We have suppressed the dependence on $\boldsymbol{\omega}_0$ in the notation for U_{inc} and will do so in other functions, where the dependence on $\boldsymbol{\omega}_0$ is implicitly understood. The formula (2.1.8) defines an incident plane wave which oscillates sinusoidally in the direction of $-\boldsymbol{\omega}_0$ and is constant in the directions orthogonal to $-\boldsymbol{\omega}_0$. The solution U is then obtained by finding U_{sc} which satisfies (2.1.3) and (2.1.5) along with appropriate boundary conditions found by substituting (2.1.4) into (2.1.2) and (2.1.7).

Definition 2.1. We define the problem of finding a solution to the Helmholtz equation (2.1.3) with the conditions (2.1.2), (2.1.5), (2.1.7) and (2.1.8) as the (acoustic) planar incidence scattering problem.

As stated above we are interested in the behaviour of the solution $U(\mathbf{x}, k)$ at “high-frequencies” or short wavelengths i.e. when the wavelength $\lambda := 2\pi/k$ is significantly smaller than some characteristic length of the scattering obstacle.

Mathematically we are concerned, in general, with the asymptotics of $U_{sc}(\mathbf{x}, k)$ as $k \rightarrow \infty$.

The Ray method, geometric optics and its further modification, the Geometric Theory of Diffraction (GTD), provide a set of recipes for constructing such asymptotics for the scattered field (see [60], [54], [51] and [17]). From these methods, we expect the asymptotics of the scattered field to be composed of a number of contributions corresponding to scattering by particular parts of the boundary. Those contributions may include “simple reflections” caused by non-grazing incidence at smooth parts of the obstacle D , or more complicated “grazing incidence” diffraction which leads to asymptotics of the “creeping waves” in the shadow [59] and special boundary-layer asymptotics in the “penumbra”, i.e. the zone between regions of complete shadow and complete illumination (see e.g. [6]).

The scattered wave’s asymptotics may also contain components arising from diffraction by non-smooth “singular” points of the scattering surface such as edges or conical points. The diffraction by conical points is the main topic of this thesis.

Using the Ray Method we get a formal recipe for constructing such asymptotics (see e.g. [15, §8.2]). The intuitive idea is the expectation that in the high-frequency regime the component solution to the scattering problem will appear “locally” to be a plane wave, rapidly oscillating but with slowly varying amplitude, propagation direction and phase. This can be written as a well known “ray ansatz”

$$U(\mathbf{x}) = e^{ik\tau(\mathbf{x})} \sum_{j=0}^{\infty} A_j(\mathbf{x})(ik)^{\alpha-j}, \quad (2.1.9)$$

where the “eikonal” τ must satisfy the *eikonal equation*, $|\nabla\tau|^2 = 1$, the “amplitudes” A_j are solutions of equations known as the *transport equations* [15, 8.2.19] and α is a constant depending on the physical nature of the relevant component wave. The so-called “rays” emerge in the process of solving the eikonal equation (which is a first order nonlinear partial differential equation) by the method of Hamilton-Jacobi (the method of characteristics). The rays’ “directions” correspond to the vector $\nabla\tau$ and the surfaces of constant τ are called “wave fronts”. The transport equations describe the way the amplitude varies along these rays. (The scattered rays are constructed by a modified version of Fermat’s principle [60]: the wave field travels along the shortest route between two points via the surface of D .) The eikonal and transport equations lead to a system of first order ordinary differential equations along the rays and the only missing information are the initial conditions along the rays. These initial conditions are found via the “localisation principle” by considering the appropriate “canonical problem”

which depends on the “local geometry” of the part of the obstacle the ray is being scattered from. Solving these canonical problems and finding the “far field” asymptotics of the solutions allows us to find $\tau(\mathbf{x})$ and $A_j(\mathbf{x})$ in (2.1.9) via the procedure of “matched asymptotics”, and hence ultimately allows us to find the contributions to the component scattered wave in the form (2.1.9). So, the underlying idea behind the localisation principle is that the high-frequency incident wave “sees” only local features of the scatterer.

For the problem of scattering by a point \mathbf{x} on a smooth portion of D , the obstacle appears locally to be a plane interface (which is the tangent plane to the actual scatterer at \mathbf{x}) and so the scattered rays are determined by the usual laws of reflection via geometrical optics (with the canonical problem being that of the reflection of a plane wave by a tangent plane which can easily be solved by the method of images). The initial data is found from the reflection coefficient of the incident wave by the tangent plane to ∂D at \mathbf{x} . These reflection coefficients are an example of the more general *diffraction coefficients* which determine how a family of rays which are scattered by a point (which may be a singular point) on the surface of the obstacle propagate.

The case of diffraction by “wedge-type” singularities reduces to a canonical problem of diffraction by a wedge. This problem was solved by Sommerfeld at the end of the 19th century via a generalisation of the method of images on appropriate Riemann surfaces (see [71] [72]). This allows an explicit evaluation of the wave diffracted by the edge of the wedge.

In the same way as for the plane interface and edges, waves diffracted by a sharp singular point on D are determined by the local structure of this singularity. Hence we identify the principal asymptotics of the diffracted wave for the bounded scatterer with those of the (semi-infinite) cone Ξ , whose surface is tangent to D at the singular point (Fig. 1-1). This leads us to consider diffraction by cones with “arbitrary” cross sections, which has been a particular challenge in diffraction theory for many years.

This strategy of considering the canonical problem has been rigorously justified e.g. for the reflected wave [48], [7] and [20], see also [43] for a 2D wave diffracted by a (curved) corner and [64] for a 3D wave diffracted by a conical point. (Using the same reasoning as above we can argue that the problem of scattering of an electromagnetic incident wave by a bounded obstacle with singular points can also be reduced to a canonical conical electromagnetic diffraction problem. This will be discussed in §2.2.)

So we consider the scattering problem when the obstacle is Ξ , a cone of

arbitrary cross section. To characterise the geometry of Ξ , we assume its vertex is at the origin (Fig. 1-2). Then every point $\mathbf{x} \in \mathbb{R}^3$, can be represented as $\mathbf{x} = r\boldsymbol{\omega}$ where $r = |\mathbf{x}|$ and $\boldsymbol{\omega} \in S^2$, the unit sphere centred at the origin. As \mathbf{x} varies within the domain of propagation, $\mathbb{R}^3 \setminus \Xi$, $\boldsymbol{\omega}$ varies within M , the manifold consisting of the portion of S^2 exterior to the cone. The manifold M characterizes the cross section of the cone and has boundary $\ell = S^2 \cap \partial\Xi$. We next describe the precise assumptions on the conical geometry and introduce some notation.

Notation 2.2. We assume that the cone's surface $\partial\Xi$ has a finite number of smooth (i.e. analytic) faces, joined at lateral edges (and meeting at the tip), and that the angle between pairs of adjacent faces lies in $(0, 2\pi)$ (i.e. cuspid edges are excluded). We also assume that M and $S^2 \setminus \bar{M}$ are simply connected subsets of S^2 and that the contour ℓ is a simple closed curve consisting of a finite number of analytic arcs on the sphere also joined at non-cuspid corners. For much of what we are going to do below, a lower order of smoothness for the faces would be sufficient, but we suppress this extra generality in the interests of readability.

For $\boldsymbol{\omega}, \boldsymbol{\omega}' \in S^2$ we define $\theta(\boldsymbol{\omega}, \boldsymbol{\omega}')$ to be the geodesic distance between two points $\boldsymbol{\omega}$ and $\boldsymbol{\omega}'$ on the sphere S^2 (the arclength of the “shortest” curve lying on S^2 connecting $\boldsymbol{\omega}$ and $\boldsymbol{\omega}'$, i.e. $\cos \theta(\boldsymbol{\omega}, \boldsymbol{\omega}') = \boldsymbol{\omega} \cdot \boldsymbol{\omega}'$).

We denote the contribution to U_{sc} from the field diffracted by the tip of the cone by U_{diff} . The field U_{diff} takes the following form (see e.g. [9, pg. 541]),

$$U_{diff}(\mathbf{x}) = 2\pi \frac{e^{ikr}}{kr} f(\boldsymbol{\omega}, \boldsymbol{\omega}_0) + O((kr)^{-2}), \quad k \rightarrow \infty. \quad (2.1.10)$$

Here $f(\boldsymbol{\omega}, \boldsymbol{\omega}_0)$ is the *diffraction coefficient*, which depends only on the geometry of the cone, the incident angle $-\boldsymbol{\omega}_0$ and the angle of observation $\boldsymbol{\omega}$. The diffraction coefficients are exactly the initial conditions required to formulate the wave diffracted by the singularity in the original problem in the form (2.1.9). The formula (2.1.10) is directly related to the representation (2.1.9) (with $\alpha = -1$) insofar that the diffraction coefficient $f(\boldsymbol{\omega}, \boldsymbol{\omega}_0)$ derived from the canonical conical problem describes the contribution of the tip diffracted wave to the principal amplitude $A_0(\mathbf{x})$ of the solution to the planar incidence scattering problem (via $\tau = r$, $A_0 = 2\pi i f(\boldsymbol{\omega}, \boldsymbol{\omega}_0)$). We aim at deriving a formula for $f(\boldsymbol{\omega}, \boldsymbol{\omega}_0)$ from far field asymptotics of the canonical problem of diffraction of a plane wave by a semi-infinite cone. The latter is a boundary value problem with an unbounded scatterer for which a proper formulation of the radiation conditions is unclear. To bypass this, we consider first a “point-source” problem. (The radiation conditions in the form (2.1.5) still apply for the point source problem and uniqueness

is known to hold, see e.g. [56] for the electromagnetic case. Although there are no publications known to us that address the question of uniqueness in the acoustic case and/or lateral edge case, there is no doubt that the methods of proving uniqueness e.g. in [56] can be adapted in a straightforward way to these cases. This has not been pursued in this thesis.) By allowing the source $\mathbf{x}_0 = r_0\boldsymbol{\omega}_0$ to approach infinity, i.e. $r_0 \rightarrow \infty$, with $\boldsymbol{\omega}_0$ fixed, we recover a solution to the planar incidence scattering problem. There are other techniques which one could use, i.e. the so-called “limiting absorption” procedure, but we do not discuss them here.

2.1.1 The point source and planar incidence problem

In this subsection we consider the conical scattering problem for a point source incident wave in \mathbb{R}^3 following [67], [68] and [9] i.e. we wish to find the Green’s function satisfying

$$(\Delta + k^2)G(\mathbf{x}, \mathbf{x}_0) = -\delta(\mathbf{x} - \mathbf{x}_0) \quad \text{for } \mathbf{x} \in \mathbb{R}^3 \setminus \Xi, \quad (2.1.11)$$

with boundary conditions

$$G(\mathbf{x}, \mathbf{x}_0) = 0 \quad \text{or} \quad \frac{\partial G(\mathbf{x}, \mathbf{x}_0)}{\partial \mathbf{n}} = 0 \quad \text{for } \mathbf{x} \in \partial\Xi, \quad (2.1.12)$$

and radiation, tip and edge conditions (if any) given by (2.1.5), (2.1.7). In (2.1.12) $\delta(\mathbf{x} - \mathbf{x}_0)$ is the Dirac delta generalised function which physically corresponds to the “point source” at $\mathbf{x} = \mathbf{x}_0$. We can write $G = G_{inc} + G_{sc}$ where G_{inc} is the point source incident wave which is given by the solution to (2.1.11) in \mathbb{R}^3 which satisfies the radiation conditions (2.1.5). It is well known (e.g. [30, §2.8.1]) that G_{inc} is given by

$$G_{inc}(\mathbf{x}, \mathbf{x}_0) = \frac{e^{ik|\mathbf{x}-\mathbf{x}_0|}}{4\pi|\mathbf{x} - \mathbf{x}_0|}. \quad (2.1.13)$$

Definition 2.3. We define the problem of finding a solution to the Helmholtz equation (2.1.11) along with the conditions (2.1.2), (2.1.5), (2.1.7) as the point source scattering problem.

We formulate the solution to the point source scattering problem via separation of variables in coordinates $(r, \boldsymbol{\omega})$. The radial part of G is given by Bessel and Hankel functions of the first kind, J_ν and $H_\nu^{(1)}$. The angular part is given by the eigenfunctions of the operator $-\Delta^* + 1/4$. Here Δ^* is defined as the Laplace-Beltrami operator, in standard spherical coordinates (θ, ϕ) we write it

as,

$$\Delta^* = \frac{1}{\sin \theta} \frac{\partial}{\partial \theta} \left(\sin \theta \frac{\partial}{\partial \theta} \right) + \frac{1}{\sin^2 \theta} \frac{\partial^2}{\partial \phi^2}.$$

From the general theory of elliptic differential operators [63, Ch. II §4,5], $-\Delta^* + 1/4$, with specified (Dirichlet or Neumann) boundary conditions, is a self-adjoint operator in $L^2(M)$ with discrete non-negative spectrum and corresponding eigenfunctions. We denote the eigenfunctions by $\Phi_{B,j}(\boldsymbol{\omega})$, $j = 1, 2, \dots$, with the eigenvalues $\nu_{B,j}^2$, $\nu_{B,j} > 1/2$ for $B = D$ and N for the Dirichlet and Neumann problems respectively. We assume these are ordered so that $\nu_{B,j} \leq \nu_{B,j+1}$, $j = 1, 2, \dots$.

Therefore

$$\left(\Delta^* + \nu_{B,j}^2 - \frac{1}{4} \right) \Phi_{B,j}(\boldsymbol{\omega}) = 0 \text{ on } M, \text{ for } B = D \text{ or } N, \quad (2.1.14)$$

with Dirichlet or Neumann boundary conditions respectively.

Definition 2.4. We refer to the eigenvalues defined by (2.1.14) as the external Dirichlet or external Neumann eigenvalues depending on the boundary conditions. Similarly we can define the internal Dirichlet and internal Neumann eigenvalues which are given by $\widehat{\nu}_{B,j} \geq 1/2$, $B = D, N$, $j = 1, 2, \dots$, satisfying,

$$\left(\Delta^* + \widehat{\nu}_{B,j}^2 - \frac{1}{4} \right) \widehat{\Phi}_{B,j}(\boldsymbol{\omega}) = 0 \text{ on } S^2 \setminus (M \cup \ell), \text{ for } B = D \text{ or } N,$$

for some (interior) eigenfunctions $\widehat{\Phi}_{B,j}$, $j = 1, 2, \dots$, with Dirichlet or Neumann boundary conditions on ℓ .

It follows from the general theory of elliptic operators (see above) that $1/2 < \nu_{D,j}$ for $j = 1, 2, \dots$ and $1/2 = \nu_{N,1} < \nu_{N,j}$ for $j = 2, 3, \dots$. The eigenfunctions $\Phi_{B,j}$, $B = D, N$, $j = 1, 2, \dots$ can always be selected so that they form an orthonormal basis in $L^2(M)$, the Lebesgue space of square integrable functions defined on M , see e.g. [63, Ch. II §4,5], i.e. in particular,

$$\int_M \Phi_{B,j}(\boldsymbol{\omega}) \Phi_{B,k}(\boldsymbol{\omega}) dS(\boldsymbol{\omega}) = \delta_{jk}, \quad B = D, N,$$

where δ_{jk} is the usual Kronecker delta symbol,

$$\delta_{jk} = \begin{cases} 1 & j = k \\ 0 & j \neq k \end{cases}.$$

Hence in $L^2(M)$, the first Neumann's normalised eigenfunction $\Phi_{N,1}$ (associated with $\nu_{N,1}$) is a constant function given by $\Phi_{N,1}(\boldsymbol{\omega}) \equiv |M|^{-1/2}$, where $|M|$ is the

surface area of the manifold M . (It is clear that $\Phi_{N,1}$ satisfies (2.1.14) and that $\int_M (\Phi_{N,1}(\boldsymbol{\omega}))^2 dS(\boldsymbol{\omega}) = 1$.) From now on we drop the subscripts D, N and write ν_j for $\nu_{B,j}$ and Φ_j for $\Phi_{B,j}$, $B = D, N$, in this section with the dependence on the boundary conditions to be understood implicitly.

Writing $\mathbf{x}_0 = r_0 \boldsymbol{\omega}_0$ and applying separation of variables to the point source scattering problem, we get the formula (see e.g. [9] or, for a more rigorous derivation and justification, [61]),

$$G(\mathbf{x}, \mathbf{x}_0) = -\frac{\pi}{2i} \sum_{j=1}^{\infty} (rr_0)^{-1/2} J_{\nu_j}(kr_<) H_{\nu_j}^{(1)}(kr_>) \Phi_j(\boldsymbol{\omega}) \Phi_j(\boldsymbol{\omega}_0). \quad (2.1.15)$$

where $r_< := \min\{r, r_0\}$ and $r_> := \max\{r, r_0\}$ and J_{ν_j} and $H_{\nu_j}^{(1)}$ are Bessel functions. Note that the asymptotics of $J_{\nu_j}(kr_<)$ and $H_{\nu_j}^{(1)}(kr_>)$ when $kr \rightarrow 0$ and $kr \rightarrow \infty$, respectively, ensure the tip condition (2.1.7) and the radiation condition (2.1.5). (It is shown in [61] that (2.1.15) is the solution to the point source scattering problem therefore *a posteriori* establishes the existence of a solution. The ‘‘eigenvalue decomposition’’ leading to (2.1.15) might also be used as an alternative proof of the uniqueness of a solution to the point source scattering problem.) The series convergence is understood in the distributional sense, see [61, Pg. 3710] for the exact description of the relevant distribution space.

Using a procedure often referred to as ‘‘Watson’s transformation’’ we can transform (2.1.15) into the contour integral

$$G(\mathbf{x}, \mathbf{x}_0) = -\frac{1}{2} (rr_0)^{-1/2} \int_{\gamma_1} J_{\nu}(kr_<) H_{\nu}^{(1)}(kr_>) g(\boldsymbol{\omega}, \boldsymbol{\omega}_0, \nu) \nu d\nu, \quad (2.1.16)$$

where the convergence of the integral is also understood initially in the distributional sense. (The equivalence of (2.1.15) and (2.1.16) is verified for $r \neq r_0$ in Lemma 2.8.) The integration in (2.1.16) is over a contour, γ_1 , in the complex plane which bends around $\nu_j, j = 1, 2, \dots$. The points ν_j are represented schematically by dots on the real axis in Fig. 2-1. In (2.1.16) $g(\boldsymbol{\omega}, \boldsymbol{\omega}_0, \nu)$ is the spherical Green’s function satisfying

$$(\Delta^* + \nu^2 - 1/4)g(\boldsymbol{\omega}, \boldsymbol{\omega}_0, \nu) = \delta(\boldsymbol{\omega} - \boldsymbol{\omega}_0), \quad \text{for } \boldsymbol{\omega} \in M, \quad (2.1.17)$$

and $g(\boldsymbol{\omega}, \boldsymbol{\omega}_0, \nu)$ also satisfies a Dirichlet or Neumann boundary condition on ℓ , the boundary of M , whichever is given in the original scattering problem. It is known (e.g. from spectral theory cf. [33, Ch. VII]) that g is analytic with respect to ν with poles $\nu_j, j = 1, 2, \dots$. (It is shown in [61] that the series (2.1.15) is

rapidly convergent due to the asymptotic properties of J_ν and $H_\nu^{(1)}$ when $\text{Im}(\nu)$ is bounded and $\text{Re}(\nu) \rightarrow +\infty$. Using similar techniques it follows the integral in (2.1.16) is rapidly convergent when $r \neq r_0$ and $\boldsymbol{\omega} \neq \boldsymbol{\omega}_0$ also, although we do not show this here.)

To show that the formulations (2.1.15) and (2.1.16) are equivalent we use Lemma 2.6, but first we introduce the following definition.

Definition 2.5. Suppose that $v(\boldsymbol{\omega})$ and $w(\boldsymbol{\omega})$ are two generalised functions (distributions), i.e. linear continuous functionals defined by their “actions” on an appropriate space of test functions. The distributions v and w are equal if their actions on a test function ψ are equal, namely $\langle v(\boldsymbol{\omega}), \psi(\boldsymbol{\omega}) \rangle = \langle w(\boldsymbol{\omega}), \psi(\boldsymbol{\omega}) \rangle$ where for a “regular” function y , $\langle y(\boldsymbol{\omega}), \psi(\boldsymbol{\omega}) \rangle = \int_M y(\boldsymbol{\omega}) \psi(\boldsymbol{\omega}) dS(\boldsymbol{\omega})$, (see e.g. [41, §1.3] for details).

The exact distribution space in the present context depends on whether we are working in a Dirichlet or Neumann setting. In the Dirichlet setting we consider a space of test functions given by

$$F_D(M) := \{\psi \in C^\infty(\bar{M}) : \psi|_\ell = 0, \Delta^{*j}\psi|_\ell = 0, j = 1, 2, \dots\}.$$

In the Neumann setting we consider

$$F_N(M) := \{\psi \in C^\infty(\bar{M}) : (\partial\psi/\partial\mathbf{m})|_\ell = 0, \frac{\partial}{\partial\mathbf{m}}\{\Delta^{*j}\psi\}|_\ell = 0, j = 1, 2, \dots\}.$$

A sequence of functions $\psi_n \in F_B(M)$, $n \in \mathbb{N}$, $B = D, N$ converges to $\psi \in F_B(M)$ if for any $j = 0, 1, \dots$

$$\|\Delta^{*j}(\psi_n - \psi)\|_{L^2(M)} \rightarrow 0,$$

as $n \rightarrow \infty$. (For more details see [9, Appendix B], also cf. [61, Pg. 3710], [42], [23], [73, Ch 5 Appedix A].)

By definition, a series $\sum_{j=1}^\infty v_j(\boldsymbol{\omega})$ converges in the distributional sense if

$$\left\langle \sum_{j=1}^\infty v_j(\boldsymbol{\omega}), \psi(\boldsymbol{\omega}) \right\rangle = \lim_{N \rightarrow \infty} \left\langle \sum_{j=1}^N v_j(\boldsymbol{\omega}), \psi(\boldsymbol{\omega}) \right\rangle$$

exists for every test function ψ .

Similarly the integral of $v(\boldsymbol{\omega}, \nu)$ of γ_1 converges in the distributional sense if

$$\left\langle \int_{\gamma_1} v(\boldsymbol{\omega}, \nu) d\nu, \psi(\boldsymbol{\omega}) \right\rangle = \lim_{C \rightarrow \infty} \left\langle \int_{\tilde{\gamma}_C} v(\boldsymbol{\omega}, \nu) d\nu, \psi(\boldsymbol{\omega}) \right\rangle$$

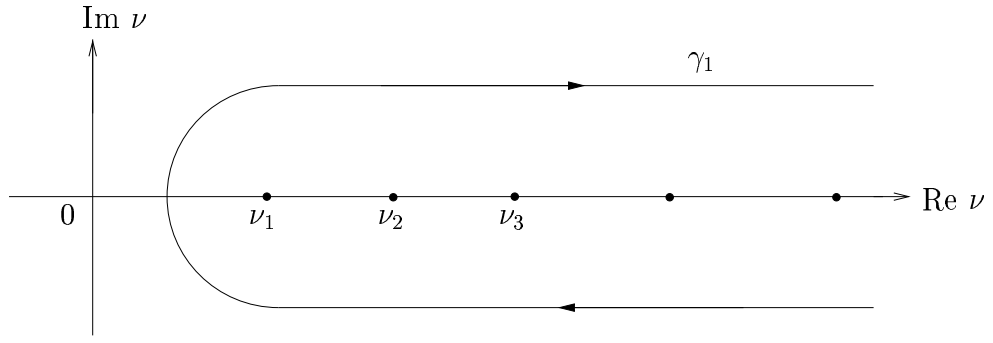


Figure 2-1: Contour of integration γ_1

exists for every test function ψ . Here $\tilde{\gamma}_C$ is the part of the contour γ_1 in the half-plane $\text{Re}(\nu) \leq C$.

Lemma 2.6. For $\text{Re}(\nu) > 0$, $\nu \neq \nu_j$ $j = 1, 2, \dots$ and fixed $\omega_0 \in M$, $g(\omega, \omega_0, \nu)$ defined in (2.1.17) can be represented in the form

$$g(\omega, \omega_0, \nu) = \sum_{j=1}^{\infty} (\nu^2 - \nu_j^2)^{-1} \Phi_j(\omega) \Phi_j(\omega_0), \quad (2.1.18)$$

holding in the distributional sense.

Proof We prove this result for the case when g satisfies Dirichlet boundary conditions, the proof for the Neumann case is analogous. We seek $g(\omega, \omega_0, \nu)$ in the form of a spectral decomposition with respect to the orthonormal eigenfunctions $\{\Phi_j\}$. So $g(\omega, \omega_0, \nu)$ is sought in the form,

$$g(\omega, \omega_0, \nu) = \sum_{j=1}^{\infty} \mathcal{G}_j(\omega_0, \nu) \Phi_j(\omega), \quad \omega \in M, \quad (2.1.19)$$

where \mathcal{G}_j are to be found.

We next claim that, in the distributional sense, the “spherical” delta function can be represented in the form

$$\delta(\omega - \omega_0) = \sum_{j=1}^{\infty} \Phi_j(\omega) \Phi_j(\omega_0), \quad (2.1.20)$$

(with the series in (2.1.20) converging in the distributional sense). To prove the

claim consider, for $\psi \in F_D(M)$,

$$\begin{aligned} \langle \sum_{j=1}^{\infty} \Phi_j(\boldsymbol{\omega}) \Phi_j(\boldsymbol{\omega}_0), \psi(\boldsymbol{\omega}) \rangle &= \sum_{j=1}^{\infty} \int_M \Phi_j(\boldsymbol{\omega}) \Phi_j(\boldsymbol{\omega}_0) \psi(\boldsymbol{\omega}) dS(\boldsymbol{\omega}) \\ &= \sum_{j=1}^{\infty} \Phi_j(\boldsymbol{\omega}_0) \int_M \Phi_j(\boldsymbol{\omega}) \psi(\boldsymbol{\omega}) dS(\boldsymbol{\omega}). \end{aligned} \quad (2.1.21)$$

The right-hand side of (2.1.21) is the orthogonal expansion of ψ evaluated at $\boldsymbol{\omega}_0$, with the series convergent in the classical sense (uniformly) since for any $\psi \in F_D(M)$, the “Fourier coefficients”, $\int_M \Phi_j(\boldsymbol{\omega}) \psi(\boldsymbol{\omega}_0) dS(\boldsymbol{\omega})$ are known to decay faster than any inverse power of j and $|\Phi_j(\boldsymbol{\omega})| \leq Cj$, cf. [9, Appendix B]. Thus,

$$\langle \sum_{j=1}^{\infty} \Phi_j(\boldsymbol{\omega}) \Phi_j(\boldsymbol{\omega}_0), \psi \rangle = \psi(\boldsymbol{\omega}_0) = \langle \delta(\boldsymbol{\omega} - \boldsymbol{\omega}_0), \psi \rangle, \quad \text{when } \boldsymbol{\omega}, \boldsymbol{\omega}_0 \in M.$$

The last equality follows from [41, §1.3]. This along with Definition 2.5 establishes the claim.

Now $g(\boldsymbol{\omega}, \boldsymbol{\omega}_0, \nu)$ satisfies (2.1.17) and so

$$\begin{aligned} \langle \delta(\boldsymbol{\omega} - \boldsymbol{\omega}_0), \psi(\boldsymbol{\omega}) \rangle &= \langle (\Delta^* + \nu^2 - 1/4)g(\boldsymbol{\omega}, \boldsymbol{\omega}_0, \nu), \psi(\boldsymbol{\omega}) \rangle \\ &= \langle g(\boldsymbol{\omega}, \boldsymbol{\omega}_0, \nu), (\Delta^* + \nu^2 - 1/4)\psi(\boldsymbol{\omega}) \rangle \\ &= \langle \sum_{j=1}^{\infty} \mathcal{G}_j(\boldsymbol{\omega}_0, \nu) \Phi_j(\boldsymbol{\omega}), (\Delta^* + \nu^2 - 1/4)\psi(\boldsymbol{\omega}) \rangle \\ &= \lim_{N \rightarrow \infty} \sum_{j=1}^N \mathcal{G}_j(\boldsymbol{\omega}_0, \nu) \langle \Phi_j(\boldsymbol{\omega}), (\Delta^* + \nu^2 - 1/4)\psi(\boldsymbol{\omega}) \rangle. \end{aligned} \quad (2.1.22)$$

Since $\Phi_j(\boldsymbol{\omega})$ is a “regular” distribution

$$\begin{aligned} \langle \Phi_j(\boldsymbol{\omega}), (\Delta^* + \nu^2 - 1/4)\psi(\boldsymbol{\omega}) \rangle &= \int_M \Phi_j(\boldsymbol{\omega}) (\Delta^* + \nu^2 - 1/4)\psi(\boldsymbol{\omega}) dS(\boldsymbol{\omega}) \\ &= \int_{\ell} \Phi_j(\boldsymbol{\omega}) \frac{\partial \psi(\boldsymbol{\omega})}{\partial \mathbf{m}} - \frac{\partial \Phi_j(\boldsymbol{\omega})}{\partial \mathbf{m}} \psi(\boldsymbol{\omega}) d\boldsymbol{\omega} \\ &\quad + \int_M \psi(\boldsymbol{\omega}) (\Delta^* + \nu^2 - 1/4)\Phi_j(\boldsymbol{\omega}) dS(\boldsymbol{\omega}) \\ &= \langle \psi(\boldsymbol{\omega}), (\Delta^* + \nu^2 - 1/4)\Phi_j(\boldsymbol{\omega}) \rangle \\ &= \langle \psi(\boldsymbol{\omega}), (\Delta^* + \nu_j^2 - 1/4)\Phi_j(\boldsymbol{\omega}) + (\nu^2 - \nu_j^2)\Phi_j(\boldsymbol{\omega}) \rangle \\ &= (\nu^2 - \nu_j^2) \langle \psi(\boldsymbol{\omega}), \Phi_j(\boldsymbol{\omega}) \rangle. \end{aligned} \quad (2.1.23)$$

The last equality follows from (2.1.14). Substituting (2.1.23) into (2.1.22) we obtain

$$\begin{aligned} \langle \delta(\boldsymbol{\omega} - \boldsymbol{\omega}_0), \psi(\boldsymbol{\omega}) \rangle &= \lim_{N \rightarrow \infty} \sum_{j=1}^N \mathcal{G}_j(\boldsymbol{\omega}_0, \nu) (\nu^2 - \nu_j^2) \langle \Phi_j(\boldsymbol{\omega}), \psi(\boldsymbol{\omega}) \rangle \\ &= \left\langle \sum_{j=1}^{\infty} \mathcal{G}_j(\boldsymbol{\omega}_0, \nu) (\nu^2 - \nu_j^2) \Phi_j(\boldsymbol{\omega}), \psi(\boldsymbol{\omega}) \right\rangle. \end{aligned} \quad (2.1.24)$$

Therefore, by substituting (2.1.20) into the left-hand side of (2.1.24) we have $\mathcal{G}_j(\boldsymbol{\omega}_0, \nu) = (\nu^2 - \nu_j^2)^{-1} \Phi_j(\boldsymbol{\omega}_0)$ and substituting this into (2.1.19) gives (2.1.18). Finally notice that the right-hand side of (2.1.18) converges in the distributional sense (for $\nu \neq \nu_j$) using the same argument as the one establishing distributional convergence of (2.1.20). Since we have shown that (2.1.18) satisfies (2.1.17) in the distributional sense, the uniqueness of a distributional solution to (2.1.17) (see e.g. [41], [53]) implies the result. \square

To show the representations (2.1.15) and (2.1.16) of $G(\mathbf{x}, \mathbf{x}_0)$ are equivalent we use a variant of the Cauchy residue theorem which we formulate below in a suitable form without proof.

Theorem 2.7. *Suppose that v is a function defined on \mathbb{C} which is analytic everywhere except at infinitely many poles, $\pm \nu_j$, $j = 1, 2, \dots$, such that $0 < \nu_1 < \nu_2 < \dots$ and $\nu_j \rightarrow \infty$ as $j \rightarrow \infty$. Suppose also that γ_1 crosses the real axis at a point in the interval $(0, \nu_1)$. Let the integral of v over the contour γ_1 be convergent. Also let the series $\sum_{j=1}^{\infty} \text{res}\{v(\nu); \nu_j\}$ be convergent, where $\text{res}\{v(\nu); \nu_j\}$ is the residue of $v(\nu)$ at $\nu = \nu_j$, in particular, provided the poles are simple,*

$$\text{res}\{v(\nu); \nu_j\} := \lim_{\nu \rightarrow \nu_j} (\nu - \nu_j) v(\nu). \quad (2.1.25)$$

In addition suppose that

$$\int_{\gamma'_a} v(\nu) d\nu \rightarrow 0 \quad (2.1.26)$$

when $a \neq \nu_j$, $a \in \mathbb{R}$, $a \rightarrow \infty$, where γ'_a is a vertical contour (part of $\text{Re}(\nu) = a$) connecting the “lower” and “upper” branches of γ_1 :

$$\gamma'_a = \{\nu : \text{Re}(\nu) = a, b_1 \leq \text{Im}(\nu) \leq b_2, a + ib_k \in \gamma_1, k = 1 \text{ and } 2\}.$$

Then the integral of v over the contour γ_1 can be represented in the following

form (noting that the contour is negatively oriented),

$$\int_{\gamma_1} v(\nu) d\nu = -2\pi i \sum_{j=1}^{\infty} \text{res}\{v(\nu); \nu_j\}.$$

Lemma 2.8. *The representations (2.1.15) and (2.1.16) of $G(\mathbf{x}, \mathbf{x}_0)$, the solution to the point-source problem, are equivalent in the distributional sense when $r \neq r_0$.*

We do not give all the technical details for the proof of this result but instead give a sketched proof. We wish to show that for $\psi \in F_B(M)$,

$$\begin{aligned} \left\langle -\frac{1}{2}(rr_0)^{-1/2} \int_{\gamma_1} J_\nu(kr_<) H_\nu^{(1)}(kr_>) g(\boldsymbol{\omega}, \boldsymbol{\omega}_0, \nu) \nu d\nu, \psi(\boldsymbol{\omega}) \right\rangle = \\ \left\langle -\frac{\pi}{2i} \sum_{j=1}^{\infty} (rr_0)^{-1/2} J_{\nu_j}(kr_<) H_{\nu_j}^{(1)}(kr_>) \Phi_j(\boldsymbol{\omega}) \Phi_j(\boldsymbol{\omega}_0), \psi(\boldsymbol{\omega}) \right\rangle. \end{aligned} \quad (2.1.27)$$

We aim to show this using Theorem 2.7. Hence we need to check that the hypotheses of Theorem 2.7 hold for

$$v(\nu) = \left\langle -\frac{1}{2}(rr_0)^{-1/2} J_\nu(kr_<) H_\nu^{(1)}(kr_>) g(\boldsymbol{\omega}, \boldsymbol{\omega}_0, \nu), \psi(\boldsymbol{\omega}) \right\rangle. \quad (2.1.28)$$

The convergence of the action of the series in (2.1.27) on a test function is proved in [61, Theorem 1]. To prove convergence of the action of the integral on a test function in (2.1.27) we show

$$\lim_{C \rightarrow \infty} \left\{ -\frac{1}{2}(rr_0)^{-1/2} \int_{\tilde{\gamma}_C} J_\nu(kr_<) H_\nu^{(1)}(kr_>) \langle g(\boldsymbol{\omega}, \boldsymbol{\omega}_0, \nu) \nu, \psi(\boldsymbol{\omega}) \rangle d\nu \right\} \quad (2.1.29)$$

exists. Now it follows from [61, Pg. 3712] that

$$\left| -\frac{1}{2}(rr_0)^{-1/2} J_\nu(kr_<) H_\nu^{(1)}(kr_>) \right| \leq C |\nu| \left(\frac{r_<}{r_>} \right)^{\text{Re}(\nu)} \quad (2.1.30)$$

when $\nu \in \gamma_1$. Also from [9, Appendix B]

$$\begin{aligned} \langle g(\boldsymbol{\omega}, \boldsymbol{\omega}_0, \nu), \psi(\boldsymbol{\omega}) \rangle &= \left\langle \frac{1}{\nu^2} \delta(\boldsymbol{\omega} - \boldsymbol{\omega}_0) + \frac{1}{\nu^2} \left(\frac{1}{4} - \Delta^* \right) g(\boldsymbol{\omega}, \boldsymbol{\omega}_0, \nu), \psi(\boldsymbol{\omega}) \right\rangle \\ &= \frac{1}{\nu^2} \psi(\boldsymbol{\omega}_0) + \frac{1}{\nu^2} \langle g(\boldsymbol{\omega}, \boldsymbol{\omega}_0, \nu), \left(\frac{1}{4} - \Delta^* \right) \psi(\boldsymbol{\omega}) \rangle. \end{aligned} \quad (2.1.31)$$

It can be shown that the contribution of the first term on the right-hand side of

(2.1.31) to (2.1.29) vanishes, see [9], and that

$$\left| \frac{1}{\nu^2} \langle g, \left(\frac{1}{4} - \Delta^* \right) \psi(\boldsymbol{\omega}) \rangle \right| \leq \frac{C' \| (1/4 - \Delta^*)^5 \psi \|_{L^2(M)}}{2\nu^2 \operatorname{Re}(\nu) |\operatorname{Im}(\nu)|}, \quad (2.1.32)$$

see also [9]. Thus combining (2.1.29) - (2.1.32) implies that the limit in (2.1.29) exists.

Now we consider the last condition (2.1.26) of Theorem 2.7. A way to show this is by using the representation

$$\langle g(\boldsymbol{\omega}, \boldsymbol{\omega}_0, \nu), \psi(\boldsymbol{\omega}) \rangle = \sum_{j=1}^{\infty} \frac{\Phi_j(\boldsymbol{\omega}_0)}{\nu^2 - \nu_j^2} \langle \Phi_j(\boldsymbol{\omega}), \psi(\boldsymbol{\omega}) \rangle, \quad (2.1.33)$$

where $\Phi_j(\boldsymbol{\omega}_0) \langle \Phi_j(\boldsymbol{\omega}), \psi(\boldsymbol{\omega}) \rangle$ are known to decay faster than any inverse power of j , for any $\boldsymbol{\omega}_0, \psi$. Combining (2.1.33), (2.1.28) in (2.1.26) we interchange the summation and integration over γ'_a and integrate by parts to “regularise” the potential singularity which arises when ν is close to ν_j . Then we use a bound akin to (2.1.30) for the derivative of $J_\nu(kr_<) H_\nu^{(1)}(kr_>)$ gives (2.1.26). Therefore the conditions of Theorem 2.7 are satisfied. Hence since $g(\boldsymbol{\omega}, \boldsymbol{\omega}, \nu)$ is analytic with respect to ν with poles at $\nu_j, j = 1, 2, \dots$ [33] we get,

$$\begin{aligned} & -\frac{1}{2} (rr_0)^{-1/2} \int_{\gamma_1} J_\nu(kr_<) H_\nu^{(1)}(kr_>) \langle g(\boldsymbol{\omega}, \boldsymbol{\omega}_0, \nu), \psi(\boldsymbol{\omega}) \rangle \nu \, d\nu \\ &= \frac{1}{2} (rr_0)^{-1/2} 2\pi i \sum_{j=1}^{\infty} \operatorname{res} \{ J_\nu(kr_<) H_\nu^{(1)}(kr_>) \langle g(\boldsymbol{\omega}, \boldsymbol{\omega}_0, \nu), \psi(\boldsymbol{\omega}) \rangle \nu; \nu_j \}. \end{aligned} \quad (2.1.34)$$

Now from (2.1.18) we have,

$$\begin{aligned} \lim_{\nu \rightarrow \nu_j} (\nu - \nu_j) \langle g(\boldsymbol{\omega}, \boldsymbol{\omega}_0, \nu), \psi(\boldsymbol{\omega}) \rangle \nu &= \lim_{\nu \rightarrow \nu_j} \sum_{k=1}^{\infty} \frac{(\nu - \nu_j) \nu}{\nu^2 - \nu_k^2} \Phi_k(\boldsymbol{\omega}_0) \langle \Phi_k(\boldsymbol{\omega}), \psi(\boldsymbol{\omega}) \rangle \\ &= \frac{1}{2} \Phi_j(\boldsymbol{\omega}_0) \langle \Phi_j(\boldsymbol{\omega}), \psi(\boldsymbol{\omega}) \rangle. \end{aligned}$$

Therefore from (2.1.34),

$$\begin{aligned} & -\frac{1}{2} (rr_0)^{-1/2} \int_{\gamma_1} J_\nu(kr_<) H_\nu^{(1)}(kr_>) \langle g(\boldsymbol{\omega}, \boldsymbol{\omega}_0, \nu), \psi(\boldsymbol{\omega}) \rangle \nu \, d\nu \\ &= -\frac{\pi}{2i} \sum_{j=1}^{\infty} (rr_0)^{-1/2} J_{\nu_j}(kr_<) H_{\nu_j}^{(1)}(kr_>) \Phi_j(\boldsymbol{\omega}_0) \langle \Phi_j(\boldsymbol{\omega}), \psi(\boldsymbol{\omega}) \rangle, \end{aligned}$$

for $r \neq r_0$ as required. \square

The formulae (2.1.15) or (2.1.16) give the solution to the point source problem. We will use this to obtain a solution to the planar incidence scattering problem. The following result gives a relationship between the point source incident wave G_{inc} and the planar incident wave, U_{inc} defined in (2.1.8).

Lemma 2.9. *For all $\mathbf{x} \in \mathbb{R}^3 \setminus \Xi$ and $\boldsymbol{\omega}_0 \in M$,*

$$U_{inc}(\mathbf{x}; \boldsymbol{\omega}_0) = \lim_{r_0 \rightarrow \infty} \left\{ G_{inc}(\mathbf{x}, \mathbf{x}_0) \left(\frac{e^{ikr_0}}{4\pi r_0} \right)^{-1} \right\}.$$

Proof We want to find the limit of

$$G_{inc}(\mathbf{x}; \boldsymbol{\omega}_0) \left(\frac{e^{ikr_0}}{4\pi r_0} \right)^{-1} = \frac{e^{ik|\mathbf{x}-\mathbf{x}_0|} r_0}{|\mathbf{x} - \mathbf{x}_0| e^{ikr_0}}$$

as $r_0 \rightarrow \infty$. First we note that, with $\mathbf{x} = r\boldsymbol{\omega}$, $r > 0$ and $\boldsymbol{\omega} \in S^2$, we have

$$\begin{aligned} |\mathbf{x} - \mathbf{x}_0| &= ((\mathbf{x} - \mathbf{x}_0) \cdot (\mathbf{x} - \mathbf{x}_0))^{1/2} = (r^2 + r_0^2 - 2\mathbf{x} \cdot \mathbf{x}_0)^{1/2} \\ &= (r^2 + r_0^2 - 2rr_0\boldsymbol{\omega} \cdot \boldsymbol{\omega}_0)^{1/2} = r_0(1 - 2rr_0^{-1}\boldsymbol{\omega} \cdot \boldsymbol{\omega}_0 + r^2r_0^{-2})^{1/2}. \end{aligned} \quad (2.1.35)$$

Hence

$$\lim_{r_0 \rightarrow \infty} \frac{r_0}{|\mathbf{x} - \mathbf{x}_0|} = \lim_{r_0 \rightarrow \infty} \frac{1}{(1 - 2rr_0^{-1}\boldsymbol{\omega} \cdot \boldsymbol{\omega}_0 + r^2r_0^{-2})^{1/2}} = 1.$$

Also (2.1.35) implies that

$$\begin{aligned} \lim_{r_0 \rightarrow \infty} \frac{e^{ik|\mathbf{x}-\mathbf{x}_0|}}{e^{ikr_0}} &= \lim_{r_0 \rightarrow \infty} \frac{e^{ikr_0(1-2rr_0^{-1}\boldsymbol{\omega} \cdot \boldsymbol{\omega}_0 + r^2r_0^{-2})^{1/2}}}{e^{ikr_0}} \\ &= e^{-ikr\boldsymbol{\omega} \cdot \boldsymbol{\omega}_0}. \end{aligned}$$

Therefore it follows that,

$$G_{inc}(\mathbf{x}, \mathbf{x}_0) \left(\frac{e^{ikr_0}}{4\pi r_0} \right)^{-1} \rightarrow e^{-ikr\boldsymbol{\omega} \cdot \boldsymbol{\omega}_0} = e^{-ik\boldsymbol{\omega}_0 \cdot \mathbf{x}} = U_{inc}(\mathbf{x}, \boldsymbol{\omega}_0) \quad \text{as } r_0 \rightarrow \infty,$$

by (2.1.8), the definition of U_{inc} . □

This simple result motivates us to define the solution of the plane wave scattering problem by the formula (e.g. [61]):

$$U(\mathbf{x}) = \lim_{r_0 \rightarrow \infty} \left\{ G(\mathbf{x}, \mathbf{x}_0) \left(\frac{e^{ikr_0}}{4\pi r_0} \right)^{-1} \right\}. \quad (2.1.36)$$

Using this definition for $U(\mathbf{x})$ gives the following result. It will become apparent in Lemma 2.10 that the limit in (2.1.36) exists and so is a valid definition.

Lemma 2.10. *With U defined in (2.1.36) and G defined in (2.1.15) we have, for all $\mathbf{x} = (r, \boldsymbol{\omega}) \in \mathbb{R}^3 \setminus \Xi$*

$$U(r, \boldsymbol{\omega}) = e^{i\pi/4} (2\pi)^{3/2} (kr)^{-1/2} \sum_{j=1}^{\infty} J_{\nu_j}(kr) e^{-i\nu_j\pi/2} \Phi_j(\boldsymbol{\omega}) \Phi_j(\boldsymbol{\omega}_0), \quad (2.1.37)$$

or alternatively,

$$U(r, \boldsymbol{\omega}) = -2e^{-i\pi/4} (2\pi)^{1/2} (kr)^{-1/2} \int_{\gamma_1} J_{\nu}(kr) e^{-i\pi\nu/2} g(\boldsymbol{\omega}, \boldsymbol{\omega}_0, \nu) \nu \, d\nu. \quad (2.1.38)$$

Proof The proof of this result follows [61, Theorem 4]. To prove (2.1.37) we substitute (2.1.15) into (2.1.36) and write $\mathbf{x} = (r, \boldsymbol{\omega})$ to obtain

$$U(r, \boldsymbol{\omega}) = \lim_{r_0 \rightarrow \infty} \left\{ - \left(\frac{e^{ikr_0}}{4\pi r_0} \right)^{-1} \frac{\pi}{2i} (rr_0)^{-1/2} \sum_{j=1}^{\infty} J_{\nu_j}(kr_{<}) H_{\nu_j}^{(1)}(kr_{>}) \Phi_j(\boldsymbol{\omega}) \Phi_j(\boldsymbol{\omega}_0) \right\}. \quad (2.1.39)$$

It is shown in [61, Pg. 3716] that, for sufficiently large r_0 , (e.g. $r_0 > 2r$) the series

$$\sum_{j=1}^{\infty} J_{\nu_j}(kr_{<}) H_{\nu_j}^{(1)}(kr_{>}) \Phi_j(\boldsymbol{\omega}) \Phi_j(\boldsymbol{\omega}_0)$$

is uniformly and absolutely convergent.

Since the series in (2.1.39) is absolutely convergent and the limit as $r_0 \rightarrow \infty$ for each term in the series exists, we can apply the basic theorem on interchangability of limit and summation, e.g. [19, §5.2]. Hence, noting $r_{<} \rightarrow r$ as $r_0 \rightarrow \infty$,

$$U(r, \boldsymbol{\omega}) = -\frac{2\pi^2}{i} r^{-1/2} \sum_{j=1}^{\infty} J_{\nu_j}(kr) \lim_{r_0 \rightarrow \infty} \left\{ \frac{r_0^{1/2}}{e^{ikr_0}} H_{\nu_j}^{(1)}(kr_{>}) \right\} \Phi_j(\boldsymbol{\omega}) \Phi_j(\boldsymbol{\omega}_0). \quad (2.1.40)$$

Substituting the asymptotic property of the Hankel function, [44, 8.451(3)]

$$H_{\nu}^{(1)}(kr_0) = \left(\frac{2}{\pi kr_0} \right)^{1/2} e^{ikr_0 - i\pi\nu/2 - i\pi/4} (1 + O((kr_0)^{-1})), \quad \text{as } kr_0 \rightarrow \infty,$$

into (2.1.40) and noting that $r_0/r \rightarrow 1$ as $r_0 \rightarrow \infty$, we obtain

$$\begin{aligned} U(r, \boldsymbol{\omega}) &= -\frac{2\pi^2}{i} \sum_{j=1}^{\infty} r^{-1/2} J_{\nu_j}(kr) \left(\frac{2}{\pi k} \right)^{1/2} e^{-i\pi\nu_j/2 - i\pi/4} \Phi_j(\boldsymbol{\omega}) \Phi_j(\boldsymbol{\omega}_0) \\ &= (2\pi)^{3/2} (kr)^{-1/2} e^{i\pi/4} \sum_{j=1}^{\infty} J_{\nu_j}(kr) e^{-i\pi\nu_j/2} \Phi_j(\boldsymbol{\omega}) \Phi_j(\boldsymbol{\omega}_0) \end{aligned}$$

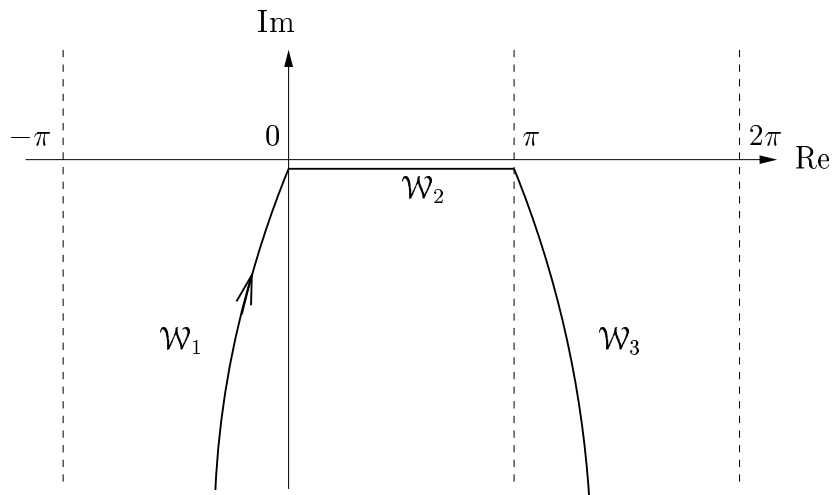


Figure 2-2: Contour of integration \mathcal{W} , $\text{Im}(\mathcal{W}_2) < -\delta$, $\delta > 0$

i.e. (2.1.37) with the latter series rapidly convergent due to the asymptotic properties of $J_{\nu_j}(kr)$ as $\nu_j \rightarrow \infty$.

The representation (2.1.38) can be verified by applying Theorem 2.7 (first in the distributional sense and then using the regularity for the distributional solutions of elliptic PDEs, e.g. [39, §8.6], [53]). \square

We now use the formulae (2.1.38) and (2.1.37) to derive a solution to the high-frequency conical scattering problem.

2.1.2 High-frequency asymptotics and the stationary phase method

We are interested in the asymptotics of (2.1.38) as the dimensionless parameter $kr \rightarrow \infty$. Following [9] and [67] it is convenient to use Sommerfeld's integral representation of the Bessel function $J_\nu(kr)$, cf. [44, 8.412(6)],

$$J_\nu(kr) = \frac{1}{2\pi} \int_{\mathcal{W}} e^{-ikr \cos s + i\nu(\pi/2 - s)} ds. \quad (2.1.41)$$

The contour $\mathcal{W} = \mathcal{W}_1 \cup \mathcal{W}_2 \cup \mathcal{W}_3$ lies in the complex half-plane $\text{Im}(s) < 0$, and is shown in Fig. 2-2. Substituting (2.1.41) into (2.1.37) we get, after interchanging the order of integration and summation [9],

$$U(r, \boldsymbol{\omega}) = e^{i\pi/4} \left(\frac{2\pi}{kr}\right)^{1/2} \int_{\mathcal{W}} e^{-ikr \cos s} \Gamma(\boldsymbol{\omega}, \boldsymbol{\omega}_0, s) ds, \quad (2.1.42)$$

where,

$$\Gamma(\boldsymbol{\omega}, \boldsymbol{\omega}_0, s) = \sum_{j=1}^{\infty} e^{-i\nu_j s} \Phi_j(\boldsymbol{\omega}) \Phi_j(\boldsymbol{\omega}_0). \quad (2.1.43)$$

Alternatively, by substituting (2.1.41) into (2.1.38) and interchanging the orders of integration we obtain (2.1.42) with Γ given by,

$$\Gamma(\boldsymbol{\omega}, \boldsymbol{\omega}_0, s) = \frac{i}{\pi} \int_{\gamma_1} e^{-i\nu s} g(\boldsymbol{\omega}, \boldsymbol{\omega}_0, \nu) \nu \, d\nu. \quad (2.1.44)$$

Note that interchanging the order of integration and summation above to obtain (2.1.42) and (2.1.43) is legitimate. Since $\text{Im}(\mathcal{W}) < -\delta$, $\delta > 0$, it follows that $\exp(-ikr \cos(s))$ decays rapidly for $s \in \mathcal{W}$ as $\text{Im}(s) \rightarrow -\infty$. This together with pointwise bounds on $|\Phi_j(\boldsymbol{\omega})|$, see e.g. [9, Appendix B], ensures that the sum-integral obtained by substituting (2.1.41) into (2.1.37) is absolutely convergent. Hence Fubini-type theorems, e.g. [40], can be applied. A similar argument (with some additional technical details) is also applicable to justify interchanging the order integration above to obtain (2.1.44) cf. [9, Appendix B].

We are interested in solving the high-frequency planar incidence scattering problem i.e. we want to calculate the asymptotics of (2.1.42) as $kr \rightarrow +\infty$. First we note that for all s satisfying $\text{Im}(s) < 0$ it holds that $\Gamma(\boldsymbol{\omega}, \boldsymbol{\omega}_0, s)$ is analytic, see [9]. (The latter follows from the uniform and absolute convergence of the series (2.1.43) for $\text{Im}(s) < -\delta$, $\delta > 0$ and the Weierstrass theorem of complex analysis on the analyticity of “locally uniform” limits e.g. [65].) Also note that $\cos s$ has a negative real part on \mathcal{W}_1 and \mathcal{W}_3 . Hence the sum and integral in (2.1.43) converge with the summand and integrand decaying exponentially for every s such that $\text{Im}(s) < 0$, see [9, Appendix B] for details. We use the fact that the integrand is analytic for $\text{Im}(s) < 0$ to allow us to deform the contour of integration \mathcal{W} . Using advanced analytic techniques (e.g. [53], [11], [57]) it can be shown that the representation of U in (2.1.42) with \mathcal{W} replaced by the contour \mathcal{W}' (in Fig. 2-3 where \mathcal{W}'_2 lies on the real axis) will hold (in the distributional sense).

Since $\cos s$ has negative real part on \mathcal{W}'_1 and \mathcal{W}'_3 the only non-negligible contribution to the asymptotics comes from the integration along \mathcal{W}'_2 . There are two types of critical points which can contribute to the asymptotic expansion of (2.1.42) when $kr \rightarrow +\infty$. Firstly there are the singular points of the “amplitude” $\Gamma(\boldsymbol{\omega}, \boldsymbol{\omega}_0, s)$. If $\Gamma(\boldsymbol{\omega}, \boldsymbol{\omega}_0, s)$ is singular at a point $s = s_0 \in (0, \pi)$ then it can be shown that integration in a neighbourhood of that point describes the asymptotics of “non-tip-diffracted” waves, i.e. incident waves, reflected waves or waves

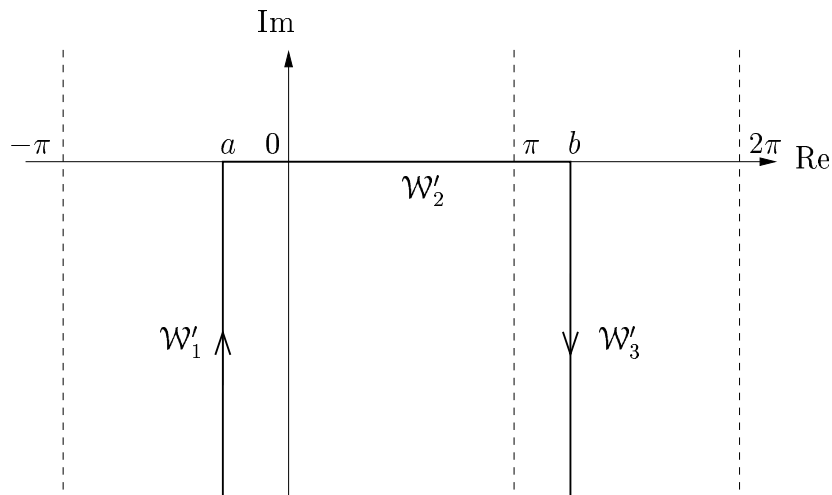


Figure 2-3: Contour of integration \mathcal{W}'

diffracted by lateral edges [67] and are not considered here. Secondly there are the stationary phase points, points s_0 such that

$$\frac{d}{ds} \cos(s)|_{s=s_0} = -\sin(s_0) = 0.$$

There are two stationary points on \mathcal{W}' , $s_0 = 0$ and $s_0 = \pi$. Contributions from these points are evaluated by the stationary phase technique (see e.g. [15, §2.7]).

We can think of the asymptotics of (2.1.42) when $kr \rightarrow \infty$ as the sum of all the contributions from the critical points. Since we are not concerned with singular points we will use a device to isolate the stationary points. However this is difficult to do when a singular point is close to a stationary point $s_0 = \pi$ and this case is not considered here although it has been shown in [67] and [9] that the contributions from these points are those corresponding to the so-called singular directions (see Definition 2.13 and also [10]). Isolating the critical points in this way will allow us to calculate the contributions from the stationary phase points using results in [15] which we do in Lemmas 2.11 and 2.15. To separate the contributions from a stationary point at s_0 from those of any other critical point we introduce “cut off” functions η which are infinitely differentiable and, when multiplied by the integrand in (2.1.42), do not affect the contributions to the asymptotic expansion of the integral. We do this by setting

$$\eta_{s_0}(s) = \begin{cases} 0, & |s - s_0| \geq \epsilon_{s_0}, \\ 1, & |s - s_0| \leq \epsilon_{s_0}/2, \end{cases} \quad (2.1.45)$$

where ϵ_{s_0} is small enough so that s_0 is the only critical point that occurs in the interval $(s_0 - \epsilon_{s_0}, s_0 + \epsilon_{s_0})$. This allows us to rewrite the formula (2.1.42) (using the new contour \mathcal{W}') as,

$$U(\mathbf{x}) = U_0(\mathbf{x}) + U_\pi(\mathbf{x}) + U_{rem}(\mathbf{x}) \quad (2.1.46)$$

where, writing $\mathbf{x} = (r, \boldsymbol{\omega})$,

$$U_{s_0}(r, \boldsymbol{\omega}) = e^{i\pi/4} \left(\frac{2\pi}{kr}\right)^{1/2} \int_{\mathcal{W}'} e^{-ikr \cos s} \Gamma(\boldsymbol{\omega}, \boldsymbol{\omega}_0, s) \eta_{s_0}(s) ds, \quad s_0 = 0, \pi,$$

and

$$U_{rem}(r, \boldsymbol{\omega}) = e^{i\pi/4} \left(\frac{2\pi}{kr}\right)^{1/2} \int_{\mathcal{W}'} e^{-ikr \cos s} \Gamma(\boldsymbol{\omega}, \boldsymbol{\omega}_0, s) (1 - \eta_0(s) - \eta_\pi(s)) ds$$

contains only the contributions to the asymptotics from non-stationary critical points (which, as mentioned above, are exactly those associated with non-tip-diffracted waves). In the remainder of this section we investigate $U_0(\mathbf{x})$ and $U_\pi(\mathbf{x})$ to obtain the asymptotics of the diffracted wave. We consider $U_0(\mathbf{x})$ first and we get the following result.

Lemma 2.11. *Suppose that $\boldsymbol{\omega}, \boldsymbol{\omega}_0 \in M$ and $\boldsymbol{\omega} \neq \boldsymbol{\omega}_0$ then*

$$U_0(r, \boldsymbol{\omega}) = O(e^{-ikr} (kr)^{-2}), \quad \text{as } kr \rightarrow \infty.$$

Proof By construction, the integral in

$$U_0(r, \boldsymbol{\omega}) = e^{i\pi/4} \left(\frac{2\pi}{kr}\right)^{1/2} \int_{\mathcal{W}'} e^{-ikr \cos s} \Gamma(\boldsymbol{\omega}, \boldsymbol{\omega}_0, s) \eta_0(s) ds \quad (2.1.47)$$

has only one critical point, namely a stationary point at $s = 0$. It follows from the stationary phase technique (see e.g. [15, pp. 73-81]) and (2.1.20) that

$$\begin{aligned} & \int_{\mathcal{W}'} e^{-ikr \cos s} \Gamma(\boldsymbol{\omega}, \boldsymbol{\omega}_0, s) \eta_{s_0}(s) ds \\ &= \left(\frac{2\pi}{kr}\right)^{1/2} e^{-ikr} \Gamma(\boldsymbol{\omega}, \boldsymbol{\omega}_0, 0) + O(e^{i\pi/4 - ikr} (kr)^{-3/2}) \\ &= \left(\frac{2\pi}{kr}\right)^{1/2} e^{-ikr} \sum_{j=1}^{\infty} \Phi_j(\boldsymbol{\omega}) \Phi_j(\boldsymbol{\omega}_0) + O(e^{i\pi/4 - ikr} (kr)^{-3/2}) \\ &= \left(\frac{2\pi}{kr}\right)^{1/2} e^{-ikr} \delta(\boldsymbol{\omega} - \boldsymbol{\omega}_0) + O(e^{i\pi/4 - ikr} (kr)^{-3/2}) \quad \text{as } kr \rightarrow \infty. \end{aligned} \quad (2.1.48)$$

Therefore (2.1.47) transforms via (2.1.48) to

$$U_0(r, \boldsymbol{\omega}) = 2\pi i \frac{e^{-ikr}}{kr} \delta(\boldsymbol{\omega} - \boldsymbol{\omega}_0) + O(e^{-ikr} (kr)^{-2}), \quad \text{as } kr \rightarrow \infty.$$

Hence the result. \square

Remark 2.12. Note from (2.1.43) that when $\boldsymbol{\omega} = \boldsymbol{\omega}_0$ then $s = 0$ is a singular point of the amplitude $\Gamma(\boldsymbol{\omega}, \boldsymbol{\omega}_0, s)$: $\Gamma(\boldsymbol{\omega}, \boldsymbol{\omega}_0, 0) = \delta(\boldsymbol{\omega} - \boldsymbol{\omega}_0)$ using (2.1.43) and (2.1.20). It has been shown in [67] that in this case the contribution to the asymptotics corresponds to the incident wave. Also we expect “physically” that the higher order $O(\exp(-ikr)/(kr)^{-2})$ term in Lemma 2.11 is in fact equal to zero for $\boldsymbol{\omega} \neq \boldsymbol{\omega}_0$ since the radiation conditions (2.1.5) for the point source problem suggest that there can be no “in going” wave. This can indeed be checked rigorously by considering more terms in the asymptotic expansion of (2.1.47) via the method of stationary phase.

It follows from Lemma 2.11 that the principal contribution to the asymptotics of the diffracted wave comes from $U_\pi(r, \boldsymbol{\omega})$. For certain angles of observation and angles of incidence it occurs that $s = \pi$ is also a singular point of the integrand in $U_\pi(r, \boldsymbol{\omega})$ and it occurs that the diffracted wave denoted by $U_{diff}(r, \boldsymbol{\omega})$ is undefined in these directions. These singular directions are defined as follows:

Definition 2.13. The singular directions are those directions where the tip-diffracted spherical wave front “interacts” with fronts of other component waves e.g. those waves reflected by the surface of the cone or diffracted by a lateral edge (if any exist) of the cone. (These are the directions that coincide with the directions of other wave components of high-frequency representation.) The set of singular directions divides M into two subdomains (this is discussed further in §6.1). The function $\Gamma(\boldsymbol{\omega}, \boldsymbol{\omega}_0, s)$ is known to have singularities at $s = \pi$ precisely for $\boldsymbol{\omega}$ coinciding with the set of singular directions [53].

There is a precise geometrical procedure for identifying the singular directions in e.g. [9, §2.3]. As in [9] we define,

$$\theta_1(\boldsymbol{\omega}, \boldsymbol{\omega}_0) = \min_{\boldsymbol{\omega}' \in \ell} \{ \theta(\boldsymbol{\omega}, \boldsymbol{\omega}') + \theta(\boldsymbol{\omega}', \boldsymbol{\omega}_0) \}. \quad (2.1.49)$$

Then for a “fully illuminated” (i.e. $-\boldsymbol{\omega}_0 \notin M$) smooth convex cone the directions $\boldsymbol{\omega}$ satisfying $\theta_1(\boldsymbol{\omega}, \boldsymbol{\omega}_0) = \pi$, are the singular directions. If the cone Ξ has lateral edges, i.e. the contour ℓ has corners then in addition to the directions $\boldsymbol{\omega}$ such that $\theta_1(\boldsymbol{\omega}, \boldsymbol{\omega}_0) = \pi$ holds, the directions $\boldsymbol{\omega}$ which satisfy $\theta(\boldsymbol{\omega}, \boldsymbol{\omega}_c) + \theta(\boldsymbol{\omega}_c, \boldsymbol{\omega}_0) = \pi$, for some corner point, $\boldsymbol{\omega}_c \in \ell$, are also singular (see Fig. 2-4).

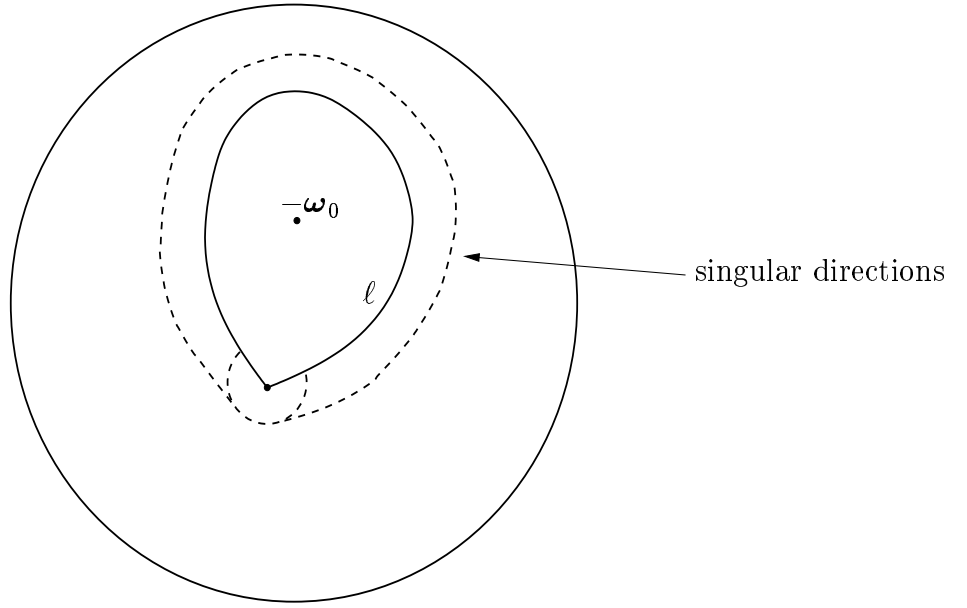


Figure 2-4: Singular directions

Example 2.14. Consider the simple example of the scattering of an axisymmetric incident wave (i.e. a plane wave travelling in the direction of the axis of the cone) by a circular cone of semi-angle $\hat{\theta}$. Then the singular directions are those directions which make an angle of $2\hat{\theta}$ with the axis of the cone.

We get the following result for nonsingular directions $\boldsymbol{\omega}$, [67], [68] and [9].

Lemma 2.15. *For angles of observation $\boldsymbol{\omega}$ which are not singular directions,*

$$U_{diff}(r, \boldsymbol{\omega}) = 2\pi \frac{e^{ikr}}{kr} f(\boldsymbol{\omega}, \boldsymbol{\omega}_0) + O((kr)^{-2}), \quad \text{as } kr \rightarrow \infty, \quad (2.1.50)$$

where $f(\boldsymbol{\omega}, \boldsymbol{\omega}_0) = \Gamma(\boldsymbol{\omega}, \boldsymbol{\omega}_0, \pi)$.

Proof By construction,

$$U_\pi(r, \boldsymbol{\omega}) = e^{i\pi/4} \left(\frac{2\pi}{kr}\right)^{1/2} \int_{\mathcal{W}'} e^{-ikr \cos s} \Gamma(\boldsymbol{\omega}, \boldsymbol{\omega}_0, s) \eta_\pi(s) ds \quad (2.1.51)$$

has only one critical point, namely a stationary point at $s = \pi$. Hence applying the stationary phase technique, e.g. [15, pp. 73-81], we get the following formula,

$$\int_{\mathcal{W}'} e^{-ikr \cos s} \Gamma(\boldsymbol{\omega}, \boldsymbol{\omega}_0, s) ds = \sqrt{2\pi} \frac{e^{-i\pi/4 + ikr}}{\sqrt{kr}} \Gamma(\boldsymbol{\omega}, \boldsymbol{\omega}_0, \pi) + O((kr)^{-3/2}),$$

as $kr \rightarrow \infty$. Therefore from (2.1.51) the asymptotic expansion of the wave

diffracted by the tip of a cone is given by

$$U_{diff}(r, \boldsymbol{\omega}) = 2\pi \frac{e^{ikr}}{kr} \Gamma(\boldsymbol{\omega}, \boldsymbol{\omega}_0, \pi) + O((kr)^{-2}) \quad \text{as } kr \rightarrow \infty, \quad (2.1.52)$$

i.e. (2.1.50). \square

The formula (2.1.50) combined with the integral in (2.1.43) gives a ‘‘Watson’s integral’’ type representation for the diffracted fields. To make the integral occurring in $f(\boldsymbol{\omega}, \boldsymbol{\omega}_0) = \Gamma(\boldsymbol{\omega}, \boldsymbol{\omega}_0, \pi)$ easier to compute we have the following strategy. We can rewrite the Green’s function, $g(\boldsymbol{\omega}, \boldsymbol{\omega}_0, \nu)$, in the form

$$g(\boldsymbol{\omega}, \boldsymbol{\omega}_0, \nu) = g_0(\boldsymbol{\omega}, \boldsymbol{\omega}_0, \nu) + g^{sc}(\boldsymbol{\omega}, \boldsymbol{\omega}_0, \nu) \quad (2.1.53)$$

where g_0 is the Green’s function for the whole sphere S^2 , given by

$$\left(\Delta^* + \nu^2 - \frac{1}{4}\right)g_0(\boldsymbol{\omega}, \boldsymbol{\omega}_0, \nu) = \delta(\boldsymbol{\omega} - \boldsymbol{\omega}_0), \quad (2.1.54)$$

and g^{sc} is the ‘‘reflected’’ part of g due to the boundary ℓ . The Green’s function g_0 is evaluated explicitly as (see e.g. [12])

$$g_0(\boldsymbol{\omega}, \boldsymbol{\omega}_0, \nu) = -\frac{1}{4 \cos(\pi\nu)} P_{\nu-\frac{1}{2}}(-\cos \theta(\boldsymbol{\omega}, \boldsymbol{\omega}_0)) \quad (2.1.55)$$

where P_ν is the Legendre special function with index ν (see e.g. [1, pg. 332]). Therefore substituting (2.1.54) into (2.1.43), the formula for $f(\boldsymbol{\omega}, \boldsymbol{\omega}_0)$ becomes

$$f(\boldsymbol{\omega}, \boldsymbol{\omega}_0) = \frac{i}{\pi} \int_{\gamma_1} e^{-i\pi\nu} g_0(\boldsymbol{\omega}, \boldsymbol{\omega}_0, \nu) \nu \, d\nu + \frac{i}{\pi} \int_{\gamma_1} e^{-i\pi\nu} g^{sc}(\boldsymbol{\omega}, \boldsymbol{\omega}_0, \nu) \nu \, d\nu.$$

Now ‘‘physically’’ the integral with g_0 in the integrand is equivalent to the diffraction coefficient in the case when there is no conical obstacle, since g_0 is the Green’s function on S^2 with no boundary ℓ , hence there is no diffraction and we can expect that its contribution will be zero. This is also shown rigorously in [9, Appendix C]. Therefore the formula for $f(\boldsymbol{\omega}, \boldsymbol{\omega}_0)$ reduces to

$$f(\boldsymbol{\omega}, \boldsymbol{\omega}_0) = \frac{i}{\pi} \int_{\gamma_1} e^{-i\pi\nu} g^{sc}(\boldsymbol{\omega}, \boldsymbol{\omega}_0, \nu) \nu \, d\nu, \quad (2.1.56)$$

The integral in (2.1.56) converges in the distribution sense, see [9, Appendix B] and Definition 2.5. Moreover $f(\boldsymbol{\omega}, \boldsymbol{\omega}_0)$ is a smooth function on M except for the singular directions (see Definition 2.13).

In general the integral in (2.1.56) only converges in the distributional sense

and so cannot be used for the practical computation of diffraction coefficients. However for certain angles of observation the contour of integration γ_1 can be deformed to make the integral in (2.1.56) rapidly convergent in the classical sense (see [67] and [68]), this is discussed in Chapter 6. For the remaining angles of observation (excluding the singular directions) other techniques can be applied to calculate the integral in (2.1.56) (see [9]). This is also discussed in Chapter 6.

Thus, in order to calculate $f(\boldsymbol{\omega}, \boldsymbol{\omega}_0)$, it follows from (2.1.56) that we need to find $g^{sc}(\boldsymbol{\omega}, \boldsymbol{\omega}_0, \nu)$ for $\nu \in \ell$. By substituting (2.1.53) into (2.1.17) and using (2.1.54) we get the boundary value problem for g^{sc} ,

$$\left(\Delta^* + \nu^2 - \frac{1}{4}\right)g^{sc}(\boldsymbol{\omega}, \boldsymbol{\omega}_0, \nu) = 0 \quad \text{for } \boldsymbol{\omega} \in M, \quad (2.1.57)$$

with the boundary conditions given by either

$$\begin{aligned} g^{sc}(\boldsymbol{\omega}, \boldsymbol{\omega}_0, \nu) &= -g_0(\boldsymbol{\omega}, \boldsymbol{\omega}_0, \nu) & \text{for } \boldsymbol{\omega} \in \ell, \\ \text{or } \frac{\partial g^{sc}}{\partial \mathbf{m}}(\boldsymbol{\omega}, \boldsymbol{\omega}_0, \nu) &= -\frac{\partial g_0}{\partial \mathbf{m}}(\boldsymbol{\omega}, \boldsymbol{\omega}_0, \nu) & \text{for } \boldsymbol{\omega} \in \ell. \end{aligned} \quad (2.1.58)$$

We need to be able to solve this boundary value problem not only for many different values of ν , but also many observation points, $\boldsymbol{\omega}$, and angles of incidence $\boldsymbol{\omega}_0$ to be able to calculate diffraction coefficients in different directions. In general there is no explicit solution therefore we need an efficient numerical method to solve (2.1.58). We now move on to the electromagnetic diffraction problem and we will return to problem (2.1.58) in Chapter 3.

2.2 The electromagnetic diffraction problem

In this section we briefly discuss the problem of the scattering of a planar electromagnetic incident wave from an obstacle D following [69]. (The technical details surrounding this problem are contained in Appendix A.) The electromagnetic field satisfies the Maxwell equations

$$\begin{aligned} \text{curl } \mathbf{E}(\mathbf{x}, t) + \mu \frac{\partial \mathbf{H}}{\partial t}(\mathbf{x}, t) &= \mathbf{0}, & \text{div } \mathbf{E}(\mathbf{x}, t) &= 0, \\ \text{curl } \mathbf{H}(\mathbf{x}, t) - \epsilon \frac{\partial \mathbf{E}}{\partial t}(\mathbf{x}, t) &= \mathbf{0}, & \text{div } \mathbf{H}(\mathbf{x}, t) &= 0, \end{aligned} \quad \mathbf{x} \in \mathbb{R}^3, t \in \mathbb{R},$$

where \mathbf{E} is the electric field, \mathbf{H} is the magnetic field, μ is the magnetic permeability and ϵ is the electric permittivity. Seeking time harmonic solutions $\mathbf{E}(\mathbf{x}, t) = \exp(-i\omega t)\mathbf{E}(\mathbf{x})$ and $\mathbf{H}(\mathbf{x}, t) = \exp(-i\omega t)\mathbf{H}(\mathbf{x})\sqrt{\epsilon/\mu}$ we get Maxwell's

equations in the frequency domain which read,

$$\begin{aligned}\operatorname{curl} \mathbf{E}(\mathbf{x}) &= ik\mathbf{H}(\mathbf{x}), \\ \operatorname{curl} \mathbf{H}(\mathbf{x}) &= -ik\mathbf{E}(\mathbf{x}),\end{aligned}\quad \mathbf{x} \in \mathbb{R}^3 \quad (2.2.1)$$

where the wave number $k = \omega\sqrt{\mu\epsilon}$. (Note that the conditions $\operatorname{div} \mathbf{E}(\mathbf{x}) = 0$ and $\operatorname{div} \mathbf{H}(\mathbf{x}) = 0$ follow automatically from (2.2.1).) We consider the field described by (2.2.1) exterior to an obstacle, D . We shall assume the usual perfectly conducting boundary condition, which means that the electric field must have a zero tangential component, i.e.

$$\mathbf{E} \wedge \mathbf{n} \Big|_{\partial D} = \mathbf{0}, \quad (2.2.2)$$

where \mathbf{n} is the exterior normal to ∂D . Again we seek \mathbf{E} and \mathbf{H} in the following form

$$\mathbf{E} = \mathbf{E}_{inc} + \mathbf{E}_{sc}, \quad \mathbf{H} = \mathbf{H}_{inc} + \mathbf{H}_{sc}, \quad (2.2.3)$$

where the subscripts *inc* and *sc* indicate the (given) incident and (to be found) scattered wave respectively.

The electromagnetic field should also satisfy certain radiation, tip and (if they exist) edge conditions (cf. §2.1 for the acoustic case) which ensure uniqueness (see e.g. [55, §1.27]). The radiation conditions (also known as the Silver-Müller conditions) are given by, writing $\mathbf{x} = r\boldsymbol{\omega}$,

$$\begin{aligned}\mathbf{E}_{sc}(\mathbf{x}) &= O(r^{-1}), \quad \mathbf{E}_{sc}(\mathbf{x}) = O(r^{-1}) \quad \text{and} \\ r(\mathbf{E}_{sc}(\mathbf{x}) + \boldsymbol{\omega} \wedge \mathbf{H}_{sc}(\mathbf{x})) &\rightarrow 0, \quad r(\mathbf{H}_{sc}(\mathbf{x}) - \boldsymbol{\omega} \wedge \mathbf{E}_{sc}(\mathbf{x})) \rightarrow 0 \quad \text{as } r \rightarrow \infty.\end{aligned} \quad (2.2.4)$$

(cf. [18, §I.2.4]). To describe the tip and edge condition recall Ω_{loc} defined in (2.1.6). We require that \mathbf{E} and \mathbf{H} satisfy

$$\int_{\Omega_{loc}} (|\mathbf{E}(\mathbf{x})|^2 + |\mathbf{H}(\mathbf{x})|^2) dV(\mathbf{x}) < \infty, \quad (2.2.5)$$

where, writing $\mathbf{E} = (E_1, E_2, E_3)$, $|\mathbf{E}|^2 = |E_1|^2 + |E_2|^2 + |E_3|^2$.

In particular we are interested in solving this problem in the case when the incident wave is planar. That is,

$$\mathbf{E}_{inc}(\mathbf{x}) = e^{-ik\boldsymbol{\omega}_0 \cdot \mathbf{x}} \mathbf{E}^0, \quad \mathbf{H}_{inc}(\mathbf{x}) = e^{-ik\boldsymbol{\omega}_0 \cdot \mathbf{x}} \mathbf{H}^0, \quad (2.2.6)$$

where $-\boldsymbol{\omega}_0$ is a unit vector describing the direction of propagation of the incident wave (as in the acoustic case) and \mathbf{E}^0 and \mathbf{H}^0 are constant unit vectors describing

the directions of \mathbf{E}_{inc} and \mathbf{H}_{inc} respectively. The vectors \mathbf{E}^0 , \mathbf{H}^0 and $-\boldsymbol{\omega}_0$ form an orthogonal right-handed triple and we refer to the directions of \mathbf{E}^0 , \mathbf{H}^0 as the polarisation of the incident wave. (One can easily check that (2.2.6) is a particular solution of (2.2.1).)

Definition 2.16. We define the problem of finding a solution to the Maxwell equations (2.2.1) with the conditions (2.2.2) - (2.2.6) as the (electromagnetic) planar incidence scattering problem.

The problem of interest is to find the asymptotics of the scattered field as $k \rightarrow \infty$. In the same way as for the acoustic problem the scattered wave in this asymptotic regime is expected to consist of different types of “component waves”. Of particular interest is the wave diffracted by a singular conical point. It can be shown using the Geometric Theory of Diffraction (adapted to the electromagnetic case) that \mathbf{E}_{diff} , \mathbf{H}_{diff} the electromagnetic wave diffracted by the singular conical point will take the form (for sufficiently large kr):

$$\left\{ \begin{array}{l} \mathbf{E}_{diff} \\ \mathbf{H}_{diff} \end{array} \right\}(\mathbf{x}) = 2\pi \frac{e^{ikr}}{kr} \left\{ \begin{array}{l} \mathcal{E}(\boldsymbol{\omega}, \boldsymbol{\omega}_0) \\ \mathcal{H}(\boldsymbol{\omega}, \boldsymbol{\omega}_0) \end{array} \right\} + O((kr)^{-2}), \quad (2.2.7)$$

where the *diffraction coefficients* $\mathcal{E}(\boldsymbol{\omega}, \boldsymbol{\omega}_0)$ and $\mathcal{H}(\boldsymbol{\omega}, \boldsymbol{\omega}_0)$ are to be found. In a way analogous to the acoustic case these diffraction coefficients are found by considering the canonical problem of the diffraction of a planar electromagnetic incident wave by the cone Ξ with surface that is tangent to D at the singular conical point (see Fig. 1-1). $\mathcal{E}(\boldsymbol{\omega}, \boldsymbol{\omega}_0)$ and $\mathcal{H}(\boldsymbol{\omega}, \boldsymbol{\omega}_0)$ depend only on the angle of observation $\boldsymbol{\omega}$, the direction and the polarisation of the incident wave and the geometry (cross section) of Ξ . We use braces in (2.2.7) and henceforth for compact writing of a pair of equations.

Following the comments above we therefore consider the canonical problem of scattering by a semi-infinite cone Ξ . It is well known that an electromagnetic field can be expressed in terms of two scalar functions. Therefore, following [69], in order to derive formulae for $\mathcal{E}(\boldsymbol{\omega}, \boldsymbol{\omega}_0)$ and $\mathcal{H}(\boldsymbol{\omega}, \boldsymbol{\omega}_0)$ we seek the electromagnetic field in terms of Debye potentials V and W :

$$\begin{aligned} \mathbf{E}(\mathbf{x}) &= \text{curl curl } (V(\mathbf{x})\mathbf{x}) + ik \text{ curl } (W(\mathbf{x})\mathbf{x}), \\ \mathbf{H}(\mathbf{x}) &= \text{curl curl } (W(\mathbf{x})\mathbf{x}) - ik \text{ curl } (V(\mathbf{x})\mathbf{x}), \end{aligned} \quad \mathbf{x} \in \mathbb{R}^3 \setminus \Xi. \quad (2.2.8)$$

We show in Appendix A that if V and W satisfy the Helmholtz equation

$$(\Delta + k^2)V(\mathbf{x}) = 0, \quad (\Delta + k^2)W(\mathbf{x}) = 0, \quad \text{for } \mathbf{x} \in \mathbb{R}^3 \setminus \Xi, \quad (2.2.9)$$

then \mathbf{E} and \mathbf{H} defined by (2.2.8) will satisfy the Maxwell equations (2.2.1). If, in addition to (2.2.9), V and W satisfy Dirichlet and Neumann boundary conditions respectively,

$$V\Big|_{\partial\Xi} = 0, \quad \frac{\partial W}{\partial \mathbf{n}}\Big|_{\partial\Xi} = 0, \quad (2.2.10)$$

then \mathbf{E} defined by (2.2.8) will also satisfy the perfectly conducting boundary condition (2.2.2).

Therefore we reduce the problem of solving the planar incidence scattering problem (2.2.1) - (2.2.6) to that of finding two scalar functions V and W which satisfy (2.2.9) and (2.2.10). To do this we write V and W in terms of the ‘‘incident part’’ and ‘‘scattered part’’,

$$V = V_{inc} + V_{sc}, \quad W = W_{inc} + W_{sc}. \quad (2.2.11)$$

Now the strategy for finding analytic formulae for \mathbf{E} and \mathbf{H} is as follows, cf. [69]: First we find solutions V_{inc} and W_{inc} satisfying the Helmholtz equations with the property

$$\begin{aligned} \mathbf{E}_{inc}(\mathbf{x}) &= \text{curl curl } (V_{inc}(\mathbf{x})\mathbf{x}) + ik \text{ curl } (W_{inc}(\mathbf{x})\mathbf{x}), \\ \mathbf{H}_{inc}(\mathbf{x}) &= \text{curl curl } (W_{inc}(\mathbf{x})\mathbf{x}) - ik \text{ curl } (V_{inc}(\mathbf{x})\mathbf{x}), \end{aligned}$$

where \mathbf{E}_{inc} and \mathbf{H}_{inc} are given by (2.2.6). Then we solve two scalar scattering problems with the incident waves given by V_{inc} and W_{inc} ,

$$(\Delta + k^2)V_{sc} = 0, \quad V_{sc}\Big|_{\partial\Xi} = -V_{inc}\Big|_{\partial\Xi}, \quad (2.2.12)$$

$$(\Delta + k^2)W_{sc} = 0, \quad \frac{\partial W_{sc}}{\partial \mathbf{n}}\Big|_{\partial\Xi} = -\frac{\partial W_{inc}}{\partial \mathbf{n}}\Big|_{\partial\Xi}. \quad (2.2.13)$$

(V_{sc} and W_{sc} also have to satisfy appropriate ‘‘radiation’’, ‘‘tip’’ and ‘‘edge’’ conditions.) From the solutions to (2.2.12) and (2.2.13) we have formulae for V and W from (2.2.11). These can then be substituted into (2.2.8) to get \mathbf{E} and \mathbf{H} . (Once we have found \mathbf{E} and \mathbf{H} the conditions (2.2.4) and (2.2.5) can be checked. We discuss (2.2.4) in Appendix A but do not concern ourselves with (2.2.5) which can also be shown to hold in a routine way.) In Appendix A we show that by investigating the high-frequency asymptotics of V and W (in a somewhat analogous way as in the acoustic case) we can find formulae for V_{diff} and W_{diff} , the Debye potentials corresponding to the electromagnetic wave diffracted by the conical point, i.e.

$$\begin{aligned} \mathbf{E}_{diff}(\mathbf{x}) &= \text{curl curl } (V_{diff}(\mathbf{x})\mathbf{x}) + ik \text{ curl } (W_{diff}(\mathbf{x})\mathbf{x}), \\ \mathbf{H}_{diff}(\mathbf{x}) &= \text{curl curl } (W_{diff}(\mathbf{x})\mathbf{x}) - ik \text{ curl } (V_{diff}(\mathbf{x})\mathbf{x}). \end{aligned} \quad (2.2.14)$$

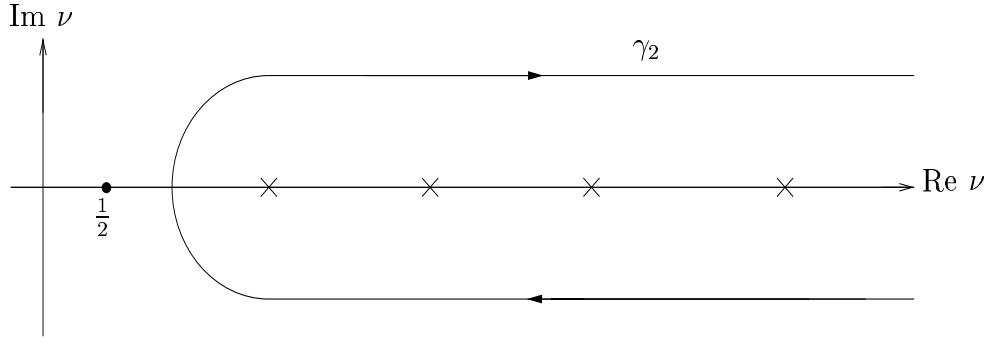


Figure 2-5: Contour of integration γ_2

We show in Appendix A that, writing $\mathbf{x} = (r, \boldsymbol{\omega})$, for $\boldsymbol{\omega}$ away from the singular directions (see Definition 2.13)

$$\left\{ \begin{array}{c} V_{diff} \\ W_{diff} \end{array} \right\} (r, \boldsymbol{\omega}) = 2\pi i \frac{e^{ikr}}{k^2 r} \left\{ \begin{array}{c} f_D \\ f_N \end{array} \right\} (\boldsymbol{\omega}, \boldsymbol{\omega}_0) + O((kr)^{-2}) \quad \text{as } kr \rightarrow \infty, \quad (2.2.15)$$

where for $B = D$ or N , $f_B(\boldsymbol{\omega}, \boldsymbol{\omega}_0)$ are scalar potentials (somewhat analogous to the acoustic diffraction coefficient $f(\boldsymbol{\omega}, \boldsymbol{\omega}_0)$ cf. (2.1.56)) given by

$$f_B(\boldsymbol{\omega}, \boldsymbol{\omega}_0) = \frac{i}{\pi} \int_{\gamma_2} e^{-i\nu\pi} g_B^{sc}(\boldsymbol{\omega}, \boldsymbol{\omega}_0, \nu) \frac{\nu}{\nu^2 - 1/4} d\nu, \quad (2.2.16)$$

holding in the distributional sense (see Appendix A for details). In (2.2.16), γ_2 is a contour of infinite extent in the complex plane (see Fig. 2-5) which crosses the real axis at a point which lies to the left of the internal Dirichlet eigenvalues $\nu_{D,j}$, $j = 1, 2, \dots$, (see Definition 2.4) and the internal Neumann eigenvalues $\nu_{N,j}$, $j = 2, 3, \dots$, (recall that $\nu_{N,1} = 1/2$) which are denoted schematically by crosses in Fig. 2-5. Also in (2.2.16), $g_B^{sc}(\boldsymbol{\omega}, \boldsymbol{\omega}_0, \nu)$ is the solution to the boundary value problem

$$(\Delta^* + \nu^2 - \frac{1}{4}) \left\{ \begin{array}{c} g_D^{sc} \\ g_N^{sc} \end{array} \right\} (\boldsymbol{\omega}, \boldsymbol{\omega}_0, \nu) = 0, \quad \boldsymbol{\omega} \in M, \quad (2.2.17)$$

$$g_D^{sc}|_{\ell} = -g_D^{inc}|_{\ell}, \quad \frac{\partial g_N^{sc}}{\partial \mathbf{m}}|_{\ell} = -\frac{\partial g_N^{inc}}{\partial \mathbf{m}}|_{\ell}. \quad (2.2.18)$$

Here

$$\begin{aligned} g_D^{inc}(\boldsymbol{\omega}, \boldsymbol{\omega}_0, \nu) &= \{ \nabla_{\boldsymbol{\omega}'} g_0(\boldsymbol{\omega}, \boldsymbol{\omega}', \nu) |_{\boldsymbol{\omega}'=\boldsymbol{\omega}_0} \} \cdot \mathbf{E}^0, \\ g_N^{inc}(\boldsymbol{\omega}, \boldsymbol{\omega}_0, \nu) &= \{ \nabla_{\boldsymbol{\omega}'} g_0(\boldsymbol{\omega}, \boldsymbol{\omega}', \nu) |_{\boldsymbol{\omega}'=\boldsymbol{\omega}_0} \} \cdot \mathbf{H}^0, \end{aligned}$$

where $\nabla_{\boldsymbol{\omega}'}$ is the spherical gradient with respect to $\boldsymbol{\omega}'$. (Recall that g_0 is the

Green's function for the whole sphere S^2 , given by (2.1.54)). Substituting (2.2.16) into (2.2.14) we obtain the following formula for \mathbf{E}_{diff} and \mathbf{H}_{diff} (see e.g. [69], [12]):

$$\begin{Bmatrix} \mathbf{E}_{diff} \\ \mathbf{H}_{diff} \end{Bmatrix}(\mathbf{x}) = 2\pi \frac{e^{ikr}}{kr} \begin{Bmatrix} \mathcal{E}(\boldsymbol{\omega}, \boldsymbol{\omega}_0) \\ \mathcal{H}(\boldsymbol{\omega}, \boldsymbol{\omega}_0) \end{Bmatrix} + O((kr)^{-2}), \text{ as } kr \rightarrow \infty, \quad (2.2.19)$$

where

$$\begin{aligned} \mathcal{E}(\boldsymbol{\omega}, \boldsymbol{\omega}_0) &= -\nabla_{\boldsymbol{\omega}} f_D(\boldsymbol{\omega}, \boldsymbol{\omega}_0) - \nabla_{\boldsymbol{\omega}} f_N(\boldsymbol{\omega}, \boldsymbol{\omega}_0) \wedge \boldsymbol{\omega}, \\ \mathcal{H}(\boldsymbol{\omega}, \boldsymbol{\omega}_0) &= -\nabla_{\boldsymbol{\omega}} f_N(\boldsymbol{\omega}, \boldsymbol{\omega}_0) + \nabla_{\boldsymbol{\omega}} f_D(\boldsymbol{\omega}, \boldsymbol{\omega}_0) \wedge \boldsymbol{\omega}. \end{aligned} \quad (2.2.20)$$

It follows from (2.2.20) that the key to calculating the vector diffraction coefficients $\mathcal{E}(\boldsymbol{\omega}, \boldsymbol{\omega}_0)$, $\mathcal{H}(\boldsymbol{\omega}, \boldsymbol{\omega}_0)$ is the computation of the scalar potentials $f_B(\boldsymbol{\omega}, \boldsymbol{\omega}_0)$, $B = D, N$ given by (2.2.16) which in turn requires solving the boundary value problem on the surface of the sphere given by (2.2.17), (2.2.18) (this is discussed in Chapters 3 and 4). Again this needs to be done many times and so we need an efficient numerical method. (Note that it is sufficient to calculate only one of the two vector diffraction coefficients \mathcal{E} and \mathcal{H} since one is a $\pi/2$ rotation of the other as follows from (2.2.20).)

Chapter 3

The Boundary Integral Method

In order to calculate the wave diffracted by a conical point (in both the acoustic and the electromagnetic cases) we need to calculate the solution to a homogeneous partial differential equation on a manifold, M , on the surface of the sphere (cf. (2.1.57), (2.1.58), (2.2.17) and (2.2.18)),

$$(\Delta^* + \nu^2 - 1/4)g^{sc}(\boldsymbol{\omega}, \boldsymbol{\omega}_0, \nu) = 0 \quad \boldsymbol{\omega} \in M, \quad (3.0.1)$$

subject to the boundary condition on ℓ

$$\left. \begin{array}{l} g^{sc}(\boldsymbol{\omega}, \boldsymbol{\omega}_0, \nu) = b_D(\boldsymbol{\omega}), \\ \text{and/or } (\partial g^{sc}/\partial \mathbf{m})(\boldsymbol{\omega}, \boldsymbol{\omega}_0, \nu) = b_N(\boldsymbol{\omega}), \end{array} \right\} \begin{array}{l} \text{the Dirichlet case} \\ \text{the Neumann case} \end{array} \quad \text{for all } \boldsymbol{\omega} \in \ell. \quad (3.0.2)$$

The boundary data for the acoustic problem are given by $b_D(\boldsymbol{\omega}) = -g_0(\boldsymbol{\omega}, \boldsymbol{\omega}_0, \nu)$ or $b_N(\boldsymbol{\omega}) = -(\partial g_0/\partial \mathbf{m})(\boldsymbol{\omega}, \boldsymbol{\omega}_0, \nu)$ and in the electromagnetic setting by $b_D(\boldsymbol{\omega}) = -g_D^{inc}(\boldsymbol{\omega}, \boldsymbol{\omega}_0, \nu)$ or $b_N(\boldsymbol{\omega}) = -(\partial g_D^{inc}/\partial \mathbf{m})(\boldsymbol{\omega}, \boldsymbol{\omega}_0, \nu)$. Also $\partial/\partial \mathbf{m}$ denotes the (outward) normal derivative with respect to $\boldsymbol{\omega} \in \ell$, i.e. differentiation along the sphere in the direction of the unit vector \mathbf{m} . To define \mathbf{m} we introduce the following notation.

Notation 3.1. With each $\boldsymbol{\omega} \in \ell$ we associate a unit normal $\mathbf{m} = \mathbf{m}(\boldsymbol{\omega})$ at $\boldsymbol{\omega} \in \ell$ which lies in the plane tangent to the unit sphere S^2 at $\boldsymbol{\omega}$ and is oriented outward from M . We also associate with $\boldsymbol{\omega}$ the unit tangent to ℓ at $\boldsymbol{\omega}$ denoted by $\mathbf{t} = \mathbf{t}(\boldsymbol{\omega})$, oriented so that $\mathbf{t}(\boldsymbol{\omega})$, $\mathbf{m}(\boldsymbol{\omega})$, $\boldsymbol{\omega}$ form an orthogonal right-handed triple (see Fig 3-1). (We often suppress the dependence on $\boldsymbol{\omega}$ from notation in order to simplify the presentation. To this end we similarly define the unit normal and tangent vectors \mathbf{m}' and \mathbf{t}' associated with a point $\boldsymbol{\omega}'$ in ℓ .)

The problem (3.0.1), (3.0.2) can now be solved by an integral equation method

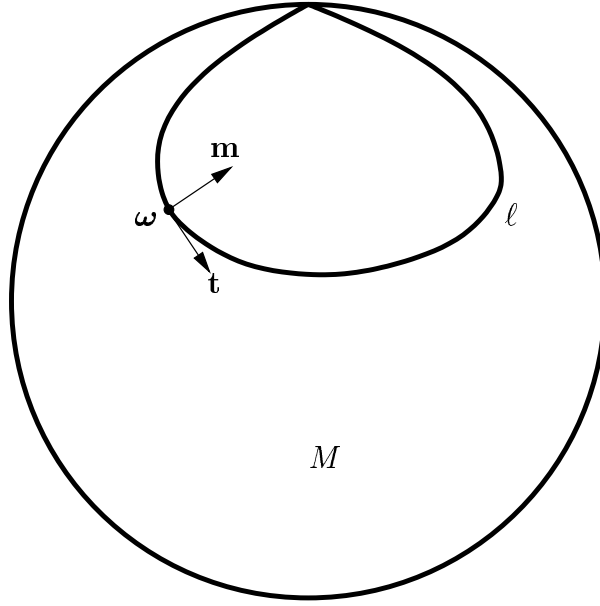


Figure 3-1: ω , \mathbf{m} and \mathbf{t}

on ℓ . In this thesis we consider only the classical indirect method which leads to a second kind equation e.g. [4]. To formulate this integral equation we introduce, for $\omega \in M$ and suitable density ψ , the single and double layer potentials,

$$\begin{aligned}
 (\mathcal{S}\psi)(\omega) &= \int_{\ell} g_0(\omega, \omega', \nu) \psi(\omega') d\omega', \\
 (\mathcal{D}\psi)(\omega) &= \int_{\ell} \frac{\partial g_0}{\partial \mathbf{m}'}(\omega, \omega', \nu) \psi(\omega') d\omega',
 \end{aligned}$$

respectively. Here $\partial/\partial \mathbf{m}'$ denotes the normal derivative outward from M at $\omega' \in \ell$. We also introduce the normal derivatives of these operators (the normal derivative of the double layer potential is also known as the hypersingular operator), for $\omega \in \ell$,

$$\begin{aligned}
 (\mathcal{S}'\psi)(\omega) &= \frac{\partial}{\partial \mathbf{m}}(\mathcal{S}\psi)(\omega) = \int_{\ell} \frac{\partial g_0}{\partial \mathbf{m}}(\omega, \omega', \nu) \psi(\omega') d\omega', \\
 (\mathcal{H}\psi)(\omega) &= \frac{\partial}{\partial \mathbf{m}}(\mathcal{D}\psi)(\omega) = \int_{\ell} \frac{\partial}{\partial \mathbf{m}} \frac{\partial g_0}{\partial \mathbf{m}'}(\omega, \omega', \nu) \psi(\omega') d\omega'.
 \end{aligned}$$

For Dirichlet problems we seek g^{sc} in the form of a double layer potential

$$g^{sc}(\omega, \omega_0, \nu) = \mathcal{D}u(\omega, \nu) = \int_{\ell} \frac{\partial g_0}{\partial \mathbf{m}'}(\omega, \omega', \nu) u(\omega', \nu) d\omega'. \quad (3.0.3)$$

By taking limits as ω tends to the contour ℓ in (3.0.3) and using the Dirichlet boundary condition from (3.0.2), one normally obtains a second-kind integral equation. However, since these integral operators are non-classical we need to verify somehow the jump properties of the double layer potential. For f defined on S^2 and $\omega^* \in \ell$, let $\lim_{\omega \rightarrow \omega_{\pm}^*} f(\omega)$ denote respectively the limit of $f(\omega)$ as $\omega \rightarrow \omega^*$ from the domain M and from the domain $S^2 \setminus \{M \cup \ell\}$. Fortunately the result we need has recently been proved.

Theorem 3.2. *If ω^* is contained in an analytic section of ℓ , then for suitable (see Remark 3.3) ψ defined on ℓ ,*

$$\begin{aligned}
(i) \quad & \lim_{\omega \rightarrow \omega_+^*} (\mathcal{S}\psi)(\omega) = (\mathcal{S}\psi)(\omega^*) = \lim_{\omega \rightarrow \omega_-^*} (\mathcal{S}\psi)(\omega) \\
(ii) \quad & \lim_{\omega \rightarrow \omega_{\pm}^*} (\mathcal{D}\psi)(\omega) = \pm \frac{1}{2} \psi(\omega^*) + (\mathcal{D}\psi)(\omega^*) \\
(iii) \quad & \lim_{\omega \rightarrow \omega_{\pm}^*} (\mathcal{S}'\psi)(\omega) = \mp \frac{1}{2} \psi(\omega^*) + (\mathcal{S}'\psi)(\omega^*) \\
(iv) \quad & \lim_{\omega \rightarrow \omega_+^*} (\mathcal{H}\psi)(\omega) = \lim_{\omega \rightarrow \omega_-^*} (\mathcal{H}\psi)(\omega)
\end{aligned}$$

Here we define, for an arbitrary function v ,

$$\lim_{\omega \rightarrow \omega_{\pm}^*} \frac{\partial v}{\partial \mathbf{m}}(\omega) = \lim_{\substack{h \rightarrow 0 \\ h > 0}} \frac{\partial v(\omega^* \pm h\mathbf{m}(\omega^*))}{\partial \mathbf{m}(\omega^*)}.$$

We do not give the proof but the result can be derived from [32, Theorem 3.6] see also [31]. This result is the analogue of the classical jump conditions for the potential operators associated with the Laplacian in e.g. [25, §2.5].

Remark 3.3. In [32] the relations in Theorem 3.2 are proved for functions ψ in suitable Sobolev spaces and if we wish to interpret them pointwise then we must impose suitable Sobolev regularity on ψ . For example (i), (ii) and (iii) hold pointwise for $\psi \in H^1(\ell)$ since $H^1(\ell) \subset C(\ell)$ whereas (iv) holds pointwise for $\psi \in H^2(\ell)$ since $\mathcal{L} : H^2(\ell) \rightarrow H^1(\ell)$ and $H^1(\ell) \subset C(\ell)$. Thus (i), (ii) and (iii) hold for $\psi \in C^1(\ell)$ and (iv) holds for $\psi \in C^2(\ell)$. These regularity requirements arising from the theory in [32] are sufficient but almost certainly not necessary.

We assume that the density u is C^1 in a neighbourhood of all non-corner points. Then applying the jump conditions in Theorem 3.2(ii) to (3.0.3) and using the Dirichlet boundary condition in (3.0.2), we obtain the second-kind

integral equation:

$$\frac{1}{2}u(\boldsymbol{\omega}, \nu) + \int_{\ell} \frac{\partial g_0}{\partial \mathbf{m}'}(\boldsymbol{\omega}, \boldsymbol{\omega}', \nu) u(\boldsymbol{\omega}', \nu) d\boldsymbol{\omega}' = b_D(\boldsymbol{\omega}), \quad (3.0.4)$$

for all smooth points $\boldsymbol{\omega} \in \ell$ [8]. For corner points the factor $1/2$ will have to be replaced by a factor related to the corner angle, cf. [22], if one wants integral equations which are correct pointwise. However in this thesis we will prove stability and convergence of numerical methods in the L^2 setting, in which case (3.0.4) is a correct representation of the integral equation even when ℓ has (a finite number of) corners.

Note that even though the numerical analysis will be carried out in L^2 , the density in (3.0.4) will always be smooth except at corners so the derivation using Theorem 3.2 is valid. Notice that, since $\boldsymbol{\omega} \in \ell$ and $\boldsymbol{\omega}_0 \in M$, the right-hand side of (3.0.4) is never singular. We can write (3.0.4) (almost everywhere) in operator form as

$$(I + \mathcal{L})u = b, \quad \text{with } (\mathcal{L}u)(\boldsymbol{\omega}) = \int_{\ell} L(\boldsymbol{\omega}, \boldsymbol{\omega}') u(\boldsymbol{\omega}') d\boldsymbol{\omega}', \quad (3.0.5)$$

with $\mathcal{L} = \mathcal{L}_D$ and the data,

$$b(\boldsymbol{\omega}) = b_D(\boldsymbol{\omega}), \quad L(\boldsymbol{\omega}, \boldsymbol{\omega}') = L_D(\boldsymbol{\omega}, \boldsymbol{\omega}') := 2 \frac{\partial g_0}{\partial \mathbf{m}'}(\boldsymbol{\omega}, \boldsymbol{\omega}', \nu). \quad (3.0.6)$$

The unknown density $u(\boldsymbol{\omega}) := u(\boldsymbol{\omega}, \nu)$ and $\boldsymbol{\omega}_0$ and ν are parameters which we suppress from the notation in (3.0.5) for simplicity.

Analogously, the solution to the Neumann problem can be sought using a single layer potential

$$g^{sc}(\boldsymbol{\omega}, \boldsymbol{\omega}_0, \nu) = \mathfrak{S}u(\boldsymbol{\omega}, \nu) = \int_{\ell} g_0(\boldsymbol{\omega}, \boldsymbol{\omega}', \nu) u(\boldsymbol{\omega}', \nu) d\boldsymbol{\omega}'. \quad (3.0.7)$$

We assume again that u is C^1 in a neighbourhood of non-corner points. Taking the normal derivative, using Theorem 3.2 (iii) and fitting the boundary condition leads again to an equation of the form (3.0.5) with $\mathcal{L} = \mathcal{L}_N$,

$$b(\boldsymbol{\omega}) = b_N(\boldsymbol{\omega}), \quad L(\boldsymbol{\omega}, \boldsymbol{\omega}') = L_N(\boldsymbol{\omega}, \boldsymbol{\omega}') := -2 \frac{\partial g_0}{\partial \mathbf{m}}(\boldsymbol{\omega}, \boldsymbol{\omega}', \nu), \quad (3.0.8)$$

and density $u(\boldsymbol{\omega}, \nu)$ again denoted by $u(\boldsymbol{\omega})$.

Although the operators in (3.0.5), with the kernels from (3.0.6) or (3.0.8) are not classical, we will show in this chapter that their properties are analogous to

those of the standard layer potentials for the Helmholtz equation on the boundary of a planar domain.

3.1 Preliminary results

The main aim of this subsection is to identify the principal parts of the kernels L_D and L_N defined in (3.0.6) and (3.0.8). This is done in Theorem 3.6. To prove Theorem 3.6 we need two technical lemmas.

Lemma 3.4. *For $\boldsymbol{\omega}, \boldsymbol{\omega}' \in \ell$,*

$$L_D(\boldsymbol{\omega}, \boldsymbol{\omega}') = \frac{1}{2 \cos(\pi\nu)} P'_{\nu-\frac{1}{2}}(-\cos \theta(\boldsymbol{\omega}, \boldsymbol{\omega}')) \mathbf{t}' \cdot (\boldsymbol{\omega} \wedge \boldsymbol{\omega}') \quad (3.1.1)$$

$$L_N(\boldsymbol{\omega}, \boldsymbol{\omega}') = -\frac{1}{2 \cos(\pi\nu)} P'_{\nu-\frac{1}{2}}(-\cos \theta(\boldsymbol{\omega}, \boldsymbol{\omega}')) \mathbf{t} \cdot (\boldsymbol{\omega}' \wedge \boldsymbol{\omega}) \quad (3.1.2)$$

Proof First note that by employing spherical polar coordinates

$$\boldsymbol{\omega}' = (\sin \theta' \cos \phi', \sin \theta' \sin \phi', \cos \theta')^T.$$

Then for any $v : S^2 \rightarrow \mathbb{R}$, we have the representation

$$\frac{\partial v}{\partial \mathbf{m}'}(\boldsymbol{\omega}') = \nabla_{\boldsymbol{\omega}'} \{v \circ \boldsymbol{\omega}'\} \cdot \mathbf{m}',$$

where $\nabla_{\boldsymbol{\omega}'}$ is the spherical gradient:

$$\nabla_{\boldsymbol{\omega}'} = \frac{1}{\sin \theta'} \mathbf{e}_{\phi'} \frac{\partial}{\partial \phi'} + \mathbf{e}_{\theta'} \frac{\partial}{\partial \theta'}, \quad (3.1.3)$$

with

$$\mathbf{e}_{\phi'} = (-\sin \phi', \cos \phi', 0)^T \quad \text{and} \quad \mathbf{e}_{\theta'} = (\cos \theta' \cos \phi', \cos \theta' \sin \phi', -\sin \theta')^T.$$

Since $\cos \theta(\boldsymbol{\omega}, \boldsymbol{\omega}') = \boldsymbol{\omega} \cdot \boldsymbol{\omega}'$, we have

$$\frac{\partial}{\partial \mathbf{m}'} P'_{\nu-\frac{1}{2}}(-\cos \theta(\boldsymbol{\omega}, \boldsymbol{\omega}')) = -P'_{\nu-\frac{1}{2}}(-\cos \theta(\boldsymbol{\omega}, \boldsymbol{\omega}')) \nabla_{\boldsymbol{\omega}'} \{\boldsymbol{\omega} \cdot \boldsymbol{\omega}'\} \cdot \mathbf{m}'.$$

Now to calculate $\nabla_{\boldsymbol{\omega}'}(\boldsymbol{\omega} \cdot \boldsymbol{\omega}')$ note that,

$$\frac{\partial}{\partial \phi'}(\boldsymbol{\omega} \cdot \boldsymbol{\omega}') = \boldsymbol{\omega} \cdot \left(\frac{\partial}{\partial \phi'} \boldsymbol{\omega}' \right) = \boldsymbol{\omega} \cdot (\sin \theta' \mathbf{e}_{\phi'}),$$

and similarly,

$$\frac{\partial}{\partial \theta'}(\boldsymbol{\omega} \cdot \boldsymbol{\omega}') = \boldsymbol{\omega} \cdot \mathbf{e}_{\theta'}.$$

Therefore it follows from (3.1.3) that $\nabla_{\boldsymbol{\omega}'}(\boldsymbol{\omega} \cdot \boldsymbol{\omega}') = \mathbf{e}_{\phi'}(\mathbf{e}_{\phi'} \cdot \boldsymbol{\omega}) + \mathbf{e}_{\theta'}(\mathbf{e}_{\theta'} \cdot \boldsymbol{\omega})$. Expressing $\boldsymbol{\omega}$ as its decomposition in terms of the orthonormal vectors $\mathbf{e}_{r'} = \boldsymbol{\omega}'$, $\mathbf{e}_{\theta'}$ and $\mathbf{e}_{\phi'}$ it follows that

$$\nabla_{\boldsymbol{\omega}'}(\boldsymbol{\omega} \cdot \boldsymbol{\omega}') = \boldsymbol{\omega} - \boldsymbol{\omega}'(\boldsymbol{\omega} \cdot \boldsymbol{\omega}'). \quad (3.1.4)$$

Thus from (2.1.54) and (3.0.6) and the fact $\boldsymbol{\omega}' \cdot \mathbf{m} = 0$, we have,

$$L_D(\boldsymbol{\omega}, \boldsymbol{\omega}') = \frac{1}{2 \cos(\pi\nu)} P'_{\nu-\frac{1}{2}}(-\cos \theta(\boldsymbol{\omega}, \boldsymbol{\omega}')) \boldsymbol{\omega} \cdot \mathbf{m}'. \quad (3.1.5)$$

Since \mathbf{t}' , \mathbf{m}' and $\boldsymbol{\omega}'$ form a right-handed triple (see Notation 3.1), we have $\mathbf{m}' = \boldsymbol{\omega}' \wedge \mathbf{t}'$, and so

$$L_D(\boldsymbol{\omega}, \boldsymbol{\omega}') = \frac{1}{2 \cos(\pi\nu)} P'_{\nu-\frac{1}{2}}(-\cos \theta(\boldsymbol{\omega}, \boldsymbol{\omega}')) \boldsymbol{\omega} \cdot (\boldsymbol{\omega}' \wedge \mathbf{t}'),$$

which is equivalent to (3.1.1) by cyclic permutation. The proof of (3.1.2) follows easily since $L_N(\boldsymbol{\omega}, \boldsymbol{\omega}') = -L_D(\boldsymbol{\omega}', \boldsymbol{\omega})$. \square

The next lemma identifies the asymptotic behaviour of $P'_{\nu+\frac{1}{2}}(x)$ for x close to -1 . We will combine this with (3.1.1), (3.1.2) to identify the behaviour of L_D and L_N near $\boldsymbol{\omega} = \boldsymbol{\omega}'$.

Lemma 3.5. *For all $k \in \mathbb{C}$, $P_k(x)$ is an analytic function of $x \in (-1, 1)$. Also for $x \in (-3, 1)$,*

$$P_k(x) = a_k(x) \log \left(\frac{1+x}{2} \right) + b_k(x),$$

with $a_k(x)$ and $b_k(x)$ both analytic on $(-3, 1)$. Moreover,

$$a_k(-1) = \frac{\sin(\pi k)}{\pi} \quad \text{and} \quad b_k(-1) = \frac{\sin(\pi k)}{\pi} \{ \psi(k) + \psi(-k-1) + 2\gamma \},$$

where $\psi(k) = -\gamma - \sum_{r=1}^{\infty} (1/(k+r) - 1/r)$ and γ is the Euler constant.

Proof From [1, Equation 8.1.2] we get the following representation of P_k :

$$P_k(x) = F(-k, k+1; 1; \frac{1-x}{2}) \quad (3.1.6)$$

where F is the hypergeometric function. It follows from [1, pg. 556] that

$F(-k, k+1; 1; z)$ has a convergent power series for $-1 \leq z < 1$. Therefore, by (3.1.6), $P_k(x)$ is analytic for $x \in (-1, 3)$ and in particular for $x \in (-1, 1)$. This proves the first statement in the lemma.

Furthermore from [52, Ch V. Eq 53] we have that

$$P_k(x) = a_k(x) \log \left(\frac{1+x}{2} \right) + b_k(x), \quad (3.1.7)$$

where

$$a_k(x) = \frac{\sin(\pi k)}{\pi} F(-k, k+1; 1; (1+x)/2) \quad (3.1.8)$$

and

$$b_k(x) = \frac{\sin(\pi k)}{\pi} \left\{ [\psi(k) + \psi(-k-1) + 2\gamma] F(-k, k+1; 1; (1+x)/2) + \sum_{r=1}^{\infty} B(k, r) \phi(k, r) \left(\frac{1+x}{2} \right)^r \right\}. \quad (3.1.9)$$

Here

$$B(k, r) = \frac{(-k) \dots (-k+r-1)(k+1) \dots (k+r)}{(r!)^2}$$

and

$$\phi(k, r) = \sum_{j=1}^r \left\{ \frac{2k(k+1) + j}{(j^2 - k^2 - k - j)j} \right\}.$$

As remarked above, $F(-k, k+1; 1; (1+x)/2)$ has a convergent power series for $-1 \leq (1+x)/2 < 1$, so $a_k(x)$ is analytic for $x \in (-3, 1)$. Moreover $a_k(-1) = \sin(\pi k)/\pi$ follows from [1, pg. 556]). Turning to b_k , it is clear that the first term on the right-hand side of (3.1.9) is also analytic for $x \in (-3, 1)$ and that the assertions about b_k will then follow provided the domain of convergence of the power series

$$\sum_{r=1}^{\infty} B(k, r) \phi(k, r) \left(\frac{1+x}{2} \right)^r \quad (3.1.10)$$

can be shown to be $(-3, 1)$.

To obtain this result we note that $\lim_{r \rightarrow \infty} \phi(k, r)$ is clearly finite. Now if

$\lim_{r \rightarrow \infty} \phi(k, r) \neq 0$ then it follows that $|\phi(k, r+1)/\phi(k, r)| \rightarrow 1$ as $r \rightarrow \infty$ so,

$$\begin{aligned} \lim_{r \rightarrow \infty} \frac{|B(k, r+1) \phi(k, r+1) (\frac{1+x}{2})^{r+1}|}{|B(k, r) \phi(k, r) (\frac{1+x}{2})^r|} &= \left| \frac{1+x}{2} \right| \lim_{r \rightarrow \infty} \left| \frac{(-k+r)(k+r+1)}{(r+1)^2} \right| \\ &= \left| \frac{1+x}{2} \right|. \end{aligned} \quad (3.1.11)$$

and (3.1.10) is convergent for $x \in (-3, 1)$ by the ratio test. If, on the other hand, $\lim_{r \rightarrow \infty} \phi(k, r) = 0$ then, for large enough r , $|\phi(k, r)| < 1$. Since (3.1.11) also shows that the power series $\sum_{r=1}^{\infty} B(k, r) ((1+x)/2)^r$ converges for $x \in (-3, 1)$, the comparison test then ensures that (3.1.10) also converges for $x \in (-3, 1)$. \square

We now combine Lemmas 3.4 and 3.5 to obtain:

Theorem 3.6. *With the notational conventions 3.1 we have:*

(i) For $\omega, \omega' \in \ell$,

$$L_D(\omega, \omega') = -\frac{\mathbf{t}' \cdot (\omega \wedge \omega')}{\pi |\omega - \omega'|^2} + F_D(\omega, \omega'), \quad (3.1.12)$$

$$L_N(\omega, \omega') = \frac{\mathbf{t} \cdot (\omega' \wedge \omega)}{\pi |\omega - \omega'|^2} + F_N(\omega, \omega'), \quad (3.1.13)$$

where F_D and F_N are bounded functions on $\ell \times \ell$.

(ii) Suppose ω is a fixed non-corner point of ℓ . Then the components

$$\frac{\mathbf{t}' \cdot (\omega \wedge \omega')}{\pi |\omega - \omega'|^2} \quad \text{and} \quad \frac{\mathbf{t} \cdot (\omega' \wedge \omega)}{\pi |\omega - \omega'|^2} \quad (3.1.14)$$

of L_D and L_N are both C^∞ functions of ω' in a neighbourhood of ω and, for $B = D$ or N , the remainder functions F_B satisfy,

$$F_B(\omega, \omega') = O(|\omega - \omega'|^2 \log |\omega - \omega'|), \quad \text{as } \omega' \rightarrow \omega. \quad (3.1.15)$$

Proof We give the proof for L_D , the argument for L_N is analogous.

(i) First suppose that $0 \leq \theta(\omega, \omega') \leq \pi - \delta$ for some $0 < \delta < \pi/2$. From Lemma 3.5 with $k = \nu - 1/2$, we have, for $x \in (-1, 1)$,

$$P'_{\nu-1/2}(x) = \frac{-\cos(\pi\nu)}{\pi} \left\{ \frac{1}{x+1} \right\} + r(x) \quad (3.1.16)$$

where

$$r(x) = \frac{a_{\nu-1/2}(x) - a_{\nu-1/2}(-1)}{x - (-1)} + a'_{\nu-1/2}(x) \log \left(\frac{x+1}{2} \right) + b'_{\nu-1/2}(x). \quad (3.1.17)$$

Also note that, since $\boldsymbol{\omega}, \boldsymbol{\omega}' \in S^2$, we have

$$-\cos \theta(\boldsymbol{\omega}, \boldsymbol{\omega}') + 1 = -\boldsymbol{\omega} \cdot \boldsymbol{\omega}' + 1 = \frac{1}{2} |\boldsymbol{\omega} - \boldsymbol{\omega}'|^2 . \quad (3.1.18)$$

Hence

$$P'_{\nu-\frac{1}{2}}(-\cos \theta(\boldsymbol{\omega}, \boldsymbol{\omega}')) = -\frac{2 \cos(\pi\nu)}{\pi |\boldsymbol{\omega} - \boldsymbol{\omega}'|^2} + r(-1 + |\boldsymbol{\omega} - \boldsymbol{\omega}'|^2/2). \quad (3.1.19)$$

Therefore combining the first result in Lemma 3.4 with (3.1.17) and (3.1.19), we obtain (3.1.12) where

$$F_D(\boldsymbol{\omega}, \boldsymbol{\omega}') = \frac{1}{2 \cos(\pi\nu)} r(-1 + |\boldsymbol{\omega} - \boldsymbol{\omega}'|^2/2) \mathbf{t}' \cdot (\boldsymbol{\omega} \wedge \boldsymbol{\omega}') . \quad (3.1.20)$$

To complete the proof of (i) for the case $0 \leq \theta(\boldsymbol{\omega}, \boldsymbol{\omega}') \leq \pi - \delta$ we show that F_D is bounded on $\ell \times \ell$. Substituting (3.1.17) into (3.1.20) we obtain

$$\begin{aligned} & 2 \cos(\pi\nu) F_D(\boldsymbol{\omega}, \boldsymbol{\omega}') = \\ & \mathbf{t}' \cdot (\boldsymbol{\omega} \wedge \boldsymbol{\omega}') \left\{ \frac{a_{\nu-\frac{1}{2}}(-1 + |\boldsymbol{\omega} - \boldsymbol{\omega}'|^2/2) - a_{\nu-\frac{1}{2}}(-1)}{|\boldsymbol{\omega} - \boldsymbol{\omega}'|^2/2} + b'_{\nu-\frac{1}{2}}(-1 + |\boldsymbol{\omega} - \boldsymbol{\omega}'|^2/2) \right\} \end{aligned} \quad (3.1.21)$$

$$+ a'_{\nu-\frac{1}{2}}(-1 + |\boldsymbol{\omega} - \boldsymbol{\omega}'|^2/2) \{ \mathbf{t}' \cdot (\boldsymbol{\omega} \wedge \boldsymbol{\omega}') \log(|\boldsymbol{\omega} - \boldsymbol{\omega}'|^2/4) \} . \quad (3.1.22)$$

To obtain the desired result for F_D , recall from Lemma 3.5 that $a_{\nu-\frac{1}{2}}$ and $b'_{\nu-\frac{1}{2}}$ are both analytic on $(-3, 1)$. Also note that $0 \leq \theta(\boldsymbol{\omega}, \boldsymbol{\omega}') \leq \pi - \delta$ implies that there exists $\epsilon > 0$ such that $-1 \leq -\cos \theta(\boldsymbol{\omega}, \boldsymbol{\omega}') \leq 1 - \epsilon$, . Hence, it follows from (3.1.18) that

$$-1 \leq -1 + |\boldsymbol{\omega} - \boldsymbol{\omega}'|^2/2 \leq 1 - \epsilon. \quad (3.1.23)$$

Since $|\boldsymbol{\omega} - \boldsymbol{\omega}'|^2$ is a smooth function of $\boldsymbol{\omega}, \boldsymbol{\omega}'$, it follows that the terms inside the braces in (3.1.21) are smooth functions of $\boldsymbol{\omega}, \boldsymbol{\omega}' \in \ell$. Moreover

$$\begin{aligned} |\mathbf{t}' \cdot (\boldsymbol{\omega} \wedge \boldsymbol{\omega}')| & \leq |\mathbf{t}'| |\boldsymbol{\omega} \wedge \boldsymbol{\omega}'| = \sin \theta(\boldsymbol{\omega}, \boldsymbol{\omega}') = \{1 - \cos^2 \theta(\boldsymbol{\omega}, \boldsymbol{\omega}')\}^{1/2} \\ & = \{1 - (\boldsymbol{\omega} \cdot \boldsymbol{\omega}')^2\}^{1/2} = \{(1 - \boldsymbol{\omega} \cdot \boldsymbol{\omega}')(1 + \boldsymbol{\omega} \cdot \boldsymbol{\omega}')\}^{1/2} \\ & = \{((\boldsymbol{\omega} - \boldsymbol{\omega}') \cdot (\boldsymbol{\omega} - \boldsymbol{\omega}')/2)((\boldsymbol{\omega} + \boldsymbol{\omega}') \cdot (\boldsymbol{\omega} + \boldsymbol{\omega}')/2)\}^{1/2} \\ & = \frac{1}{2} |\boldsymbol{\omega} - \boldsymbol{\omega}'| |\boldsymbol{\omega} + \boldsymbol{\omega}'|. \end{aligned} \quad (3.1.24)$$

which ensures the boundedness of (3.1.21). The boundedness of (3.1.22) follows in a similar way, using the above remarks and the analyticity of $a'_{\nu-\frac{1}{2}}$ on $(-3, 1)$.

To complete the proof of (i) we now consider the case $\pi - \delta \leq \theta(\boldsymbol{\omega}, \boldsymbol{\omega}') \leq \pi$. For this case recall from (3.1.6) that $P_{\nu-1/2}(x)$ is analytic for $x \in (-1, 3)$. Therefore (3.1.1) implies that $L_D(\boldsymbol{\omega}, \boldsymbol{\omega}')$ is bounded for $\pi - \delta \leq \theta(\boldsymbol{\omega}, \boldsymbol{\omega}') \leq \pi$. Thus setting

$$F_D(\boldsymbol{\omega}, \boldsymbol{\omega}') = L_D(\boldsymbol{\omega}, \boldsymbol{\omega}') + \frac{\mathbf{t}' \cdot (\boldsymbol{\omega} \wedge \boldsymbol{\omega}')}{\pi |\boldsymbol{\omega} - \boldsymbol{\omega}'|^2}$$

ensures that the representation (3.1.12) holds and $F_D(\boldsymbol{\omega}, \boldsymbol{\omega}')$ is bounded.

(ii) Now suppose that $\boldsymbol{\omega}$ is not a corner point and that $\boldsymbol{\omega}'$ is sufficiently close to $\boldsymbol{\omega}$ so as to ensure that there is no corner point between $\boldsymbol{\omega}$ and $\boldsymbol{\omega}'$ on ℓ . Also suppose that 2Λ is the length of ℓ and let $\boldsymbol{\rho}$ denote an arclength parameterisation of ℓ from any fixed reference point oriented so that $\boldsymbol{\rho}(s)$ travels around ℓ with M on the right-hand side (as indicated by the arrow in Fig. 3-2) as s travels from $-\Lambda$ to Λ . Set $\boldsymbol{\omega} = \boldsymbol{\rho}(s)$ then it follows that the unit tangent \mathbf{t} at $\boldsymbol{\omega}$ is given by $\mathbf{t} = \boldsymbol{\rho}_s(s)$, the derivative of $\boldsymbol{\rho}(s)$. So for $\boldsymbol{\omega}'$ near $\boldsymbol{\omega}$ with $\boldsymbol{\omega}' = \boldsymbol{\rho}(\sigma)$, we have

$$|\boldsymbol{\omega} - \boldsymbol{\omega}'|/|s - \sigma| = O(1) \quad \text{and} \quad |s - \sigma|/|\boldsymbol{\omega} - \boldsymbol{\omega}'| = O(1) \quad \text{as } \sigma \rightarrow s. \quad (3.1.25)$$

Also,

$$\boldsymbol{\omega} \wedge \boldsymbol{\omega}' = \boldsymbol{\rho}(s) \wedge \boldsymbol{\rho}(\sigma) = (\boldsymbol{\rho}(s) - \boldsymbol{\rho}(\sigma)) \wedge \boldsymbol{\rho}(\sigma).$$

Hence

$$\mathbf{t}' \cdot (\boldsymbol{\omega} \wedge \boldsymbol{\omega}') = \boldsymbol{\rho}_s(\sigma) \cdot ((\boldsymbol{\rho}(s) - \boldsymbol{\rho}(\sigma)) - (s - \sigma)\boldsymbol{\rho}_s(\sigma)) \wedge \boldsymbol{\rho}(\sigma)). \quad (3.1.26)$$

Since $|\boldsymbol{\omega} - \boldsymbol{\omega}'|^2 = (\boldsymbol{\rho}(s) - \boldsymbol{\rho}(\sigma)) \cdot (\boldsymbol{\rho}(s) - \boldsymbol{\rho}(\sigma))$, it follows from Taylor's Theorem that (3.1.14) are smooth functions as $\sigma \rightarrow s$ (i.e. $\boldsymbol{\omega}' \rightarrow \boldsymbol{\omega}$). Moreover (3.1.25) and (3.1.26) imply that $|\mathbf{t}' \cdot (\boldsymbol{\omega} \wedge \boldsymbol{\omega}')| = O(|\boldsymbol{\omega} - \boldsymbol{\omega}'|^2)$ as $\boldsymbol{\omega} \rightarrow \boldsymbol{\omega}'$, and so (3.1.15) follows from (3.1.22), completing the proof of the theorem. \square

To prepare for the following results we rewrite (3.0.5) on $[-\Lambda, \Lambda]$ via the arclength parameterisation, $\boldsymbol{\rho}$, introduced in the proof of Theorem 3.6(ii). We rewrite (3.0.5) on $[-\Lambda, \Lambda]$ by putting $\boldsymbol{\omega} = \boldsymbol{\rho}(s)$ and $\boldsymbol{\omega}' = \boldsymbol{\rho}(\sigma)$. Thus we obtain

$$(I + \widehat{\mathcal{L}}_B)\widehat{u} = \widehat{b}_B, \quad \text{with} \quad (\widehat{\mathcal{L}}_B\widehat{u})(s) = \int_{-\Lambda}^{\Lambda} \widehat{L}_B(s, \sigma)\widehat{u}(\sigma)d\sigma, \quad s \in [-\Lambda, \Lambda], \quad B = D, N, \quad (3.1.27)$$

where $\widehat{u}(s) = u(\boldsymbol{\rho}(s))$. In the case of Dirichlet boundary data, using (3.0.6) and

Lemma 3.4 we have $B = D$ and

$$\begin{aligned}\widehat{b}_D(s) &:= -2g_0(\boldsymbol{\rho}(s), \boldsymbol{\omega}_0, \nu) \quad \text{and} \\ \widehat{L}_D(s, \sigma) &:= \frac{1}{2 \cos(\pi\nu)} P'_{\nu-\frac{1}{2}}(-\cos \theta(\boldsymbol{\rho}(s), \boldsymbol{\rho}(\sigma))) \boldsymbol{\rho}_s(\sigma) \cdot (\boldsymbol{\rho}(s) \wedge \boldsymbol{\rho}(\sigma)).\end{aligned}\quad (3.1.28)$$

(Note that since $\boldsymbol{\rho}$ is the arclength parameterisation, the Jacobian does not appear explicitly in the kernel since it satisfies $|\boldsymbol{\rho}_s(\sigma)| = 1$.) For Neumann boundary data, using (3.0.8) and Lemma 3.4 we obtain (3.1.27) with $B = N$ and

$$\begin{aligned}\widehat{b}_N(s) &:= 2 \frac{\partial g_0}{\partial \mathbf{m}(s)}(\boldsymbol{\rho}(s), \boldsymbol{\omega}_0, \nu) \quad \text{and} \\ \widehat{L}_N(s, \sigma) &:= -\frac{1}{2 \cos(\pi\nu)} P'_{\nu-\frac{1}{2}}(-\cos \theta(\boldsymbol{\rho}(s), \boldsymbol{\rho}(\sigma))) \boldsymbol{\rho}_s(s) \cdot (\boldsymbol{\rho}(\sigma) \wedge \boldsymbol{\rho}(s)),\end{aligned}\quad (3.1.29)$$

where $\mathbf{m}(s)$ is the corresponding normal to ℓ at $\boldsymbol{\rho}(s)$.

The remainder of this chapter is devoted to the analysis of the equation (3.1.27) in the space $L^2[-\Lambda, \Lambda]$ equipped with the norm

$$\|v\|_{L^2[-\Lambda, \Lambda]} = \left\{ \int_{-\Lambda}^{\Lambda} |v(\sigma)|^2 d\sigma \right\}^{1/2}.$$

This allows us to include both the Neumann and Dirichlet problems, whether ℓ has corners or not in a unified setting. (There is a corresponding theory in the space $L^\infty[-\Lambda, \Lambda]$ which applies to the Dirichlet problem for corner domains but not to the Neumann problem. Of course, for smooth ℓ , analysis in any standard space is possible; but the corner case is one of the goals of this work.)

The case when ℓ has corners will be considered in earnest in the next section. But first we consider the simpler case of smooth ℓ . The well-posedness of (3.1.27) is established in the next result.

Theorem 3.7. *For $B = D$ or N , suppose that ℓ is \mathcal{C}^∞ and that the homogeneous version of (3.1.27) has only the trivial solution, i.e.*

$$(I + \widehat{\mathcal{L}}_B)\widehat{u} = 0 \Rightarrow \widehat{u} = 0, \quad \text{for } \widehat{u} \in L^2[-\Lambda, \Lambda], \quad (3.1.30)$$

then $I + \widehat{\mathcal{L}}_B$ is invertible on $L^2[-\Lambda, \Lambda]$ and (3.1.27) has a unique solution for all $\widehat{b}_B \in L^2[-\Lambda, \Lambda]$.

Proof To prove this theorem we need only show that $\widehat{\mathcal{L}}_B$ is a compact operator on $L^2[-\Lambda, \Lambda]$ and then the result is a consequence of the Fredholm alternative. Compactness of $\widehat{\mathcal{L}}_B$ follows from Theorem 3.6, which implies that, for $B = D$ or

$N, L_B(\boldsymbol{\omega}, \boldsymbol{\omega}_0)$ are bounded on $\ell \times \ell$. Hence we have from (3.1.28) and (3.1.29) that $\widehat{L}_B(s, \sigma)$ is bounded on $[-\Lambda, \Lambda] \times [-\Lambda, \Lambda]$. Therefore $\widehat{\mathcal{L}}_B$ is a compact operator (see e.g. [58, pg. 326]). Thus the result follows from the Fredholm alternative. \square

In the final result of this section we establish the hypothesis (3.1.30) of Theorem 3.7. The result is given in Theorem 3.8. Its proof is essentially a reworking of the classical argument from standard planar potential theory to the spherical case. The key to the argument are the jump relations in Theorem 3.2.

Theorem 3.8. (i) *Suppose that ν is not an external Dirichlet eigenvalue nor an internal Neumann eigenvalue (see Definition 2.4). Also suppose that*

$$(I + \widehat{\mathcal{L}}_D)\widehat{u} = 0 \quad \text{for some } \widehat{u} \in L^2[-\Lambda, \Lambda]. \quad (3.1.31)$$

Then $\widehat{u}(s) = 0$, for all $s \in [-\Lambda, \Lambda]$.

(ii) *Suppose that ν is not an external Neumann eigenvalue nor an internal Dirichlet eigenvalue. Also suppose that*

$$(I + \widehat{\mathcal{L}}_N)\widehat{u} = 0 \quad \text{for some } \widehat{u} \in L^2[-\Lambda, \Lambda].$$

Then $\widehat{u}(s) = 0$, for all $s \in [-\Lambda, \Lambda]$.

Proof (i) If (3.1.31) holds then by the inverse of the transformation which took (3.0.5) to (3.1.27), we have,

$$(I + \mathcal{L}_D)u = 0 \quad (3.1.32)$$

where $u(\boldsymbol{\omega}) = \widehat{u}(\boldsymbol{\rho}^{-1}(\boldsymbol{\omega}))$. Now consider the double layer potential

$$U(\boldsymbol{\omega}) = (\mathcal{D}u)(\boldsymbol{\omega}), \quad \boldsymbol{\omega} \in S^2. \quad (3.1.33)$$

It is clear that U solves the PDE $(\Delta^* + \nu^2 - 1/4)U(\boldsymbol{\omega}) = 0$ for $\boldsymbol{\omega} \in M \cup M'$, where $M' = S^2 \setminus \{M \cup \ell\}$. Moreover taking the limit of $U(\boldsymbol{\omega})$ as $\boldsymbol{\omega} \rightarrow \boldsymbol{\omega}^* \in \ell$, we have as a consequence of Theorem 3.2(ii) and (3.1.32) that,

$$\lim_{\boldsymbol{\omega} \rightarrow \boldsymbol{\omega}_+^*} U(\boldsymbol{\omega}) = \frac{1}{2}u(\boldsymbol{\omega}^*) + (\mathcal{D}u)(\boldsymbol{\omega}^*) = \frac{1}{2}(I + \mathcal{L}_D)u(\boldsymbol{\omega}^*) = 0. \quad (3.1.34)$$

Thus U solves the boundary value problem

$$\begin{aligned} (\Delta^* + \nu^2 - 1/4)U(\boldsymbol{\omega}) &= 0 & \boldsymbol{\omega} \in M, \\ U(\boldsymbol{\omega}) &= 0 & \boldsymbol{\omega} \in \ell. \end{aligned}$$

It follows, since we have assumed ν does not coincide with any exterior Dirichlet eigenvalues, that $U \equiv 0$ in M and so

$$\lim_{\boldsymbol{\omega} \rightarrow \boldsymbol{\omega}_+^*} \left(\frac{\partial}{\partial \mathbf{m}} U(\boldsymbol{\omega}) \right) = 0.$$

Hence it follows from Theorem 3.2(iv) that

$$\lim_{\boldsymbol{\omega} \rightarrow \boldsymbol{\omega}_-^*} \left(\frac{\partial}{\partial \mathbf{m}} U(\boldsymbol{\omega}) \right) = 0,$$

so U is a solution to the homogeneous interior Neumann problem therefore arguing again this time using the assumption that ν is not an interior Neumann eigenvalue it follows that $U \equiv 0$ in M' and so using Theorem 3.2(ii) we find that $u(\boldsymbol{\omega}^*) = \lim_{\boldsymbol{\omega} \rightarrow \boldsymbol{\omega}_+^*} U(\boldsymbol{\omega}) - \lim_{\boldsymbol{\omega} \rightarrow \boldsymbol{\omega}_-^*} U(\boldsymbol{\omega}) = 0$ and this implies the result. (The whole argument can be cast in an appropriate Sobolev space, see Remark 3.3.)

(ii) This is proved in an analogous way to (i) interchanging the roles of Dirichlet and Neumann eigenvalues and single and double layer potentials. \square

Recall that in general ℓ is composed of smooth curves on S^2 , joined at a finite number (which may be 0) of corners (see Notation 2.2). We expect that when ℓ does contain corners then Theorem 3.8 will still be true. The proof of this result is beyond the scope of this thesis. Its counterpart on planar polygonal domains is well known [27]. For this reason we will assume in the next section that Theorem 3.8 remains true when ℓ contains corners.

When ℓ does contain a corner, compactness of $\widehat{\mathcal{L}}_B$ is lost and the proof of Theorem 3.7 fails, so another approach is needed to prove the well-posedness of (3.1.27). The approach we will use in the following subsection is to compare the integral operator $\widehat{\mathcal{L}}_B$ with a corresponding plane Laplace integral operator $\widehat{\mathcal{K}}_B$ and then use well-posedness results which are known for the planar Laplace problem.

3.2 Relation to the planar Laplace case

To simplify the presentation, we assume that the contour ℓ has one corner which we will denote by the point $\boldsymbol{\omega}_c \in S^2$. The case of several corners is obtained analogously. Without loss of generality, we assume $\boldsymbol{\omega}_c = (0, 0, 1)^T$.

Let $\boldsymbol{\rho}$ denote the arclength parameterisation of ℓ defined above along with the additional property that $\boldsymbol{\rho}(0) = \boldsymbol{\omega}_c$. Then we can introduce the “wedge” w in the tangent plane to S^2 at $\boldsymbol{\omega}_c$ as follows.

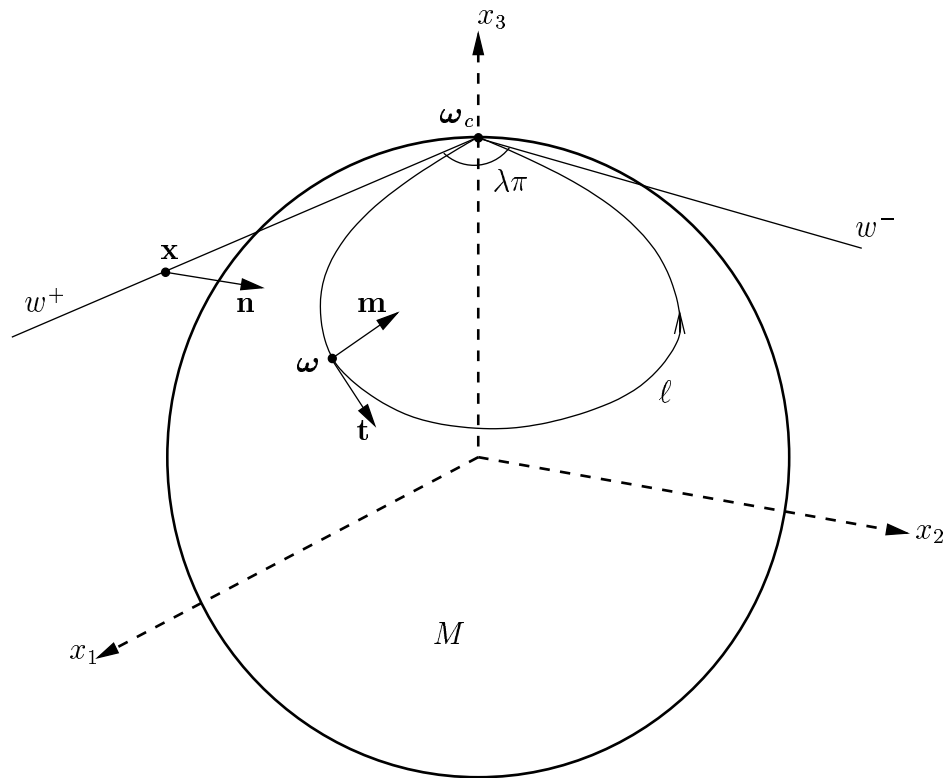


Figure 3-2: Wedge w and contour ℓ

Definition 3.9. The wedge w is defined to be the union of two straight line segments:

$$w = w^- \cup w^+,$$

$$w^- = \{(0, 0, 1)^T + s\mathbf{t}_c^- : s \in [-\Lambda, 0]\}, \quad w^+ = \{(0, 0, 1)^T + s\mathbf{t}_c^+ : s \in [0, \Lambda]\},$$

and $\mathbf{t}_c^\pm = \lim_{s \rightarrow 0^\pm} \boldsymbol{\rho}_s(s)$ (see Fig 3-2). The angle between the tangents \mathbf{t}_c^+ and $-\mathbf{t}_c^-$ is measured “anticlockwise” about the x_3 axis (when viewed from outside the sphere) from w^+ to w^- and is denoted $\lambda\pi$, where $\lambda \in (0, 2) \setminus \{1\}$. Without loss of generality we choose our coordinate system so that \mathbf{t}_c^+ is in the direction of the x_1 axis. Each $\mathbf{x} = s\mathbf{t}_c^\pm \in w^\pm$ can be associated with a unique $\boldsymbol{\omega} = \boldsymbol{\rho}(s) \in \ell$, and with a unit normal \mathbf{m} at $\boldsymbol{\omega} \in \ell$ oriented outward from M . To \mathbf{x} we associate a unit normal \mathbf{n} to w in the plane tangent to S^2 at $\boldsymbol{\omega}_c$, oriented so that $\mathbf{n} \cdot \mathbf{m} \rightarrow 1$ as $s \rightarrow 0$. (See also Fig 3-2.)

The fundamental solution of Laplace’s equation on the plane is given by

$(1/2\pi) \log |\mathbf{x} - \mathbf{x}'|$. Using this we introduce the operators

$$(\mathcal{K}_B u)(\mathbf{x}) = \int_w K_B(\mathbf{x}, \mathbf{x}') u(\mathbf{x}') d\mathbf{x}' \quad B = D, N$$

Analogously to (3.0.6), (3.0.8), the Dirichlet and Neumann kernels are

$$K_D(\mathbf{x}, \mathbf{x}') := \frac{1}{\pi} \frac{\partial}{\partial \mathbf{n}'} \{ \log |\mathbf{x} - \mathbf{x}'| \} = -\frac{(\mathbf{x} - \mathbf{x}') \cdot \mathbf{n}'}{\pi |\mathbf{x} - \mathbf{x}'|^2} \quad (3.2.1)$$

$$K_N(\mathbf{x}, \mathbf{x}') := -\frac{1}{\pi} \frac{\partial}{\partial \mathbf{n}} \{ \log |\mathbf{x} - \mathbf{x}'| \} = -\frac{(\mathbf{x} - \mathbf{x}') \cdot \mathbf{n}}{\pi |\mathbf{x} - \mathbf{x}'|^2}. \quad (3.2.2)$$

Here \mathbf{n}, \mathbf{n}' are unit normals to w at $\mathbf{x}, \mathbf{x}' \in w$ respectively, as described in Definition 3.9.

Theorem 3.10 will show that the principal singularity of L_B near $\boldsymbol{\omega} = \boldsymbol{\omega}' = \boldsymbol{\omega}_c$ is the same as K_B near $\mathbf{x} = \mathbf{x}' = \boldsymbol{\omega}_c$. This is useful because the properties of the integral operator \mathcal{K}_B with kernel K_B are well-understood [27], [22], [38] [5].

If we denote the arclength parameterisation of the wedge w by \mathbf{r} , with

$$\mathbf{r}(-\Lambda) = (0, 0, 1)^T - \Lambda \mathbf{t}_c^-, \quad \mathbf{r}(0) = \boldsymbol{\omega}_c, \quad \text{and} \quad \mathbf{r}(\Lambda) = (0, 0, 1)^T + \Lambda \mathbf{t}_c^+,$$

then, analogously to (3.1.27), we can rewrite \mathcal{K} as an operator

$$(\widehat{\mathcal{K}}\widehat{u})(s) = \int_{-\Lambda}^{\Lambda} \widehat{K}(s, \sigma) \widehat{u}(\sigma) d\sigma \quad s \in [-\Lambda, \Lambda]$$

where from (3.2.1) and (3.2.2),

$$\widehat{K}_D(s, \sigma) := -\frac{(\mathbf{r}(s) - \mathbf{r}(\sigma)) \cdot \mathbf{n}(\sigma)}{\pi |\mathbf{r}(s) - \mathbf{r}(\sigma)|^2}, \quad (3.2.3)$$

$$\widehat{K}_N(s, \sigma) := -\frac{(\mathbf{r}(s) - \mathbf{r}(\sigma)) \cdot \mathbf{n}(s)}{\pi |\mathbf{r}(s) - \mathbf{r}(\sigma)|^2}, \quad (3.2.4)$$

for the Dirichlet and Neumann problems respectively. Here $\mathbf{n}(\sigma)$ is the normal to w at $\mathbf{x} = \mathbf{r}(\sigma)$. The following theorem shows that \widehat{K}_B contains the principal singularity of \widehat{L}_B near the corner point $s = \sigma = 0$ in both the Dirichlet and Neumann cases, $B = D, N$.

Theorem 3.10. *Let $B = D$ or N . Then for $(s, \sigma) \in [-\Lambda, \Lambda] \times [-\Lambda, \Lambda]$, $\widehat{L}_B(s, \sigma) - \widehat{K}_B(s, \sigma)$ is a bounded function.*

Proof We give the proof for the case $B = D$. The proof for the case $B = N$ is analogous. First we consider the kernel \widehat{K}_D . From Definition 3.9 the parametric

equation, \mathbf{r} , for w , is given by

$$\mathbf{r}(\sigma) = \begin{cases} (-\sigma \cos(\lambda\pi), -\sigma \sin(\lambda\pi), 1)^T, & \sigma \in [-\Lambda, 0] \\ (\sigma, 0, 1)^T, & \sigma \in [0, \Lambda]. \end{cases} \quad (3.2.5)$$

Notice that if $-\Lambda \leq s, \sigma \leq 0$ or $0 \leq s, \sigma \leq \Lambda$ then $\mathbf{r}(s)$ and $\mathbf{r}(\sigma)$ lie on the same arm of w and so it follows from (3.2.3) that $\widehat{K}_D(s, \sigma) = 0$ and, by Theorem 3.6(ii), $\widehat{L}_D(s, \sigma)$ is bounded. So we have to consider only the case when s and σ are on different sides of 0.

First consider the case $-\Lambda \leq s \leq 0 \leq \sigma \leq \Lambda$. Then (3.2.5) implies that $\mathbf{r}(s) - \mathbf{r}(\sigma) = (-s \cos(\lambda\pi) - \sigma, -s \sin(\lambda\pi), 0)^T$ and $\mathbf{n}(\sigma) = (0, 1, 0)^T$. Therefore

$$(\mathbf{r}(s) - \mathbf{r}(\sigma)) \cdot \mathbf{n}(\sigma) = -s \sin(\lambda\pi) \quad \text{and} \quad |\mathbf{r}(s) - \mathbf{r}(\sigma)|^2 = s^2 + 2s\sigma \cos(\lambda\pi) + \sigma^2.$$

So from (3.2.3),

$$\widehat{K}_D(s, \sigma) = \frac{1}{\pi} \frac{s \sin(\lambda\pi)}{(s^2 + 2s\sigma \cos(\lambda\pi) + \sigma^2)}, \quad -\Lambda \leq s \leq 0 \leq \sigma \leq \Lambda. \quad (3.2.6)$$

A similar calculation shows analogously that

$$\widehat{K}_D(s, \sigma) = -\frac{1}{\pi} \frac{s \sin(\lambda\pi)}{(s^2 + 2s\sigma \cos(\lambda\pi) + \sigma^2)}, \quad -\Lambda \leq \sigma \leq 0 \leq s \leq \Lambda, \quad (3.2.7)$$

which is a result we need later, in Theorem 3.14.

Now we turn our attention to the kernel, $\widehat{L}_D(s, \sigma)$. Using Taylor's theorem we can write the parameterisation $\boldsymbol{\rho}$ as,

$$\boldsymbol{\rho}(\sigma) = \begin{cases} \mathbf{r}(\sigma) + \sigma^2(\alpha_1(-\sigma), \beta_1(-\sigma), \gamma_1(-\sigma))^T, & \sigma \in [-\Lambda, 0] \\ \mathbf{r}(\sigma) + \sigma^2(\alpha_2(\sigma), \beta_2(\sigma), \gamma_2(\sigma))^T, & \sigma \in [0, \Lambda], \end{cases} \quad (3.2.8)$$

where $\alpha_i(s), \beta_i(s)$ and $\gamma_i(s)$ are smooth functions on $[0, \Lambda]$, $i = 1, 2$. Thus, for $-\Lambda \leq s \leq 0 \leq \sigma \leq \Lambda$, we have, from (3.2.5) and (3.2.8),

$$\boldsymbol{\rho}(s) \wedge \boldsymbol{\rho}(\sigma) = (-s \sin(\lambda\pi), s \cos(\lambda\pi) + \sigma, 0)^T + O(\max\{|s|, |\sigma|\}^2), \quad (3.2.9)$$

as $\max\{|s|, |\sigma|\} \rightarrow 0$. Hence, with $\boldsymbol{\omega} = \boldsymbol{\rho}(s)$ and $\boldsymbol{\omega}' = \boldsymbol{\rho}(\sigma)$, we have,

$$\begin{aligned} \mathbf{t}' &= \boldsymbol{\rho}_s(\sigma) = (1, 0, 0)^T + O(\sigma), \\ -\mathbf{t}' \cdot (\boldsymbol{\omega} \wedge \boldsymbol{\omega}') &= s \sin(\lambda\pi) + O(\max\{|s|, |\sigma|\}^2) \\ \text{and } |\boldsymbol{\omega} - \boldsymbol{\omega}'|^2 &= s^2 + 2s\sigma \cos(\lambda\pi) + \sigma^2 + O(\max\{|s|, |\sigma|\}^3), \end{aligned} \quad (3.2.10)$$

as $\max\{|s|, |\sigma|\} \rightarrow 0$. Therefore we have from (3.1.12)

$$\widehat{L}_D(s, \sigma) = \frac{\sin(\lambda\pi)}{\pi} \frac{s + \eta_2(s, \sigma)}{s^2 + 2s\sigma \cos(\lambda\pi) + \sigma^2 + \eta_3(s, \sigma)} + \widehat{F}_D(s, \sigma),$$

where $\widehat{F}_D(s, \sigma) = F_D(\boldsymbol{\rho}(s), \boldsymbol{\rho}(\sigma))$ and

$$\eta_i(s, \sigma) = O(\max\{|s|, |\sigma|\}^i), \quad i = 2, 3. \quad (3.2.11)$$

Hence, for $-\Lambda \leq s \leq 0 \leq \sigma \leq \Lambda$,

$$\begin{aligned} (\widehat{L}_D - \widehat{K}_D)(s, \sigma) = \frac{\sin(\lambda\pi)}{\pi} \left\{ \frac{s + \eta_2(s, \sigma)}{s^2 + 2s\sigma \cos(\lambda\pi) + \sigma^2 + \eta_3(s, \sigma)} \right. \\ \left. - \frac{s}{s^2 + 2s\sigma \cos(\lambda\pi) + \sigma^2} \right\} + \widehat{F}_D(s, \sigma), \end{aligned} \quad (3.2.12)$$

which is clearly continuous for $(s, \sigma) \neq (0, 0)$. Now in order to show that $(\widehat{L}_D - \widehat{K}_D)(s, \sigma)$ is bounded near $(s, \sigma) = (0, 0)$ we need to show that the limit (as $(s, \sigma) \rightarrow (0, 0)$) of the first term on the right-hand side of (3.2.12) is bounded.

We do this for $0 < -s \leq \sigma$. The case $0 < \sigma \leq -s$ is analogous.

To obtain the result, write

$$\begin{aligned} & \frac{s + \eta_2(s, \sigma)}{s^2 + 2s\sigma \cos(\lambda\pi) + \sigma^2 + \eta_3(s, \sigma)} - \frac{s}{s^2 + 2s\sigma \cos(\lambda\pi) + \sigma^2} \\ = & \frac{\eta_2(s, \sigma)(s^2 + 2s\sigma \cos(\lambda\pi) + \sigma^2) - \eta_3(s, \sigma)s}{(s^2 + 2s\sigma \cos(\lambda\pi) + \sigma^2)(s^2 + 2s\sigma \cos(\lambda\pi) + \sigma^2 + \eta_3(s, \sigma))} \\ = & \frac{\frac{\eta_2(s, \sigma)}{\sigma^2} \left(\left(\frac{s}{\sigma} \right)^2 + 2 \frac{s}{\sigma} \cos(\lambda\pi) + 1 \right) - \frac{\eta_3(s, \sigma)}{\sigma^3} \frac{s}{\sigma}}{\left(\left(\frac{s}{\sigma} \right)^2 + 2 \frac{s}{\sigma} \cos(\lambda\pi) + 1 \right) \left(\left(\frac{s}{\sigma} \right)^2 + 2 \frac{s}{\sigma} \cos(\lambda\pi) + 1 + \frac{\eta_3(s, \sigma)}{\sigma^2} \right)}. \end{aligned} \quad (3.2.13)$$

Now when $0 < -s \leq \sigma$ we have $0 < |s| \leq |\sigma|$ and from (3.2.11) it follows that $\eta_2(s, \sigma)/\sigma^2 = O(1)$, $\eta_3(s, \sigma)/\sigma^3 = O(1)$ and $\eta_3(s, \sigma)/\sigma^2 \rightarrow 0$ as $(s, \sigma) \rightarrow (0, 0)$. Moreover since $\lambda \in (0, 2) \setminus 1$,

$$x^2 + 2x \cos(\lambda\pi) + 1 \geq \sin^2(\lambda\pi) > 0 \quad \text{for all } x \in \mathbb{R}.$$

Combining all these facts with (3.2.13) shows that the first term in (3.2.12) is bounded as $(s, \sigma) \rightarrow (0, 0)$. Since \widehat{F}_D is a bounded function, it follows that $\widehat{L}_D(s, \sigma) - \widehat{K}_D(s, \sigma)$ is bounded for $-\Lambda \leq s \leq 0 \leq \sigma \leq \Lambda$.

For $-\Lambda \leq \sigma \leq 0 \leq s \leq \Lambda$ the result follows analogously. \square

The next result follows directly from Theorem 3.10.

Corollary 3.11. For $B = D$ or N , $\widehat{\mathcal{L}}_B - \widehat{\mathcal{K}}_B$ is a compact operator on $L^2[-\Lambda, \Lambda]$.

Proof The kernel of $\widehat{\mathcal{L}}_B - \widehat{\mathcal{K}}_B$ is $(\widehat{L}_B - \widehat{K}_B)(s, \sigma)$ which, from Theorem 3.10, is a bounded function and the result follows from [58, pg. 326]. \square

The remainder of this chapter is devoted to proving the well-posedness of (3.1.27) in $L^2[-\Lambda, \Lambda]$. This is done in Corollary 3.15. Since $\widehat{\mathcal{L}}_B$ is a compact perturbation of $\widehat{\mathcal{K}}_B$, the key part of the proof of Corollary 3.15 is contained in Theorem 3.14, which is of key importance also when we come to the numerical analysis in Chapter 4. First we need the following two results from functional analysis.

Theorem 3.12. Let X be a Banach space, and let S be a bounded operator from X into X , with $\|S\|_X < 1$. Then the inverse of $I - S : X \rightarrow X$, exists and is bounded

$$\|(I - S)^{-1}\|_X \leq \frac{1}{1 - \|S\|_X}.$$

For a proof of the above result see e.g [58, pg. 154].

Lemma 3.13. Suppose that X and Y are two Banach spaces and that S and T are two bounded linear operators $S, T : X \rightarrow Y$ such that S^{-1} exists from Y to X and $\|S - T\|_{X \rightarrow Y} < \frac{1}{\|S^{-1}\|_{Y \rightarrow X}}$. Then T^{-1} exists from Y to X and

$$\|T^{-1}\|_{Y \rightarrow X} \leq \frac{\|S^{-1}\|_{Y \rightarrow X}}{1 - \|S - T\|_{X \rightarrow Y} \|S^{-1}\|_{Y \rightarrow X}}. \quad (3.2.14)$$

Proof Since $\|(S - T)S^{-1}\|_{Y \rightarrow Y} \leq \|(S - T)\|_{X \rightarrow Y} \|S^{-1}\|_{Y \rightarrow X} < 1$. It follows from Theorem 3.12 that $(I - (S - T)S^{-1})^{-1}$ exists from Y to Y and

$$\|(I - (S - T)S^{-1})^{-1}\|_{Y \rightarrow Y} \leq \frac{1}{1 - \|(S - T)S^{-1}\|_{Y \rightarrow Y}}.$$

Now $T = S - (S - T) = (I - (S - T)S^{-1})S$ therefore $T^{-1} = S^{-1}(I - (S - T)S^{-1})^{-1}$ exists from Y to X . Moreover

$$\begin{aligned} \|T^{-1}\|_{Y \rightarrow X} &\leq \|S^{-1}\|_{Y \rightarrow X} \|(I - (S - T)S^{-1})^{-1}\|_{Y \rightarrow Y} \\ &\leq \frac{\|S^{-1}\|_{Y \rightarrow X}}{1 - \|(S - T)S^{-1}\|_{Y \rightarrow Y}} \\ &\leq \frac{\|S^{-1}\|_{Y \rightarrow X}}{1 - \|(S - T)\|_{X \rightarrow Y} \|S^{-1}\|_{Y \rightarrow X}}, \end{aligned}$$

as required. \square

Theorem 3.14. For $B = D$ or N , $(I + \widehat{\mathcal{K}}_B)^{-1}$ exists and is bounded on $L^2[-\Lambda, \Lambda]$.

Proof The first step is to write the operator $(I + \widehat{\mathcal{K}}_B)$ on $L^2[-\Lambda, \Lambda]$ as two coupled convolution operators on $[0, \Lambda]$. For $(w_1, w_2) \in L^2[0, \Lambda] \times L^2[0, \Lambda]$ we introduce the norm

$$\|(w_1, w_2)\| = \{\|w_1\|_{L^2[0, \Lambda]}^2 + \|w_2\|_{L^2[0, \Lambda]}^2\}^{1/2}.$$

Also we define the map $\Pi : L^2[-\Lambda, \Lambda] \rightarrow L^2[0, \Lambda] \times L^2[0, \Lambda]$ by

$$\Pi v := (v_1, v_2), \quad (3.2.15)$$

where

$$v_1(s) = v(-s) + v(s) \quad \text{and} \quad v_2(s) = v(-s) - v(s), \quad s \in [0, \Lambda].$$

Clearly Π is a bijection and

$$\|\Pi v\|^2 = 2\|v\|_{L^2[-\Lambda, \Lambda]}^2. \quad (3.2.16)$$

To rewrite $(I + \widehat{\mathcal{K}}_B)$ as two coupled convolution operators we consider the application of Π to the image of $\widehat{\mathcal{K}}_B$. First we write the operator $\widehat{\mathcal{K}}_B$, using (3.2.6) and (3.2.7), in the form,

$$\widehat{\mathcal{K}}_B v(s) = \begin{cases} \int_0^\Lambda \widehat{\kappa}_B(s/\sigma) v(\sigma) \frac{d\sigma}{\sigma}, & s \in [-\Lambda, 0], \\ -\int_{-\Lambda}^0 \widehat{\kappa}_B(s/\sigma) v(\sigma) \frac{d\sigma}{\sigma}, & s \in [0, \Lambda]. \end{cases} \quad (3.2.17)$$

where

$$\widehat{\kappa}_B(s) = \frac{\sin(\lambda\pi)}{\pi} \frac{s}{1 + 2s \cos \lambda\pi + s^2}, \quad B = D, \quad (3.2.18)$$

$$\widehat{\kappa}_B(s) = \frac{\sin(\lambda\pi)}{\pi} \frac{1}{1 + 2s \cos \lambda\pi + s^2}, \quad B = N. \quad (3.2.19)$$

Moreover we have from (3.2.17) that, for $s \in [0, 1]$,

$$\begin{aligned}
\widehat{\mathcal{K}}_B v(-s) + \widehat{\mathcal{K}}_B v(s) &= \int_0^\Lambda \widehat{\kappa}_B(-s/\sigma) v(\sigma) \frac{d\sigma}{\sigma} - \int_{-\Lambda}^0 \widehat{\kappa}_B(s/\sigma) v(\sigma) \frac{d\sigma}{\sigma} \\
&= \int_0^\Lambda \widehat{\kappa}_B(-s/\sigma) v(\sigma) \frac{d\sigma}{\sigma} + \int_0^\Lambda \widehat{\kappa}_B(-s/\sigma) v(-\sigma) \frac{d\sigma}{\sigma} \\
&= \int_0^\Lambda \widehat{\kappa}_B(-s/\sigma) \{v(-\sigma) + v(\sigma)\} \frac{d\sigma}{\sigma}, \tag{3.2.20}
\end{aligned}$$

and similarly,

$$\widehat{\mathcal{K}}_B v(-s) - \widehat{\mathcal{K}}_B v(s) = - \int_0^\Lambda \widehat{\kappa}_B(-s/\sigma) \{v(-\sigma) - v(\sigma)\} \frac{d\sigma}{\sigma}. \tag{3.2.21}$$

Therefore it follows from (3.2.20) and (3.2.21) together with (3.2.15) that,

$$\Pi \widehat{\mathcal{K}}_B = \widetilde{\mathbb{K}}_B \Pi. \tag{3.2.22}$$

Here $\widetilde{\mathbb{K}}_B$ is the matrix operator

$$\widetilde{\mathbb{K}}_B = \begin{pmatrix} \widetilde{\mathcal{K}}_B & 0 \\ 0 & -\widetilde{\mathcal{K}}_B \end{pmatrix},$$

and $\widetilde{\mathcal{K}}_B$ is the *Mellin convolution* operator on $L^2[0, \Lambda]$ defined by

$$(\widetilde{\mathcal{K}}_B v)(s) = \int_0^\Lambda \widetilde{\kappa}_B(s/\sigma) v(s) \frac{d\sigma}{\sigma}$$

with kernel,

$$\widetilde{\kappa}_B(s) = \widehat{\kappa}_B(-s). \tag{3.2.23}$$

It therefore follows that,

$$\Pi(I + \widehat{\mathcal{K}}_B) = (I + \widetilde{\mathbb{K}}_B)\Pi, \tag{3.2.24}$$

The identity (3.2.24) shows that, since Π is a bijection, to finish the proof we need to show that $I + \widetilde{\mathbb{K}}_B$ is invertible on $(L^2[0, \Lambda])^2$. Since $I + \widetilde{\mathbb{K}}_B$ is a 2×2 operator matrix, with $I \pm \widetilde{\mathcal{K}}_B$ on the diagonal and 0 off the diagonal, this will follow if we show that the operators $I \pm \widetilde{\mathcal{K}}_B$ are invertible on $L^2[0, \Lambda]$. We do this by proving that the operators $\widetilde{\mathcal{K}}_B$ are a contraction for $B = D, N$. We introduce

the Mellin transform,

$$\mathcal{M}\{v(s); z\} = \int_0^\infty s^{z-1}v(s)ds, \quad \text{for } z \in \mathbb{C}. \quad (3.2.25)$$

It can be shown that (see e.g. [21])

$$\|\tilde{\mathcal{K}}_B\|_{L^2[0,\Lambda]} = \sup_{\operatorname{Re}(z)=1/2} |\mathcal{M}\{\tilde{\kappa}_B(s); z\}|. \quad (3.2.26)$$

In order to use (3.2.26) to compute the norms of $\tilde{\mathcal{K}}_B$, $B = D$ or N we need to calculate the Mellin transforms of $\tilde{\kappa}_B$, $B = D, N$. We consider $\tilde{\kappa}_N$ first. From (3.2.23) and (3.2.19)

$$\tilde{\kappa}_N(s) = \frac{\sin(\lambda\pi)}{\pi} \frac{1}{1 - 2s \cos(\lambda\pi) + s^2} = \frac{\sin(\chi\pi)}{\pi} \frac{1}{1 + 2s \cos(\chi\pi) + s^2}$$

where $\chi = 1 - \lambda$. Then from e.g. [35, pg. 489],

$$\mathcal{M}\{\tilde{\kappa}_N(s); z\} = \frac{\sin(\chi\pi(1-z))}{\sin(\pi z)}. \quad (3.2.27)$$

Note from (3.2.18), (3.2.19) and (3.2.23), that $\tilde{\kappa}_D(s) = -s\tilde{\kappa}_N(s)$ therefore, from (3.2.25), $\mathcal{M}\{\tilde{\kappa}_D(s); z\} = -\mathcal{M}\{\tilde{\kappa}_N(s); z+1\}$ hence it follows from (3.2.27) that

$$\mathcal{M}\{\tilde{\kappa}_D(s); z\} = -\frac{\sin(\chi\pi z)}{\sin(\pi z)}. \quad (3.2.28)$$

Hence for all $\xi \in \mathbb{R}$

$$\begin{aligned} |\mathcal{M}\{\tilde{\kappa}_N(s); 1/2 + i\xi\}|^2 &= |\mathcal{M}\{\tilde{\kappa}_D(s); 1/2 - i\xi\}|^2 = \left| \frac{\sin(\chi\pi(1/2 - i\xi))}{\sin(\pi(1/2 - i\xi))} \right|^2 \\ &= \left| \frac{\sin(\chi\pi/2) \cosh(\chi\pi\xi)}{\cosh(\pi\xi)} - \frac{i \cos(\chi\pi/2) \sinh(\chi\pi\xi)}{\cosh(\pi\xi)} \right|^2 \\ &= \frac{\sin^2(\chi\pi/2) \cosh^2(\chi\pi\xi)}{\cosh^2(\pi\xi)} + \frac{\cos^2(\chi\pi/2) \sinh^2(\chi\pi\xi)}{\cosh^2(\pi\xi)} \\ &= \frac{\cosh^2(\chi\pi\xi) - \cos^2(\chi\pi/2)}{\cosh^2(\pi\xi)} \\ &= \frac{\sinh^2(\chi\pi\xi) + \sin^2(\chi\pi/2)}{\cosh^2(\pi\xi)} =: w_1(\xi). \end{aligned} \quad (3.2.29)$$

To complete the proof that the operators $\tilde{\mathcal{K}}_B$ are contractions, we simply need

to show that $\max_{\xi \in \mathbb{R}} w_1(\xi) \leq C < 1$. In fact, since $w_1(\xi) = w_1(-\xi)$, we only need to show $\max_{\xi \in [0, \infty)} w_1(\xi) \leq C < 1$. Since $w_1(0) = \sin^2(\chi\pi/2) < 1$, we do this by showing that

$$w_1(0) \geq w_1(\xi), \quad \text{for all } \xi \in [0, \infty), \quad (3.2.30)$$

which is equivalent to,

$$\sin^2(\chi\pi/2) \sinh^2(\pi\xi) / \sinh^2(\chi\pi\xi) \geq 1, \quad \text{for all } \xi \in [0, \infty). \quad (3.2.31)$$

To obtain (3.2.31), we first claim that for $a, b \in \mathbb{R}$ such that $|a| < |b|$

$$\left| \frac{\sinh(b)}{\sinh(a)} \right| \geq \left| \frac{b}{a} \right|. \quad (3.2.32)$$

To prove the claim note that it is sufficient to show only

$$\frac{\sinh(b)}{\sinh(a)} \geq \frac{b}{a}, \quad \text{for } 0 \leq a < b, \quad (3.2.33)$$

since, for any configurations of a, b satisfying $|a| < |b|$, (3.2.32) can be rewritten in the form (3.2.33). To show (3.2.33), consider the function v defined on $[0, b]$ by $v(x) := x \sinh(b) / b \sinh(x)$. If $v(x) \geq 1$ for all $x \in [0, b]$, then the claim is proved. It is trivially true that $v(b) = 1$. Moreover,

$$\begin{aligned} v'(x) &= \frac{\sinh(b)}{b} \left\{ \frac{\sinh(x) - x \cosh(x)}{\sinh^2(x)} \right\} \\ &= \frac{\sinh(b)}{b \sinh^2(x)} \sum_{j=1}^{\infty} \left(\frac{1}{(2j+1)!} - \frac{1}{2j!} \right) x^{2j+1} \leq 0. \end{aligned}$$

Hence it follows that $v(x) \geq 1$ for all $x \in [0, b]$. This proves the claim (3.2.32). As a consequence of this claim, we have

$$\frac{\sinh^2(\pi\xi)}{\sinh^2(\chi\pi\xi)} \geq \frac{1}{\chi^2}$$

and hence (3.2.31) follows provided

$$(\sin(\chi\pi/2)/\chi)^2 \geq 1. \quad (3.2.34)$$

To prove (3.2.34) define $w_2(\chi) = \sin(\chi\pi/2)/\chi$. Now $w_2(\chi) = w_2(-\chi)$ and $w_2(1) = 1$, so if we can show that $w_2(\chi)$ is a decreasing function on $[0, 1)$ then it

is clear that (3.2.34) is true. Differentiating w_2 we get,

$$w_2'(\chi) = \frac{\chi\pi \cos(\chi\pi/2)/2 - \sin(\chi\pi/2)}{\chi^2}. \quad (3.2.35)$$

Consider the numerator on the right-hand side of (3.2.35),

$$w_3(\chi) := \chi\pi \cos(\chi\pi/2)/2 - \sin(\chi\pi/2).$$

Now $w_3'(\chi) = -\chi\pi^2 \sin(\chi\pi/2)/4 - \pi \cos(\chi\pi/2) \leq 0$ for $\chi \in [0, 1)$ so $w_3(\chi)$ is decreasing on $[0, 1)$. Thus, since $w_3(0) = 0$, it follows that $w_3(\chi) \leq 0$ for $\chi \in [0, 1)$. Hence (3.2.35) implies that $w_2'(\chi) \leq 0$ and so $w_2(\chi)$ is decreasing on $[0, 1)$. Therefore (3.2.34) follows and so does (3.2.30)

Hence from (3.2.29),

$$|\mathcal{M}\{\tilde{\kappa}_N(s); 1/2 + i\xi\}|^2 = |\mathcal{M}\{\tilde{\kappa}_D(s); 1/2 - i\xi\}|^2 \leq \sin^2(\chi\pi/2) < 1 \quad \text{for all } \xi \in \mathbb{R}. \quad (3.2.36)$$

Therefore from (3.2.26) and (3.2.36) it follows that

$$\|\tilde{\mathcal{K}}_B\|_{L^2[0, \Lambda]} < 1,$$

i.e $\tilde{\mathcal{K}}_B$ is a contraction. Hence Lemma 3.12 implies that $I \pm \tilde{\mathcal{K}}_B$ are invertible on $L^2[0, \Lambda]$, therefore it follows that $(I + \tilde{\mathcal{K}}_B)^{-1}$ exists, in fact $(I + \tilde{\mathcal{K}}_B)^{-1}$ is a 2×2 operator matrix with diagonal entries given by $(I \pm \tilde{\mathcal{K}}_B)^{-1}$ and off diagonal entries equal to 0. Finally it follows from (3.2.24) that

$$(I + \hat{\mathcal{K}}_B)^{-1} = \Pi^{-1}(I + \tilde{\mathcal{K}}_B)\Pi$$

exists and is bounded. □

Corollary 3.15. *For $B = D$ or N , suppose that (3.1.30) holds then $(I + \hat{\mathcal{L}}_B)^{-1}$ exists and is bounded on $L^2[-\Lambda, \Lambda]$.*

Proof Using Lemma 3.14 the equation (3.1.27) can be rewritten as

$$(I + (I + \hat{\mathcal{K}}_B)^{-1}(\hat{\mathcal{L}}_B - \hat{\mathcal{K}}_B))\hat{u} = (I + \hat{\mathcal{K}}_B)^{-1}\hat{b}. \quad (3.2.37)$$

Since $(I + \hat{\mathcal{K}}_B)^{-1}(\hat{\mathcal{L}}_B - \hat{\mathcal{K}}_B)$ is a compact operator it follows from the Fredholm alternative that (3.2.37) has a unique solution if and only if the homogeneous equation

$$(I + \hat{\mathcal{L}}_B)\hat{u} = 0$$

has only the zero solution which we have assumed. It also follows that the operator on the left-hand side of (3.2.37) has a bounded inverse therefore,

$$\|\widehat{u}\|_{L^2[-\Lambda,\Lambda]} \leq C\|(I + \widehat{\mathcal{K}}_B)^{-1}\widehat{b}\|_{L^2[-\Lambda,\Lambda]} \leq C\|\widehat{b}\|_{L^2[-\Lambda,\Lambda]},$$

and the result follows. □

Chapter 4

Numerical Method for the Integral Equation

We wish to solve approximately and efficiently integral equations of the form,

$$(I + \widehat{\mathcal{L}})\widehat{u}(s) = \widehat{b}(s), \quad \text{with} \quad \widehat{\mathcal{L}}\widehat{u}(s) = \int_{-\Lambda}^{\Lambda} \widehat{L}(s, \sigma)\widehat{u}(\sigma) d\sigma, \quad (4.0.1)$$

for some kernel $\widehat{L}(s, \sigma)$ defined on $[-\Lambda, \Lambda] \times [-\Lambda, \Lambda]$ and some function \widehat{b} . We can do this by seeking a solution in a family of finite dimensional spaces, X_n . This solution is required to satisfy (4.0.1) only approximately. We denote the basis of X_n by $\{\phi_1, \dots, \phi_n\}$ and seek $\widehat{u}_n \in X_n$, i.e.

$$\widehat{u}_n(s) = \sum_{i=1}^n c_i \phi_i(s), \quad s \in [-\Lambda, \Lambda],$$

where the coefficients c_1, \dots, c_n are found by substituting u_n into (4.0.1) and forcing the equation to hold in some sense. There are different senses in which (4.0.1) can be satisfied approximately and this leads to different numerical schemes. The two most popular schemes are the Galerkin and the collocation method.

For the Galerkin method we let (\cdot, \cdot) denote the inner-product on $L^2[-\Lambda, \Lambda]$, then, defining the residual $r_n(s) = \widehat{u}_n(s) + \widehat{\mathcal{L}}\widehat{u}_n(s) - \widehat{b}(s)$, we require that $(r_n, \phi_j) = 0$ for $j = 1, \dots, n$ i.e. c_1, \dots, c_n are found by solving the linear system,

$$\sum_{i=1}^n c_i ((\phi_i, \phi_j) + (\widehat{\mathcal{L}}\phi_i, \phi_j)) = (\widehat{b}, \phi_j), \quad j = 1, \dots, n.$$

Whilst the theory for this method is well known, it has the disadvantage of being expensive to implement due to the need to calculate the double integrals

$(\widehat{\mathcal{L}}\phi_i, \phi_j)$. However the collocation method requires that for the distinct points $x_1, \dots, x_n \in [-\Lambda, \Lambda]$, $r_n(x_j) = 0$ for $j = 1, \dots, n$. This leads to the simpler linear system

$$\sum_{i=1}^n c_i(\phi_i(x_j) + \widehat{\mathcal{L}}\phi_i(x_j)) = \widehat{b}(x_j), \quad j = 1, \dots, n.$$

Although the theory is not as complete as for the Galerkin method, and we are still required to calculate integrals, this method is clearly cheaper to implement than the Galerkin method and for this reason we will consider the collocation method in this thesis.

In this chapter we describe collocation with piecewise polynomial functions as our approximation space. Then we turn our attention to the particular problem of solving (3.0.5), equivalently (3.1.27). First in §4.2 we shall consider the case when the contour ℓ is smooth, using standard theories for the numerical analysis of second kind Fredholm integral equations to give stability and convergence results. Then in §4.3 we consider the problem when ℓ has a corner. This time the standard arguments do not hold since the integral operator in (4.0.1) is not compact and so we need a more detailed analysis of the collocation method based on the theory for the planar Laplace problem in a region with a corner. This will give us stability and optimal convergence of the method.

In order to compute the collocation solution we need to calculate integrals which in general cannot be done explicitly. Therefore we will also look at fully discrete methods which approximate these integrals numerically and give sufficient conditions for the quadrature rules implemented here to ensure the same theoretical rates of convergence as the exact collocation methods. This is done in §4.4.

4.1 The collocation method

We consider using collocation by piecewise polynomial trial functions to find a numerical solution to (4.0.1). To describe this method we introduce a mesh on $[-\Lambda, \Lambda]$, $-\Lambda = x_0 < x_1 < \dots < x_n = \Lambda$. Define $I_i = [x_{i-1}, x_i]$ and $h_i = x_i - x_{i-1}$, for $i = 1, \dots, n$ and let \mathbf{r} be an n -dimensional vector of polynomial orders. We define our approximation space $S_n^{\mathbf{r}}[-\Lambda, \Lambda]$ as the set of piecewise polynomials which have order r_i on I_i ,

$$S_n^{\mathbf{r}}[-\Lambda, \Lambda] = \{v \in L^\infty[-\Lambda, \Lambda] : v|_{I_i} \in \mathbf{P}_{r_i}\}. \quad (4.1.1)$$

where \mathbf{P}_{r_i} denotes the set of polynomials of order r_i (i.e. degree $r_i - 1$) for $r_i \geq 1$.

Collocation points on any subinterval, I_i , for a given order r will be obtained by mapping a fixed set of points $0 < \xi_1^r < \xi_2^r < \dots < \xi_r^r < 1$ to the subinterval. Thus, on each interval, I_i , we can define the r_i collocation points,

$$x_{ij}^{r_i} = x_{i-1} + h_i \xi_j^{r_i}. \quad (4.1.2)$$

We also define the index set $\mathcal{J} = \{(i, j) : 1 \leq i \leq n, 1 \leq j \leq r_i\}$. The basis functions, ϕ_{ij} , $(i, j) \in \mathcal{J}$, of $S_n^r[-\Lambda, \Lambda]$, are given by Lagrange interpolating polynomials,

$$\begin{aligned} \phi_{ij}(x) &= \prod_{\substack{1 \leq k \leq r_i \\ k \neq j}} \frac{x - x_{ik}^{r_i}}{x_{ij}^{r_i} - x_{ik}^{r_i}} \chi_i(x), \quad \text{when } r_i > 1, \\ \phi_{i1}(x) &= \chi_i(x), \quad \text{when } r_i = 1, \end{aligned} \quad (4.1.3)$$

where χ_i is the characteristic function on I_i . Clearly $\phi_{ij}|_{I_i} \in \mathbf{P}_{r_i}$ and $\phi_{ij}(x_{i'j'}^{r_{i'}}) = \delta_{ii'} \delta_{jj'}$. Now the collocation method for (3.1.27) seeks a solution $\hat{u}_n \in S_n^r[-\Lambda, \Lambda]$,

$$\hat{u}_n(s) = \sum_{i=1}^n \sum_{j=1}^{r_i} \hat{\mu}_{ij} \phi_{ij}(s),$$

where $\hat{\mu}_{ij}$ are to be found. This is substituted into (4.0.1) and $\hat{\mu}_{ij}$ are found by forcing the resulting residual to vanish at the collocation points $x_{i'j'}^{r_{i'}}$. This leads to a linear system,

$$\hat{\mu}_{i'j'} + \sum_{i=1}^n \sum_{j=1}^{r_i} \hat{\mu}_{ij} \int_{I_i} \hat{L}(x_{i'j'}^{r_{i'}}, \sigma) \phi_{ij}(\sigma) d\sigma = \hat{b}(x_{i'j'}^{r_{i'}}), \quad (i', j') \in \mathcal{J}. \quad (4.1.4)$$

This is an $m \times m$ linear system

$$(I + \hat{\mathbb{L}}) \hat{\boldsymbol{\mu}} = \hat{\mathbf{b}}, \quad (4.1.5)$$

where m is the dimension of S_n^r given by $m = \sum_{i=1}^n r_i$. The vector entries of $\hat{\mathbf{b}}$ are

$$\hat{\mathbf{b}}_{ij} = \hat{b}(x_{ij}^{r_i}), \quad \text{for } (i, j) \in \mathcal{J},$$

and the matrix entries of $\hat{\mathbb{L}}$ are given by

$$\hat{\mathbb{L}}_{i'j',ij} = \int_{I_i} \hat{L}(x_{i'j'}^{r_{i'}}, \sigma) \phi_{ij}(\sigma) d\sigma = (\hat{\mathcal{L}} \phi_{ij})(x_{i'j'}^{r_{i'}}), \quad (4.1.6)$$

for $(i, j), (i', j') \in \mathcal{J}$. Note that the matrix entries are integrals which in general need to be evaluated numerically, this is discussed in §4.4.

To analyse this method we write (4.1.5) in operator form. We do this by introducing a projection operator onto $S_n^{\mathbf{r}}[-\Lambda, \Lambda]$ denoted by $\widehat{\mathcal{P}}_n$, defined in the following way. For any function v , continuous at $x_{ij}^{r_i}$,

$$(\widehat{\mathcal{P}}_n v)(x) = \sum_{i=1}^n \sum_{j=1}^{r_i} v(x_{ij}^{r_i}) \phi_{ij}(x). \quad (4.1.7)$$

Clearly $(\widehat{\mathcal{P}}_n v)(x)$ is the unique function in $S_n^{\mathbf{r}}[-\Lambda, \Lambda]$ that interpolates v at the collocation points $x_{ij}^{r_i}$, $(i, j) \in \mathcal{J}$. Obviously $\widehat{\mathcal{P}}_n$ depends on the choice of the mesh nodes but this dependence is suppressed from the notation for simplicity. We write (4.1.4) in operator form as follows,

$$(I + \widehat{\mathcal{P}}_n \widehat{\mathcal{L}}) \widehat{u}_n = \widehat{\mathcal{P}}_n \widehat{b}. \quad (4.1.8)$$

Note that since the collocation points $x_{ij}^{r_i}$ all lie in the interior of I_i . The corner point is a mesh point, hence the corner point is not a collocation point. The functions $\widehat{\mathcal{L}} \phi_{ij}(s)$ are all continuous at $x_{ij}^{r_i}$, $(i, j) \in \mathcal{J}$ so $\widehat{\mathcal{P}}_n \widehat{\mathcal{L}}$ is well defined on $S_n^{\mathbf{r}}[-\Lambda, \Lambda]$.

4.2 Smooth contour ℓ

We consider first the problem of solving (3.0.5) when the contour ℓ is smooth. As described in Chapter 3, we can use the arclength parameterisation of ℓ to rewrite (3.0.5) in the form (4.0.1) with the integral operator,

$$(\widehat{\mathcal{L}} \widehat{u})(s) = (\widehat{\mathcal{L}}_B \widehat{u})(s) = \int_{-\Lambda}^{\Lambda} \widehat{L}_B(s, \sigma) \widehat{u}(\sigma) d\sigma,$$

where $\widehat{L}_B(s, \sigma)$ is given by (3.1.28) or (3.1.29) for $B = D$ or N respectively. Note, from Theorem 3.6, that $\widehat{\mathcal{L}}_B$ is compact on $L^2[-\Lambda, \Lambda]$.

In this section we use a h -refinement method based on a uniform mesh where accuracy is achieved by increasing the number of nodes only. We choose the node points x_i so that $x_i - x_{i-1} = 2\Lambda/n$ for $i = 1, \dots, n$. We also fix the order of the approximating polynomial equal to r for some $r > 0$ on each interval I_i . So we define \mathbf{r} to be the constant vector $r_i = r$ for $i = 1, \dots, n$ and $\widehat{\mathcal{P}}_n$ to be the corresponding projection onto $S_n^{\mathbf{r}}[-\Lambda, \Lambda]$. Then the collocation equations can be

written as,

$$(I + \widehat{\mathcal{P}}_n \widehat{\mathcal{L}}_B) \widehat{u}_n = \widehat{\mathcal{P}}_n \widehat{b} \quad (4.2.1)$$

with $B = D$ or N depending on the boundary conditions of the original problem. Using the fact that $\widehat{\mathcal{L}}_B$ is compact we shall show the stability of this method and hence we obtain its convergence below.

This is a standard exercise, but we include it for completeness, since, although computations on smooth boundaries have been performed in e.g. [9] [8], this method has not been analysed. First we need the following two results.

Lemma 4.1. *Let X, Y be Banach spaces and let $\mathcal{A}_n : X \rightarrow Y$, $n \geq 1$ be a sequence of bounded linear operators. Assume $\|\mathcal{A}_n v\|_X \rightarrow 0$ as $n \rightarrow \infty$ for all $v \in X$. Then the convergence is uniform on compact subsets of X .*

For a proof of the above result see [4, Lemma 3.1.1].

Lemma 4.2. *For $B = D$ or N , $\|\widehat{\mathcal{L}}_B - \widehat{\mathcal{P}}_n \widehat{\mathcal{L}}_B\|_{L^2[-\Lambda, \Lambda]} \rightarrow 0$ as $n \rightarrow \infty$.*

Proof First let $w \in C[-\Lambda, \Lambda]$ be an arbitrary continuous function. Then since $(I - \widehat{\mathcal{P}}_n)w \rightarrow 0$ as $n \rightarrow \infty$, it follows from Lemma 4.1 that on a compact subset, Z , of $C[-\Lambda, \Lambda]$,

$$\sup_{w \in Z} \|(I - \widehat{\mathcal{P}}_n)w\|_{L^\infty[-\Lambda, \Lambda]} \rightarrow 0 \quad \text{as } n \rightarrow \infty. \quad (4.2.2)$$

Here $\|\cdot\|_{L^\infty[-\Lambda, \Lambda]}$ is the usual uniform norm. Now from the definition of an operator norm it follows

$$\|\widehat{\mathcal{L}}_B - \widehat{\mathcal{P}}_n \widehat{\mathcal{L}}_B\|_{L^2[-\Lambda, \Lambda]} = \sup_{\|v\|_{L^2[-\Lambda, \Lambda]} \leq 1} \|\widehat{\mathcal{L}}_B v - \widehat{\mathcal{P}}_n \widehat{\mathcal{L}}_B v\|_{L^2[-\Lambda, \Lambda]} = \sup_{v \in \widehat{\mathcal{L}}_B(\mathcal{B})} \|v - \widehat{\mathcal{P}}_n v\|_{L^2[-\Lambda, \Lambda]},$$

where \mathcal{B} is the unit ball in $L^2[-\Lambda, \Lambda]$ and $\widehat{\mathcal{L}}_B(\mathcal{B})$ is the set $\{\widehat{\mathcal{L}}_B z : z \in \mathcal{B}\}$. The space $\widehat{\mathcal{L}}_B(\mathcal{B})$ has compact closure in $C[-\Lambda, \Lambda]$ since $\widehat{\mathcal{L}}_B$, regarded as an operator from $L^2[-\Lambda, \Lambda]$ into $C[-\Lambda, \Lambda]$, is compact (see e.g. [47, Theorem 3]). Therefore, from (4.2.2)

$$\sup_{v \in \widehat{\mathcal{L}}_B(\mathcal{B})} \|v - \widehat{\mathcal{P}}_n v\|_{L^2[-\Lambda, \Lambda]} \leq (2\Lambda)^{1/2} \sup_{v \in \widehat{\mathcal{L}}_B(\mathcal{B})} \|v - \widehat{\mathcal{P}}_n v\|_{L^\infty[-\Lambda, \Lambda]} \rightarrow 0, \quad \text{as } n \rightarrow \infty.$$

This proves the lemma. □

The following result shows that the collocation equations (4.2.1) are stable.

Theorem 4.3. For $B = D$ or N , and for sufficiently large n , $(I + \widehat{\mathcal{P}}_n \widehat{\mathcal{L}}_B)^{-1}$ exists and $\|(I + \widehat{\mathcal{P}}_n \widehat{\mathcal{L}}_B)^{-1}\|_{L^2[-\Lambda, \Lambda]}$ is uniformly bounded. Also, with \widehat{u} , denoting the exact solution of (4.0.1), we have, for some constant C ,

$$\|\widehat{u} - \widehat{u}_n\|_{L^2[-\Lambda, \Lambda]} \leq C \|(I - \widehat{\mathcal{P}}_n) \widehat{u}\|_{L^2[-\Lambda, \Lambda]}. \quad (4.2.3)$$

So $\|\widehat{u} - \widehat{u}_n\|_{L^2[-\Lambda, \Lambda]}$ converges to zero at least as fast as $\|(I - \widehat{\mathcal{P}}_n) \widehat{u}\|_{L^2[-\Lambda, \Lambda]}$, as $n \rightarrow \infty$.

Proof By Lemma 4.2, there exists $n_0 \in \mathbb{N}$ such that

$$\sup_{n \geq n_0} \|\widehat{\mathcal{L}}_B - \widehat{\mathcal{P}}_n \widehat{\mathcal{L}}_B\|_{L^2[-\Lambda, \Lambda]} \leq 1 / \|(I + \widehat{\mathcal{L}}_B)^{-1}\|_{L^2[-\Lambda, \Lambda]}.$$

It follows from Theorems 3.7 and 3.8 that $I + \widehat{\mathcal{L}}_B$ is invertible, hence for $n \geq n_0$,

$$\|(I + \widehat{\mathcal{L}}_B) - (I + \widehat{\mathcal{P}}_n \widehat{\mathcal{L}}_B)\|_{L^2[-\Lambda, \Lambda]} \leq 1 / \|(I + \widehat{\mathcal{L}}_B)^{-1}\|_{L^2[-\Lambda, \Lambda]}.$$

Therefore by Lemma 3.13, $(I + \widehat{\mathcal{P}}_n \widehat{\mathcal{L}}_B)^{-1}$ exists and is uniformly bounded in the $L^2[-\Lambda, \Lambda]$ norm. To obtain the estimate (4.2.3) write

$$\widehat{u} - \widehat{u}_n = \widehat{u} - (I + \widehat{\mathcal{P}}_n \widehat{\mathcal{L}}_B)^{-1} \widehat{\mathcal{P}}_n \widehat{u} = (I + \widehat{\mathcal{P}}_n \widehat{\mathcal{L}}_B)^{-1} (\widehat{u} - \widehat{\mathcal{P}}_n \widehat{u}),$$

and then take norms. □

Assuming $\widehat{u} \in C^\infty[-\Lambda, \Lambda]$, we obtain a quantitative convergence estimate from Theorem 4.3 using the standard estimate

$$\|(I - \widehat{\mathcal{P}}_n) \widehat{u}\|_{L^2[-\Lambda, \Lambda]} \leq C n^{-r} \|\widehat{u}\|_{H^r[-\Lambda, \Lambda]}.$$

where $H^r[-\Lambda, \Lambda]$ is the usual Sobolev space. Hence, by Theorem 4.3, \widehat{u}_n converges to \widehat{u} with $O(n^{-r})$.

These rates of convergence are shown empirically in §5.4 for the test case when ℓ is the contour associated with a circular cone.

Now we analyse the collocation method described in §4.1 in the case when ℓ contains a corner.

4.3 Nonsmooth contour ℓ

In this section we are interested in the solution to (3.0.5) when ℓ has a corner ω_c . As in Chapter 3 we will use the parametric representation, ρ , where $\rho(0) = \omega_c$

to write (3.0.5) in the form (4.0.1). In this case the integral equation (4.0.1) no longer has a compact integral operator $\widehat{\mathcal{L}} = \widehat{\mathcal{L}}_B$. However, as shown in Corollary 3.11, $\widehat{\mathcal{L}}_B$ is a compact perturbation of a planar Laplace integral operator, $\widehat{\mathcal{K}}_B$, and so we apply techniques used to solve Laplacian problems to solve and analyse (4.0.1).

Since there is a corner at $\boldsymbol{\rho}(0)$ we define the mesh so that the nodes satisfy $-\Lambda = x_0 < x_1 < \dots < x_m = 0 < x_{m+1} < \dots < x_n = \Lambda$ where $n = 2m$ and we choose r_i , x_i and $\xi_j^{r_i}$, $(i, j) \in \mathcal{J}$ so that the collocation points lie symmetrically about 0. More precisely, we define,

$$r_{m+i} = r_{m-i+1}, \quad \text{and} \quad x_{m+i} = -x_{m-i}. \quad (4.3.1)$$

We also require the points $\{\xi_j^{r_i} : j = 1, \dots, r_i\}$ to be chosen symmetrically about the point $1/2$ for all i . An example is the Gauss-Legendre points.

We consider two types of collocation method. Firstly we will look at a modification of the h -refinement method. Secondly we consider a hp -method where the approximating function has a linear distribution of polynomial orders along the subintervals. In the hp -version we simultaneously increase the number of nodes and the order of the approximating polynomials to achieve accuracy, whereas in the h -version we only increase the number of nodes.

4.3.1 The h -refinement method

In the h -refinement method, to ensure optimal convergence, we choose the nodes so that the mesh is graded towards the singularity at 0, that is,

$$x_{m\pm i} = \pm(i/m)^q \Lambda \quad \text{for } i = 1, \dots, m, \quad \text{and } x_0 = 0, \quad (4.3.2)$$

where $q \geq 1$ is the grading exponent (note that if $q = 1$ we have a uniform mesh and recall that the length of ℓ is 2Λ). We also need the technical condition that on some intervals nearest to 0 the approximating function, \widehat{u}_n , is exactly zero. We introduce the parameter $i_0 \in \mathbb{N}_0 = \mathbb{N} \cup 0$ independent of n . We seek $\widehat{u}_n \in S_n^{\mathbf{r}}$, where, in this subsection, we take $r_i = 1$ (in fact the approximating polynomial is set equal to zero) for $m - i_0 < i < m + 1 + i_0$ and $r_i = r$ for $i \leq m - i_0$ and $i \geq m + i_0 + 1$ for some $r > 0$. We define the corresponding projection of $L^2[-\Lambda, \Lambda]$ onto $S_n^{\mathbf{r}}$ by $\widehat{\mathcal{P}}_n$. The projection operator $\widehat{\mathcal{P}}_n$ depends on i_0 and r but we suppress this from the notation. To show stability of the h -refinement

collocation equation,

$$(I + \widehat{\mathcal{P}}_n \widehat{\mathcal{L}}_B) \widehat{u}_n = \widehat{\mathcal{P}}_n \widehat{b}_B, \quad \text{for } B = D, N \quad (4.3.3)$$

with respect to this approximation space we need the following result on the stability of $(I + \widehat{\mathcal{P}}_n \widehat{\mathcal{K}}_B)^{-1}$. (Recall that $\widehat{\mathcal{K}}_B$ is the integral operator associated with the planar Laplace's equation in the presence of the wedge w tangent to ℓ at ω_c , see Definition 3.9.)

Theorem 4.4. *For $B = D$ or N there exists a fixed i_0 so that for n sufficiently large, $(I + \widehat{\mathcal{P}}_n \widehat{\mathcal{K}}_B)^{-1}$ exists and is bounded on $S_n^r[-\Lambda, \Lambda]$.*

Proof First we write $I + \widehat{\mathcal{P}}_n \widehat{\mathcal{K}}_B$ as two coupled convolution operators on $[0, \Lambda]$. First recall from the proof of Theorem 3.14 that $\widehat{\mathcal{K}}_B$ can be written in the form

$$\widehat{\mathcal{K}}_B v(s) = \begin{cases} \int_0^\Lambda \widehat{\kappa}_B(s/\sigma) v(\sigma) \frac{d\sigma}{\sigma}, & s \in [-\Lambda, 0], \\ - \int_{-\Lambda}^0 \widehat{\kappa}_B(s/\sigma) v(\sigma) \frac{d\sigma}{\sigma}, & s \in [0, \Lambda]. \end{cases}$$

with $\widehat{\kappa}_B$ given by (3.2.18) and (3.2.19) for $B = D$ and N respectively. Hence, from (4.1.7) it follows that for $v \in L^2[-\Lambda, \Lambda]$,

$$(\widehat{\mathcal{P}}_n \widehat{\mathcal{K}}_B v)(s) = \begin{cases} \sum_{i=1}^{m-i_0} \sum_{j=1}^r \left\{ \int_0^\Lambda \widehat{\kappa}_B(x_{ij}^r/\sigma) v(\sigma) \frac{d\sigma}{\sigma} \right\} \phi_{ij}(s), & s \in [-\Lambda, 0], \\ - \sum_{i=m+1+i_0}^n \sum_{j=1}^r \left\{ \int_{-\Lambda}^0 \widehat{\kappa}_B(x_{ij}^r/\sigma) v(\sigma) \frac{d\sigma}{\sigma} \right\} \phi_{ij}(s), & s \in [0, \Lambda]. \end{cases} \quad (4.3.4)$$

Using the symmetry assumption (4.3.1) we can rewrite this operator as

$$(\widehat{\mathcal{P}}_n \widehat{\mathcal{K}}_B v)(s) = \begin{cases} \sum_{i=m+1+i_0}^n \sum_{j=1}^r \int_0^\Lambda \widehat{\kappa}_B(-x_{ij}^r/\sigma) v(\sigma) \frac{d\sigma}{\sigma} \phi_{ij}(-s), & s \in [-\Lambda, 0], \\ \sum_{i=m+1+i_0}^n \sum_{j=1}^r \int_0^\Lambda \widehat{\kappa}_B(-x_{ij}^r/\sigma) v(-\sigma) \frac{d\sigma}{\sigma} \phi_{ij}(s), & s \in [0, \Lambda]. \end{cases} \quad (4.3.5)$$

Hence, for $s > 0$,

$$(\widehat{\mathcal{P}}_n \widehat{\mathcal{K}}_B v)(-s) \pm (\widehat{\mathcal{P}}_n \widehat{\mathcal{K}}_B v)(s) = \sum_{i=m+1+i_0}^n \sum_{j=1}^r \left[\int_0^\Lambda \widetilde{\kappa}_B(x_{ij}^r/\sigma) \{v(\sigma) \pm v(-\sigma)\} \frac{d\sigma}{\sigma} \right] \phi_{ij}(s),$$

with $\widetilde{\kappa}_B(x) = \widehat{\kappa}_B(-x)$ as defined in (3.2.23). Therefore, following the same lines

as the decoupling argument in the proof of Theorem 3.14 with Π and $\tilde{\mathbb{K}}_B$ defined therein, we can write,

$$\Pi \widehat{\mathcal{P}}_n \widehat{\mathcal{K}}_B = \tilde{\mathbb{P}}_n \tilde{\mathbb{K}}_B \Pi \quad (4.3.6)$$

where

$$\tilde{\mathbb{P}}_n = \begin{pmatrix} \tilde{\mathcal{P}}_n & 0 \\ 0 & \tilde{\mathcal{P}}_n \end{pmatrix}.$$

Here $\tilde{\mathcal{P}}_n$ is defined as the restriction of $\widehat{\mathcal{P}}_n$ to $L^2[0, \Lambda]$, so for $v \in L^2[0, \Lambda]$

$$\tilde{\mathcal{P}}_n v = \sum_{i=m+1}^n \sum_{j=1}^r v(x_{ij}^r) \phi_{ij}(x). \quad (4.3.7)$$

Therefore, it follows from (4.3.6) that,

$$\Pi(I + \widehat{\mathcal{P}}_n \widehat{\mathcal{K}}_B) = (I + \tilde{\mathbb{P}}_n \tilde{\mathbb{K}}_B) \Pi. \quad (4.3.8)$$

To complete the proof, note that $I + \tilde{\mathbb{P}}_n \tilde{\mathbb{K}}_B$ is a 2×2 operator matrix with entries given by $I \pm \tilde{\mathcal{P}}_n \tilde{\mathcal{K}}_B$ on the diagonal and 0 off the diagonal. Recall that $\tilde{\mathcal{K}}_B$ the Mellin convolution operator on $L^2[0, \Lambda]$ given by

$$(\tilde{\mathcal{K}}_B v)(s) = \int_0^\Lambda \tilde{\kappa}_B(s/\sigma) v(s) \frac{d\sigma}{\sigma}.$$

By showing the operators $I \pm \tilde{\mathcal{P}}_n \tilde{\mathcal{K}}_B$ are invertible, it will follow from (4.3.8) that $I + \widehat{\mathcal{P}}_n \widehat{\mathcal{K}}_B$ is invertible.

The question of the stability of $I + \widehat{\mathcal{P}}_n \widehat{\mathcal{K}}_B$ is equivalent to the question of stability of piecewise polynomial collocation methods for Mellin convolution equations on $[0, \Lambda]$. This has been well investigated, e.g. [22], [45], [35] and [38]. Much of the earliest work in this field concerned stability in $L^\infty[0, \Lambda]$. However in this work we need stability in the space $L^2[0, \Lambda]$ because the integral equation for the Neumann problem is not well-posed in $L^\infty[0, \Lambda]$. For results in $L^2[0, \Lambda]$ the fundamental reference is [35], see also the review [38].

It follows from results in [35] that, for i_0 and n sufficiently large, $I \pm \tilde{\mathcal{P}}_n \tilde{\mathcal{K}}_B$ are invertible on $S_n^r[0, \Lambda]$ and have inverses which are uniformly bounded in the $L^2[-\Lambda, \Lambda]$ norm as $n \rightarrow \infty$ if the kernel, $\tilde{\kappa}_B$, of $\tilde{\mathcal{K}}_B$ defined in (3.2.23) satisfies

the following conditions (see [35, Theorem 3.1]):

$$\int_0^\infty x^{j-1/2} |D^j \tilde{\kappa}_B(x)| dx < \infty, \quad \text{for } j = 0, 1, \quad (4.3.9)$$

$$1 \pm \mathcal{M}\{\tilde{\kappa}_B; z\} \neq 0 \quad \text{for } \operatorname{Re}(z) = 1/2 \quad (4.3.10)$$

$$\text{and } \{ \arg(1 \pm \mathcal{M}\{\tilde{\kappa}_B; 1/2 + i\xi\}) \}_{-\infty}^\infty = 0, \quad (4.3.11)$$

where \mathcal{M} denotes the Mellin transform as defined in (3.2.25) and $D = d/dx$. To use Elschner's result we need to verify the conditions (4.3.9) - (4.3.11).

First note from (3.2.18), (3.2.19) and (3.2.23) that

$$x^{j-1/2} |D^j \tilde{\kappa}_D(x)| = O(x^{1/2}) \quad \text{and} \quad x^{j-1/2} |D^j \tilde{\kappa}_N(x)| = O(x^{-1/2}) \quad \text{as } x \rightarrow 0,$$

for $j = 0$ and 1 . Also note that

$$x^{j-1/2} |D^j \tilde{\kappa}_D(x)| = O(x^{-3/2}) \quad \text{and} \quad x^{j-1/2} |D^j \tilde{\kappa}_N(x)| = O(x^{-5/2}) \quad \text{as } x \rightarrow \infty,$$

for $j = 0$ and 1 . Hence it is clear that (4.3.9) holds. Second, it is shown that $|\mathcal{M}\{\tilde{\kappa}_B; z\}| \leq C < 1$ for all z with $\operatorname{Re}(z) = 1/2$ in (3.2.36). Hence (4.3.10) and (4.3.11) are true. Thus Elschner's result implies that $(I \pm \tilde{\mathcal{P}}_n \tilde{\mathcal{K}}_B)^{-1}$ exists and is bounded. Therefore it follows that $(I + \tilde{\mathcal{P}}_n \tilde{\mathcal{K}}_B)^{-1}$ exists and is given by the 2×2 operator matrix with $(I \pm \tilde{\mathcal{P}}_n \tilde{\mathcal{K}})^{-1}$ on the diagonal and 0 off the diagonal. Moreover, it follows from (4.3.8) that

$$(I + \hat{\mathcal{P}}_n \hat{\mathcal{K}}_B)^{-1} = \Pi^{-1} (I + \tilde{\mathcal{P}}_n \tilde{\mathcal{K}}_B)^{-1} \Pi$$

exists and is bounded, as required. \square

Remark 4.5. Here we give a flavour as to why the conditions (4.3.9) - (4.3.11) imply stability of $(I \pm \tilde{\mathcal{P}}_n \tilde{\mathcal{K}}_B)^{-1}$, $B = D, N$. It follows from the general results in [38] (see Theorem 3.1 there and the remarks following it) that for all $v_n \in S_n^r[0, \Lambda]$, these conditions imply $\|(I - \tilde{\mathcal{P}}_n) \tilde{\mathcal{K}}_B v_n\|_{L^2(I_i)} \leq C(1/i_0) \|x(D \tilde{\mathcal{K}}_B v_n)(x)\|_{L^2(I_i)}$. It can be shown that the L^2 norm of $x(D \tilde{\mathcal{K}}_B v_n)(x)$ is bounded (using condition (4.3.9)). Hence it follows that for all $\epsilon > 0$ and sufficiently large n there exists i_0 such that

$$\|(I \pm \tilde{\mathcal{P}}_n \tilde{\mathcal{K}}_B) v_n - (I \pm \tilde{\mathcal{K}}_B) v_n\|_{L^2[-\Lambda, \Lambda]} < \epsilon \|v_n\|_{L^2[-\Lambda, \Lambda]},$$

for all $v_n \in S_n^r[0, \Lambda]$. Therefore stability of $(I \pm \tilde{\mathcal{P}}_n \tilde{\mathcal{K}}_B)^{-1}$ on $S_n^r[0, \Lambda]$ follows from Lemma 3.13 the fact that $I \pm \tilde{\mathcal{K}}_B$ are invertible (see the proof of Theorem 3.14).

Similarly for sufficiently large n and all $\epsilon > 0$, there exists i_0 such that for $v_n \in S_n[-\Lambda, \Lambda]$

$$\|(I - \widehat{\mathcal{P}}_n)\widehat{\mathcal{K}}_B v_n\|_{L^2[-\Lambda, \Lambda]} < \epsilon \|v_n\|_{L^2[-\Lambda, \Lambda]},$$

which is a result which we use in the proof of Theorem 4.6.

Now we can use this result to show stability of the collocation equation (4.3.3).

Theorem 4.6. *For $B = D$ or N there exists a modification parameter i_0 such that for all sufficiently large n , the collocation equation (4.3.3) is stable in $L^2[-\Lambda, \Lambda]$. That is $(I + \widehat{\mathcal{P}}_n \widehat{\mathcal{L}}_B)^{-1}$ exists and is uniformly bounded on $S_n^r[-\Lambda, \Lambda]$ with respect to n .*

Proof We shall show that, for each $\epsilon > 0$, there exists a modification such that for n sufficiently large,

$$\|(I - \widehat{\mathcal{P}}_n)\widehat{\mathcal{L}}_B v_n\|_{L^2[-\Lambda, \Lambda]} \leq \epsilon \|v_n\|_{L^2[-\Lambda, \Lambda]}, \quad (4.3.12)$$

for all $v_n \in S_n^r[-\Lambda, \Lambda]$. Then, since

$$I + \widehat{\mathcal{P}}_n \widehat{\mathcal{L}}_B = (I + \widehat{\mathcal{L}}_B) - (I - \widehat{\mathcal{P}}_n)\widehat{\mathcal{L}}_B,$$

existence and stability of $(I + \widehat{\mathcal{P}}_n \widehat{\mathcal{L}}_B)^{-1}$ on $S_n^r[-\Lambda, \Lambda]$ follows from Lemma 3.13 by taking $\epsilon < 1/\|(I + \widehat{\mathcal{L}}_B)^{-1}\|_{L^2[-\Lambda, \Lambda]}$ and recalling Corollary 3.15. To obtain (4.3.12), note that by the triangle inequality,

$$\|(I - \widehat{\mathcal{P}}_n)\widehat{\mathcal{L}}_B v_n\|_{L^2[-\Lambda, \Lambda]} \leq \|(I - \widehat{\mathcal{P}}_n)\widehat{\mathcal{K}}_B v_n\|_{L^2[-\Lambda, \Lambda]} + \|(I - \widehat{\mathcal{P}}_n)(\widehat{\mathcal{L}}_B - \widehat{\mathcal{K}}_B)v_n\|_{L^2[-\Lambda, \Lambda]}. \quad (4.3.13)$$

Now recall that $\widehat{\mathcal{P}}_n$ projects to zero on the $2i_0$ intervals nearest 0. Thus

$$\begin{aligned} \|(I - \widehat{\mathcal{P}}_n)(\widehat{\mathcal{L}}_B - \widehat{\mathcal{K}}_B)v_n\|_{L^2[-\Lambda, \Lambda]}^2 &\leq \|(\widehat{\mathcal{L}}_B - \widehat{\mathcal{K}}_B)v_n\|_{L^2[x_{m-i_0}, x_{m+i_0}]}^2 \\ &\quad + \|(I - \widehat{\mathcal{P}}_n)(\widehat{\mathcal{L}}_B - \widehat{\mathcal{K}}_B)v_n\|_{L^2([-\Lambda, \Lambda] \setminus [x_{m-i_0}, x_{m+i_0}])}^2. \end{aligned} \quad (4.3.14)$$

It follows from Theorem 3.10 that $\widehat{\mathcal{L}}_B - \widehat{\mathcal{K}}_B$ is a bounded function. This implies that $(\widehat{\mathcal{L}}_B - \widehat{\mathcal{K}}_B)$ is compact from $L^2[-\Lambda, \Lambda]$ to $L^\infty[-\Lambda, \Lambda]$, [58, pp. 534-535]. Thus the first term on the right-hand side of (4.3.14) may be estimated by

$$\begin{aligned} \|(\widehat{\mathcal{L}}_B - \widehat{\mathcal{K}}_B)v_n\|_{L^2[x_{m-i_0}, x_{m+i_0}]}^2 &\leq 2x_{m+i_0} \|(\widehat{\mathcal{L}}_B - \widehat{\mathcal{K}}_B)v_n\|_{L^\infty[x_{m-i_0}, x_{m+i_0}]}^2 \\ &\leq Cn^{-q} \|v_n\|_{L^2[-\Lambda, \Lambda]}^2. \end{aligned} \quad (4.3.15)$$

We now consider the second term on the right-hand side of (4.3.14). First we write

$$\begin{aligned} \|(I - \widehat{\mathcal{P}}_n)(\widehat{\mathcal{L}}_B - \widehat{\mathcal{K}}_B)v_n\|_{L^2([- \Lambda, \Lambda] \setminus [x_{m-i_0}, x_{m+i_0}])}^2 &= \sum_{i \leq m-i_0} \|(I - \widehat{\mathcal{P}}_n)(\widehat{\mathcal{L}}_B - \widehat{\mathcal{K}}_B)v_n\|_{L^2(I_i)}^2 \\ &+ \sum_{i \geq m+i_0+1} \|(I - \widehat{\mathcal{P}}_n)(\widehat{\mathcal{L}}_B - \widehat{\mathcal{K}}_B)v_n\|_{L^2(I_i)}^2. \end{aligned} \quad (4.3.16)$$

We will estimate the second sum in (4.3.16). (The first sum can be dealt with in a similar way.) To do this we recall the standard results for piecewise polynomial interpolation (e.g. [34, pg. 554]) and write

$$\begin{aligned} \sum_{i \geq m+i_0+1} \|(I - \widehat{\mathcal{P}}_n)(\widehat{\mathcal{L}}_B - \widehat{\mathcal{K}}_B)v_n\|_{L^2(I_i)}^2 &\leq C \sum_{i \geq m+i_0+1} h_i^2 \|D(\widehat{\mathcal{L}}_B - \widehat{\mathcal{K}}_B)v_n\|_{L^2(I_i)}^2 \\ &\leq C \sum_{i \geq m+i_0+1} h_i^3 \|s^{-1} sD(\widehat{\mathcal{L}}_B - \widehat{\mathcal{K}}_B)v_n\|_{L^\infty(I_i)}^2. \end{aligned}$$

It can be shown, using the same argument as in the proof of Theorem 3.10, that the operator $sD(\widehat{\mathcal{L}}_B - \widehat{\mathcal{K}}_B)$ has a bounded kernel. Hence, noting that $h_i \leq Cn^{-1}$, we obtain

$$\begin{aligned} \sum_{i \geq m+i_0+1} \|(I - \widehat{\mathcal{P}}_n)(\widehat{\mathcal{L}}_B - \widehat{\mathcal{K}}_B)v_n\|_{L^2(I_i)}^2 &\leq Cn^{-1} \sum_{i \geq m+i_0+1} (h_i x_{i-1}^{-1})^2 \|v_n\|_{L^2[- \Lambda, \Lambda]}^2 \\ &\leq C \max_{i \geq m+i_0+1} (h_i x_{i-1}^{-1})^2 \|v_n\|_{L^2[- \Lambda, \Lambda]}^2. \end{aligned} \quad (4.3.17)$$

Now for $i \geq i_0 + 1$, (4.3.2) implies

$$h_{m+i} = \left(\frac{i}{m}\right)^q \Lambda - \left(\frac{i-1}{m}\right)^q \Lambda \leq q\Lambda \frac{1}{m} \left(\frac{i}{m}\right)^{q-1}.$$

Hence,

$$h_{m+i} x_{m+i-1}^{-1} \leq q \frac{1}{m} \left(\frac{i}{m}\right)^{q-1} \left(\frac{m}{i-1}\right)^q \leq q \frac{1}{i-1} \leq q \frac{1}{i_0}. \quad (4.3.18)$$

By substituting (4.3.18) into (4.3.17) it follows that

$$\sum_{i \geq m+i_0+1} \|(I - \widehat{\mathcal{P}}_n)(\widehat{\mathcal{L}}_B - \widehat{\mathcal{K}}_B)v_n\|_{L^2(I_i)}^2 \leq C \left(\frac{1}{i_0}\right)^2 \|v_n\|_{L^2[- \Lambda, \Lambda]}^2.$$

A similar estimate holds for the first sum in (4.3.16) and so

$$\begin{aligned} \|(I - \widehat{\mathcal{P}}_n)(\widehat{\mathcal{L}}_B - \widehat{\mathcal{K}}_B)v_n\|_{L^2([- \Lambda, \Lambda] \setminus [x_{m-i_0}, x_{m+i_0}])} &\leq C \frac{1}{i_0} \|v_n\|_{L^2[- \Lambda, \Lambda]} \\ &\leq \frac{\epsilon}{2} \|v_n\|_{L^2[- \Lambda, \Lambda]}, \end{aligned} \quad (4.3.19)$$

for sufficiently large i_0 .

Therefore, it follows from (4.3.14), (4.3.15) and (4.3.19) that, for sufficiently large n , there exists i_0 such that,

$$\|(I - \widehat{\mathcal{P}}_n)(\widehat{\mathcal{L}}_B - \widehat{\mathcal{K}}_B)v_n\|_{L^2[- \Lambda, \Lambda]} \leq \frac{\epsilon}{2} \|v_n\|_{L^2[- \Lambda, \Lambda]}.$$

Also, for sufficiently large n , it follows from Remark 4.5 that there exists i_0 such that

$$\|(I - \widehat{\mathcal{P}}_n)\widehat{\mathcal{K}}_B v_n\|_{L^2[- \Lambda, \Lambda]} < \frac{\epsilon}{2} \|v_n\|_{L^2[- \Lambda, \Lambda]}.$$

Hence (4.3.12) follows from (4.3.13). \square

Remark 4.7. The introduction of the parameter i_0 is solely a device to prove stability of the collocation method applied to the particular problem when ℓ contains a corner. The proof that these methods are stable without modification has eluded researchers for 15 years. However, no unmodified practical collocation method has ever been observed to be unstable. For this reason and to simplify the presentation we assume that Theorem 4.6 holds for $i_0 = 0$ (i.e. no modification) for the remainder of this section.

Theorem 4.6 implies that the collocation equation (4.3.3) is uniquely solvable for all n sufficiently large. We use this result in Lemma 4.9 to find a bound for the error $\|\widehat{u} - \widehat{u}_n\|_{L^2[- \Lambda, \Lambda]}$. First we need the following result which gives an estimate for $\|\widehat{\mathcal{P}}_n v\|_{L^2(I_i)}$ for an arbitrary function v .

Lemma 4.8. *Let $v : [- \Lambda, \Lambda] \rightarrow \mathbb{R}$, then*

$$\|\widehat{\mathcal{P}}_n v\|_{L^2(I_i)}^2 \leq C h_i \max_{j=1, \dots, r} |v(x_{ij}^r)|^2,$$

with C independent of i and n .

Proof First note that since v is well defined at the collocation points x_{ij}^r for $(i, j) \in \mathcal{J}$ we have

$$\|\widehat{\mathcal{P}}_n v\|_{L^2(I_i)}^2 \leq h_i \|\widehat{\mathcal{P}}_n v\|_{L^\infty(I_i)}^2.$$

Also for $x \in I_i$,

$$|(\widehat{\mathcal{P}}_n v)(x)| = \left| \sum_{j=1}^r v(x_{ij}^r) \phi_{ij}(x) \right| \leq \left\{ \sum_{j=1}^r |\phi_{ij}(x)| \right\} \max_{j=1, \dots, r} |v(x_{ij}^r)|. \quad (4.3.20)$$

Clearly $\sum_{j=1}^r |\phi_{ij}(x)|$ is bounded when $r = 1$. If $r > 1$, then for $x \in I_i$, we can write, $x = x_{i-1} + h_i \xi$ for some $\xi \in [0, 1]$. Now since $x_{ij}^r = x_{i-1} + h_i \xi_j$, we have, using (4.1.3),

$$\sum_{j=1}^r |\phi_{ij}(x)| = \sum_{j=1}^r \left| \prod_{\substack{1 \leq k \leq r \\ k \neq j}} \left(\frac{\xi - \xi_k}{\xi_j - \xi_k} \right) \right|$$

which is bounded independently of i and $x \in I_i$. Hence the result follows from (4.3.20). \square

Lemma 4.9. *For the exact solution, \widehat{u} , to (4.0.1) and approximate solution, \widehat{u}_n , determined by (4.1.8), we have the following error estimate,*

$$\|\widehat{u} - \widehat{u}_n\|_{L^2[-\Lambda, \Lambda]} \leq C \|(I - \widehat{\mathcal{P}}_n) \widehat{u}\|_{L^2[-\Lambda, \Lambda]}$$

for some constant C independent of n and \widehat{u} .

Proof First applying the triangle inequality we have,

$$\|\widehat{u} - \widehat{u}_n\|_{L^2[-\Lambda, \Lambda]} \leq \|\widehat{u} - \widehat{\mathcal{P}}_n \widehat{u}\|_{L^2[-\Lambda, \Lambda]} + \|\widehat{\mathcal{P}}_n \widehat{u} - \widehat{u}_n\|_{L^2[-\Lambda, \Lambda]}. \quad (4.3.21)$$

It follows from Theorem 4.6 that the second term on the right-hand side of (4.3.21) can be estimated by

$$\begin{aligned} \|\widehat{\mathcal{P}}_n \widehat{u} - \widehat{u}_n\|_{L^2[-\Lambda, \Lambda]} &\leq C \|(I + \widehat{\mathcal{P}}_n \widehat{\mathcal{L}}_B)(\widehat{\mathcal{P}}_n \widehat{u} - \widehat{u}_n)\|_{L^2[-\Lambda, \Lambda]} \\ &\leq C \|\widehat{\mathcal{P}}_n \widehat{\mathcal{L}}_B (I - \widehat{\mathcal{P}}_n) \widehat{u}\|_{L^2[-\Lambda, \Lambda]} \\ &\leq C \{ \|\widehat{\mathcal{P}}_n \widehat{\mathcal{K}}_B (I - \widehat{\mathcal{P}}_n) \widehat{u}\|_{L^2[-\Lambda, \Lambda]} \\ &\quad + \|\widehat{\mathcal{P}}_n (\widehat{\mathcal{L}}_B - \widehat{\mathcal{K}}_B) (I - \widehat{\mathcal{P}}_n) \widehat{u}\|_{L^2[-\Lambda, \Lambda]} \}. \end{aligned} \quad (4.3.22)$$

It can be shown that the first term on the right-hand side of (4.3.22) satisfies , cf. [36, Theorem 3.3]

$$\|\widehat{\mathcal{P}}_n \widehat{\mathcal{K}}_B (I - \widehat{\mathcal{P}}_n) \widehat{u}\|_{L^2[-\Lambda, \Lambda]} \leq C \|(I - \widehat{\mathcal{P}}_n) \widehat{u}\|_{L^2[-\Lambda, \Lambda]}. \quad (4.3.23)$$

Moreover, applying Lemma 4.8,

$$\begin{aligned}
\|\widehat{\mathcal{P}}_n(\widehat{\mathcal{L}}_B - \widehat{\mathcal{K}}_B)(I - \widehat{\mathcal{P}}_n)\widehat{u}\|_{L^2[-\Lambda, \Lambda]}^2 &= \sum_{i=1}^n \|\widehat{\mathcal{P}}_n(\widehat{\mathcal{L}}_B - \widehat{\mathcal{K}}_B)(I - \widehat{\mathcal{P}}_n)\widehat{u}\|_{L^2(I_i)}^2 \\
&\leq C \sum_{i=1}^n h_i \max_{j=1, \dots, r} |(\widehat{\mathcal{L}}_B - \widehat{\mathcal{K}}_B)(I - \widehat{\mathcal{P}}_n)\widehat{u}(x_{ij}^r)|^2 \\
&\leq C \left\{ \sum_{i=1}^n h_i \right\} \|(I - \widehat{\mathcal{P}}_n)\widehat{u}\|_{pL^2[-\Lambda, \Lambda]}^2 \quad (4.3.24)
\end{aligned}$$

$$\leq C \|(I - \widehat{\mathcal{P}}_n)\widehat{u}\|_{L^2[-\Lambda, \Lambda]}^2. \quad (4.3.25)$$

(The inequality (4.3.24) follows because the kernel of $\widehat{\mathcal{L}}_B - \widehat{\mathcal{K}}_B$ is bounded.) The result now follows by combining (4.3.21), (4.3.22), (4.3.23) and (4.3.25). \square

It follows from Lemma 4.9 that to obtain convergence rates we need estimates on the interpolation error $\|\widehat{u} - \widehat{\mathcal{P}}_n\widehat{u}\|_{L^2[-\Lambda, \Lambda]}$. These of course depend on the regularity of the solution. To describe this regularity we introduce the weighted Sobolev space for an interval $J \subset \mathbb{R}$. For $k \in \mathbb{N}$ and $\alpha \in \mathbb{R}$

$$L_\alpha^{2,k}(J) = \{v : |x|^{j-\alpha} D^j v \in L^2(J), j = 0, 1, \dots, k\}, \quad (4.3.26)$$

equipped with the norm $\|v\|_{L_\alpha^{2,k}(J)} = \sum_{j=0}^k \| |x|^{j-\alpha} D^j v \|_{L^2(J)}$, (see [35]). Note that when $r < \alpha$,

$$L_\alpha^{2,r}[-\Lambda, \Lambda] \subset H^r[-\Lambda, \Lambda] := \{v \in L^2[-\Lambda, \Lambda] : D^r v \in L^2[-\Lambda, \Lambda]\}. \quad (4.3.27)$$

Examples 4.10.

(i) The function

$$\widehat{u}(x) = C' + C''|x|^\theta, \quad \text{where } 1/2 < \theta < 1, \quad (4.3.28)$$

satisfies $\widehat{u}(x) - C' \in L_\alpha^{2,k}[-\Lambda, \Lambda]$ for all $k \geq 0$ and $\alpha < \theta + 1/2$.

(ii) The function

$$\widehat{u}(x) = C|x|^{\theta-1}, \quad \text{where } 1/2 < \theta < 1, \quad (4.3.29)$$

satisfies $\widehat{u}(x) \in L_\alpha^{2,k}[-\Lambda, \Lambda]$ for all $k \geq 0$ and $\alpha < \theta - 1/2$.

Remark 4.11. When we solve the Dirichlet problem for the Laplace equation in the region interior to a planar polygon using the indirect boundary integral method the solution of the resulting integral equation has its principal singularity

in the form (4.3.28) where the corner is at $x = 0$ and $\theta = 1/(1 + |\chi|)$, where $(1 - \chi)\pi$ is the angle subtended by the corner ($\chi \in (-1, 1) \setminus \{0\}$). When we solve the Neumann problem with the same geometry again using the indirect boundary method the density has its principal singularity in the form (4.3.29), again with $\theta = 1/(1 + |\chi|)$ (see e.g [27], [45], [36]).

Since the integral operator in the spherical boundary integral equations which we are solving in this thesis has a principal part which coincides with the Laplace operator we conjecture that the solutions of our integral equations have the same principal singularity as identified in Examples 4.10 (i) and (ii). The numerical results below support this conjecture.

Following Remark 4.11 in Theorems 4.12 and 4.13 we will prove estimates for $\|(I - \widehat{\mathcal{P}}_n)\widehat{u}\|_{L^2[-\Lambda, \Lambda]}$ under assumptions which encapsulate Examples 4.10(i) and (ii).

Theorem 4.12. *Suppose there exists a constant $C' = C'(\widehat{u})$ such that $\widehat{u} - C' \in L_\alpha^{2,r}[-\Lambda, \Lambda]$ for some $\alpha > 1$. Then,*

$$\|(I - \widehat{\mathcal{P}}_n)\widehat{u}\|_{L^2[-\Lambda, \Lambda]} \leq Cn^{-r}\|\widehat{u} - C'\|_{L_\alpha^{2,r}[-\Lambda, \Lambda]},$$

when $q \geq \max\{r/\alpha, 1\}$ for some C independent of n and \widehat{u} .

Proof Throughout the proof C denotes a generic constant independent of n . Due to the symmetry of the collocation points about the origin it is sufficient to prove

$$\|(I - \widehat{\mathcal{P}}_n)\widehat{u}\|_{L^2[0, \Lambda]} \leq Cn^{-r}\|\widehat{u} - C'\|_{L_\alpha^{2,r}[0, \Lambda]}. \quad (4.3.30)$$

First of all recall the standard estimates for piecewise polynomial interpolation, cf. [34, pg. 554],

$$\|(I - \widehat{\mathcal{P}}_n)\widehat{u}\|_{L^2(I_i)} \leq Ch_i^j \|D^j \widehat{u}\|_{L^2(I_i)} \quad (4.3.31)$$

for $j = 1, \dots, r$, provided the norm on the right-hand side is finite.

When $r < \alpha$, $\widehat{u} - C' \in H^r[-\Lambda, \Lambda]$ by (4.3.27). We can apply (4.3.31) with the mesh (4.3.2) taken to be uniform, (i.e. $q = 1$) and $j = r$ to obtain

$$\begin{aligned} \|(I - \widehat{\mathcal{P}}_n)\widehat{u}\|_{L^2[0, \Lambda]} &\leq Cn^{-r}\|D^r \widehat{u}\|_{L^2[0, \Lambda]} = Cn^{-r}\|D^r(\widehat{u} - C')\|_{L^2[0, \Lambda]} \\ &\leq Cn^{-r}\|\widehat{u} - C'\|_{L_\alpha^{2,r}[0, \Lambda]}. \end{aligned}$$

Now assume $r \geq \alpha$. Applying (4.3.31) on $I_{m+1}(= [0, x_{m+1}])$ with $j = 1$ we

obtain

$$\begin{aligned}
\|(I - \widehat{\mathcal{P}}_n)\widehat{u}\|_{L^2(I_{m+1})} &\leq Ch_{m+1}\|D\widehat{u}\|_{L^2(I_{m+1})} \\
&= Ch_{m+1}\left\{\int_0^{h_{m+1}} x^{2\alpha-2}|x^{1-\alpha}D\widehat{u}(x)|^2 dx\right\}^{1/2} \\
&\leq Ch_{m+1}^\alpha\|x^{1-\alpha}D\widehat{u}\|_{L^2(I_{m+1})} = Cm^{-q\alpha}\|x^{1-\alpha}D(\widehat{u} - C')\|_{L^2(I_{m+1})} \\
&\leq Cn^{-r}\|\widehat{u} - C'\|_{L_\alpha^{2,r}(I_{m+1})}, \tag{4.3.32}
\end{aligned}$$

when $q \geq r/\alpha$ (note from (4.3.2) that $h_{m+1} = Cm^{-q} = O(n^{-q})$).

For the other intervals I_i , $i > m + 1$, we apply (4.3.31) with $j = r$ to obtain

$$\|(I - \widehat{\mathcal{P}}_n)\widehat{u}\|_{L^2(I_i)} \leq Ch_i^r \left\{ \int_{I_i} x^{2\alpha-2r} |x^{r-\alpha} D^r \widehat{u}(x)|^2 dx \right\}^{1/2}. \tag{4.3.33}$$

Since $r \geq \alpha$ this yields,

$$\|(I - \widehat{\mathcal{P}}_n)\widehat{u}\|_{L^2(I_i)} \leq Ch_i^r x_{i-1}^{\alpha-r} \|x^{r-\alpha} D^r \widehat{u}\|_{L^2(I_i)} \leq Ch_i^r x_i^{\alpha-r} \|\widehat{u} - C'\|_{L_\alpha^{2,r}(I_i)}. \tag{4.3.34}$$

(Here we have used the fact that for $i > m + 1$, there exist constants C_1, C_2 independent of i and n such that $C_2 \leq x_{i-1}/x_i \leq C_1$.) From (4.3.2), $x_i = ((i - m)/m)^q \Lambda$ and so,

$$h_i = \left(\frac{i - m}{m}\right)^q \Lambda - \left(\frac{i - m - 1}{m}\right)^q \Lambda \leq C \left(\frac{i - m}{m}\right)^q \frac{1}{i - m},$$

where C depends on q but is independent of n . Therefore, since $\alpha q \geq r$ we have

$$\begin{aligned}
h_i^r x_i^{\alpha-r} &\leq C \left(\frac{i - m}{m}\right)^{qr} (i - m)^{-r} \left(\frac{i - m}{m}\right)^{q(\alpha-r)} = C \left(\frac{i - m}{m}\right)^{q\alpha-r} m^{-r} \\
&\leq Cm^{-r} \leq Cn^{-r}. \tag{4.3.35}
\end{aligned}$$

Hence it follows from (4.3.34) that,

$$\|(I - \widehat{\mathcal{P}}_n)\widehat{u}\|_{L^2(I_i)} \leq Cn^{-r} \|\widehat{u} - C'\|_{L_\alpha^{2,r}(I_i)}. \tag{4.3.36}$$

Combining (4.3.32) and (4.3.36) gives (4.3.30) and the result follows. \square

Theorem 4.13. *Suppose that $\widehat{u} \in L_\alpha^{2,r}[-\Lambda, \Lambda]$ for some $\alpha > 0$. Then*

$$\|(I - \widehat{\mathcal{P}}_n)\widehat{u}\|_{L^2[-\Lambda, \Lambda]} \leq Cn^{-r} \|\widehat{u}\|_{L_\alpha^{2,r}[-\Lambda, \Lambda]},$$

when $q \geq \max\{r/\alpha, 1\}$.

Proof As in the proof of Theorem 4.12 it is sufficient to show

$$\|(I - \widehat{\mathcal{P}}_n)\widehat{u}\|_{L^2[0,\Lambda]} \leq Cn^{-r} \|\widehat{u}\|_{L_\alpha^{2,r}[0,\Lambda]}, \quad (4.3.37)$$

and this is trivial when $r < \alpha$. So assuming $r \geq \alpha$, and repeating the argument in the proof of Theorem 4.12 it follows from the inequality on the left-hand side of (4.3.34) that, for $i > m + 1$,

$$\|(I - \widehat{\mathcal{P}}_n)\widehat{u}\|_{L^2(I_i)} \leq Ch_i^r x_{i-1}^{\alpha-r} \|x^{r-\alpha} D^r \widehat{u}\|_{L^2(I_i)} \leq Ch_i^r x_i^{\alpha-r} \|\widehat{u}\|_{L_\alpha^{2,r}(I_i)}$$

hence, by (4.3.35),

$$\|(I - \widehat{\mathcal{P}}_n)\widehat{u}\|_{L^2(I_i)} \leq Cn^{-r} \|\widehat{u}\|_{L_\alpha^{2,r}(I_i)}, \quad (4.3.38)$$

when $q \geq r/\alpha$. Therefore to complete the proof we need to show (4.3.38) holds when $i = m + 1$. To do this, note that Lemma 4.8 applied on I_{m+1} implies,

$$\|\widehat{\mathcal{P}}_n \widehat{u}\|_{L^2(I_{m+1})}^2 \leq Ch_{m+1} \max_{j=1,\dots,r} |\widehat{u}(\xi_j^r h_{m+1})|^2, \quad (4.3.39)$$

(recall from (4.1.2) and (4.3.2) that $x_{m+1,j} = \xi_j^r h_{m+1}$). (Note that \widehat{u} is well defined at the collocation points since $D\widehat{u}$ is integrable on any open interval in $[-\Lambda, \Lambda] \setminus \{0\}$.) Now following [34, Lemma 4.1], for each $j = 1, \dots, r$ we can write

$$h_{m+1} |\widehat{u}(\xi_j^r h_{m+1})|^2 = (\xi_j^r)^{-2} h_{m+1}^{-1} \left| \int_0^{\xi_j^r h_{m+1}} D\{x\widehat{u}(x)\} dx \right|^2. \quad (4.3.40)$$

(Note that $x\widehat{u}(x)$ must vanish at $x = 0$ since $\widehat{u} \in L_\alpha^{2,r}[-\Lambda, \Lambda]$ with $\alpha > 0$.) Hence applying the product rule followed by the Cauchy-Schwartz inequality to (4.3.40), we have,

$$\begin{aligned} h_{m+1} |\widehat{u}(\xi_j^r h_{m+1})|^2 &= (\xi_j^r)^{-2} h_{m+1}^{-1} \left| \int_0^{\xi_j^r h_{m+1}} \{\widehat{u}(x) + xD\widehat{u}(x)\} dx \right|^2 \\ &\leq (\xi_j^r)^{-2} h_{m+1}^{-1} \left\{ \int_0^{\xi_j^r h_{m+1}} 1 dx \right\} \left\{ \int_0^{\xi_j^r h_{m+1}} |\widehat{u}(x) + xD\widehat{u}(x)|^2 dx \right\} \\ &\leq (\xi_j^r)^{-1} \int_0^{h_{m+1}} |\widehat{u}(x) + xD\widehat{u}(x)|^2 dx \leq C \|\widehat{u}(x) + xD\widehat{u}(x)\|_{L^2(I_{m+1})}^2. \end{aligned}$$

Combining this with (4.3.39) and applying the triangle inequality gives,

$$\|\widehat{\mathcal{P}}_n \widehat{u}\|_{L^2(I_{m+1})} \leq C \{ \|\widehat{u}\|_{L^2(I_{m+1})} + \|xD\widehat{u}(x)\|_{L^2(I_{m+1})} \}. \quad (4.3.41)$$

(Note that $\widehat{\mathcal{P}}_n$ is not bounded on $L^2(I_{m+1})$. The estimate (4.3.41) reflects this but is enough for our purposes.) Thus, using (4.3.41) we obtain, after another application of the triangle inequality,

$$\|(I - \widehat{\mathcal{P}}_n)\widehat{u}\|_{L^2(I_{m+1})} \leq C\{\|\widehat{u}\|_{L^2(I_{m+1})} + \|xD\widehat{u}(x)\|_{L^2(I_{m+1})}\}. \quad (4.3.42)$$

We now estimate each term on the right-hand side of (4.3.42).

First consider $\|\widehat{u}\|_{L^2(I_{m+1})}$. For this quantity, we have

$$\begin{aligned} \|\widehat{u}\|_{L^2(I_{m+1})} &= \left\{ \int_0^{h_{m+1}} x^{2\alpha} |x^{-\alpha}\widehat{u}(x)|^2 dx \right\}^{1/2} \leq Ch_{m+1}^\alpha \|\widehat{u}\|_{L_\alpha^{2,r}(I_{m+1})} \\ &\leq Cn^{-r} \|\widehat{u}\|_{L_\alpha^{2,r}(I_{m+1})}, \end{aligned} \quad (4.3.43)$$

when $q \geq r/\alpha$. Arguing in the same way, it is clear that

$$\|xD\widehat{u}(x)\|_{L^2(I_{m+1})} \leq Cn^{-r} \|\widehat{u}\|_{L_\alpha^{2,r}(I_{m+1})}. \quad (4.3.44)$$

Therefore, combining (4.3.42), (4.3.43) and (4.3.44) we obtain

$$\|(I - \widehat{\mathcal{P}}_n)\widehat{u}\|_{L^2(I_{m+1})} \leq Cn^{-r} \|\widehat{u}\|_{L_\alpha^{2,r}(I_{m+1})},$$

which, along with (4.3.38) gives (4.3.37) and hence the result. \square

Theorem 4.14. (i) Suppose that $B = D$ and that the exact solution to (4.0.1) satisfies $\widehat{u} - C' \in L_\alpha^{2,r}[-\Lambda, \Lambda]$ with $1 < \alpha < 3/2$, then for sufficiently large n the collocation method described by (4.3.3) converges with error

$$\|\widehat{u} - \widehat{u}_n\|_{L^2[-\Lambda, \Lambda]} = Cn^{-r} \|\widehat{u} - C'\|_{L_\alpha^{2,r}[-\Lambda, \Lambda]} \quad \text{as } n \rightarrow \infty, \quad (4.3.45)$$

provided the grading parameter $q \geq \max\{r/\alpha, 1\}$.

(ii) Suppose that $B = N$ and that the exact solution to (4.0.1) satisfies $\widehat{u} \in L_\alpha^{2,r}[-\Lambda, \Lambda]$ for some $0 < \alpha < 1/2$, then for sufficiently large n the collocation method described by (4.3.3) converges with error

$$\|\widehat{u} - \widehat{u}_n\|_{L^2[-\Lambda, \Lambda]} = Cn^{-r} \|\widehat{u}\|_{L_\alpha^{2,r}[-\Lambda, \Lambda]} \quad \text{as } n \rightarrow \infty, \quad (4.3.46)$$

provided the grading parameter $q \geq r/\alpha$.

Proof It follows from Lemma 4.9 that for both the Dirichlet problem and the

Neumann problem

$$\|\widehat{u} - \widehat{u}_n\|_{L^2[-\Lambda, \Lambda]} \leq C \|(I - \widehat{\mathcal{P}}_n)\widehat{u}\|_{L^2[-\Lambda, \Lambda]}. \quad (4.3.47)$$

Therefore the proofs of (i) and (ii) now follow by applying Theorems 4.12 and 4.13, respectively. \square

Theorem 4.14 is a theoretical result which assumes the matrix entries (4.1.6) are computed exactly. In practice numerical approximations are needed. In §4.4 we give sufficient conditions for the accuracy of the approximations needed to calculate the matrix entries (4.1.6). Before we do this we briefly discuss the *hp*-version of collocation for the remainder of this section. (We insert this discussion because the *hp*-version is used for some of the experiments in Chapter 6.)

4.3.2 The *hp*-refinement method

We investigate here the *hp*-version of collocation which we obtain by simultaneously refining the mesh and increasing the order of the approximating piecewise polynomial. The *hp*-refinement method has been thoroughly investigated in its application to the finite element method on planar polygonal domains. Moreover, for the finite element method, it has been shown in [49] that if the boundary data is piecewise analytic then the *hp*-version converges exponentially whilst the *h*-version has a polynomial rate of convergence (with respect to the number of degrees of freedom). Following [49] corresponding results have been shown for the *hp*-method applied to the boundary element method see e.g. [37] [66].

For the *hp*-version of collocation we use a geometric mesh with refinement towards 0. For fixed $\sigma \in (0, 1)$ we define the nodes of the mesh by

$$x_{m \pm i} = \pm \sigma^{m-i} \Lambda, \quad \text{for } i = 1, \dots, m, \quad x_0 = 0.$$

(This is different from the algebraically refined mesh in (4.3.2).) We seek an approximate solution on the space, S_n^r associated with this mesh. A typical distribution of orders \mathbf{r} in the *hp*-version of collocation would be:

$$r_i = \lceil (m+1-i)\beta \rceil \quad \text{for } i = 1, \dots, m-1, \quad r_i = \lceil (i-m)\beta \rceil \quad \text{for } i = m+2, \dots, n, \quad (4.3.48)$$

for some fixed parameter $\beta > 0$ and $r_i = 1$ for $i = m, m+1$ (in fact, we set the approximating polynomial equal to zero for $i = m, m+1$). Here, for $x \in \mathbb{R}$,

$[x]$ denotes the smallest integer greater than or equal to x . Thus close to 0 we approximate the solution on small subintervals, using low order methods, while further away we use higher order on larger subintervals. The maximum order increases linearly with m and hence also n . Again we define the corresponding projection of $L^2[-\Lambda, \Lambda]$ onto $S_n^{\mathbf{r}}$ by $\widehat{\mathcal{P}}_n$ with the dependence on σ, β and \mathbf{r} suppressed from the notation.

The next result shows that the hp -version of collocation is stable.

Theorem 4.15. *For $B = D$ or N and for n sufficiently large, $(I + \widehat{\mathcal{P}}_n \widehat{\mathcal{L}}_B)^{-1}$ exists and is bounded on $L^2[-\Lambda, \Lambda]$.*

Proof The proof is analogous to the proof of the stability of the h -version of collocation. First consider $I \pm \widetilde{\mathcal{P}}_n \widetilde{\mathcal{K}}_B$, $B = D, N$ where $\widetilde{\mathcal{K}}_B$ is defined in the proof of Theorem 3.14 and $\widetilde{\mathcal{P}}_n$ is defined as in (4.3.7) (but obviously with respect to the approximation space $S_n^{\mathbf{r}}$ with \mathbf{r} defined by (4.3.48)). It follows from [37, Theorem 4.3] that $I \pm \widetilde{\mathcal{P}}_n \widetilde{\mathcal{K}}_B$ are invertible on $L^2[0, \Lambda]$ if $\widetilde{\kappa}_B$ satisfies the conditions (4.3.9) - (4.3.11) (verified in the proof of Theorem 4.4). In addition to these conditions we also require that the kernel $\widetilde{\kappa}_B$ satisfies the following smoothness condition:

$$\int_0^\infty x^{-1/2} |x^j D^j \widetilde{\kappa}_B(x)| dx < \infty, \quad \text{for } j = 1, 2,$$

which can be verified after some manipulation. Therefore by repeating the argument in Theorem 4.4 it follows that $I + \widehat{\mathcal{P}}_n \widehat{\mathcal{K}}_B$ is invertible on $L^2[-\Lambda, \Lambda]$. It is clear that the result follows using the same argument as in Theorem 4.6. \square

Remark 4.16. Note that the parameter i_0 does not appear in Theorem 4.15. However the approximating polynomial is set to zero on the two subintervals containing the corner and the order of the approximating polynomial increases as the mesh is refined.

As we have shown, the collocation equation (4.3.3) is convergent in a Sobolev space setting for the h -version of collocation. However in order to derive exponential convergence of the hp -method we need to have estimates in a certain countably normed space of real-analytic functions on $[-\Lambda, \Lambda] \setminus \{0\}$ (see [37]). This space is defined as follows For $\alpha > 0$, we define

$$B_\alpha(I) = \{v : \exists d > 0 \text{ independent of } j \text{ such that} \\ \|x^{j-\alpha} D^j v\|_{L^2(I)} \leq d^{j+1} j!, j = 0, 1, 2, \dots\}.$$

In view of this we can now state the following theorem which is key in proving the exponential convergence of the hp -method.

Theorem 4.17. *Suppose that $\widehat{u} \in B_\alpha[-\Lambda, \Lambda]$ and β in (4.3.48) is sufficiently large, then*

$$\|(I - \widehat{\mathcal{P}}_n)\widehat{u}\|_{L^2(I_I)} \leq Ce^{-bn},$$

where C and b depend on \widehat{u} , β , σ and α but are independent of n .

We do not give a proof here but the result can be derived from [37, pp. 58-61]

By assuming regularity of the exact solution to (3.1.27) we get the following lemma on the convergence of the hp -method.

Lemma 4.18. *Suppose that $\widehat{u} \in B_\alpha[-\Lambda, \Lambda]$ and that β and n are sufficiently large. Then the hp -collocation method on the approximation space $S_n^{\mathbf{r}}[-\Lambda, \Lambda]$ (with \mathbf{r} defined by (4.3.48)) converges with error,*

$$\|\widehat{u} - \widehat{u}_n\|_{L^2[-\Lambda, \Lambda]} \leq Ce^{-bn}, \quad \text{as } n \rightarrow \infty, \quad (4.3.49)$$

where C and b depend on \widehat{u} , β , σ and α but are independent of n .

Proof From Theorem 4.15 and recalling the proof of Theorem 4.14 we have the following bound

$$\|\widehat{u} - \widehat{u}_n\|_{L^2[-\Lambda, \Lambda]} \leq C\|\widehat{u} - \widehat{\mathcal{P}}_n\widehat{u}\|_{L^2[-\Lambda, \Lambda]}. \quad (4.3.50)$$

The result follows from Theorem 4.17. \square

Remark 4.19. The required regularity condition, $\widehat{u} \in B_\alpha[-\Lambda, \Lambda]$, is proved in [37, Theorem 2.1] for the pure Mellin convolution operator, $\widetilde{\mathcal{K}}_B$. Since the operator $\widehat{\mathcal{L}}_B$ of interest in this thesis is a smoothing perturbation of $\widehat{\mathcal{K}}_B$ we expect the same regularity to hold in our application, it is not immediately obvious that the regularity assumption in Lemma 4.18 holds for our application and it is outside the scope of the thesis to prove it. However the results in §6.3.1 indicate that the hp -method does converge exponentially in this case.

In the next section we consider a fully discrete collocation method which maintains optimal convergence only for the h -refinement method. However the theoretical rates of convergence for the hp -refinement method seen here are also observed numerically in §6.3.1, by employing an analogous quadrature scheme to calculate the matrix entries (4.1.6).

4.4 The discrete collocation method

In §4.2 and §4.3 we have given theoretical convergence results for the collocation method based on the assumption that the matrix entries are computed exactly. However in practice numerical techniques are required. In this section we consider the collocation equation

$$(I + \widehat{\mathcal{P}}_n \widehat{\mathcal{L}}) \widehat{u}_n = \widehat{b}, \quad (4.4.1)$$

(we have dropped the dependence on boundary conditions from the notation to simplify the presentation in this section). We aim to give sufficient conditions on the degree of exactness of the quadrature rules used to compute the corresponding matrix entries in order to maintain optimal convergence of the overall method.

Recall that for general collocation method (4.4.1) the matrix entries are given by (4.1.6), i.e.

$$\widehat{\mathbb{L}}_{i'j',ij} = \int_{I_i} \widehat{L}(x_{i'j'}^{r_{i'}}, \sigma) \phi_{ij}(\sigma) d\sigma, \quad \text{for } (i, j), (i', j') \in \mathcal{J},$$

where ϕ_{ij} is the j th basis function for polynomials of order r_i on the interval I_i . In general these integrals have no explicit formula and so they will need to be calculated numerically. We call the resulting method for approximating the solution to (4.4.1) the *discrete collocation method*. To define this method more precisely we introduce the possibility of approximating $(\widehat{\mathcal{L}}\phi_{ij})(s)$ by $\widehat{\mathbb{L}}_{ij}^d(s)$, $\widehat{\mathbb{L}}_{ij}^d(s) \approx (\widehat{\mathcal{L}}\phi_{ij})(s)$, where d stands for discrete.

For any $v_n \in S_n^r[-\Lambda, \Lambda]$, $v_n(s) = \sum_{i=1}^n \sum_{j=1}^{r_i} v_{ij} \phi_{ij}(s)$, the action of $\widehat{\mathcal{L}}$ on v_n is

$$\widehat{\mathcal{L}}v_n(s) = \sum_{i=1}^n \sum_{j=1}^{r_i} (\widehat{\mathcal{L}}\phi_{ij})(s) v_{ij}. \quad (4.4.2)$$

The corresponding approximation of this is,

$$\widehat{\mathcal{L}}^d v_n(s) = \sum_{i=1}^n \sum_{j=1}^{r_i} \widehat{\mathbb{L}}_{ij}^d(s) v_{ij}. \quad (4.4.3)$$

Note, $\widehat{\mathcal{L}}^d$ is defined only on $S_n^r[-\Lambda, \Lambda]$. Recall that the functions $\widehat{\mathcal{L}}\phi_{ij}(s)$ are all continuous at $x_{ij}^{r_i}$ so $\widehat{\mathcal{P}}_n \widehat{\mathcal{L}}$ is well defined on $S_n^r[-\Lambda, \Lambda]$. We assume that $\widehat{\mathbb{L}}_{ij}^d$ are also continuous at $x_{ij}^{r_i}$ so that $\widehat{\mathcal{P}}_n \widehat{\mathcal{L}}^d$ is also well defined on $S_n^r[-\Lambda, \Lambda]$. The discrete collocation solution $\widehat{u}_n^d \in S_n^r[-\Lambda, \Lambda]$ is defined by,

$$(I + \widehat{\mathcal{P}}_n \widehat{\mathcal{L}}^d) \widehat{u}_n^d = \widehat{\mathcal{P}}_n \widehat{b}. \quad (4.4.4)$$

If we write $\widehat{u}_n^d(s) = \sum_{i=1}^n \sum_{j=1}^{r_i} \widehat{\mu}_{ij}^d \phi_{ij}(s)$ then $\widehat{\mu}_{ij}^d$ may be found from the linear system,

$$\widehat{\mu}_{i'j'}^d + \sum_{i=1}^n \sum_{j=1}^{r_i} \widehat{\mu}_{ij}^d \widehat{\mathbb{L}}_{i'j',ij}^d = \widehat{b}(x_{i'j'}^{r_{i'}}), \quad (i', j'), (i, j) \in \mathcal{J}, \quad (4.4.5)$$

where

$$\widehat{\mathbb{L}}_{i'j',ij}^d = \widehat{\mathbb{L}}_{ij}^d(x_{i'j'}^{r_{i'}}). \quad (4.4.6)$$

Comparing this with (4.1.4) we see that $\widehat{\boldsymbol{\mu}}^d$ satisfies the same equation as $\widehat{\boldsymbol{\mu}}$ but with matrix entry $\widehat{\mathbb{L}}_{i'j',ij}$ replaced by its approximation $\widehat{\mathbb{L}}_{i'j',ij}^d$.

This leads to different versions of the discrete collocation method, depending on how the functions $\widehat{\mathbb{L}}_{ij}^d(s)$ are defined. For the remainder of this section we consider only a h -version of the collocation method and take $\widehat{\mathcal{P}}_n$ to be the projection onto the h -refinement approximation space $S_n^r[-\Lambda, \Lambda]$ defined in §4.2 and §4.3.1, i.e. $\widehat{\mathcal{P}}_n$ projects onto a space of piecewise polynomials of order $r_i = r$, for each $i = 1, \dots, n$. We describe the sufficient conditions that the functions $\widehat{\mathbb{L}}_{ij}^d$ should satisfy to ensure that the discrete collocation solution \widehat{u}_n^d converges to the exact solution \widehat{u} optimally i.e. $\|\widehat{u} - \widehat{u}_n^d\|_{L^2[-\Lambda, \Lambda]} = O(n^{-r})$. To analyse (4.4.4) we use the following lemma:

Lemma 4.20. *Assuming $(I + \widehat{\mathcal{P}}_n \widehat{\mathcal{L}}^d)^{-1}$ exists, then*

$$\widehat{u} - \widehat{u}_n^d = (\widehat{u} - \widehat{u}_n) + \widehat{\delta}_n \quad (4.4.7)$$

where the perturbation $\widehat{\delta}_n$ is given by

$$\widehat{\delta}_n = (I + \widehat{\mathcal{P}}_n \widehat{\mathcal{L}}^d)^{-1} \widehat{\mathcal{P}}_n (\widehat{\mathcal{L}} - \widehat{\mathcal{L}}^d) \widehat{u}_n. \quad (4.4.8)$$

Proof Clearly (4.4.7) holds with

$$\widehat{\delta}_n := \widehat{u}_n - \widehat{u}_n^d. \quad (4.4.9)$$

Now observe that,

$$\begin{aligned} (I + \widehat{\mathcal{P}}_n \widehat{\mathcal{L}}^d) \widehat{\delta}_n &= (I + \widehat{\mathcal{P}}_n \widehat{\mathcal{L}}^d) \widehat{u}_n - (I + \widehat{\mathcal{P}}_n \widehat{\mathcal{L}}^d) \widehat{u}_n^d \\ &= (I + \widehat{\mathcal{P}}_n \widehat{\mathcal{L}}) \widehat{u}_n - (I + \widehat{\mathcal{P}}_n \widehat{\mathcal{L}}^d) \widehat{u}_n^d + \widehat{\mathcal{P}}_n (\widehat{\mathcal{L}}^d - \widehat{\mathcal{L}}) \widehat{u}_n, \end{aligned} \quad (4.4.10)$$

which implies (4.4.8) since the first two terms on the right-hand side of (4.4.10) are each equal to $\widehat{\mathcal{P}}_n \widehat{b}$. \square

In order to use Lemma 4.20, we need to establish that $(I + \widehat{\mathcal{P}}_n \widehat{\mathcal{L}}^d)^{-1}$ exists as an operator on $S_n^r[-\Lambda, \Lambda]$ and is uniformly bounded. In view of the stability of

the true collocation method (Theorem 4.6) a sufficient condition for this is that

$$\|\widehat{\mathcal{P}}_n(\widehat{\mathcal{L}} - \widehat{\mathcal{L}}^d)|_{S_n^r}\|_{L^2[-\Lambda, \Lambda]} \rightarrow 0 \quad \text{as } n \rightarrow \infty. \quad (4.4.11)$$

When (4.4.11) holds, the rate of convergence of \widehat{u}_n^d to \widehat{u} depends on the rate of convergence in (4.4.11). We make this more precise in the next theorem. In what follows we use C to denote a generic constant whose value may change from line to line.

Theorem 4.21. *Suppose that the collocation method (4.4.1) is stable. Suppose also that for each n there exist $\epsilon_n \in \mathbb{R}$ such that*

$$\|\widehat{\mathcal{P}}_n(\widehat{\mathcal{L}} - \widehat{\mathcal{L}}^d)v_n\|_{L^2[-\Lambda, \Lambda]} \leq \epsilon_n \|v_n\|_{L^2[-\Lambda, \Lambda]}, \quad (4.4.12)$$

for all $v_n \in S_n^r[-\Lambda, \Lambda]$.

If $\epsilon_n \rightarrow 0$ as $n \rightarrow \infty$ then the discrete collocation equation (4.4.4) is stable, i.e. $(I + \widehat{\mathcal{P}}_n \widehat{\mathcal{L}}^d)^{-1}$ exists and is uniformly bounded on $S_n^r[-\Lambda, \Lambda]$ for n sufficiently large. Moreover,

$$\|\widehat{u} - \widehat{u}_n^d\|_{L^2[-\Lambda, \Lambda]} \leq \|\widehat{u} - \widehat{u}_n\|_{L^2[-\Lambda, \Lambda]} + C \epsilon_n \|\widehat{b}\|_{L^\infty[-\Lambda, \Lambda]}, \quad (4.4.13)$$

where C depends on \widehat{b} but is independent of n .

Proof As we have assumed the method for computing \widehat{u}_n is stable, $\|(I + \widehat{\mathcal{P}}_n \widehat{\mathcal{L}})^{-1}\|_{L^2[-\Lambda, \Lambda]}$ is uniformly bounded in n . Therefore,

$$\|(I + \widehat{\mathcal{P}}_n \widehat{\mathcal{L}})v_n\|_{L^2[-\Lambda, \Lambda]} \geq C \|v_n\|_{L^2[-\Lambda, \Lambda]} \quad (4.4.14)$$

for some constant $C > 0$ and all $v_n \in S_n^r[-\Lambda, \Lambda]$. Now notice that, by (4.4.12),

$$\begin{aligned} \|(I + \widehat{\mathcal{P}}_n \widehat{\mathcal{L}}^d)v_n - (I + \widehat{\mathcal{P}}_n \widehat{\mathcal{L}})v_n\|_{L^2[-\Lambda, \Lambda]} &= \|\widehat{\mathcal{P}}_n(\widehat{\mathcal{L}}^d - \widehat{\mathcal{L}})v_n\|_{L^2[-\Lambda, \Lambda]} \\ &\leq \epsilon_n \|v_n\|_{L^2[-\Lambda, \Lambda]}. \end{aligned} \quad (4.4.15)$$

Therefore, using the reverse triangle inequality,

$$\|(I + \widehat{\mathcal{P}}_n \widehat{\mathcal{L}})v_n\|_{L^2[-\Lambda, \Lambda]} - \|(I + \widehat{\mathcal{P}}_n \widehat{\mathcal{L}}^d)v_n\|_{L^2[-\Lambda, \Lambda]} \leq \epsilon_n \|v_n\|_{L^2[-\Lambda, \Lambda]}.$$

Combining this with (4.4.15) and (4.4.14), we get that, for all $v_n \in S_n^r[-\Lambda, \Lambda]$,

$$\begin{aligned} \|(I + \widehat{\mathcal{P}}_n \widehat{\mathcal{L}}^d)v_n\|_{L^2[-\Lambda, \Lambda]} &\geq \|(I + \widehat{\mathcal{P}}_n \widehat{\mathcal{L}})v_n\|_{L^2[-\Lambda, \Lambda]} - \epsilon_n \|v_n\|_{L^2[-\Lambda, \Lambda]} \\ &\geq (C - \epsilon_n) \|v_n\|_{L^2[-\Lambda, \Lambda]} \\ &\geq C' \|v_n\|_{L^2[-\Lambda, \Lambda]}, \end{aligned} \tag{4.4.16}$$

for some positive constant C' and sufficiently large n . This implies stability of the discrete collocation method. The bound (4.4.13) is a simple consequence of Lemma 4.20. It follows from (4.4.7), (4.4.8) and (4.4.12) that

$$\begin{aligned} \|\widehat{u} - \widehat{u}_n^d\|_{L^2[-\Lambda, \Lambda]} &\leq \|\widehat{u} - \widehat{u}_n\|_{L^2[-\Lambda, \Lambda]} + \|(I + \widehat{\mathcal{P}}_n \widehat{\mathcal{L}}^d)^{-1} P_n (\widehat{\mathcal{L}} - \widehat{\mathcal{L}}^d) \widehat{u}_n\|_{L^2[-\Lambda, \Lambda]} \\ &\leq \|\widehat{u} - \widehat{u}_n\|_{L^2[-\Lambda, \Lambda]} + C \epsilon_n \|\widehat{u}_n\|_{L^2[-\Lambda, \Lambda]}. \end{aligned}$$

Therefore, using the fact that $\widehat{u}_n = (I + \widehat{\mathcal{P}}_n \widehat{\mathcal{L}})^{-1} \widehat{\mathcal{P}}_n \widehat{b}$,

$$\begin{aligned} \|\widehat{u} - \widehat{u}_n^d\|_{L^2[-\Lambda, \Lambda]} &\leq \|\widehat{u} - \widehat{u}_n\|_{L^2[-\Lambda, \Lambda]} + C \epsilon_n \|\widehat{\mathcal{P}}_n \widehat{b}\|_{L^2[-\Lambda, \Lambda]} \\ &\leq \|\widehat{u} - \widehat{u}_n\|_{L^2[-\Lambda, \Lambda]} + C \epsilon_n \|\widehat{\mathcal{P}}_n \widehat{b}\|_{L^\infty[-\Lambda, \Lambda]} \\ &\leq \|\widehat{u} - \widehat{u}_n\|_{L^2[-\Lambda, \Lambda]} + C \epsilon_n \|\widehat{b}\|_{L^\infty[-\Lambda, \Lambda]}. \end{aligned}$$

Hence the result is proved. \square

Remark 4.22. When the collocation method converges optimally we have the following estimate, $\|\widehat{u} - \widehat{u}_n\|_{L^2[-\Lambda, \Lambda]} = O(n^{-r})$. Therefore it is natural to seek quadrature methods which satisfy $\epsilon_n = O(n^{-r})$.

Sufficient conditions for this are the subject of the next theorem. First we need the following inverse estimate.

Lemma 4.23. $\|v_n\|_{L^\infty(I_i)} \leq C h_i^{-1/2} \|v_n\|_{L^2(I_i)}$ for all $v_n \in S_n^r$, where $\|\cdot\|_{L^\infty(I_i)}$ is defined by $\|v_n\|_{L^\infty(I_i)} = \max_{x \in I_i} |v_n(x)|$.

Proof Since the space of polynomials of degree r is finite dimensional, we have,

$$\|p\|_{L^\infty[0,1]} \leq C \|p\|_{L^2[0,1]},$$

for all such polynomials, where C is a constant that depends on r but not on p . Applying this inequality to $p(x) = v_n(x_{i-1} + h_i x)$ (which is clearly a polynomial on $[0, 1]$) we get

$$\|v_n\|_{L^\infty(I_i)} = \|p\|_{L^\infty[0,1]} \leq C \|p\|_{L^2[0,1]},$$

and so since,

$$\|v_n\|_{L^2(I_i)}^2 = \int_{I_i} (v_n(x))^2 dx = \int_0^1 (v_n(x_{i-1} + xh_i))^2 h_i dx = h_i \|p\|_{L^2[0,1]}^2,$$

the result follows. \square

Theorem 4.24. *Define*

$$e_{i'j',ij} := |\mathbb{I}_{i'j',ij} - \mathbb{I}_{i'j',ij}^d| \quad (4.4.17)$$

and suppose

$$e_{i'j',ij} \leq Ch_i n^{-r}, \quad (4.4.18)$$

for some C independent of i' , j' , i and j then (4.4.12) holds with $\epsilon_n \leq Cn^{-r}$.

Proof First note that by applying Lemma 4.8 to $(\widehat{\mathcal{L}} - \widehat{\mathcal{L}}^d)v_n$ on the interval $I_{i'}$, for some $v_n \in S_n^r[-\Lambda, \Lambda]$, we have that

$$\|\widehat{\mathcal{P}}_n(\widehat{\mathcal{L}} - \widehat{\mathcal{L}}^d)v_n\|_{L^2(I_{i'})}^2 \leq Ch_{i'} \max_{j'=1,\dots,r} |(\widehat{\mathcal{L}} - \widehat{\mathcal{L}}^d)v_n(x_{i'j'}^r)|^2. \quad (4.4.19)$$

We will use this estimate to prove the result, therefore we need to investigate $|(\widehat{\mathcal{L}} - \widehat{\mathcal{L}}^d)v_n(x_{i'j'}^r)|$.

By writing $v_n(s) = \sum_{i=1}^n \sum_{j=1}^r v_{ij} \phi_{ij}(s)$, it follows from (4.1.6), (4.4.3), (4.4.6) and (4.4.2) that

$$\begin{aligned} |((\widehat{\mathcal{L}} - \widehat{\mathcal{L}}^d)v_n)(x_{i'j'}^r)| &= \left| \sum_{i=0}^n \sum_{j=0}^r (\widehat{\mathbb{I}}_{i'j',ij} - \widehat{\mathbb{I}}_{i'j',ij}^d) v_{ij} \right| \\ &\leq \sum_{i=0}^n \sum_{j=0}^r e_{i'j',ij} |v_{ij}| \leq Cn^{-r} \sum_{i=0}^n h_i \|v_n\|_{L^\infty(I_i)}, \end{aligned}$$

where in the last line we have used the assumption (4.4.18). Hence using the inverse estimate in Lemma 4.23 and the Cauchy-Schwartz inequality we have

$$\begin{aligned} |((\widehat{\mathcal{L}} - \widehat{\mathcal{L}}^d)v_n)(x_{i'j'}^r)| &\leq Cn^{-r} \sum_{i=0}^n h_i^{1/2} \|v_n\|_{L^2(I_i)} \\ &\leq Cn^{-r} \left\{ \sum_{i=0}^n h_i \right\}^{1/2} \left\{ \sum_{i=0}^n \|v_n\|_{L^2(I_i)}^2 \right\}^{1/2} \\ &\leq Cn^{-r} \|v_n\|_{L^2[-\Lambda, \Lambda]}. \end{aligned}$$

This together with (4.4.19) implies,

$$\|\widehat{\mathcal{P}}_n(\widehat{\mathcal{L}} - \widehat{\mathcal{L}}^d)v_n\|_{L^2[-\Lambda, \Lambda]}^2 \leq \sum_{i'=1}^n \|\widehat{\mathcal{P}}_n(\widehat{\mathcal{L}} - \widehat{\mathcal{L}}^d)v_n\|_{L^2(I_{i'})}^2 \leq C \left\{ \sum_{i'=1}^n h_{i'} \right\} n^{-2r} \|v_n\|_{L^2[-\Lambda, \Lambda]}^2,$$

hence the result. \square

As a consequence of Theorems 4.21 and 4.24 we have sufficient conditions on $e_{i'j',ij}$, the error between the exact and approximated matrix entries, which give us a stable, optimally convergent and fully discrete method for solving (4.0.1). In Chapter 5 we construct efficient quadrature rules that require a minimal amount of kernel evaluations whilst simultaneously satisfying these conditions.

Chapter 5

Quadrature

In this chapter we devise the quadrature rules required so that the fully discrete collocation method described in Chapter 4 converges optimally. Following on from §4.4 we only consider finding these quadrature rules for the h -version of collocation with an approximation space of piecewise polynomials of order r . We shall do this for a general class of integral equations,

$$(I + \widehat{\mathcal{L}})\widehat{u}(s) = \widehat{b}(s), \quad \text{with} \quad \widehat{\mathcal{L}}\widehat{u}(s) = \int_{-\Lambda}^{\Lambda} \widehat{L}(s, \sigma)\widehat{u}(\sigma)d\sigma,$$

where the kernel satisfies the following conditions. We introduce the distance function dist defined by

$$\text{dist}(s, \sigma) = \min\{|s - \sigma|, |s - \sigma + 2\Lambda|, |s - \sigma - 2\Lambda|\}, \quad \text{for } s, \sigma \in [-\Lambda, \Lambda]. \quad (5.0.1)$$

We make the assumption on the kernel that for $k \in \mathbb{N}_0 := \mathbb{N} \cup \{0\}$

$$\left| \frac{\partial^k}{\partial \sigma^k} \widehat{L}(s, \sigma) \right| \leq C \text{dist}(s, \sigma)^{-1-k}. \quad (5.0.2)$$

We do not prove (5.0.2) explicitly for our application. However we note that it is completely natural since the Mellin convolution kernel $\widehat{\kappa}_B(s/\sigma)1/\sigma$ which occurs in the operator $\widehat{\mathcal{K}}_B$ (see (3.2.17)) satisfies

$$\frac{\partial^k}{\partial \sigma^k} \{\widehat{\kappa}_B(s/\sigma)1/\sigma\} \leq C(1/\sigma)^{k+1}, \quad k \in \mathbb{N} \cup 0.$$

(Note that $\widehat{\kappa}_B$ is infinitely continuously differentiable with all its derivatives bounded on \mathbb{R} .) Also note that with respect to our application this is the worst case scenario and the behaviour displayed in (5.0.2) only occurs in the vicinity of

points corresponding to a corner, if any, on the boundary ℓ . In fact, away from the corners the kernel L_B , $B = D, N$, satisfies

$$\left| \frac{\partial^k}{\partial \sigma^k} \widehat{L}_B(s, \sigma) \right| \leq C \max\{1, \text{dist}(s, \sigma)^{2-\epsilon-k}\},$$

for any arbitrarily small ϵ , $0 < \epsilon < 1$ (see Theorem 3.6). We shall also need in Lemma 5.10 a certain analyticity property of L_B which we state and motivate there.

It follows from Theorems 4.21 and 4.24 that if $\|\widehat{u} - \widehat{u}_n\|_{L^2[-\Lambda, \Lambda]} = O(n^{-r})$, then the discrete collocation solution, \widehat{u}_n^d , will converge optimally to \widehat{u} in $L^2[-\Lambda, \Lambda]$ if the matrix entry errors, $e_{i'j',ij} := |\widehat{\mathbb{L}}_{i'j',ij} - \widehat{\mathbb{L}}_{i'j',ij}^d|$, satisfy

$$e_{i'j',ij} \leq Ch_i n^{-r}, \quad \text{for } (i, j), (i', j') \in \mathcal{J}, \quad (5.0.3)$$

with C independent of i, i', j and j' . (Recall that the index set \mathcal{J} is given by $\mathcal{J} = \{(i, j) : 1 \leq i \leq n, 1 \leq j \leq r\}$.)

In Lemmas 5.5, 5.12 and 5.15 below we shall derive suitable quadrature schemes which ensure (5.0.3) holds. In these Lemmas we distinguish three cases: the “smooth”, “nearly singular” and “weakly singular” integrals. More precisely we define

$$\text{dist}(I_{i'}, I_i) = \min_{j'=0, \dots, r} \text{dist}(x_{i'j'}^r, I_i).$$

Then we choose a fixed parameter, $\theta \in [0, 1)$, and we distinguish the three cases:

$$\text{Case 1 :} \quad \text{dist}(I_{i'}, I_i) \geq h_i^\theta, \quad (5.0.4)$$

$$\text{Case 2 :} \quad \text{dist}(I_{i'}, I_i) < h_i^\theta, \quad i \neq i', \quad (5.0.5)$$

$$\text{Case 3 :} \quad i = i'. \quad (5.0.6)$$

We assume throughout this chapter that n , the number of nodes in the collocation mesh, is sufficiently large so that $h_i < 1$ for all $i = 1, \dots, n$. Since the stability results in Chapter 4 are proved for sufficiently large n this represents no loss of generality.

When i, i' satisfy Case 1 then $x_{i'j'}^r$ remains reasonably far from σ and so we shall find that a straightforward error analysis is sufficient to analyse the accuracy of standard quadrature approximation of the matrix entries. Also this is the most common case (e.g. on a uniform mesh and for, θ close to 1, there are $O(n^2)$ pairs (i, i') satisfying Case 1 and close to $O(n)$ pairs (i, i') satisfying Cases 2 and 3). Therefore it is particularly important that the numerical scheme implemented

when i, i' satisfy Case 1 is an efficient method.

We consider finding quadrature rules that satisfy (5.0.3) for the computationally significant Case 1 first.

5.1 Case 1 : Smooth integrands

For this so-called “far-field” case we consider using quadrature rules that are exact for polynomials of order $t_{i',i}$ (i.e. degree $t_{i',i} - 1$) for each pair (i', i) satisfying (5.0.4). The main aim of this subsection is to find sufficient conditions on $t_{i',i}$ to ensure that (5.0.3) holds for all i, i' satisfying (5.0.4) and $j, j' = 1, \dots, r$.

First we introduce another family of points $\boldsymbol{\eta}^d \in \mathbb{R}^d$ for $d \in \mathbb{N}$ such that $0 \leq \eta_1^d < \eta_2^d < \dots < \eta_d^d \leq 1$. (These can be the same as, or different from, the collocation points ξ_j^r introduced in §4.1.) We also introduce a class of quadrature rules on $[0, 1]$ which are exact for all polynomials of order $\leq t$, with $d \leq t \leq 2d$. These use function evaluations at the points η_k^d for $k = 1, \dots, d$, and have the form

$$\int_0^1 v(\sigma) d\sigma \approx \sum_{k=1}^d w_k^d v(\eta_k^d). \quad (5.1.1)$$

We assume that the weights, w_k^d , in (5.1.1) are positive. An example is the Gauss-Legendre quadrature rule which is found by treating w_k^d and η_k^d as $2d$ unknowns and are chosen so that the rule (5.1.1) is exact for all polynomials of order $\leq 2d$. Transforming (5.1.1) to a rule on rule I_i yields:

$$\int_{I_i} v(\sigma) d\sigma \approx \sum_{k=1}^d h_i w_k^d v(\sigma_{ik}^d), \quad (5.1.2)$$

where $\sigma_{ik}^d = x_{i-1} + \eta_k^d h_i$. Note that if we use Gauss-Legendre quadrature and collocate at the Gauss-Legendre points then the σ_{ij}^d will coincide with the points x_{ij}^r , introduced in (4.1.2), when $r = d$.

The following result gives a derivative-based error estimate for general quadrature rules of the form (5.1.2).

Lemma 5.1. *Suppose that $v \in C^t(I_i)$ and that the quadrature rule in (5.1.2) is exact for polynomials of order less than or equal to t . Then,*

$$\left| \int_{I_i} v(\sigma) d\sigma - \sum_{k=1}^d h_i w_k^d v(\sigma_{ik}^d) \right| \leq C h_i^{t+1} \|D^t v\|_{L^\infty(I_i)}. \quad (5.1.3)$$

Proof Let $p \in \mathbf{P}_t$ then since the quadrature rule (5.1.2) is exact for p , we have

$$\begin{aligned} \left| \int_{I_i} v(\sigma) d\sigma - \sum_{k=1}^d h_i w_k^d v(\sigma_{ik}^d) \right| &= \left| \int_{I_i} (v-p)(\sigma) d\sigma - \sum_{k=1}^d h_i w_k^d (v-p)(\sigma_{ik}^d) \right| \\ &\leq h_i \|v-p\|_{L^\infty(I_i)} + \left\{ h_i \sum_{k=1}^d w_k^d \right\} \|v-p\|_{L^\infty(I_i)} \\ &= 2h_i \|v-p\|_{L^\infty(I_i)}, \end{aligned} \quad (5.1.4)$$

since $\sum_{k=1}^d w_k^d = 1$. To estimate (5.1.4) we expand v as a Taylor series of degree $t-1$ about x_{i-1} with Lagrange remainder,

$$v(\sigma) = p(\sigma) + (\sigma - x_{i-1})^t \frac{D^t v(\xi)}{t!}, \quad (5.1.5)$$

for some $\xi \in I_i$ and p is the Taylor polynomial:

$$p(\sigma) = \sum_{k=0}^{t-1} (\sigma - x_{i-1})^k \frac{D^k v(x_{i-1})}{k!}.$$

It follows from (5.1.5) that $\|v-p\|_{L^\infty(I_i)} \leq h_i^t \|D^t v\|_{L^\infty(I_i)}$ and (5.1.3) follows from (5.1.4). \square

To compute the matrix entries $\widehat{\mathbb{L}}_{i'j',ij}^d$, defined in (4.4.6), we shall use a quadrature rule based on $d_{i',i}$ points depending on i' and i in order to ensure a certain order of exactness. This will yield computable matrix entries given by

$$\widehat{\mathbb{L}}_{i'j',ij}^d = \sum_{k=1}^{d_{i',i}} h_i w_k^{d_{i',i}} L(x_{i'j'}^r, \sigma_{ik}^{d_{i',i}}) \phi_{ij}(\sigma_{ik}^{d_{i',i}}). \quad (5.1.6)$$

Note that if we are able to choose $\boldsymbol{\eta}^{d_{i',i}} = \boldsymbol{\xi}^{r_i}$ then the sum in (5.1.6) collapses to one term. This is because the quadrature nodes $\sigma_{ik}^{d_{i',i}}$ will coincide with the collocation points $x_{ij}^{d_{i',i}}$ and since $\phi_{ij}(x_{ik}^r) = \delta_{jk}$ the summand in (5.1.6) will vanish for all k except when $k = j$. Thus in this case only one kernel evaluation is required to compute (5.1.6). This is useful in our application since each evaluation of the kernel is relatively expensive, see §6.2.

Now recall the quantity $e_{i'j',ij}$ which has to be estimated as in (5.0.3). It is given by (using (5.1.6)):

$$e_{i'j',ij} = \left| \int_{I_i} \widehat{L}(x_{i'j'}^r, \sigma) \phi_{ij}(\sigma) d\sigma - \sum_{k=1}^{d_{i',i}} h_i w_k^{d_{i',i}} \widehat{L}(x_{i'j'}^r, \sigma_{ik}^{d_{i',i}}) \phi_{ij}(\sigma_{ik}^{d_{i',i}}) \right|.$$

The choice of $t_{i',i}$, the order of the quadrature rule (on which the number and position of abscissae will depend), so that the requirement (5.0.3) is satisfied is now our main consideration. If we can find a bound on the derivatives of $L(x_{i'j}^r, \sigma)\phi_{ij}(\sigma)$ as a function of σ then we can use Lemma 5.1 to achieve the required accuracy in (5.0.3). This is the purpose of Lemma 5.2.

First we note that the basis function, ϕ_{ij} , restricted to the interval I_i , is the Lagrange interpolating polynomial of degree $r - 1$ on $[-1, 1]$ translated to I_i . More precisely, with ϕ_{ij} as defined in (4.1.3), when $\sigma = x_{i-1} + h_i\xi \in I_i$, we have,

$$\phi_{ij}(\sigma) = \lambda_j(\xi) := \prod_{\substack{1 \leq k \leq r \\ k \neq j}} \frac{\xi - \xi_k^r}{\xi_j^r - \xi_k^r}.$$

Hence,

$$\phi_{ij}(\sigma) = \lambda_j\left(\frac{\sigma - x_{i-1}}{h_i}\right),$$

(if $r = 1$ then $\phi_{ij}(\sigma) = \chi_i(\sigma)$) and from this we obtain

$$\begin{aligned} \|D^k \phi_{ij}\|_{L^\infty(I_i)} &\leq C_k h_i^{-k}, & k = 0, \dots, r-1, & \quad \text{and} \\ \|D^k \phi_{ij}\|_{L^\infty(I_i)} &= 0, & k \geq r, & \end{aligned} \quad (5.1.7)$$

where C_k depends on k (and r) but not on the mesh or on i . Here and henceforth we use C , C_1 , C_2 , C_k etc. to denote generic constants which are mesh independent and whose value may change from line to line. Using this observation, we can bound the derivatives of $\widehat{L}(x_{i'j}^r, \sigma)\phi_{ij}(\sigma)$.

Lemma 5.2. *Suppose $i, i' \in \{1, \dots, n\}$ satisfy (5.0.4), then for all $k \geq 0$*

$$\|D_\sigma^k \{\widehat{L}(x_{i'j}^r, \sigma)\phi_{ij}(\sigma)\}\|_{L^\infty(I_i)} \leq C_k \text{dist}(I_{i'}, I_i)^{-1-k} \left\{ \frac{\text{dist}(I_{i'}, I_i)}{h_i} \right\}^{\min\{k, r-1\}},$$

for some mesh independent constants C_k .

Proof By the Leibnitz rule we can write

$$\|D_\sigma^k \{\widehat{L}(x_{i'j}^r, \sigma)\phi_{ij}(\sigma)\}\|_{L^\infty(I_i)} \leq C_k \max_{l=0, \dots, k} \left\{ \|D_\sigma^{k-l} \widehat{L}(x_{i'j}^r, \sigma)\|_{L^\infty(I_i)} \|D^l \phi_{ij}\|_{L^\infty(I_i)} \right\}.$$

From (5.0.2) and (5.1.7) we get

$$\begin{aligned}
\|D_\sigma^k \{\widehat{L}(x_{i'j}^r, \sigma)\phi(\sigma)\}\|_{L^\infty(I_i)} &\leq C_k \max_{l=0, \dots, \min\{k, r-1\}} \text{dist}(I_{i'}, I_i)^{-1-k+l} h_i^{-l} \\
&= C_k \max_{l=0, \dots, \min\{k, r-1\}} \text{dist}(I_{i'}, I_i)^{-1-k} \left\{ \frac{\text{dist}(I_{i'}, I_i)}{h_i} \right\}^l.
\end{aligned} \tag{5.1.8}$$

From (5.0.4) and using the fact that $\theta \in [0, 1)$ (and the assumption $h_i < 1$), we see that $\text{dist}(I_{i'}, I_i) \geq h_i^\theta > h_i$. Thus, $\text{dist}(I_{i'}, I_i)/h_i > 1$ and so (5.1.8) implies the result. \square

Combining Lemmas 5.1 and 5.2 we obtain an estimate of the error for a quadrature rule of the form (5.1.6) applied to a typical ‘‘far field’’ matrix entry.

Corollary 5.3. *Let $i, i' \in \{1, \dots, n\}$ satisfy (5.0.4). Then using a quadrature rule which is exact for polynomials of order $t_{i',i}$ we get*

$$e_{i'j',ij} \leq C \left\{ \frac{h_i}{\text{dist}(I_{i'}, I_i)} \right\}^{t_{i',i}+1-\min\{t_{i',i}, r-1\}}.$$

Proof By Lemma 5.1,

$$\begin{aligned}
e_{i'j',ij} &= \left| \int_{I_i} \widehat{L}(x_{i'j'}^r, \sigma) \phi_{ij}(\sigma) d\sigma - \sum_{k=1}^{d_{i',i}} h_i w_k^{d_{i',i}} \widehat{L}(x_{i'j'}^r, \sigma_{ik}^{d_{i',i}}) \phi_{ij}(\sigma_{ik}^{d_{i',i}}) \right| \\
&\leq C h_i^{t_{i',i}+1} \|D_\sigma^{t_{i',i}} \{\widehat{L}(x_{i'j}^r, \sigma)\phi(\sigma)\}\|_{L^\infty(I_i)}.
\end{aligned}$$

Hence by Lemma 5.2,

$$\begin{aligned}
e_{i'j',ij} &\leq C h_i^{t_{i',i}+1} \text{dist}(I_{i'}, I_i)^{-1-t_{i',i}} \left\{ \frac{\text{dist}(I_{i'}, I_i)}{h_i} \right\}^{\min\{t_{i',i}, r-1\}} \\
&= C \left\{ \frac{h_i}{\text{dist}(I_{i'}, I_i)} \right\}^{t_{i',i}+1-\min\{t_{i',i}, r-1\}}.
\end{aligned} \quad \square$$

Remark 5.4. Under the conditions of Corollary 5.3, if the quadrature rule for $\mathbb{L}_{i'j',ij}$ is chosen to have order $t_{i',i} \geq r-1$ then

$$e_{i'j',ij} \leq C \left\{ \frac{h_i}{\text{dist}(I_{i'}, I_i)} \right\}^{t_{i',i}-r+2}.$$

This now leads to the next result which tells us what degree of precision is sufficient to ensure that (5.0.3) holds. This is obtained by arguments similar to those used in [46].

Lemma 5.5. *Let the assumptions of Corollary 5.3 hold. Suppose n is sufficiently large and that, for each pair (i', i) in Case 1, we use a quadrature rule based on at least r abscissae chosen so that the order of precision, $t_{i',i}$, is the smallest integer such that*

$$t_{i',i} \geq r - 1, \quad (5.1.9)$$

$$t_{i',i} \geq r - 1 + \frac{r + \log(\text{dist}(I_{i'}, I_i)) / \log(h_i)}{1 - \log(\text{dist}(I_{i'}, I_i)) / \log(h_i)}, \quad (5.1.10)$$

then (5.0.3) holds.

Remark 5.6. As the mesh is refined $h_i \rightarrow 0$, the right-hand side of (5.1.10) approaches $2r - 1$ and the condition (5.1.9) becomes redundant.

Proof Firstly we have from (5.0.4) (using our assumption that $h_i < 1$) that

$$\frac{\log(\text{dist}(I_{i'}, I_i))}{\log(h_i)} \leq \theta < 1.$$

Therefore (5.1.10) implies

$$\left(1 - \frac{\log(\text{dist}(I_{i'}, I_i))}{\log(h_i)}\right)(t_{i',i} - r + 1) \geq r + \frac{\log(\text{dist}(I_{i'}, I_i))}{\log(h_i)}.$$

Multiplying by $\log(h_i) < 0$, this implies

$$(\log(h_i) - \log(\text{dist}(I_{i'}, I_i)))(t_{i',i} - r + 1) \leq r \log(h_i) + \log(\text{dist}(I_{i'}, I_i)).$$

Hence (5.1.10) implies

$$\left(\frac{h_i}{\text{dist}(I_{i'}, I_i)}\right)^{t_{i',i} - r + 1} \leq h_i^r \text{dist}(I_{i'}, I_i).$$

Rearranging this gives

$$\left(\frac{h_i}{\text{dist}(I_{i'}, I_i)}\right)^{t_{i',i} - r + 2} \leq h_i^{r+1}.$$

Therefore, by Remark 5.4 and assumption (5.1.9), we have

$$e_{i'j',ij} \leq Ch_i^{r+1} \leq Ch_i \frac{1}{n^r},$$

as required. □

We can use this lemma to devise sufficient quadrature methods in the “far-field” case that will ensure optimal convergence of the collocation method. In the following subsection we restrict to the case of Gauss-Legendre quadrature rules which leads to a particularly efficient scheme.

5.1.1 Gauss-Legendre quadrature

Consider a special case where the collocation points on I_i coincide with the Gauss points translated to I_i and $\widehat{\mathbb{L}}_{i_j, i'_j}$ is approximated by the r -point Gauss-Legendre rule (based on the same points). Then $t_{i', i} = 2r$ (see e.g. [28]). As explained above, since the quadrature points coincide with the collocation points and because of the special form of the basis functions ϕ_{ij} , there is only one kernel evaluation required to calculate the matrix entries. The matrix entries which we can estimate using this particular method is described in the next result.

Lemma 5.7. *Suppose we use the h -version of collocation with approximating piecewise polynomials of order r on each subinterval and collocate at the Gauss-Legendre points of subintervals. Then (5.1.9) and (5.1.10) will hold if we use Gauss-Legendre quadrature of order r to calculate the matrix entries (4.1.6) for pairs (i', i) satisfying,*

$$\text{dist}(I_{i'}, I_i) \geq h_i^{1/(r+2)}. \quad (5.1.11)$$

Proof Clearly (5.1.9) holds since $t_{i', i} = 2r$. Starting from (5.1.11), we see that this implies,

$$\frac{\log(\text{dist}(I_{i'}, I_i))}{\log(h_i)} \leq \frac{1}{r+2} < 1.$$

After a little algebra, it can be shown that this implies

$$r+1 \geq \frac{r + \log(\text{dist}(I_{i'}, I_i))/\log(h_i)}{1 - \log(\text{dist}(I_{i'}, I_i))/\log(h_i)}$$

Hence,

$$t_{i', i} = 2r \geq r - 1 + \frac{r + \log(\text{dist}(I_{i'}, I_i))/\log(h_i)}{1 - \log(\text{dist}(I_{i'}, I_i))/\log(h_i)},$$

so (5.1.10) holds. \square

The consequence of this lemma is that if we take $\theta = 1/(r+2)$ then we can calculate the matrix entries (4.1.6) for all pairs (i', i) in Case 1 with one kernel evaluation. Since the right-hand side of (5.1.11) approaches 0 as $n \rightarrow \infty$, an increasing proportion of the off diagonal matrix entries in $\widehat{\mathbb{L}}$ can be approximated using one point quadrature rules as the mesh is refined.

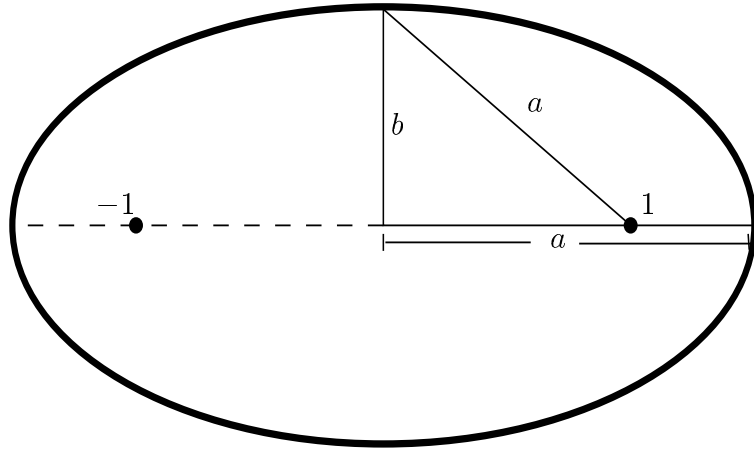


Figure 5-1: The ellipse $\mathcal{E}_{a,b}$

5.2 Case 2 : Nearly singular integrands

Now we consider Case 2, the nearly singular integrals. Gaussian quadrature can handle many near singular integrals very effectively and so we consider such rules here. However for this case (and also for Case 3) we no longer use derivatives of $L(x_{ij'}, \sigma)\phi_{ij}(\sigma)$ to estimate the quadrature error since these derivatives blow up so quickly that the analysis in §5.1 fails. Instead we shall use so-called “derivative-free” error estimates for the quadrature. Fortunately such estimates exist for Gauss-Legendre quadrature rules. Let $\mathcal{E}_{a,b} \subset \mathbb{C}$ denote the closed ellipse with foci at -1 and 1 , with semi-major axis of length $a > 1$ and semi-minor axis of length $b = \sqrt{a^2 - 1} > 0$ (see Fig 5-1).

Now consider the integral of some function v over $[-1, 1]$ and the d -point Gauss-Legendre approximation of this integral, denoted by $G^d v$. A classical estimate for the error is given by the following lemma.

Lemma 5.8. *Let v be analytic on $[-1, 1]$ and admit an analytic continuation into the ellipse $\mathcal{E}_{a,b}$. Then*

$$\left| \int_{-1}^1 v(\sigma) d\sigma - G^d v \right| \leq C(a+b)^{-2d} \max_{z \in \mathcal{E}_{a,b}} |v(z)|$$

Proof The result follows from [28, 4.6.1.11].

Note that this is quite different in flavour to the more usual estimates in Lemma 5.1 in that derivatives of v do not appear explicitly on the right-hand side. We use this result to find a bound (given in Lemma 5.10) for $e_{ij', ij}$, when Gauss-Legendre rules are applied on I_i , in Case 2.

For Lemma 5.10 we need an analyticity assumption on the kernel \widehat{L} . Precisely we shall assume:

Assumption 5.9. For each i, i', j' the function $\widehat{L}(x_{i'j'}^r, \sigma)$ for $\sigma \in I_i$ has an analytic extension to $\sigma \in \mathbb{C}$ with its only singularity at $\sigma = x_{i'j'}$.

This assumption is reasonable because: (a) Fundamental solutions of general elliptic PDEs are analytic except at the origin see e.g. [46, §2.2]. (b) The contour ℓ is assumed to be piecewise analytic (see Notation 2.2) and since the corners of ℓ are not allowed to be interior points of I_i , the parameterisation $\boldsymbol{\rho}$ in (3.1.27) is analytic on \bar{I}_i . Note that the definition of the distance function (5.0.1) and the assumption (5.0.2) can be extended in a straightforward way for $\sigma \in \mathbb{C}$.

Lemma 5.10. *Assume Assumption 5.9 and that (5.0.2) holds for $\sigma \in \mathbb{C}$. Suppose we use the $d_{i',i}$ -point Gauss-Legendre rule in (5.0.3) for all pairs (i', i) in Case 2. Also suppose the meshes have a bounded local mesh ratio, i.e. there exist constants C_1, C_2 such that*

$$C_2 \leq \frac{h_{i+1}}{h_i} \leq C_1. \quad (5.2.1)$$

Then,

$$\epsilon_{i'j',ij} \leq Ch_i \rho^{-2d_{i',i}}$$

for some $\rho = \rho(i', j', i) > 1$, which is bounded away from 1 and independent of n .

Remark 5.11. The condition (5.2.1) is satisfied for uniform meshes or the graded mesh introduced in (4.3.2).

Proof Firstly, we employ a change of variable to rewrite $\mathbb{L}_{i'j',ij}$ as an integral over $[-1, 1]$. Let $\sigma = x_{i-1} + h_i(y + 1)/2$,

$$\mathbb{L}_{i'j',ij} = \int_{I_i} L(x_{i'j'}^r, \sigma) \phi_{ij}(\sigma) d\sigma = \frac{h_i}{2} \int_{-1}^1 v_{i'j',ij}(y) dy, \quad (5.2.2)$$

where

$$v_{i'j',ij}(y) = L(x_{i'j'}^r, x_{i-1} + h_i(y + 1)/2) \phi_{ij}(x_{i-1} + h_i(y + 1)/2). \quad (5.2.3)$$

Now if we use the Gauss-Legendre rule on I_i to approximate the middle integral in (5.2.2) we get the same result as if we use the Gauss-Legendre rule to approximate the right hand-side of (5.2.2). So the error is,

$$e_{i'j',ij} = \left| \frac{h_i}{2} \int_{-1}^1 v_{i'j',ij}(y) dy - G^{d_{i',i}} v_{i'j',ij} \right|. \quad (5.2.4)$$

Now we need to construct an ellipse with foci at -1 and 1 so that $v_{i'j',ij}$ satisfies the conditions of Lemma 5.8. So we need to know where the singularities of $v_{i'j',ij}$ lie. Now ϕ_{ij} has an analytic extension to any ellipse but $L(x_{i'j'}^r, \sigma)$ has a singularity at $\sigma = x_{i'j'}^r$. Suppose that $x_{i'j'}^r > x_i$ (we return to the possibility of $x_{i'j'}^r < x_{i-1}$ later) then

$$x_{i'j'}^r = x_i + \eta h_{i+1}, \quad (5.2.5)$$

for some η which depends on i', j' and i . Note that $\eta \geq \xi_1^r$, i.e. η is bounded away from 0. Thus, the continuation of $v_{i'j',ij}$ into \mathbb{C} has a weak singularity at the point $y_s \notin [-1, 1]$ which is given by the change of variable that was used in (5.2.2), i.e. $x_{i-1} + h_i(y_s + 1)/2 = x_i + \eta h_{i+1}$. This yields

$$y_s = 1 + 2\eta \frac{h_{i+1}}{h_i}.$$

Hence if we chose $\mathcal{E}_{a,b}$ so that $a = a(i', j', i)$ satisfies $1 < a < y_s = 1 + 2\eta h_{i+1}/h_i$ (say, by setting $a = 1 + \eta h_{i+1}/h_i$) then the continuation of the integrand into $\mathcal{E}_{a,b}$ is analytic. By choosing $b = b(i', j', i)$ accordingly (i.e. so that $b^2 + 1 = a^2$, see Fig 5-1) and setting $\rho = a + b$ it follows from Lemma 5.8 and (5.2.4) that,

$$e_{i'j',ij} = C\rho^{-2d_{i',i}} \frac{h_i}{2} \max_{z \in \mathcal{E}_{a,b}} |v_{i'j',ij}(z)|,$$

for all pairs (i', i) in Case 2 and $j, j' = 1, \dots, r$. It follows from (5.0.2) (extended to include $\sigma \in \mathbb{C}$) that

$$|v_{i'j',ij}(z)| \leq Ch_i^{-1},$$

for all $z \in \mathcal{E}_{a,b}$ with C independent of the mesh. Hence,

$$e_{i'j',ij} = C\rho^{-2d_{i',i}}.$$

If $x_{i'j'}^r < x_{i-1}$ then the singularity of f occurs at $y_s = -1 - 2\eta h_{i-1}/h_i$ for some $\eta \geq 1 - \xi_r^r$ and the result follows in the same way as above. \square

Lemma 5.10 can now be used to derive the sufficient degree of precision to ensure that (5.0.3) holds.

Lemma 5.12. *Suppose that i, i' satisfy (5.0.5) and that each matrix entry $\mathbb{L}_{i'j',ij}$ is approximated by a $d_{i',i}$ -point Gauss-Legendre, where $d_{i',i}$ is the smallest integer satisfying*

$$d_{i',i} \geq \frac{-(r+1) \log(h_i)}{2 \log(\rho)}, \quad (5.2.6)$$

where ρ is the minimum of all the $\rho(i', j', i)$ identified in Lemma 5.10, then (5.0.3)

holds.

Proof From (5.2.6) we get

$$-2d_{i',i} \log(\rho) \leq (r+1) \log(h_i).$$

Hence $\rho^{-2d_{i',i}} \leq h_i^{r+1}$, and so by Lemma 5.10

$$e_{i'j',ij} \leq C\rho^{-2d_{i',i}} \leq Ch_i^{r+1} \leq Ch_i \frac{1}{n^r}.$$

□

We now have a sufficient quadrature rule for i', i satisfying Case 2. Note from Lemma 5.12 that as n increases an $O(\log(n))$ point Gauss-Legendre rule is needed to achieve the order of accuracy in (5.0.3). Hence we have a quadrature scheme that requires $O(\log(n))$ kernel evaluations per matrix entry.

5.3 Case 3 : Weakly singular integrands

We now consider the weakly singular integrals in Case 3. In this case the integrand is weakly singular at some point on the range of integration and so neither Corollary 5.3 nor Lemma 5.10 can be used. We consider here the case when the integrand has a log singularity i.e. when the kernel is of the form

$$\widehat{L}(s, \sigma) = p(s, \sigma) \log(|s - \sigma|) + r(s, \sigma), \quad (5.3.1)$$

where p and r are smooth functions. With regard to the problem of interest in Chapter 3 by ensuring that any corner points on ℓ coincide with a node on the collocation mesh then each subinterval I_i will correspond to a smooth section of the contour ℓ . Hence it follows from Theorem 3.6 that the kernel $\widehat{L}_B(s, \sigma)$, $B = D, N$ will take the form (5.3.1). In fact by substituting the representation of $P_{\nu-1/2}$ from Lemma 3.5 into the expressions (3.1.1) and (3.1.2) for L_D and L_N , respectively, it can be shown that p and r can be written in terms of the functions $a_{\nu-1/2}$ and $b_{\nu-1/2}$ defined in (3.1.8), (3.1.9) and their derivatives. The functions $a_{\nu-1/2}$ and $b_{\nu-1/2}$ can be computed explicitly in terms of hypergeometric functions.

Using (5.3.1) the integral we wish to calculate can be split into two parts

$$\begin{aligned} \int_{I_i} \widehat{L}(x_{ij}^r, \sigma) \phi_{ij}(\sigma) d\sigma &= \int_{I_i} p(x_{ij}^r, \sigma) \log(|x_{ij}^r - \sigma|) \phi_{ij}(\sigma) d\sigma \\ &+ \int_{I_i} r(x_{ij}^r, \sigma) \phi_{ij}(\sigma) d\sigma. \end{aligned} \quad (5.3.2)$$

The second integral on the right-hand side has a smooth integrand and can be estimated using a Gauss-Legendre quadrature rule. For the first integral we use product integration.

To describe product integration consider the general problem of integrating $w(\sigma)v(\sigma)$, where v is a smooth, possibly complicated function and w is a simple and possibly singular function. We approximate v on I_i by its interpolant at some points σ_{ij} , $j = 1, \dots, d$:

$$\Pi_d v(\sigma) = \sum_{j=0}^d v(\sigma_{ij}) l_{ij}(\sigma),$$

where

$$l_{ij}(\sigma) = \prod_{k \neq j} \frac{\sigma - \sigma_{ik}}{\sigma_{ik} - \sigma_{ij}}.$$

This leads to the approximation

$$\begin{aligned} \int_{I_i} w(\sigma)v(\sigma) d\sigma &\approx \int_{I_i} w(\sigma)(\Pi_d v)(\sigma) d\sigma = \int_{I_i} w(\sigma) \sum_{j=0}^d v(\sigma_{ij}) l_{ij}(\sigma) d\sigma \\ &= \sum_{j=0}^{d_i} v(\sigma_{ij}) \int_{I_i} w(\sigma) l_{ij}(\sigma) d\sigma = \sum_{j=0}^{d_i} w_{ij} v(\sigma_{ij}), \end{aligned} \quad (5.3.3)$$

where $w_{ij} = \int_{I_i} w(\sigma) l_{ij}(\sigma) d\sigma$. If w is simple enough, the weights w_{ij} in (5.3.3) can be computed analytically.

We apply this to the first integral on the right-hand side of (5.3.2).

Lemma 5.13. *Suppose that we use the quadrature rule in (5.3.3) with $d = d_{i',i}$ nodes, $w(\sigma) = \log|x_{ij}^r - \sigma| \phi_{ij}(\sigma)$ and $v(\sigma) = p(x_{ij}^r, \sigma)$ then we get the following error bound*

$$\begin{aligned} &\left| \int_{I_i} p(x_{ij}^r, \sigma) \log(|x_{ij}^r - \sigma|) \phi_{ij}(\sigma) d\sigma - \sum_{j=0}^{d_{i',i}} w_{ij} p(x_{ij}^r, \sigma_{ij}) \right| \\ &\leq C \|p(x_{ij}^r, \sigma) - \Pi_{d_{i',i}} p(x_{ij}^r, \sigma)\|_{L^\infty(I_i)} \int_{I_i} |\log(|x_{ij}^r - \sigma|)| d\sigma, \end{aligned} \quad (5.3.4)$$

where $w_{ij} = \int_{I_i} \log(|x_{ij}^r - \sigma|) \phi_{ij}(\sigma) l_{ij}(\sigma) d\sigma$.

Remark 5.14. Note that ϕ_{ij} and l_{ij} are polynomials. Therefore the integral describing the weights w_{ij} have an integrand which is a product of a log function and a polynomial. Hence w_{ij} can be computed analytically.

Proof By (5.3.3) and (5.1.7) we have,

$$\begin{aligned} & \left| \int_{I_i} p(x_{ij}^r, \sigma) \log(|x_{ij}^r - \sigma|) \phi_{ij}(\sigma) d\sigma - \sum_{j=0}^{d_{i',i}} w_{ij} p(x_{ij}^r, \sigma_{ij}) \right| \\ &= \left| \int_{I_i} (p(x_{ij}^r, \sigma) - (\Pi_{d_{i',i}} p)(x_{ij}^r, \sigma)) \log(|x_{ij}^r - \sigma|) \phi_{ij}(\sigma) d\sigma \right| \\ &\leq C \|p(x_{ij}^r, \sigma) - (\Pi_{d_{i',i}} p)(x_{ij}^r, \sigma)\|_{L^\infty(I_i)} \int_{I_i} |\log(|x_{ij}^r - \sigma|)| d\sigma, \quad (5.3.5) \end{aligned}$$

as required. \square

So the accuracy of the quadrature rule depends on the accuracy of the interpolating polynomial, $\Pi_{d_{i',i}} p$, compared with p . We use Lemma 5.13 in the next result which gives a sufficient numerical technique for approximating the matrix entries $\mathbb{L}_{i'j',ij}$ for pairs (i', i) satisfying Case 3.

Lemma 5.15. *Suppose that $i = i'$ and that we approximate the matrix entries $\mathbb{L}_{i'j',ij}$ using the representation (5.3.2). Also suppose that we compute $\mathbb{L}_{i'j',ij}^d$, the numerical approximation of $\mathbb{L}_{i'j',ij}$, by using the product integration method described in Lemma 5.13, with $d_{i',i} = r + 1$, to approximate the first integral on the right-hand side of (5.3.2) and by using the $\lceil r/2 \rceil$ -point Gauss-Legendre rule to compute the second integral on the right-hand side of (5.3.2). Then it follows that the matrix entry approximation error satisfies*

$$e_{i'j',ij} \leq Ch_i n^{-r}.$$

Proof First we write

$$e_1 := \left| \int_{I_i} p(x_{ij}^r, \sigma) \log(|x_{ij}^r - \sigma|) \phi_{ij}(\sigma) d\sigma - \sum_{j=0}^{r+1} w_{ij} p(x_{ij}^r, \sigma_{ij}) \right|,$$

where $w_{ij} = \int_{I_i} \log(|s - \sigma|) l_{ij}(\sigma) d\sigma$. We also define

$$e_2 := \left| \int_{I_i} r(x_{ij}^r, \sigma) \phi_{ij}(\sigma) d\sigma - G^{\lceil r/2 \rceil} \{r(x_{ij}^r, \cdot) \phi_{ij}(\cdot)\} \right|,$$

where, for an arbitrary function v , $G^{\lceil r/2 \rceil} v$ is the $\lceil r/2 \rceil$ point Gauss-Legendre approximation of the integral of v over I_i . It follows that

$$e_{i'j',ij} \leq e_1 + e_2. \quad (5.3.6)$$

From Lemma 5.13 it follows that

$$e_1 \leq \|p(x_{ij}^r, \sigma) - \Pi_{r+1} p(x_{ij}^r, \sigma)\|_{L^\infty(I_i)} \int_{I_i} |\log(|x_{ij}^r - \sigma|)| d\sigma.$$

Therefore using the standard estimate $\|p(x_{ij}^r, \sigma) - \Pi_{r+1} p(x_{ij}^r, \sigma)\|_{L^\infty(I_i)} \leq Ch_i^{r+1}$ where C is a constant that depends on p , it follows that

$$e_1 \leq Ch_i^{r+1}.$$

Now we consider e_2 . Since the Gauss-Legendre rule on $\lceil r/2 \rceil$ points is exact for all polynomials of order $\leq 2r$ (see e.g. [28]) it follows from Lemma 5.1 that

$$e_2 \leq Ch_i^{r+1} \|D_\sigma^{r+1} r(x_{ij}^r, \sigma) \phi_{ij}(\sigma)\|_{L^\infty[-\Lambda, \Lambda]} \leq Ch_i^{r+1}.$$

Hence (5.3.6) implies that $e_{i'j',ij} \leq Ch_i^{r+1} \leq Ch_i n^{-r}$. \square

Combining all three cases (5.0.4)-(5.0.6) we see that $O(n^2)$ kernel evaluations are needed to compute the whole matrix to ensure (5.0.3) holds for all pairs (i, i') (in fact a large proportion of matrix entries can be computed with only one kernel evaluation).

We have described here an efficient strategy for assembling the matrix $\widehat{\mathbb{L}}^d$ while maintaining the optimal convergence of the h -version of collocation method described in Chapter 4. In the next section we present the results of some numerical experiments which use these approximation rules for the matrix assembly and demonstrate the rates of convergence expected from Chapter 4 and the theory above.

5.4 Numerical results

We shall illustrate the performance of the numerical method described Chapter 4 with the quadrature rules above for two example problems. Throughout the computations we use collocation at the Gauss points of subintervals.

Example 1

First we consider the numerical solution to the integral equation that results from the acoustic diffraction problem for a circular cone. We consider both Dirichlet and Neumann boundary conditions and fix $\nu = i$. We chose a circular cone with semi angle (the angle between the surface of the cone and its axis of symmetry) equal to $\pi/6$ and an axisymmetric incident wave, $U_{inc}(\mathbf{x}) = \exp(-ik\boldsymbol{\omega}_0 \cdot \mathbf{x})$, where $-\boldsymbol{\omega}_0$ is the direction of the axis of symmetry. The boundary value problem (3.0.1), (3.0.2), associated with this example has an explicit solution. We do not concern ourselves with this fact here but we will return to it when we consider the accuracy of the single/double layer representations in §6.3. Unfortunately there is no explicit formula for the solution to the integral equation (4.3.3).

In Table 5.1 and 5.2 we give results for the h -version of collocation (4.3.3) with piecewise constant and piecewise linear basis functions (i.e. $r = 1$ and 2 respectively). For the evaluation of the boundary integrals we used Gauss quadrature at the collocation points (i.e. the r -point Gauss Legendre rule) for pairs (i', i) satisfying (5.0.4) with $\theta = 1/(r + 2)$. We increase the number of Gauss quadrature points, d , logarithmically as n increases for the nearly singular integrals, according to the formula

$$d \geq \frac{(r + 1) \log(n)}{2 \log(2)}.$$

This arises from taking $\rho = 2$ and $h_i = 1/n$ in (5.2.6). This is not strictly equivalent to (5.2.6) but is convenient and of the right order as $n \rightarrow \infty$. When the observation point lies in the interval of integration then, since $r \leq 2$ and $L_D(\boldsymbol{\omega}, \boldsymbol{\omega}') = O(|\boldsymbol{\omega} - \boldsymbol{\omega}'|^2 \log(|\boldsymbol{\omega} - \boldsymbol{\omega}'|))$ as $|\boldsymbol{\omega} - \boldsymbol{\omega}'| \rightarrow 0$ (Theorem 3.6(ii)), we simply apply the r -point Gauss-Legendre rule to compute the weakly singular integrals. We shall see that our numerical results support the theoretical predictions.

Table 5.1: Estimated errors for the piecewise constant collocation method for example 1

n	Dirichlet Problem		Neumann Problem	
	err _n ¹	ratio	err _n ¹	ratio
4	6.831E-3		8.471E-5	
8	5.003E-4	13.7	6.392E-6	13.3
16	1.626E-5	30.8	2.083E-7	30.7
32	2.875E-5	0.56	3.268E-7	0.64
64	1.051E-5	2.74	1.092E-7	3.00
128	2.870E-6	3.66	3.132E-8	3.49

Table 5.2: Estimated errors for the piecewise linear collocation method for example 1

n	Dirichlet Problem		Neumann Problem	
	err _n ¹	ratio	err _n ¹	ratio
4	5.248E-4		6.703E-6	
8	6.389E-5	8.21	8.178E-7	8.20
16	7.653E-6	8.34	9.799E-9	8.35
32	8.259E-7	9.26	1.058E-9	9.26
64	2.936E-9	281	3.223E-11	307

Since the true value of the density \hat{u} is unknown, to illustrate convergence, we have computed an “exact” solution \hat{u}^* by using piecewise linear collocation on a mesh with 500 nodes. In Tables 5.1 and 5.2, the quantity err_n^1 is an estimation of the L^2 norm of $\hat{u}^* - \hat{u}_n$ computed using r -point Gauss quadrature with respect to the mesh with n nodes. That is the L^2 norm of $\hat{u}^* - \hat{u}_n$ is estimated using values of \hat{u}_n at the collocation points.

The column labelled ratio is the ratio of successive values of err_n^1 as n doubles. The rate of convergence is given by $\log(\text{ratio})/\log(2)$, hence it appears empirically that the error is approaching $O(n^{-2})$ for piecewise constant approximation and close to $O(n^{-3})$ for piecewise linear approximation. These rates of convergence are faster than the convergence given in §4.2. This apparent discrepancy is explained in the discussion on superconvergence below.

Example 2

To test how the collocation method performs when ℓ contains corners, the second example we consider is the numerical solution to the integral equation resulting from the diffraction of acoustic waves by a trihedral cone. In the asymptotics literature this is an unsolved *canonical problem* - i.e. it is a relatively simple geometry which often occurs in applications, but there is no known closed form expression for the diffraction coefficients. Again we consider both Dirichlet and Neumann boundary conditions with ν fixed, $\nu = i$.

Our cone is determined by three rays which emanate from the origin and pass through the points $\omega_{c_i} \in S^2$, $i = 1, 2, 3$, specified by spherical polar coordinates $(\theta^*, 0)$, $(\theta^*, 2\pi/3)$ and $(\theta^*, 4\pi/3)$ respectively, where $\cos \theta^* = 1/\sqrt{3}$. The conical scatterer Ξ has surface composed of the three planar segments determined by each pair of rays and the contour ℓ is made up of three smooth geodesic curves in S^2 , with each pair of smooth curves meeting at an angle of $\pi/2$ at one of the

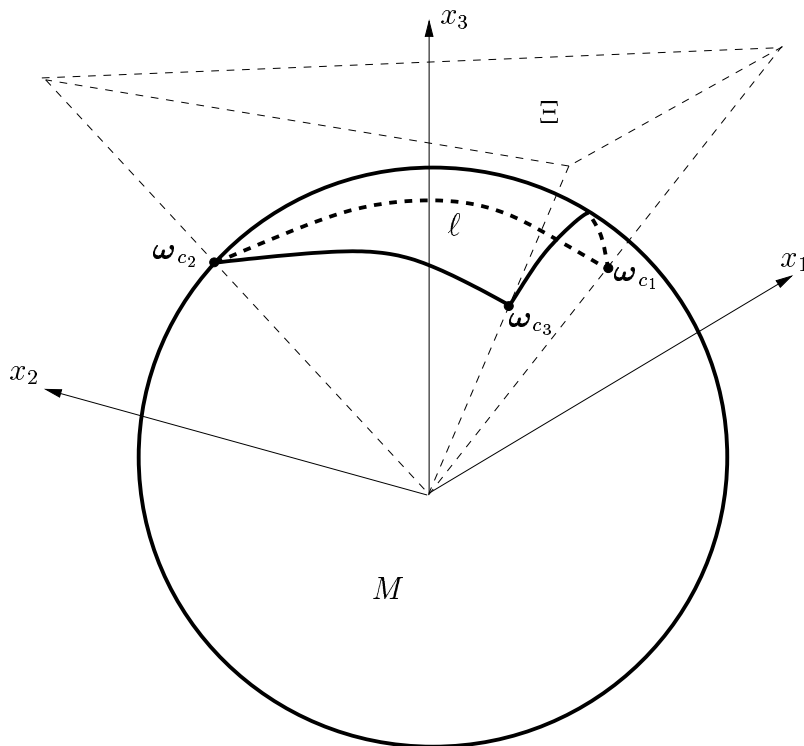


Figure 5-2: The contour ℓ associated with a trihedral cone

points ω_{c_i} . The geometry is depicted in Fig. 5-2. The contour ℓ is drawn in bold.

We consider a test problem where $\omega_0 = -\omega_{c_1}$. Again an explicit formula for the double layer density \hat{u} in the boundary integral equation is not known. However we expect from Remark 4.11 and Examples 4.10 that in the presence of Dirichlet boundary conditions there exists a constant C' such that, $\hat{u} - C' \in L_\alpha^{2,r}$, with $\alpha < 7/6$, and when Neumann boundary conditions are prescribed, $\hat{u} \in L_\alpha^{2,r}$, $\alpha < 1/6$. So for the Dirichlet problem, piecewise constant approximation should yield optimal $O(n^{-1})$ convergence (in the L^2 sense) on a uniform mesh ($q = 1$, cf. Theorem 4.14) and on this mesh we can expect that piecewise linear approximations will give a slightly faster rate of convergence. On the other hand for the Neumann problem we expect a rate of convergence close to $O(n^{-1/6})$ on a uniform mesh.

For this example we have again computed an “exact” solution \hat{u}^* by using piecewise linear collocation on a mesh with $n = 498$ nodes. (To obtain the “exact” Dirichlet solution we grade the mesh towards the corners with $q = 2$ and for the the “exact” Neumann solution, since the optimal grading is rather severe, we only use a grading with exponent $q = 3$.) The “exact” solutions \hat{u}^* to the integral equation with Dirichlet and Neumann boundary conditions are shown in

Figs. 5-3 and 5-4 respectively. The singular behaviour of the solution is seen at the points corresponding to the corners of ℓ (i.e. at the points $s = 0, \pi/2, \pi, 3\pi/2$).

The L^2 error is computed and the stiffness matrix \mathbb{L}_B^d is assembled using the same quadrature scheme as in Example 1. Note that for this geometry $L_B(\boldsymbol{\omega}, \boldsymbol{\omega}') = 0$ when $\boldsymbol{\omega}$ and $\boldsymbol{\omega}'$ both lie on the same edge of the geodesic triangle ℓ . Hence, one third of the matrix entries are zero, included in these zero entries are the weakly singular integrals in Case 3, which in this case do not need to be approximated. The errors err_n^1 are computed as in Example 1.

The results for the uniform mesh are given in Tables 5.3 and 5.4. As expected, a convergence rate close to $O(n^{-1})$ is observed for the Dirichlet problem and close to $O(n^{-1/6})$ for the Neumann problem.

Table 5.3: Estimated errors for the piecewise constant collocation method for example 2 on a uniform mesh

n	Dirichlet Problem		Neumann Problem	
	err_n^1	ratio	err_n^1	ratio
24	9.957E-2		1.609E-3	
48	5.285E-2	1.88	1.530E-3	1.05
96	2.472E-2	2.14	1.229E-3	1.24
192	1.074E-2	2.30	1.077E-3	1.14
384	4.992E-3	2.15	9.589E-4	1.12

As we have shown, mesh grading will improve the rates of convergence, (except in the piecewise constant approximation of the Dirichlet problem case where optimal convergence is obtained using a uniform mesh). Consider the Neumann problem, the required grading exponent $q > 6r$ needed for optimal convergence

Table 5.4: Estimated errors for the piecewise linear collocation method for example 2 on a uniform mesh

n	Dirichlet Problem		Neumann Problem	
	err_n^1	ratio	err_n^1	ratio
24	5.638E-4		1.178E-3	
48	8.785E-4	0.64	8.211E-4	1.44
96	3.654E-4	2.40	6.254E-4	1.31
192	1.343E-4	2.72	5.668E-4	1.10
384	5.754E-4	2.33	5.252E-4	1.08

(cf. Theorem 4.14) is rather severe here. However, note that, because the Neumann solution, $\widehat{u} \in L_\alpha^{2,r}$, $\alpha = 1/6$, it can be shown that with $q' \leq 6r$ a rate of convergence of $O(n^{-q'/6})$ in the L^2 norm can be attained when a graded mesh is used with grading exponent $q > q'$. We illustrate the correctness of this result with $q = 3$. The results are in Table 5.5. Here we find that the Neumann problem now converges with a rate close to $O(n^{-1/2})$ as expected. The Dirichlet problem now appears to converge with a superoptimal rate, but this could be expected to subside back to $O(n^{-1})$ asymptotically.

Table 5.5: Estimated errors for the piecewise constant collocation method for example 2 on a graded mesh, $q=3$

n	Dirichlet Problem		Neumann Problem	
	err_n^1	ratio	err_n^1	ratio
24	1.257E-2		6.307E-3	
48	4.948E-3	2.54	6.106E-3	1.03
96	2.147E-3	2.30	4.744E-3	1.29
192	7.842E-4	2.74	3.553E-3	1.34
384	2.442E-4	3.21	2.738E-3	1.30

Now returning to the Dirichlet problem, it follows from Theorem 4.14 that optimal convergence for the piecewise linear collocation method can be attained when a graded mesh with exponent $q \geq 2/(7/6)$ is used. Our results with $q = 2$ are illustrated in Table 5.6. Here we find that the Dirichlet problem now converges with a rate close to $O(n^{-2})$ and the Neumann problem converges with a rate close to $O(n^{-1/3})$, as expected. These results indicate that our integral equation solver is working as predicted by the theory.

Table 5.6: Estimated errors for the piecewise linear collocation method for example 2 on a graded mesh, $q=2$

n	Dirichlet Problem		Neumann Problem	
	err_n^1	ratio	err_n^1	ratio
24	2.722E-4		1.279E-3	
48	2.607E-4	1.04	8.573E-4	1.49
96	5.449E-5	4.78	6.162E-4	1.39
192	1.148E-5	4.75	4.843E-4	1.27
384	4.527E-6	2.54	4.348E-4	1.11

Superconvergence

As we have stated earlier, sometimes the computations converge at a faster rate than so far proved. This maybe due to \widehat{u}_n being superconvergent at the collocation points. To give a flavour of why superconvergence may occur, consider (4.1.8). We introduce the iterated collocation solution, \widehat{u}_n^I , defined by $\widehat{u}_n^I = \widehat{b} - \widehat{\mathcal{L}}\widehat{u}_n$. Then $\widehat{\mathcal{P}}_n\widehat{u}_n^I = \widehat{u}_n$ and so u_n and u_n^I are equal at the collocation points. Also $(I - \widehat{\mathcal{L}}\widehat{\mathcal{P}}_n)\widehat{u}_n^I = \widehat{b}$. Now assuming (4.1.8) is stable in $L^2[-\Lambda, \Lambda]$, $(I - \widehat{\mathcal{L}}\widehat{\mathcal{P}}_n)^{-1}$ is bounded and

$$(I + \widehat{\mathcal{L}}\widehat{\mathcal{P}}_n)^{-1} = I + \widehat{\mathcal{P}}_n(I + \widehat{\mathcal{P}}_n\widehat{\mathcal{L}})^{-1}\widehat{\mathcal{L}} \quad \text{on } L^2[-\Lambda, \Lambda],$$

which shows $(I + \widehat{\mathcal{L}}\widehat{\mathcal{P}}_n)^{-1}$ is also bounded. Therefore since

$$(I + \widehat{\mathcal{L}}\widehat{\mathcal{P}}_n)(\widehat{u} - \widehat{u}_n^I) = -\widehat{\mathcal{L}}(I - \widehat{\mathcal{P}}_n)\widehat{u}$$

it follows that

$$\|\widehat{u} - \widehat{u}_n^I\|_{L^2[-\Lambda, \Lambda]} \leq C\|\widehat{\mathcal{L}}(I - \widehat{\mathcal{P}}_n)\widehat{u}\|_{L^2[-\Lambda, \Lambda]},$$

and we expect from e.g. [22] that, depending on where we chose to place the collocation points, $\|\widehat{\mathcal{L}}(I - \widehat{\mathcal{P}}_n)\widehat{u}\|_{L^2[-\Lambda, \Lambda]} = O(n^{-r'})$ for some $2r \geq r' \geq r$. A prime candidate is the Gauss points. When we collocate at the Gauss points a superconvergence of $O(n^{-2r})$ can be expected for the solution at the Gauss points.

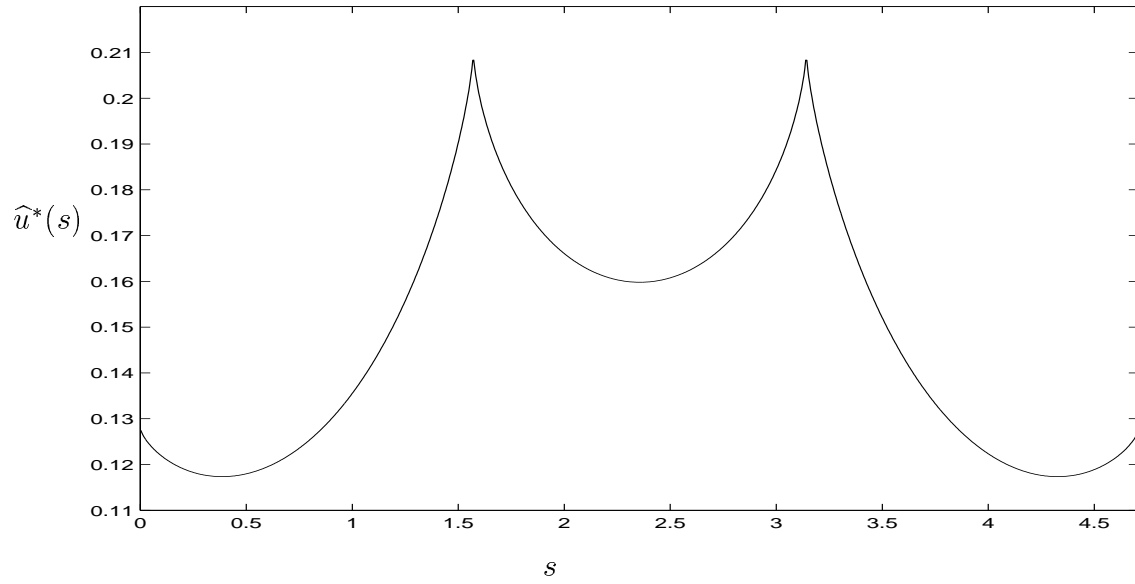


Figure 5-3: The “exact” solution to the integral equation (Dirichlet boundary conditions)

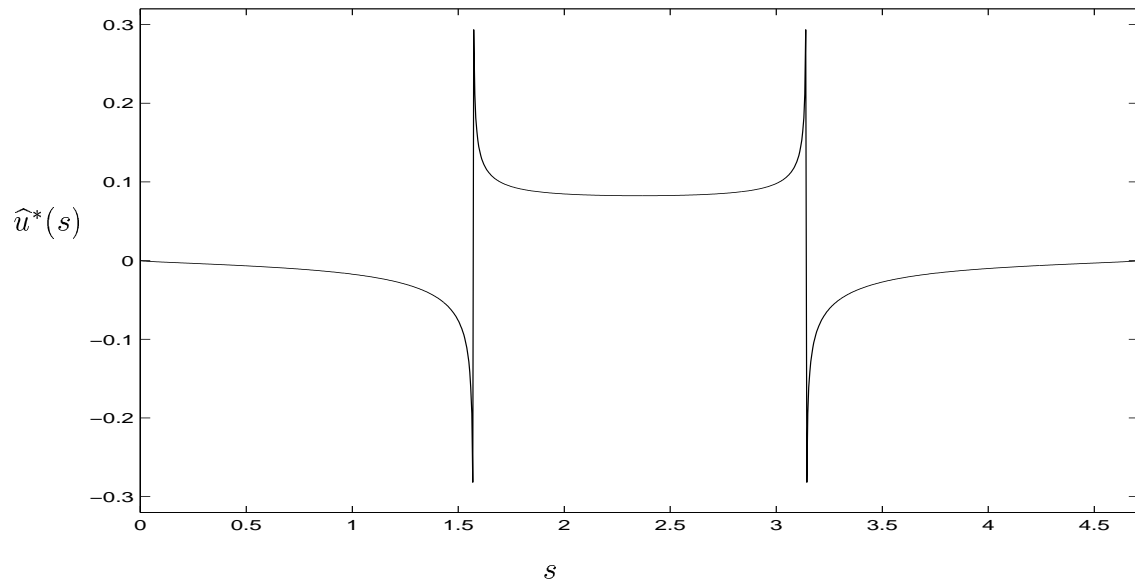


Figure 5-4: The “exact” solution to the integral equation (Neumann boundary conditions)

Chapter 6

Practical Computation of Diffraction Coefficients

In this chapter we describe some of the practical aspects of calculating the acoustic diffraction coefficient, $f(\boldsymbol{\omega}, \boldsymbol{\omega}_0)$, and the electromagnetic diffraction coefficients, $\mathcal{E}(\boldsymbol{\omega}, \boldsymbol{\omega}_0)$ and $\mathcal{H}(\boldsymbol{\omega}, \boldsymbol{\omega}_0)$. To summarise, the basic strategy of calculating the acoustic diffraction coefficient is as follows.

Algorithm A

- (a.i) Firstly we find \hat{u}_n , a numerical approximation of the solution to the integral equation $(I + \hat{\mathcal{L}}_B)\hat{u}(s) = \hat{b}_B(s)$, $B = D$ or N . Here $\hat{\mathcal{L}}_B$ are integral operators as defined in (3.1.27) with kernels $\hat{L}_B(s, \sigma)$ defined in (3.1.28), (3.1.29), and \hat{b}_B depends on the boundary conditions (2.1.2) of the original problem. This needs to be done for many values of $\nu \in \gamma_1$ (see Fig. 2-1).
- (a.ii) Next we find a numerical solution, g_n^{sc} , to the boundary value problem (3.0.1), (3.0.2) with boundary conditions depending on the original problem. We do this by rewriting the integrals along ℓ in (3.0.3) and (3.0.7) as integrals along $[-\Lambda, \Lambda]$ using the parameterisation $\boldsymbol{\rho}$ (the transformation which took (3.0.5) to (3.1.27)) in (3.0.3) and (3.0.7). We then replace \hat{u} by \hat{u}_n in the parameterised versions of (3.0.3) and (3.0.7) to approximate the double and single layer potentials respectively.
- (a.iii) Finally we need to calculate $f(\boldsymbol{\omega}, \boldsymbol{\omega}_0)$ by substituting g_n^{sc} into (2.1.56)

$$f(\boldsymbol{\omega}, \boldsymbol{\omega}_0) \approx \frac{i}{\pi} \int_{\gamma_1} e^{-i\nu\pi} g_n^{sc}(\boldsymbol{\omega}, \boldsymbol{\omega}_0, \nu) \nu \, d\nu. \quad (6.0.1)$$

Recall that in general the integral in (6.0.1) only converges in the distributional sense. We discuss techniques which will transform this integral to one which converges in the classical sense in §6.1.

We have a similar scheme for calculating the electromagnetic diffraction coefficients.

Algorithm B

(b.i) Firstly we find numerical approximations of the solutions of both of the integral equations $(I + \widehat{\mathcal{L}}_B)\widehat{u}(s) = \widehat{b}_B(s)$ for $B = D$ and N , where $\widehat{\mathcal{L}}_B$ are the same integral operators as in (a.i), and \widehat{b}_B depends on the boundary conditions (2.1.2) of the original problem. Again this needs to be done for many values of ν . For the electromagnetic diffraction coefficients $\nu \in \gamma_2$ (Fig. 2-5).

(b.ii) We approximate the solution to the boundary value problems

$$(\Delta^* + \nu^2 - 1/4)g_B^{sc}(\boldsymbol{\omega}, \boldsymbol{\omega}_0, \nu) = 0, \quad B = D, N,$$

with Dirichlet and Neumann boundary conditions (2.2.18) respectively. In a similar way to (a.ii) we rewrite (3.0.3) and (3.0.7) on $[-\Lambda, \Lambda]$ and we replace \widehat{u} by \widehat{u}_n to obtain the approximations $g_{B,n}^{sc}$ for $B = D$ and N respectively.

(b.iii) Finally we calculate $\mathcal{E}(\boldsymbol{\omega}, \boldsymbol{\omega}_0)$ and $\mathcal{H}(\boldsymbol{\omega}, \boldsymbol{\omega}_0)$ by substituting $g_{B,n}^{sc}$ into the formula (2.2.16) for $f_B(\boldsymbol{\omega}, \boldsymbol{\omega}_0)$ for $B = D, N$, i.e. for the electric diffraction coefficient we have from (2.2.20) and (2.2.16) the following,

$$\begin{aligned} \mathcal{E}(\boldsymbol{\omega}, \boldsymbol{\omega}_0) &= -\nabla_{\boldsymbol{\omega}} f_D(\boldsymbol{\omega}, \boldsymbol{\omega}_0) - \nabla_{\boldsymbol{\omega}} f_N(\boldsymbol{\omega}, \boldsymbol{\omega}_0) \wedge \boldsymbol{\omega} \\ &\approx \frac{-i}{\pi} \int_{\gamma_2} e^{-i\nu\pi} (\nabla_{\boldsymbol{\omega}} g_{D,n}^{sc}(\boldsymbol{\omega}, \boldsymbol{\omega}_0, \nu) + \nabla_{\boldsymbol{\omega}} g_{N,n}^{sc}(\boldsymbol{\omega}, \boldsymbol{\omega}_0, \nu) \wedge \boldsymbol{\omega}) \frac{\nu}{\nu^2 - 1/4} d\nu. \end{aligned} \tag{6.0.2}$$

By using (2.2.20) and (2.2.16) again, we obtain an analogous formula for $\mathcal{H}(\boldsymbol{\omega}, \boldsymbol{\omega}_0)$. Again we need to employ the techniques discussed in §6.1 to make the integral in (6.0.2) convergent in the classical sense.

There are several aspects of these schemes which need to be considered before we can go ahead and calculate the diffraction coefficients. Firstly, to solve the integral equation in steps (a.i) and (b.i) we need to be able to calculate the kernel, $\widehat{\mathcal{L}}_B(\boldsymbol{\omega}, \boldsymbol{\omega}')$, and the right-hand side \widehat{b}_B for $B = D, N$. This involves calculating

Legendre functions with a complex index. The computation of such Legendre functions is examined in §6.2. Another issue to be considered (occurring in steps (a.ii) and (b.ii)) is how we calculate the integral in the single and double layer potentials. This we discuss in §6.3, where we also present convergence results for our method of approximating the potentials.

The final issue is the calculation of the contour integrals (over contours of infinite extent) which appear in the formulae (6.0.1) and (6.0.2) for the diffraction coefficients. It turns out that these contour integrals can be rewritten as rapidly convergent integrals along the imaginary axis for certain values of ω . This helps with the implementation and is described in §6.1 while quadrature rules that are used to calculate the deformed integrals are given in §6.4.

Diffraction coefficient calculations are carried out for several conical geometries and are also presented in §6.4.

6.1 Domains of observation

In both the acoustic and the electromagnetic cases the observation domain, M , can be divided into two sub-domains, M_1 and M_2 , separated by the singular directions (see Definition 2.13).

In the case of a fully illuminated convex cone the subdomain M_2 contains observation directions that are inside the domain in which the waves reflected by the surface of the cone and diffracted by lateral edges propagate. The subdomain M_1 is the domain outside of this region and in which only the tip diffracted wave propagates. Recall the function $\theta_1(\omega, \omega_0)$ in Definition 2.13. The domain M_1 is defined by the angles of observation ω such that $\theta_1(\omega, \omega_0)$ is greater than π and M_2 contains all the remaining non-singular directions in M . That is,

$$\begin{aligned} M_1 &= \{\omega \in M : \theta_1(\omega, \omega_0) > \pi\}, \\ M_2 &= \{\omega \in M : \omega \notin M_1 \text{ and } \omega \text{ is not a singular direction}\}. \end{aligned}$$

For a cone that is not fully illuminated, M is still split into two subdomains, M_1 and M_2 . This time, as for the fully illuminated case, M_2 contains observation directions in the “reflected wave” and “edge diffracted wave” domain. In addition to this M_2 contains the “shadow” domain (where neither the scattered nor incident wave penetrate). To simplify presentation we consider only the case when the cone is fully illuminated.

It is in the domain M_1 that it is possible to deform the contours of integration

in (2.1.56) and (2.2.16) to obtain a rapidly convergent integral. This is discussed in §6.1.1 and §6.1.2. However when $\boldsymbol{\omega} \in M_2$ this technique fails. We do not consider this case in depth here but we note that in [9] it is shown that the acoustic diffraction coefficient, $f(\boldsymbol{\omega}, \boldsymbol{\omega}_0)$, and the scalar potentials, $f_B(\boldsymbol{\omega}, \boldsymbol{\omega}_0)$, $B = D, N$, can be determined in the form of Abel-Poisson regularisations. For example, the acoustic diffraction coefficient may be written in the form

$$f(\boldsymbol{\omega}, \boldsymbol{\omega}_0) = \lim_{\epsilon \rightarrow 0^+} \frac{i}{\pi} \int_{\gamma_1} e^{-i\nu\pi - \epsilon\nu} g^{sc}(\boldsymbol{\omega}, \boldsymbol{\omega}_0, \nu) \nu \, d\nu. \quad (6.1.1)$$

The integral in (6.1.1) converges absolutely for fixed ϵ (although as ϵ gets smaller the convergence becomes slower) see [9, Appendix B]. Also, although the convergence with respect to ϵ in (6.1.1) is *a priori* in the distributional sense (see e.g. [9]), it is in fact “classical” (and uniform with respect to $\boldsymbol{\omega}$) in subdomains of M that remain a positive distance away from the singular directions, see [11], [57]. An analogous formula is available for $f_B(\boldsymbol{\omega}, \boldsymbol{\omega}_0)$, $B = D, N$ appearing in the formula (6.0.2). The Abel-Poisson regularisation of the contour integrals allows the approximation of the diffraction coefficients for $\boldsymbol{\omega} \in M_2$ by ignoring the limit and setting ϵ equal to some fixed value. This has been implemented in [9].

For the remainder of this chapter we consider only the case when $\boldsymbol{\omega} \in M_1$.

6.1.1 Deforming the contour in the acoustic case

Recall that in the acoustic case the diffraction coefficient is given by

$$f(\boldsymbol{\omega}, \boldsymbol{\omega}_0) = \frac{i}{\pi} \int_{\gamma_1} e^{-i\nu\pi} g^{sc}(\boldsymbol{\omega}, \boldsymbol{\omega}_0, \nu) \nu \, d\nu, \quad (6.1.2)$$

with the contour γ_1 given in Fig. 2-1. This integral converges only in the distributional sense (Definition 2.5), but it can be converted into a rapidly converging integral for $\boldsymbol{\omega} \in M_1$, in the classical sense. To do this we use the fact that g^{sc} behaves asymptotically like (see [9]):

$$g^{sc}(\boldsymbol{\omega}, \boldsymbol{\omega}_0, \nu) \sim e^{-|\text{Im}(\nu)|\theta_1(\boldsymbol{\omega}, \boldsymbol{\omega}_0)}, \quad \text{when } |\text{Im}(\nu)| \rightarrow +\infty.$$

This implies that if $\boldsymbol{\omega} \in M_1$, i.e. $\theta_1(\boldsymbol{\omega}, \boldsymbol{\omega}_0) > \pi$, then when $\nu = i\tau$, $\tau \in \mathbb{R}$, the integrand in (6.1.2) will decay like $O(\exp(\tau\pi - |\tau|\theta_1(\boldsymbol{\omega}, \boldsymbol{\omega}_0)))$. Therefore since the poles of the integrand in (6.1.2) lie to the right of γ_1 , (see Fig. 2-1) using results from complex analysis we can deform γ_1 onto the imaginary axis when $\boldsymbol{\omega} \in M_1$ without changing the value of the integral (rigorous proof is given in [57]). The

formula for f becomes

$$f(\boldsymbol{\omega}, \boldsymbol{\omega}_0) = -\frac{i}{\pi} \int_{-\infty}^{\infty} e^{\tau\pi} g^{sc}(\boldsymbol{\omega}, \boldsymbol{\omega}_0, i\tau) \tau \, d\tau. \quad (6.1.3)$$

Therefore (6.1.3) gives an expression for $f(\boldsymbol{\omega}, \boldsymbol{\omega}_0)$ in terms of a rapidly (exponentially) convergent integral.

6.1.2 Deforming the contour in the electromagnetic case

To calculate the electromagnetic diffraction coefficients recall from (2.2.20) that we need to calculate $f_B(\boldsymbol{\omega}, \boldsymbol{\omega}_0)$, $B = D, N$,

$$f_B(\boldsymbol{\omega}, \boldsymbol{\omega}_0) = \frac{i}{\pi} \int_{\gamma_2} e^{-i\nu\pi} g_B^{sc}(\boldsymbol{\omega}, \boldsymbol{\omega}_0, \nu) \frac{\nu}{\nu^2 - 1/4} \, d\nu. \quad (6.1.4)$$

In the same way as for the acoustic case described in §6.1.1, we expect that in the domain M_1 , the integrand in (6.1.4) will be exponentially small as $\text{Im}(\nu) \rightarrow \pm\infty$. However, unlike the formula for the acoustic diffraction coefficient, the integral in (6.1.4) is along γ_2 which must lie to the right of $1/2$ (recall Fig. 2-5). Since $\nu = 1/2$ is a pole of the integrand in (6.1.4), we cannot deform γ_2 to the imaginary axis without crossing the pole $\nu = 1/2$ and therefore changing the value of the result in (6.1.4).

One way of dealing with this problem (which we shall not use here) is to follow [12] and deform γ_2 onto a contour which is parallel to the imaginary axis and to the right of $\nu = 1/2$. (We briefly discuss the strategy used in [12] here, and in §6.4.1 we will compare the results of an alternative method described below with those in [12]). The strategy in [12] is to deform the contour γ_2 on to the contour given by $\text{Re}(\nu) = C$ where C lies between $1/2$ and $\nu_{N,2}$, the next eigenvalue of the Neumann problem, or $\nu_{D,1}$, the first eigenvalue of the Dirichlet problem, whichever is smallest. To use this method, it is therefore necessary to determine these eigenvalues, or at least to have good estimates of them.

The method we use here, which will require no knowledge of the position of the eigenvalues, and is therefore more practically useful, is to deform the contour γ_2 to the imaginary axis and to compute the contribution of the residue at $\nu = 1/2$

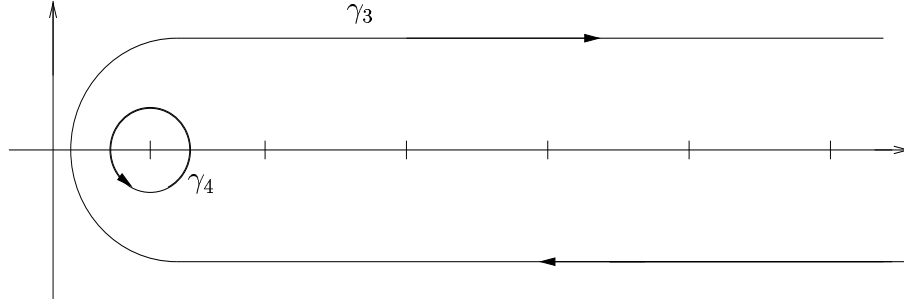


Figure 6-1: Contours of integration γ_3 and γ_4

explicitly. More precisely we write (6.1.4) as

$$\begin{aligned} f_B(\boldsymbol{\omega}, \boldsymbol{\omega}_0) &= \frac{i}{\pi} \int_{\gamma_3} e^{-i\nu\pi} g_B^{sc}(\boldsymbol{\omega}, \boldsymbol{\omega}_0, \nu) \frac{\nu}{\nu^2 - 1/4} d\nu \\ &+ \frac{i}{\pi} \int_{\gamma_4} e^{-i\nu\pi} g_B^{sc}(\boldsymbol{\omega}, \boldsymbol{\omega}_0, \nu) \frac{\nu}{\nu^2 - 1/4} d\nu, \end{aligned} \quad (6.1.5)$$

where γ_3 and γ_4 are shown in Fig. 6-1. Now the integrand has no poles to the left of γ_3 hence the integral along γ_3 can be deformed onto the imaginary axis. We shall calculate the integral around γ_4 using Cauchy's residue theorem in Lemma 6.1.

Lemma 6.1. *For $B = D$ or N it follows that,*

$$\frac{i}{\pi} \int_{\gamma_4} e^{-i\nu\pi} g_B^{sc}(\boldsymbol{\omega}, \boldsymbol{\omega}_0, \nu) \frac{\nu}{\nu^2 - 1/4} d\nu = i g_B^{sc}(\boldsymbol{\omega}, \boldsymbol{\omega}_0, 1/2). \quad (6.1.6)$$

Proof The integrand in (6.1.6) has only one pole within the closed loop formed by γ_4 , namely $\nu = 1/2$. Hence by Cauchy's residue theorem,

$$\begin{aligned} \int_{\gamma_4} e^{-i\nu\pi} g_B^{sc}(\boldsymbol{\omega}, \boldsymbol{\omega}_0, \nu) \frac{\nu}{\nu^2 - 1/4} d\nu &= 2\pi i \lim_{\nu \rightarrow 1/2} \left\{ e^{-i\nu\pi} g_B^{sc}(\boldsymbol{\omega}, \boldsymbol{\omega}_0, \nu) \frac{\nu(\nu - 1/2)}{\nu^2 - 1/4} \right\} \\ &= 2\pi i e^{-i\pi/2} g_B^{sc}(\boldsymbol{\omega}, \boldsymbol{\omega}_0, 1/2) / 2 \\ &= \pi g_B^{sc}(\boldsymbol{\omega}, \boldsymbol{\omega}, 1/2), \end{aligned}$$

and the result follows. \square

Applying this lemma, we see that (6.1.5) can be written as

$$f_B(\boldsymbol{\omega}, \boldsymbol{\omega}_0) = \frac{i}{\pi} \int_{-\infty}^{\infty} e^{\tau\pi} g_B^{sc}(\boldsymbol{\omega}, \boldsymbol{\omega}_0, i\tau) \frac{\tau}{\tau^2 + 1/4} d\tau + i g_B^{sc}(\boldsymbol{\omega}, \boldsymbol{\omega}_0, 1/2). \quad (6.1.7)$$

The integral on the right-hand side of (6.1.7) is exponentially convergent for $\boldsymbol{\omega} \in M_1$.

We can use the formula (6.1.7) to compute the electromagnetic diffraction coefficients. The functions $g_B^{sc}(\boldsymbol{\omega}, \boldsymbol{\omega}_0, i\tau)$ can be computed as described in Chapter 3. However we cannot use these techniques to compute $g_B^{sc}(\boldsymbol{\omega}, \boldsymbol{\omega}_0, 1/2)$, $B = D, N$. This is due to the fact that we seek g_B^{sc} in terms of the fundamental solution satisfying (2.1.54), which has a singularity at $\nu = 1/2$. We briefly discuss the computation of $g_B^{sc}(\boldsymbol{\omega}, \boldsymbol{\omega}_0, 1/2)$ for the remainder of this subsection.

Considering $B = D$ first, $g_D(\boldsymbol{\omega}, \boldsymbol{\omega}_0, 1/2)$ is the solution to the boundary value problem,

$$\Delta^* g_D^{sc}(\boldsymbol{\omega}, \boldsymbol{\omega}_0, 1/2) = 0, \quad \boldsymbol{\omega} \in M, \quad (6.1.8)$$

$$g_D^{sc}(\boldsymbol{\omega}, \boldsymbol{\omega}_0, 1/2) = -g_D^{inc}(\boldsymbol{\omega}, \boldsymbol{\omega}_0, 1/2), \quad \boldsymbol{\omega} \in \ell. \quad (6.1.9)$$

($g_D^{inc}(\boldsymbol{\omega}, \boldsymbol{\omega}_0, \nu)$ has a (removable) singularity at $\nu = 1/2$, see Lemma A.10 in Appendix A for details. It is explicitly given by (A.3.16).) So we henceforth define $g_D^{inc}(\boldsymbol{\omega}, \boldsymbol{\omega}_0, 1/2)$ to be the analytic continuation of $g_D^{inc}(\boldsymbol{\omega}, \boldsymbol{\omega}_0, \nu)$ as $\nu \rightarrow 1/2$.) Following a similar approach as that described in Chapter 3 we reformulate (6.1.8) directly as an integral equation. We seek the solution to (6.1.8) in the form of a “double layer potential”,

$$g_D^{sc}(\boldsymbol{\omega}, \boldsymbol{\omega}_0, 1/2) = \int_{\ell} \frac{\partial \widehat{g}_0(\boldsymbol{\omega}, \boldsymbol{\omega}', 1/2)}{\partial \mathbf{m}'} u(\boldsymbol{\omega}') d\boldsymbol{\omega}', \quad \boldsymbol{\omega} \in M, \quad (6.1.10)$$

where u is to be found and \widehat{g}_0 is by

$$\widehat{g}_0(\boldsymbol{\omega}, \boldsymbol{\omega}', 1/2) = \frac{1}{4\pi} \log(1 - \cos \theta(\boldsymbol{\omega}, \boldsymbol{\omega}')).$$

Although \widehat{g}_0 is not the fundamental solution associated with the PDE (6.1.8) on the domain S^2 it can be shown that the representation of g_D^{sc} in (6.1.10) will solve (6.1.8), (see the proof of Lemma A.10 for details). (In fact $\Delta^* \widehat{g}_0(\boldsymbol{\omega}, \boldsymbol{\omega}_0, 1/2) = \delta(\boldsymbol{\omega} - \boldsymbol{\omega}_0) - 1/4\pi$, see again the proof of Lemma A.10.) Also \widehat{g}_0 has the same local behaviour as $\boldsymbol{\omega} \rightarrow \boldsymbol{\omega}'$ as the fundamental solution of the Laplacian on the plane.

Note that (after some elementary vector calculus and using the notational convention in Notation 3.1),

$$\frac{\partial \widehat{g}_0(\boldsymbol{\omega}, \boldsymbol{\omega}', 1/2)}{\partial \mathbf{m}'} = -\frac{1}{2\pi} \frac{\mathbf{t}' \cdot (\boldsymbol{\omega} \wedge \boldsymbol{\omega}')}{|\boldsymbol{\omega} - \boldsymbol{\omega}'|^2}.$$

This is exactly the principal singularity of $(\partial g_0/\partial \mathbf{m}')(\boldsymbol{\omega}, \boldsymbol{\omega}', \nu)$, when $\nu \neq 1/2$ (this follows from (3.0.6) and (3.1.12)). It can be shown that when we take limits in (6.1.10) as $\boldsymbol{\omega}$ tends to ℓ we derive the integral equation, cf. (3.0.4)

$$u(\boldsymbol{\omega}) + \int_{\ell} 2 \frac{\partial \widehat{g}_0(\boldsymbol{\omega}, \boldsymbol{\omega}', 1/2)}{\partial \mathbf{m}'} u(\boldsymbol{\omega}') d\boldsymbol{\omega}' = 2b(\boldsymbol{\omega}), \quad \boldsymbol{\omega} \in \ell.$$

Since the kernel in this integral equation is exactly the principal singularity of $L_D(\boldsymbol{\omega}, \boldsymbol{\omega}')$ when $\nu \neq 1/2$ we apply the same techniques as in Chapters 3 and 4 to find, $g_{D,n}^{sc}$, a numerical approximation to the solution of (6.1.8) with boundary conditions given by (6.1.9).

Finally we consider $g_N^{sc}(\boldsymbol{\omega}, \boldsymbol{\omega}_0, 1/2)$. Note from the formulae for the electromagnetic diffraction coefficients (6.0.2) that we are ultimately concerned with computing the spherical gradient of $g_N^{sc}(\boldsymbol{\omega}, \boldsymbol{\omega}_0, 1/2)$. Therefore rather than solving (6.1.8), with Neumann boundary conditions, directly, we can use the relation

$$\nabla g_N^{sc}(\boldsymbol{\omega}, \boldsymbol{\omega}_0, 1/2) \wedge \boldsymbol{\omega} = \nabla g_D^{sc}(\boldsymbol{\omega}, \boldsymbol{\omega}_0, 1/2)$$

(see Lemma A.12 for details). The latter has the effect that the contributions of the residues at $\nu = 1/2$ corresponding to the terms with g_D and g_N in (6.0.2) are identical. Therefore using (6.1.5) and (6.1.6) the formula (6.0.2) for $\mathcal{E}(\boldsymbol{\omega}, \boldsymbol{\omega}_0)$ becomes,

$$\begin{aligned} \mathcal{E}(\boldsymbol{\omega}, \boldsymbol{\omega}_0) &\approx \frac{-i}{\pi} \int_{-\infty}^{\infty} (\nabla_{\boldsymbol{\omega}} g_{D,n}^{sc}(\boldsymbol{\omega}, \boldsymbol{\omega}_0, i\tau) - \nabla_{\boldsymbol{\omega}} g_{N,n}^{sc}(\boldsymbol{\omega}, \boldsymbol{\omega}_0, i\tau) \wedge \boldsymbol{\omega}) \frac{\tau e^{\tau\pi}}{\tau^2 + 1/4} d\tau \\ &+ 2i \nabla_{\boldsymbol{\omega}} g_{D,n}^{sc}(\boldsymbol{\omega}, \boldsymbol{\omega}_0, 1/2). \end{aligned}$$

An analogous formula holds for $\mathcal{H}(\boldsymbol{\omega}, \boldsymbol{\omega}_0)$.

6.2 Calculating Legendre functions

When calculating the acoustic or electromagnetic diffraction coefficients it follows from steps (a.i) and (b.i) respectively that we need to find the solution to the corresponding integral equation for various values of $\nu = i\tau$. In order to do this we need to be able to calculate the kernel $\widehat{L}_B(s, \sigma)$ for $B = D$ or N and the right-hand side $\widehat{b}_B(s)$. Hence it is necessary to calculate $P_{i\tau-1/2}(-\cos\theta)$ and $P'_{i\tau-1/2}(-\cos\theta)$. We do not know of any general-purpose software for the task of computing Legendre functions with complex indices. Thus we took the approach of [8], [9] and applied a Runge-Kutta method to the Legendre differential

equation,

$$\frac{d^2}{d\theta^2}\{P_{i\tau-\frac{1}{2}}(-\cos\theta)\} + \cot\theta\frac{d}{d\theta}\{P_{i\tau-\frac{1}{2}}(-\cos\theta)\} - (\tau^2 + 1/4)P_{i\tau-\frac{1}{2}}(-\cos\theta) = 0, \quad (6.2.1)$$

starting at $\pi/2$ and integrating forward and backward on $(0, \pi)$. For the initial data we use the formulae ([44], 8.823, 8.752 and 8.714(1))

$$P_{i\tau-\frac{1}{2}}(-\cos\theta) = \frac{1}{\pi\sqrt{2}} \int_{-\theta}^{\theta} \frac{\cos(i\tau x)}{\sqrt{\cos(x) + \cos(\theta)}} dx, \quad (6.2.2)$$

$$P'_{i\tau-\frac{1}{2}}(-\cos\theta) = \frac{\sqrt{2}}{\pi \sin\theta} \int_{-\theta}^{\theta} \cos(i\tau x) \sqrt{\cos(x) + \cos(\theta)} dx, \quad (6.2.3)$$

evaluated at $\theta = \pi/2$ using Gauss-Chebyshev quadrature with N nodes, where N is chosen so that the error is smaller than some prescribed tolerance ϵ . It turns out [29] that it is sufficient to take any $N > \{\log(\epsilon^{-1}) + |\tau|\pi\}/\{2 \log \cot(\pi/8)\}$. (In our case $\epsilon = 10^{-9}$.)

Several difficulties arise when using this method. Firstly $|\tau|$ may be large and since $P_{i\tau-1/2}(\cos\theta)$ grows exponentially in $\theta|\tau|$, this may cause overflow problems. Secondly $\theta = 0, \pi$ are singular points of the differential equation (6.2.1) and so we may expect difficulties with the Runge-Kutta integrator for $\theta = 0$ or π .

To deal with large $|\tau|$, we introduce a new unknown W_τ defined by the relation $P_{i\tau-1/2}(\cos\theta) = \exp(\theta|\tau|)W_\tau(\theta)$ (see [8]). We substitute this into (6.2.1) and rearrange to obtain an initial value system for the well behaved functions W_τ and W'_τ

$$\sin\theta\frac{d^2}{d\theta^2}W_\tau(\theta) + (2|\tau|\sin\theta + \cos\theta)\frac{d}{d\theta}W_\tau(\theta) + \left(|\tau|\cos\theta - \frac{\sin\theta}{4}\right)W_\tau(\theta) = 0, \quad (6.2.4)$$

which is again solved using the Runge-Kutta method (with the initial data derived from the integral representations (6.2.2) and (6.2.3)).

To deal with the singular point at $\theta = 0$, we use, instead of the above Runge-Kutta method, the classical expression for $P_{i\tau-1/2}(-\cos\theta)$ in terms of a hypergeometric series ([44], 8.841):

$$P_{i\tau-\frac{1}{2}}(-\cos\theta) = 1 + \frac{4\tau^2 + 1^2}{2^2} \cos^2\frac{\theta}{2} + \frac{(4\tau^2 + 1^2)(4\tau^2 + 3^2)}{2^2 4^2} \cos^4\frac{\theta}{2} + \dots \quad (6.2.5)$$

For small θ this converges rapidly. On the other hand, near the singular point

$\theta = \pi$ the formula (3.1.7) can be used

$$P_{i\tau-\frac{1}{2}}(-\cos\theta) = a_{i\tau-\frac{1}{2}}(-\cos\theta) \log\left(\frac{1-\cos\theta}{2}\right) + b_{i\tau-\frac{1}{2}}(-\cos\theta), \quad (6.2.6)$$

with explicit formulae for $a_{i\tau-\frac{1}{2}}(-\cos\theta)$ and $b_{i\tau-\frac{1}{2}}(-\cos\theta)$ in terms of hypergeometric series given in (3.1.8) and (3.1.9) (see [52, Ch V. Eq 53]). To calculate derivatives near the singular points we differentiate the formulae (6.2.5) and (6.2.6) term by term. (Note that in order to calculate the electromagnetic diffraction coefficients we also need to calculate $P''_{i\tau-1/2}(-\cos\theta)$, in (2.2.20), this is achieved by finding $P_{i\tau-\frac{1}{2}}$ and $P'_{i\tau-\frac{1}{2}}$ and then substituting into (6.2.1)).

6.3 Calculating the single and double layer potentials

In both the acoustic and electromagnetic cases we solve boundary value problems on M , a portion on the unit sphere, by the boundary integral method. This involves finding the “scattered part” g^{sc} of the Green’s function at interior points in M by evaluating potentials. Here we consider the accuracy of this process.

Consider for example the problem of calculating the solution to the boundary value problem (3.0.1) with the Dirichlet boundary conditions in (3.0.2). Recall that we seek the solution in the form of a double layer potential,

$$g^{sc}(\boldsymbol{\omega}, \boldsymbol{\omega}_0, \nu) = \int_{\ell} \frac{\partial g_0}{\partial \mathbf{m}'}(\boldsymbol{\omega}, \boldsymbol{\omega}', \nu) u(\boldsymbol{\omega}') d\boldsymbol{\omega}', \quad (6.3.1)$$

where u is to be found. We proceed by computing u_n , an approximation to u , using a collocation method as described in Chapter 4 and substituting it into (6.3.1). We are now required to calculate the integral in (6.3.1) for which, in general, there is no explicit formula. Hence we use a quadrature rule. First, in the same way as in Chapter 3 we rewrite (6.3.1) on $[-\Lambda, \Lambda]$ using $\boldsymbol{\rho}$, an arclength parameterisation of ℓ . By putting $\boldsymbol{\omega}' = \boldsymbol{\rho}(\sigma)$ and noting that $u_n(\boldsymbol{\omega}') = u_n(\boldsymbol{\rho}(\sigma)) = \hat{u}_n(\sigma)$ we obtain,

$$g^{sc}(\boldsymbol{\omega}, \boldsymbol{\omega}_0, \nu) \approx \int_{-\Lambda}^{\Lambda} N_D(\boldsymbol{\omega}, \sigma) \hat{u}_n(\sigma) d\sigma, \quad (6.3.2)$$

where, as in Lemma 3.4,

$$N_D(\boldsymbol{\omega}, \sigma) = \frac{P'_{\nu-\frac{1}{2}}(-\cos\theta(\boldsymbol{\omega}, \boldsymbol{\rho}(\sigma)))}{4 \cos(\pi\nu)} \boldsymbol{\rho}_s(\sigma) \cdot (\boldsymbol{\omega} \wedge \boldsymbol{\rho}(\sigma)).$$

Similarly if we have to solve (3.0.1) with the Neumann boundary conditions in (3.0.2) then we write the solution in the form

$$g^{sc}(\boldsymbol{\omega}, \boldsymbol{\omega}_0, \nu) = \int_{\ell} g_0(\boldsymbol{\omega}, \boldsymbol{\omega}', \nu) u(\boldsymbol{\omega}') d\boldsymbol{\omega}'. \quad (6.3.3)$$

In this case we approximate $g^{sc}(\boldsymbol{\omega}, \boldsymbol{\omega}_0, \nu)$ by

$$g^{sc}(\boldsymbol{\omega}, \boldsymbol{\omega}_0, \nu) \approx \int_{-\Lambda}^{\Lambda} N_N(\boldsymbol{\omega}, \sigma) \widehat{u}_n(\sigma) d\sigma, \quad (6.3.4)$$

where, following from (3.0.7),

$$N_N(\boldsymbol{\omega}, \sigma) = \frac{-P_{\nu-\frac{1}{2}}(-\cos\theta(\boldsymbol{\omega}, \boldsymbol{\rho}(\sigma)))}{4 \cos(\pi\nu)}.$$

Note that for $\boldsymbol{\omega}$ bounded away from ℓ the integrands in (6.3.2) and (6.3.3) are smooth (\mathcal{C}^∞) functions of σ on each subinterval of $[-\Lambda, \Lambda]$ corresponding to each smooth segment of the contour ℓ .

We aim to find a quadrature rule to calculate the integrals in (6.3.2) whilst observing the same rates of convergence as those found in Chapter 4 for the error between \widehat{u}_n and \widehat{u} . We consider here only the case of the h -refinement collocation method, hence we require a quadrature rule with an error less than $O(n^{-r})$, where n is the number of nodes on the collocation mesh and r is the order of the collocation method.

The simplest method of calculating the integral in (6.3.2) is to split the interval of integration into the n intervals I_i described in §4.1 and then use a quadrature rule on each I_i with abscissae coinciding with the collocation points x_{ij}^r . Hence we define g_n^{sc} a numerical approximation of the solution to the boundary value problem (3.0.1), (3.0.2) as follows

$$g_n^{sc}(\boldsymbol{\omega}, \boldsymbol{\omega}_0, \nu) = \sum_{i=1}^n \sum_{j=1}^r w_{ij} N_B(\boldsymbol{\omega}, x_{ij}) \widehat{u}_n(x_{ij}), \quad (6.3.5)$$

with $B = D$ or N when Dirichlet or Neumann boundary conditions are prescribed respectively. The weights can be chosen so that the quadrature rules in (6.3.5) will be exact for polynomials of degree $\leq r - 1$ at least. It follows from Lemma 5.1 that (6.3.5) will be an $O(n^{-r})$ approximation of g^{sc} , provided that \widehat{u}_n is an $O(n^{-r})$ approximation of \widehat{u} .

6.3.1 Numerical results

To test the above approach of solving the boundary value problem (3.0.1), with appropriate boundary conditions, we return to the two examples introduced in §5.4. Throughout, the implementation of the integral equation solver used to find solutions to (4.0.1) is exactly as described in §5.4.

Example 1

Recall the test example of the scattering of an axisymmetric planar acoustic incident wave by a circular cone with semi-angle $\pi/6$. As described in §2.1 the general formulae for the diffraction coefficients reduce to finding the solution of the PDE

$$(\Delta^* + \nu^2 - 1/4)g^{sc}(\boldsymbol{\omega}, \boldsymbol{\omega}_0, \nu) = 0 \quad \boldsymbol{\omega} \in M, \quad (6.3.6)$$

with Dirichlet or Neumann conditions (3.0.2) prescribed on ℓ depending on the original problem. It occurs that for any circular cone the solution g^{sc} to (6.3.6) with axisymmetric incident direction, $\boldsymbol{\omega}_0$ and Dirichlet boundary conditions has an explicit solution (see e.g. [67]) given by

$$g^{sc}(\boldsymbol{\omega}, \boldsymbol{\omega}_0, \nu) = \frac{1}{4 \cos(\pi\nu)} \frac{P_{\nu-1/2}(\cos \hat{\theta})}{P_{\nu-1/2}(-\cos \hat{\theta})} P_{\nu-1/2}(\cos \theta(\boldsymbol{\omega}, \boldsymbol{\omega}_0)),$$

where $\hat{\theta}$ is the semi-angle of the cone (i.e. in this example $\hat{\theta} = \pi/6$). Similarly if g^{sc} satisfies Neumann boundary conditions on ℓ then the solution to (6.3.6) is given by,

$$g^{sc}(\boldsymbol{\omega}, \boldsymbol{\omega}_0, \nu) = -\frac{1}{4 \cos(\pi\nu)} \frac{P'_{\nu-1/2}(\cos \hat{\theta})}{P'_{\nu-1/2}(-\cos \hat{\theta})} P_{\nu-1/2}(\cos \theta(\boldsymbol{\omega}, \boldsymbol{\omega}_0)).$$

To test the method in this case we use piecewise constant and piecewise linear collocation methods to find, u_n , the approximate solution to the corresponding integral equation. Solutions to (6.3.6) are obtained by substituting $u_n(\boldsymbol{\rho}(s)) = \hat{u}_n(s)$ into (6.3.1) (in the Dirichlet case) and (6.3.3) (in the Neumann case) and calculating the resulting integral using Gauss quadrature based at the collocation points.

For the special case $\nu = i$ we obtain the results in Table 6.1. For illustration we have estimated the order of convergence by evaluating the double/single layer potentials at the particular angle of observation $\boldsymbol{\omega} = (0, 0, -1)^T$ and calculating the error as $\text{err}_n^2 = |g^{sc}(\boldsymbol{\omega}, \boldsymbol{\omega}_0, \nu) - g_n^{sc}(\boldsymbol{\omega}, \boldsymbol{\omega}_0, \nu)|$. For other observation directions in M we obtain similar results. The figures in Table 6.1 show close

Table 6.1: Error estimates for the double/single layer potentials for Example 1

	Dirichlet Boundary Conditions				Neumann Boundary Conditions			
	constant		linear		constant		linear	
n	err_n^2	ratio	err_n^2	ratio	err_n^2	ratio	err_n^2	ratio
4	9.126E-5		7.012E-6		3.525E-6		2.790E-7	
8	6.686E-6	13.6	8.554E-7	8.20	2.660E-7	13.2	3.411E-8	8.18
16	2.154E-7	30.9	1.041E-7	8.21	8.594E-9	30.9	4.154E-9	8.21
32	3.339E-7	0.64	1.294E-8	8.05	1.352E-8	0.64	5.160E-10	8.05
64	1.120E-7	3.03	1.862E-9	6.95	4.468E-9	3.02	7.425E-11	6.95
128	3.077E-8	3.64	8.255E-10	2.25	1.227E-9	3.64	3.293E-11	2.25

to $O(n^{-2})$ convergence of the piecewise constant collocation method and close to $O(n^{-3})$ convergence of the piecewise linear collocation method illustrating the superconvergence of the method. The convergence rate of the piecewise linear approximations drop off for $n = 128$ due to the fact that the errors err_n^2 are close to machine precision.

Example 2

Recall the trihedral cone described in §5.4 (see Fig. 5-2). We wish to find a solution to (6.3.6) with Dirichlet or Neumann boundary conditions, when M is the subdomain of S^2 exterior to the cone Ξ pictured in Fig. 5-2. We consider the test case $\boldsymbol{\omega}_0 = -\boldsymbol{\omega}_{c_1}$ (see Fig. 5-2), $\boldsymbol{\omega}_0 = (0, 0, -1)$ and $\nu = i$. There is no known explicit solution for this problem. However to test the method we use the collocation method with $r = 3$ and $n = 330$ to solve (4.0.1) approximately. Then we implement the strategy described above to compute a close approximation to the exact potential. In Tables 6.2 - 6.4 we tabulate the errors, err_n^2 , which are calculated in the same way as described in Example 1 of this subsection. We have investigated the convergence of the potential when the piecewise constant and piecewise linear collocation methods are used to solve the integral equation (4.0.1). We have displayed results for the case when a uniform mesh is used (Table 6.2) along with those for graded meshes with exponent $q = 2$ and 3 (Tables 6.3 and 6.4 respectively). The results illustrate the superconvergence of the method (well-documented in the case of planar problems, e.g. [22] [4] [38]), with close to $O(n^{-2})$ convergence observed for piecewise constant approximation and faster than $O(n^{-3})$ convergence for piecewise linear approximation when $q = 3$. The extreme gradings needed for optimal convergence of the density may

Table 6.2: Error estimates for the double/single layer potentials for Example 2 using a uniform mesh, $q = 1$

n	Dirichlet Boundary Conditions				Neumann Boundary Conditions			
	constant		linear		constant		linear	
	err_n^2	ratio	err_n^2	ratio	err_n^2	ratio	err_n^2	ratio
12	3.121E-4		1.605E-5		6.251E-5		1.529E-5	
24	1.355E-4	2.30	1.648E-5	0.97	2.676E-5	2.34	5.670E-6	2.70
48	5.430E-5	2.49	5.269E-6	3.13	1.112E-5	2.41	2.196E-6	2.58
96	2.129E-5	2.55	2.003E-6	2.63	4.536E-6	2.45	8.689E-7	2.53
192	8.837E-6	2.41	8.029E-7	2.49	1.821E-6	2.49	3.442E-7	2.52

Table 6.3: Error estimates for the double/single layer potentials for Example 2 using a graded mesh, $q = 2$

n	Dirichlet Boundary Conditions				Neumann Boundary Conditions			
	constant		linear		constant		linear	
	err_n^2	ratio	err_n^2	ratio	err_n^2	ratio	err_n^2	ratio
12	3.161E-4		6.978E-6		3.743E-5		7.086E-6	
24	1.346E-4	2.35	4.387E-6	1.59	1.023E-5	3.66	1.086E-6	6.53
48	4.206E-5	3.20	5.007E-7	8.76	2.925E-6	3.50	1.725E-7	6.29
96	1.337E-5	3.15	7.214E-8	6.94	7.719E-7	3.79	2.745E-8	6.29
192	4.086E-6	3.27	1.149E-8	6.28	2.045E-7	3.77	4.334E-9	6.33

Table 6.4: Error estimates for the double/single layer potentials for Example 2 using a graded mesh, $q = 3$

n	Dirichlet Boundary Conditions				Neumann Boundary Conditions			
	constant		linear		constant		linear	
	err_n^2	ratio	err_n^2	ratio	err_n^2	ratio	err_n^2	ratio
12	4.697E-4		2.519E-5		4.451E-5		7.045E-6	
24	1.622E-4	2.90	4.039E-6	6.24	8.074E-6	5.51	7.437E-7	9.47
48	6.120E-5	2.65	3.258E-7	12.4	3.076E-6	2.62	6.417E-8	11.6
96	2.015E-5	3.04	3.179E-8	10.2	8.727E-7	3.53	5.306E-9	12.1
192	5.914E-6	3.41	2.448E-9	13.0	2.351E-7	3.71	4.083E-10	13.0

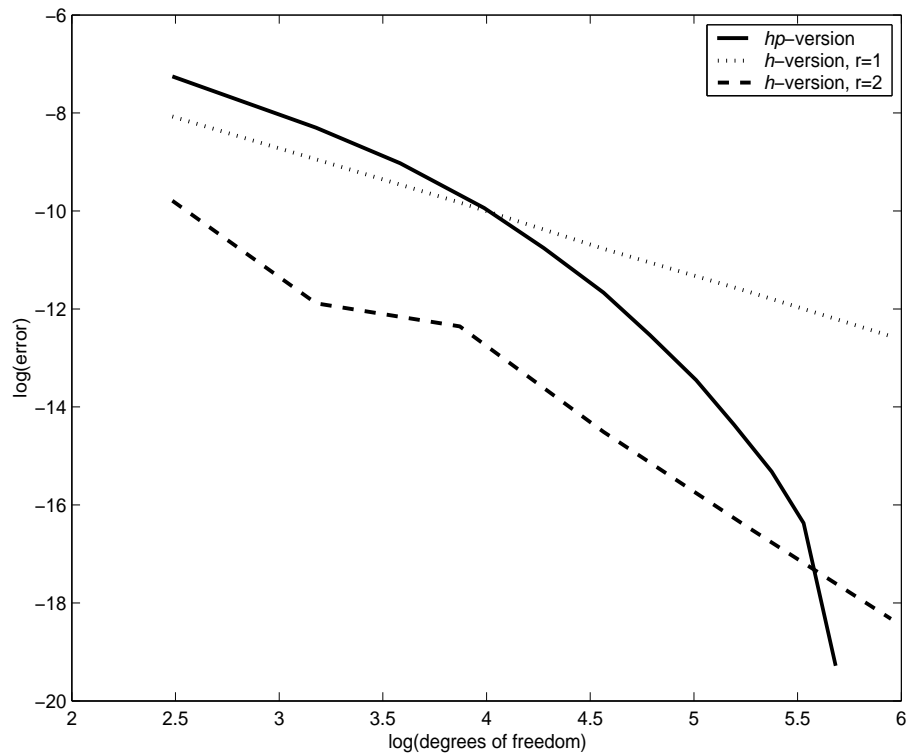


Figure 6-2: Convergence of errors for the hp -method

not be needed for the potential, and in fact better than optimal convergence may be obtained because of the smoothness of the fundamental solution away from the boundary ℓ .

We emphasise that the results in this subsection along with those in §5.4 illustrate not only the convergence theory in Chapter 4, but also show that the algorithm used to compute the Legendre function with complex index is working in a stable manner.

Recall from §5.1 that for the majority of the matrix entries only one kernel evaluation is needed *independent* of the order of the method. This suggests that the hp -version of the boundary element method with matrix entries computed using a similar quadrature scheme as the h -version should be very competitive. To demonstrate the strength of the hp -version of collocation we solve (6.3.6) with Dirichlet boundary conditions for the above trihedral cone case. We use the collocation method described in §4.3.2 to calculate \hat{u}_n with the collocation points given by the r_i Gauss points on each subinterval I_i , $i = 1, \dots, n$. We set $\sigma = 0.25$ to define the geometric mesh and set $\beta = 0.5$ in (4.3.48) to define the linear distribution of the approximating polynomials. We calculate each matrix

entry in (4.1.6) using r_i -point Gauss rules resulting in only one kernel evaluation per matrix entry.

We observe in Fig. 6-2 the exponential convergence of this scheme by plotting err_n^2 against the degrees of freedom (by degrees of freedom we mean the total number of collocation points used) on log scaled axes along with the results for piecewise constant and piecewise linear collocation methods.

6.4 Calculating the integral with respect to τ

Recall from steps (a.iii) and (b.iii) of Algorithms A and B described at the beginning of this chapter that we are required to calculate the contour integrals in the formulae (6.1.3) and (6.1.7). There is no explicit formulae to do this hence we use a numerical scheme. We consider the formula for (6.1.3) first and return to the formulae (6.1.7) later.

To calculate $f(\boldsymbol{\omega}, \boldsymbol{\omega}_0)$ we substitute g_n^{sc} into (6.1.3) and approximate the integral with respect to τ as follows. First the domain of integration is replaced by the imaginary axis truncated by two cut off points $N_1 < 0 < N_2$, with N_1 and N_2 to be chosen. Then we employ a quadrature rule to calculate the truncated integral. We define $f_n(\boldsymbol{\omega}, \boldsymbol{\omega}_0)$ to be the numerical approximation of $f(\boldsymbol{\omega}, \boldsymbol{\omega}_0)$ using this method. The cut off points and the quadrature rule are chosen so as to ensure optimal convergence of $f_n(\boldsymbol{\omega}, \boldsymbol{\omega}_0)$ to $f(\boldsymbol{\omega}, \boldsymbol{\omega}_0)$, i.e. we would like the convergence to be of the same order that g_n^{sc} converges to g^{sc} .

To find suitable values for the cut off points N_1 and N_2 we note, from [9] and [57], that $g^{sc}(\boldsymbol{\omega}, \boldsymbol{\omega}_0, i\tau)$ has the following asymptotic behaviour

$$g^{sc}(\boldsymbol{\omega}, \boldsymbol{\omega}_0, i\tau) \sim e^{-|\tau|\theta_1(\boldsymbol{\omega}, \boldsymbol{\omega}_0)}, \quad \text{as } |\tau| \rightarrow \infty. \quad (6.4.1)$$

Then for sufficiently negative N_1 ,

$$\int_{-\infty}^{N_1} e^{\tau\pi} g^{sc}(\boldsymbol{\omega}, \boldsymbol{\omega}_0, i\tau) \tau \, d\tau \sim \int_{-\infty}^{N_1} e^{\tau(\pi+\theta_1(\boldsymbol{\omega}, \boldsymbol{\omega}_0))} \tau \, d\tau. \quad (6.4.2)$$

Since the exponential term in the integrand on the right-hand side of (6.4.2) dominates the polynomial term in the integrand, to ensure that (6.4.2) is of order n^{-r} and also simplify the computation we choose N_1 so that,

$$\int_{-\infty}^{N_1} e^{\tau(\pi+\theta_1(\boldsymbol{\omega}, \boldsymbol{\omega}_0))} \tau \, d\tau \leq n^{-r}.$$

Therefore we can choose N_1 given by,

$$N_1 = \frac{-r \log(n) + \log(\theta_1(\boldsymbol{\omega}, \boldsymbol{\omega}_0) + \pi)}{\theta_1(\boldsymbol{\omega}, \boldsymbol{\omega}_0) + \pi}. \quad (6.4.3)$$

A similar argument (and recalling that $\theta_1(\boldsymbol{\omega}, \boldsymbol{\omega}_0) > \pi$) shows that we should chose

$$N_2 = \frac{r \log(n) + \log(\theta_1(\boldsymbol{\omega}, \boldsymbol{\omega}_0) - \pi)}{\theta_1(\boldsymbol{\omega}, \boldsymbol{\omega}_0) - \pi}. \quad (6.4.4)$$

To perform quadrature over $[N_1, N_2]$ we divide $[N_1, N_2]$ into $\lceil n \log(n) \rceil$ subintervals of length $(N_2 - N_1) / \lceil n \log(n) \rceil$ denoted by J_i , $i = 1, \dots, \lceil n \log(n) \rceil$. By using Gauss-Legendre rules of order $\lceil (r+1)/2 \rceil$ we obtain an $O(n^{-r})$ approximation of (6.1.3).

Using an analogous approach to calculate the integrals in the formula (6.1.7) for the scalar potentials $f_B(\boldsymbol{\omega}, \boldsymbol{\omega}_0)$, $B = D, N$, we can obtain the same result for the electromagnetic case.

To test the above technique for calculating the diffraction coefficients we return to the two example geometries of the circular cone and trihedral cone discussed in §5.4 and §6.3.1.

6.4.1 Results

We now compute diffraction coefficients for several different conical geometries. Throughout this subsection we set the angle of incidence $\boldsymbol{\omega}_0 = (0, 0, -1)^T$. In the electromagnetic setting we choose the polarisation of the incident wave so that $\mathbf{E}^0 = (1, 0, 0)^T$ and $\mathbf{H}^0 = (0, 1, 0)^T$.

Example 1

We consider here the diffraction by a circular cone (whose axis coincides with the positive x_3 axis) of semiangle $\pi/6$ in both acoustic and electromagnetic settings. We consider an axisymmetric incident wave and use piecewise constant collocation to solve the integral equation and the midpoint rule on each subinterval, I_i , to compute the potential. Since the cut off points N_1 and N_2 are determined using the expected asymptotics of g^{sc} in (6.4.1), the formulae (6.4.3) and (6.4.4) will only be valid for sufficiently large n . The computations in this subsection are only performed for relatively small values of n so to compute the integrals in (6.1.3) we truncate the range of integration to $[-2, 18]$ and split this interval into $\lceil n \log(n) \rceil$ subintervals on which we apply the mid point rule. The cut off range $[-2, 18]$ has been determined empirically to ensure accuracy for the

Table 6.5: Acoustic diffraction coefficient calculations for the circular cone

n	$\text{Im } f_n(\boldsymbol{\omega}, \boldsymbol{\omega}_0) \quad \boldsymbol{\omega} = (\sin(\pi - \theta), 0, \cos(\pi - \theta))$					
	$\theta = 0$	$\theta = \pi/24$	$\theta = 2\pi/24$	$\theta = 3\pi/24$	$\theta = 4\pi/24$	$\theta = 5\pi/24$
8	-0.049234	-0.049538	-0.050496	-0.052146	-0.054610	-0.058074
16	-0.038094	-0.038385	-0.039310	-0.040931	-0.043336	-0.046772
32	-0.038169	-0.038462	-0.039393	-0.040999	-0.043407	-0.046792
64	-0.038173	-0.038466	-0.039392	-0.041006	-0.043411	-0.046795
128	-0.038173	-0.038466	-0.039392	-0.041006	-0.043411	-0.046796

largest value of n used to evaluate the diffraction coefficients in this subsection. We evaluate $f_n(\boldsymbol{\omega}, \boldsymbol{\omega}_0)$, the estimate of the diffraction coefficient, $f(\boldsymbol{\omega}, \boldsymbol{\omega}_0)$, at several points $\boldsymbol{\omega} = (\sin(\pi - \theta), 0, \cos(\pi - \theta)) \in M_1$. In the acoustic setting we prescribe Dirichlet boundary conditions on the surface of the cone and we get results demonstrating satisfactory convergence in Table 6.5.

Due to the way we have chosen to orient the conical geometries in this subsection we will refer to the directions $\boldsymbol{\omega}$, given by $\theta = 0$ as the “back scattering” direction. The results in Table 6.5 are in good agreement with those displayed in [8, Table 1] and as expected show the magnitude of the diffraction coefficient to be increasing as $\boldsymbol{\omega}$ approaches the singular directions (which for this circular cone are given, in spherical coordinates, by: $\boldsymbol{\omega} = (\pi/3, \phi)$ for $\phi = [0, 2\pi]$, see Definition 2.13).

To investigate convergence in the electromagnetic case we introduce the “normalised” (dimensionless) radar cross section $\Sigma(\boldsymbol{\omega}, \boldsymbol{\omega}_0) = k^2\sigma(\boldsymbol{\omega}, \boldsymbol{\omega}_0)/4\pi^2$ where k is the wavenumber and σ is the conventional “radar cross section” (see e.g. [18, §I.2.5]) given by

$$\sigma(\boldsymbol{\omega}, \boldsymbol{\omega}_0) = \lim_{r \rightarrow \infty} (4\pi r^2 |\mathbf{E}_{diff}|^2).$$

This is a physical characteristic which measures the ability of the obstacle to scatter waves in particular directions. Using (2.2.19) we can write $\Sigma(\boldsymbol{\omega}, \boldsymbol{\omega}_0) = 4\pi |\mathcal{E}(\boldsymbol{\omega}, \boldsymbol{\omega}_0)|^2$. Approximations of the radar cross section (defined by Σ_n) are computed using the same strategy as used for $f_n(\boldsymbol{\omega}, \boldsymbol{\omega}_0)$ and are tabulated in Table 6.6.

The results in Table 6.6 are in good agreement with those displayed in [12, Table 1] for the same diffraction problem.

Example 2

We repeat the calculations in Example 1 for the case of diffraction by the

Table 6.6: Electromagnetic radar cross section calculations for the circular cone

n	$\Sigma_n(\boldsymbol{\omega}, \boldsymbol{\omega}_0) \quad \boldsymbol{\omega} = (\sin(\pi - \theta), 0, \cos(\pi - \theta))$					
	$\theta = 0$	$\theta = \pi/24$	$\theta = 2\pi/24$	$\theta = 3\pi/24$	$\theta = 4\pi/24$	$\theta = 5\pi/24$
8	0.003115	0.002333	0.001848	0.001506	0.001231	0.001109
16	0.002233	0.002277	0.002424	0.002702	0.003142	0.003832
32	0.002230	0.002274	0.002425	0.002697	0.003138	0.003825
64	0.002230	0.002274	0.002423	0.002698	0.003138	0.003827
128	0.002230	0.002274	0.002423	0.002698	0.003139	0.003828

trihedral cone in Fig. 5-2 in both the acoustic and the electromagnetic settings. Recall that this is an unsolved canonical problem. Again we consider an “axial” incident wave and use piecewise constant collocation to solve the integral equation and the midpoint rule on each subinterval, I_i , to compute the potential. We use the same technique as used in Example 1 to compute the integrals in (6.1.3) and (6.1.7). In Table 6.7 we present the diffraction coefficients for the acoustic scattering problem with Dirichlet boundary conditions and in Table 6.8 we display the radar cross section computations for the electromagnetic scattering problem.

Table 6.7: Acoustic diffraction coefficient calculations for the trihedral cone

n	$\text{Im } f_n(\boldsymbol{\omega}, \boldsymbol{\omega}_0) \quad \boldsymbol{\omega} = (\sin(\pi - \theta), 0, \cos(\pi - \theta))$					
	$\theta = 0$	$\theta = \pi/24$	$\theta = 2\pi/24$	$\theta = 3\pi/24$	$\theta = 4\pi/24$	$\theta = 5\pi/24$
12	-0.032628	-0.033344	-0.035596	-0.039702	-0.046298	-0.056545
24	-0.061655	-0.062447	-0.064958	-0.069587	-0.077111	-0.089053
48	-0.065966	-0.066790	-0.069406	-0.074248	-0.082160	-0.094798
96	-0.066753	-0.067591	-0.070256	-0.075197	-0.083285	-0.096233
192	-0.067187	-0.068032	-0.070720	-0.075706	-0.083874	-0.096960

The results in Table 6.7 are in qualitative agreement with those for the circular cone case: $\text{Im } f_n(\boldsymbol{\omega}, \boldsymbol{\omega}_0)$ has the same sign and the order of magnitude is smallest in the back scattering direction. Similarly the results in Table 6.8 are in qualitative agreement with those for the circular cone. Note that, in the electromagnetic setting there is a loss of symmetry due to the polarisation of the incident wave, i.e. the direction of \mathbf{E}^0 and \mathbf{H}^0 in (2.2.6).

To investigate the convergence of these results note that we can estimate the rate of convergence of an arbitrary sequence y_n by $\log((y_n - y_{2n})/(y_{2n} - y_{4n}))/\log(2)$. Using this estimate for the results displayed in Tables 6.5-6.8 we

Table 6.8: Electromagnetic radar cross section calculations for the trihedral cone

n	$\Sigma_n(\boldsymbol{\omega}, \boldsymbol{\omega}_0) \quad \boldsymbol{\omega} = (\sin(\pi - \theta), 0, \cos(\pi - \theta))$					
	$\theta = 0$	$\theta = \pi/24$	$\theta = 2\pi/24$	$\theta = 3\pi/24$	$\theta = 4\pi/24$	$\theta = 5\pi/24$
24	0.014404	0.014415	0.015294	0.017288	0.021022	0.027864
48	0.015995	0.015879	0.016707	0.018747	0.022642	0.029911
96	0.016638	0.016461	0.017257	0.019293	0.023220	0.030586
192	0.016935	0.016730	0.017510	0.019541	0.023475	0.030861
284	0.017076	0.016858	0.017631	0.019660	0.023597	0.030993

see that close to $O(n^{-1})$ convergence is achieved as expected.

Some further examples

Finally, in order to visually illustrate the computations of the diffraction coefficients for various geometries, we shall illustrate, for various choices of cone, how the computed $f(\boldsymbol{\omega}, \boldsymbol{\omega}_0)$ and $\Sigma(\boldsymbol{\omega}, \boldsymbol{\omega}_0)$ varies as the conical scatterer narrows and as the observation direction $\boldsymbol{\omega}$ ranges over a subdomain of M . Throughout we use piecewise constant collocation on a uniform mesh to compute the solution to the integral equation (4.0.1) with $n = 60$ nodes. (It follows from Theorem 4.14 and Remark 4.11 that a uniform mesh will be sufficient for optimal convergence of the piecewise constant collocation method applied to corner problems with Dirichlet boundary conditions. A uniform mesh will be suboptimal when Neumann boundary conditions are prescribed, as indicated by Theorem 4.14. However superconvergence phenomena lend to the observation of reasonable convergence rates for the derived diffraction coefficients even in the Neumann case and so we will still obtain a reasonable illustration of the behaviour of the diffraction coefficients.)

First we consider the acoustic problem. We restrict ourselves to the Dirichlet problem, as stated above we consider the axial incident direction $\boldsymbol{\omega}_0 = (0, 0, -1)^T$ and a range of observation directions written in spherical coordinates as

$$\boldsymbol{\omega} = ((\pi - \theta), \phi), \quad \text{with } 0 \leq \theta \leq \pi/3, \quad 0 \leq \phi \leq 2\pi. \quad (6.4.5)$$

Results for three different types of conical scatterer are given in Figs. 6-3 - 6-5. In Fig. 6-3 we illustrate how $|f(\boldsymbol{\omega}, \boldsymbol{\omega}_0)|$ varies as a function of θ and ϕ for three circular cones with semiangles θ^* , $3\theta^*/4$ and $\theta^*/2$. (Recall from §5.4 that θ^* is given by $\cos \theta^* = 1/\sqrt{3}$.) In Fig. 6-3 (and Figs. 6-4, 6-5) the quantity $|f(\boldsymbol{\omega}, \boldsymbol{\omega}_0)|$ is plotted on the x_3 axis against the projection of $\boldsymbol{\omega}$ onto the x_1x_2 -plane given

by: $\boldsymbol{\omega} = (\pi - \theta, \phi) \mapsto (\theta \cos \phi, \theta \sin \phi)$. Observe that the magnitude of the diffraction coefficients is smallest in the back scattering direction and increases as the observation approaches the singular directions (see Definition 2.13). Also observe that as the semiangle of the cone decreases, the magnitude of $f(\boldsymbol{\omega}, \boldsymbol{\omega}_0)$ decreases. This is to be expected since the distance between the observation domain, defined in (6.4.5), and the singular directions increases as the semiangle defining the surface of the cone decreases cf. Example 2.14.

In Fig. 6-4 we consider how $|f(\boldsymbol{\omega}, \boldsymbol{\omega}_0)|$ varies for three different elliptic cones. The surfaces of the elliptic cones are given by

$$x_3^2 = \frac{x_1^2}{a^2} + \frac{x_2^2}{b^2}, \quad (6.4.6)$$

where $a = \tan(\hat{\theta})$, $b = \tan(3\hat{\theta}/4)$, i.e. the cone has a “semi major” angle of $\hat{\theta}$ and “semi minor” angle of $3\hat{\theta}/4$. The cross sections, in a plane $x_3 = C$ for a constant C , of the cones determined by (6.4.6) are ellipses centred at the x_3 axis with major axes in the plane $x_2 = 0$. We consider $\hat{\theta} = \theta^*$, $3\theta^*/4$ and $\theta^*/2$ to investigate how $|f(\boldsymbol{\omega}, \boldsymbol{\omega}_0)|$ will vary as the angle of the cone varies. Note again that $|f(\boldsymbol{\omega}, \boldsymbol{\omega}_0)|$ is smallest in the backscattering direction. Also observe that the magnitude of $f(\boldsymbol{\omega}, \boldsymbol{\omega}_0)$ decreases as the semi major angle decreases. It follows from Definition 2.13 that, with $\boldsymbol{\omega} = (\pi - \theta, \phi)$ and $\theta > 0$ fixed, the geodesic distance between the observation directions and the singular directions will be smallest when $\phi = 0, \pi$. This is because the major axis of the cross section of the elliptic cones defined by (6.4.6) lie in the plane $x_2 = 0$, i.e. the angle subtended by the surface of the elliptic cones and its axis is greatest in the plane $x_2 = 0$. Since we expect $|f(\boldsymbol{\omega}, \boldsymbol{\omega}_0)|$ to tend to infinity as $\boldsymbol{\omega}$ approaches the singular directions this explains the faster growth, as θ increases, of $|f(\boldsymbol{\omega}, \boldsymbol{\omega}_0)|$ along the line $x_2 = 0$.

In Fig. 6-5 we illustrate similar calculations for the diffraction coefficients associated with regular trihedral cones. For this case we consider three trihedral cones whose edges lie in the directions $(\hat{\theta}, 0)$, $(\hat{\theta}, 2\pi/3)$ and $(\hat{\theta}, 4\pi/3)$ for three values of $\hat{\theta}$ (which we refer to as the semi major angle) given by θ^* , $3\theta^*/4$, $\theta^*/2$. The results are illustrated in Fig. 6-5. They show similar behaviour as that observed for the circular and elliptic cone. The magnitude of the diffraction coefficients is smallest in the back scattering direction. Also note again that if we fix $\theta > 0$ then the distance between $\boldsymbol{\omega}$ and the singular directions is smallest when $\phi = 0, 2\pi/3, 4\pi/3$. Hence the three peaks in Fig. 6-5. Also observe comparing Figs. 6-3 - 6-5 that for cones with cross sections of similar area (i.e. cones with similar semi (major) angles) the magnitudes of $f(\boldsymbol{\omega}, \boldsymbol{\omega}_0)$ are comparable.

We now consider the electromagnetic diffraction coefficients. We repeat the calculations above in the electromagnetic setting to compute the radar cross section for the same geometries. These results are illustrated in Figs. 6-6 - 6-8.

Again the quantity $\Sigma_n(\boldsymbol{\omega}, \boldsymbol{\omega}_0)$ is plotted on the x_3 axis against the projection of $\boldsymbol{\omega}$ onto the x_1x_2 -plane.

Observe again that $\Sigma_n(\boldsymbol{\omega}, \boldsymbol{\omega}_0)$ is smallest in the backscattering direction (or a direction close to the back scattering direction for the cones with edges Fig. 6-8) and increases as $\boldsymbol{\omega}$ approaches the singular direction (again notice the peaks in Figs. 6-7 and 6-8 where the distance between the observation direction and the singular directions is smallest).

Also observe a loss in the symmetry of the plots of the radar cross section compared with the plots of the acoustic diffraction coefficient for the same conical scatterer. This is most easily observed in Fig. 6-8 compared with Fig. 6-5. Note that in Fig. 6-5 the three peaks have the same magnitude whereas in Fig. 6-8 the peak at $\boldsymbol{\omega} = (2\pi/3, 0)$ is considerably smaller than the other two peaks. This is because of the loss of symmetry in the boundary conditions due to the polarisation of the incident wave.

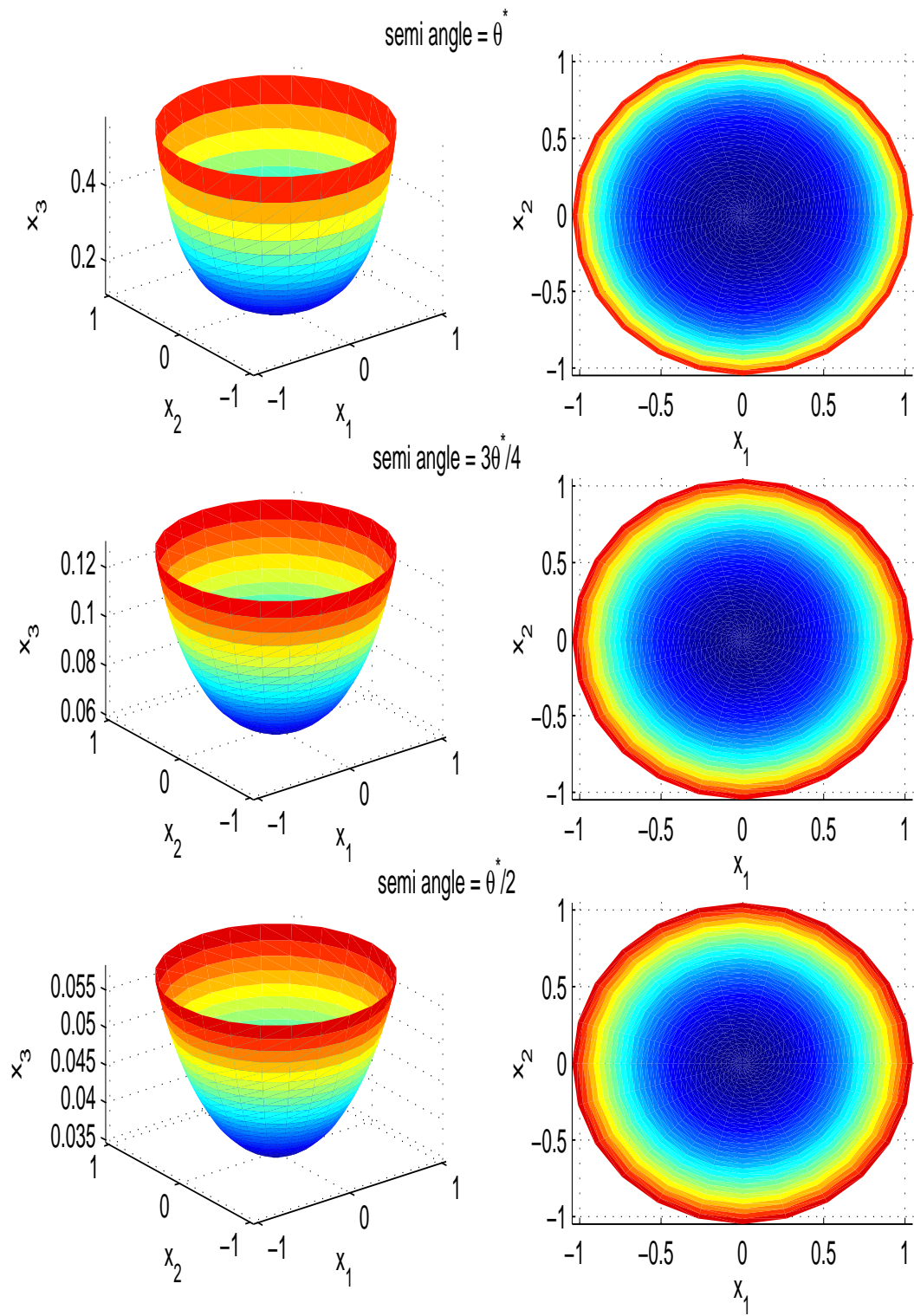


Figure 6-3: Diffraction coefficients for circular cones (acoustic)

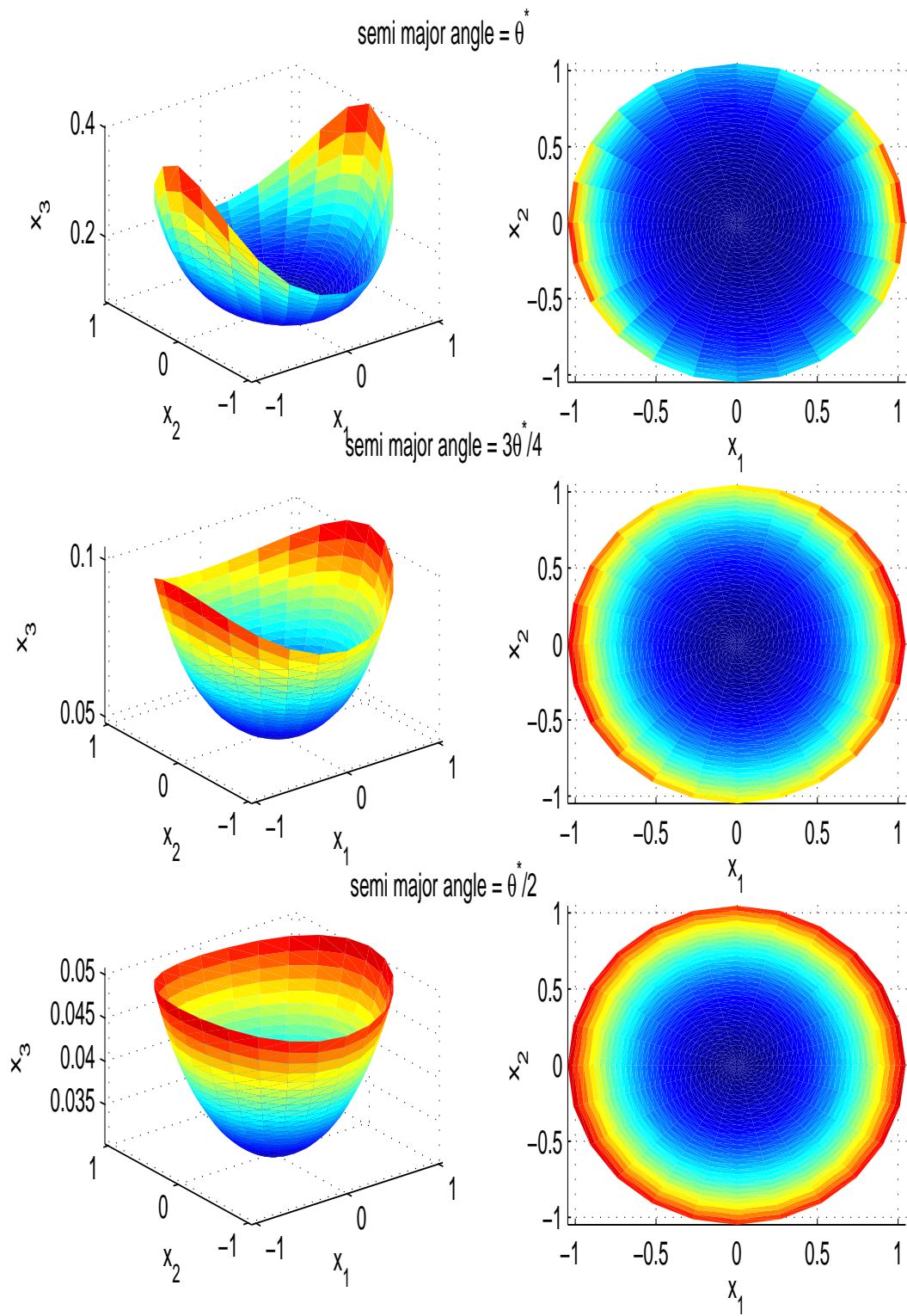


Figure 6-4: Diffraction coefficients for elliptic cones (acoustic)

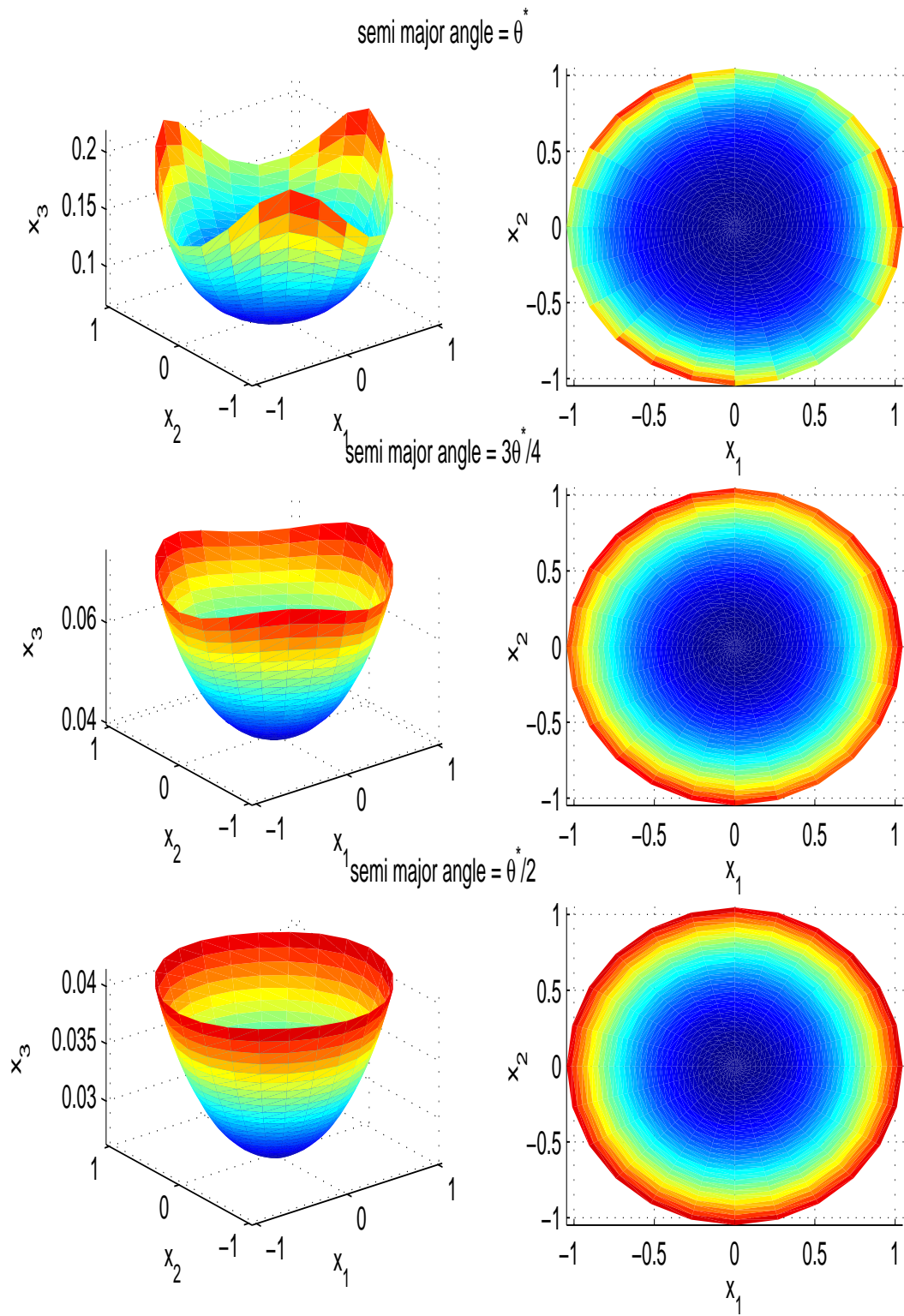


Figure 6-5: Diffraction coefficients for trihedral cones (acoustic)

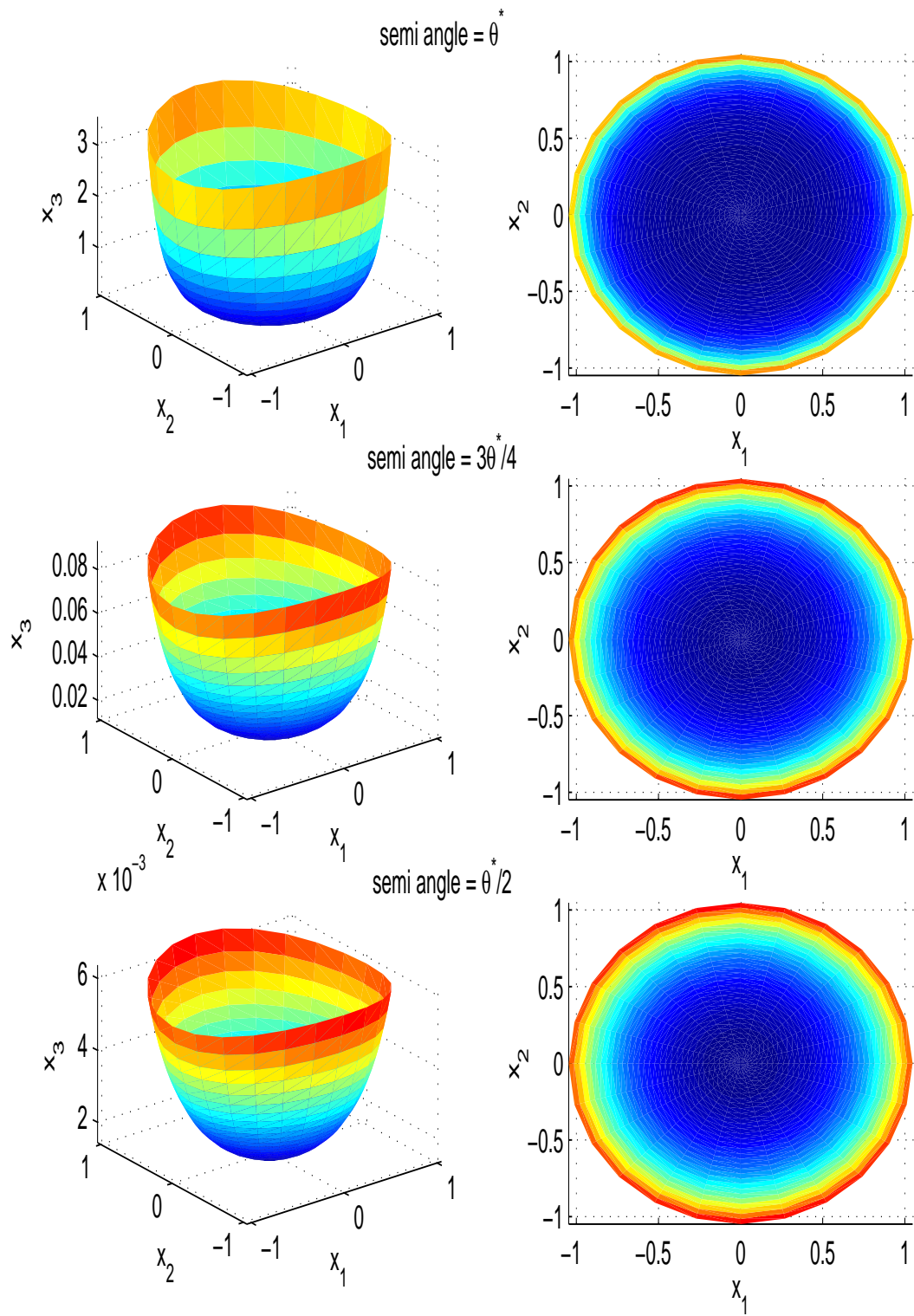


Figure 6-6: Radar cross section for circular cones (electromagnetic)

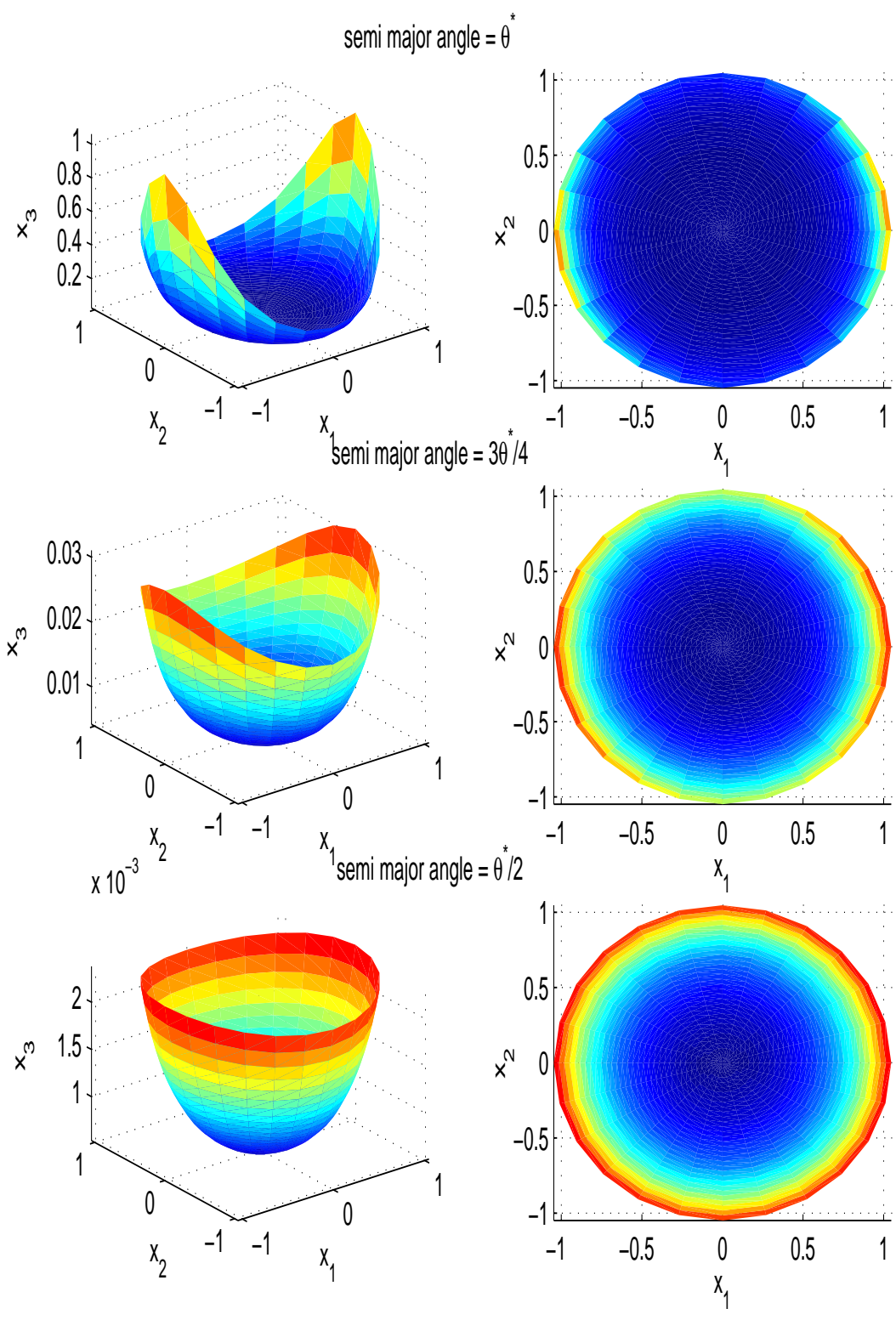


Figure 6-7: Radar cross section for elliptic cones (electromagnetic)

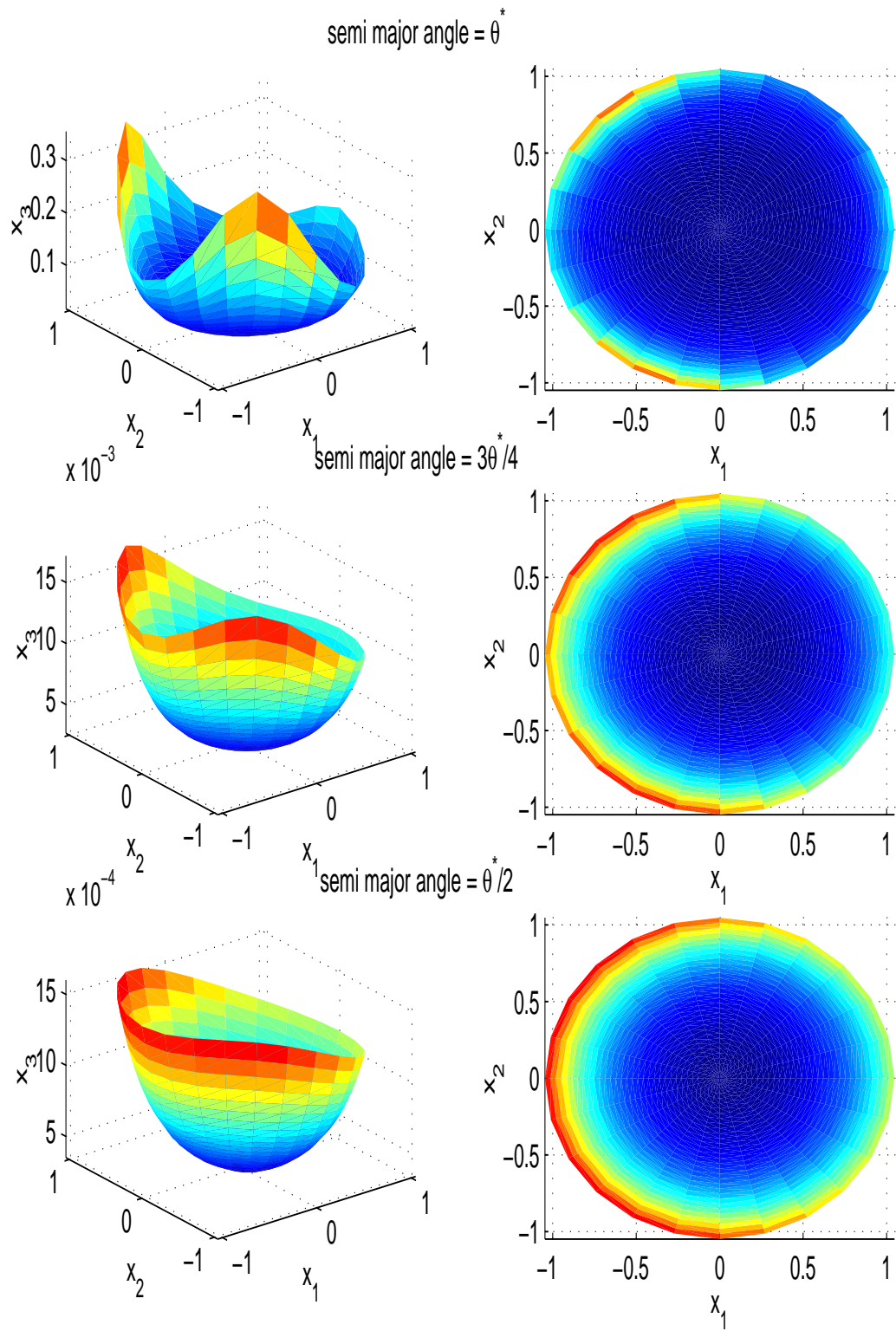


Figure 6-8: Radar cross sections for trihedral cones (electromagnetic)

Chapter 7

Conclusions and Further Work

7.1 Conclusions

We have described in detail the the derivation of the general formulae for the diffraction coefficients (in both the acoustic and electromagnetic setting). The key step in computing these diffraction coefficients is solving boundary value problems of the form

$$(\Delta^* + \nu^2 - 1/4)g^{sc}(\boldsymbol{\omega}, \boldsymbol{\omega}_0, \nu) = 0, \quad \boldsymbol{\omega} \in M, \quad (7.1.1)$$

with Dirichlet or Neumann boundary conditions. Here M is a submanifold of the surface of the unit sphere S^2 with arbitrary piecewise smooth boundary ℓ . Solving (7.1.1) needs to be done for many values of the complex parameter ν (and possibly many $\boldsymbol{\omega}_0$).

The approach we have taken in this thesis is to reformulate (7.1.1) indirectly as an integral equation of the second kind:

$$(I + \mathcal{L})u = b, \quad (7.1.2)$$

cf. (3.0.3) - (3.0.8).

We applied the collocation method to the integral equation (7.1.2) using piecewise polynomial approximating functions. We concentrated mainly on the h -version of collocation and have shown that this method for solving (7.1.2) is stable and approximates the solution to at least $O(n^{-r})$ accuracy, where n is number of elements on the boundary and r is the order of the approximating polynomial. This technique allows us to compute the acoustic and electromagnetic diffraction coefficients for rather arbitrary conical geometries with $O(n^{-r})$

accuracy.

As stated above (7.1.1) needs to be solved for many values of ν , so it is important that the numerical method for solving (7.1.2) is not only accurate but also efficient to implement. We developed a method of approximating the stiffness matrix that arises in the numerical method for computing solutions to (7.1.2) which maintains the stability and convergence properties that are known when the integrals arising in the stiffness matrix are computed exactly. Moreover, only one kernel evaluation is needed to approximate a large proportion of the matrix entries. This is especially important in our application since this will ensure that the matrix assembly process, which can dominate the overall computation time, is carried out efficiently.

7.2 Further work

Some areas for future research include:

- (i) We would like to develop and analyse the numerical scheme further to allow us to efficiently calculate diffraction coefficients for angles of observation in the domain M_2 described in §6.1, cf. [9];
- (ii) We would like to consider the matrix assembly aspect of the hp -method. In particular we are interested in sufficient quadrature rules so that the discrete hp -method enjoys the same stability and convergence properties as the true hp -method;
- (iii) We would like to consider the computation of diffraction coefficients when different boundary conditions are prescribed on the surface of the scatterer, i.e. replacing the Dirichlet/Neumann conditions in (2.1.2) by impedance boundary conditions, see [13], [14], [2];
- (iv) We would like to adapt our method to solve further challenging diffraction problems, for instance, the diffraction of a creeping wave. In [70] it has been shown by the matched asymptotics procedure that for the “inner problem” the creeping wave becomes an incident plane-like wave. This results in a boundary value problem of the form (3.0.1) and (3.0.2) with the source ω_0 on the boundary ℓ .

Appendix A

Derivation of the Formulae for the Electromagnetic Diffraction Coefficients

In this appendix we give the technical details in the derivation of the formulae for the electromagnetic diffraction coefficients given in §2.2. Recall from §2.2 that we are interested in solving the time-harmonic Maxwell equations exterior to a conical obstacle Ξ ,

$$\begin{aligned} \operatorname{curl} \mathbf{E}(\mathbf{x}) &= ik\mathbf{H}(\mathbf{x}), \\ \operatorname{curl} \mathbf{H}(\mathbf{x}) &= -ik\mathbf{E}(\mathbf{x}), \end{aligned} \quad \mathbf{x} \in \mathbb{R}^3 \setminus \Xi \quad (\text{A.0.1})$$

with perfectly conducting boundary conditions

$$\mathbf{E} \wedge \mathbf{n}|_{\partial D} = \mathbf{0}. \quad (\text{A.0.2})$$

(As stated in §2.2 we also require that \mathbf{E} and \mathbf{H} satisfy certain radiation and tip/edge conditions (2.2.4), (2.2.5).)

We are interested in solving this problem in the case when the incident wave is planar (2.2.6). In this appendix it will be convenient to choose the Cartesian coordinate system appropriately so that the direction of the incidence wave is in the negative x_3 direction and so that \mathbf{E}_0 and \mathbf{H}_0 in (2.2.6) lie in the direction of the x_2 and x_1 axes respectively (see Fig. A-1). To this end we introduce the following notation.

Notation A.1. We choose the Cartesian coordinate system so that the vectors

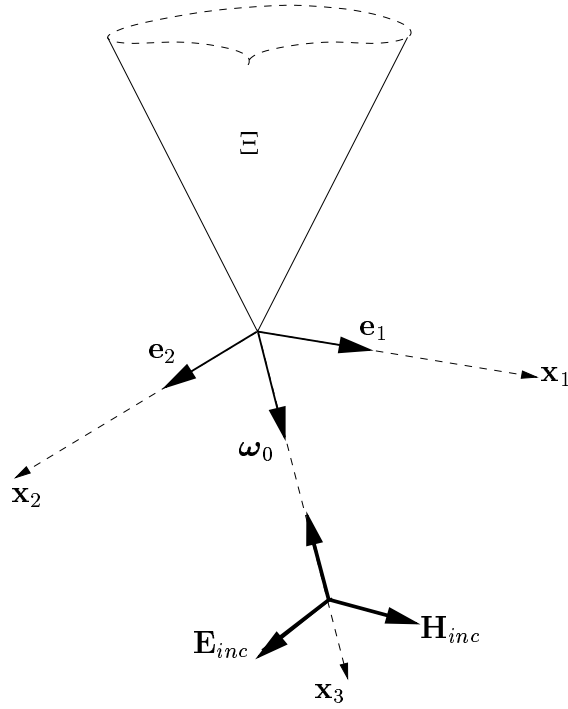


Figure A-1: Propagation of the electromagnetic incident wave

\mathbf{E}^0 , \mathbf{H}^0 , and $\boldsymbol{\omega}_0$ satisfy

$$\mathbf{E}^0 = \mathbf{e}_2 := (0, 1, 0)^T, \quad \mathbf{H}^0 = \mathbf{e}_1 := (1, 0, 0)^T, \quad \text{and} \quad \boldsymbol{\omega}_0 = \mathbf{e}_3 := (0, 0, 1)^T.$$

Then following from (2.2.6) the incident wave takes the form

$$\mathbf{E}_{inc}(\mathbf{x}) = e^{-ikx_3} \mathbf{e}_2, \quad \mathbf{H}_{inc}(\mathbf{x}) = e^{-ikx_3} \mathbf{e}_1. \quad (\text{A.0.3})$$

Also we can represent a point $\boldsymbol{\omega} \in M$ in terms of the usual spherical polar coordinates θ, ϕ as follows

$$\boldsymbol{\omega} = (\sin \theta \cos \phi, \sin \theta \sin \phi, \cos \theta)^T. \quad (\text{A.0.4})$$

(Note that in this setup θ is exactly the geodesic distance between $\boldsymbol{\omega}$ and $\boldsymbol{\omega}_0$, $\theta(\boldsymbol{\omega}, \boldsymbol{\omega}_0)$, see Notation 2.2. We also use a representation analogous to (A.0.4) to represent $\boldsymbol{\omega}' \in M$ in terms of the spherical polar coordinates θ', ϕ' .)

As in the acoustic case, the formulation of the radiation conditions for the problem of scattering by a canonical conical obstacle is a delicate issue. One approach for solving the electromagnetic planar incidence scattering problem exterior to a conical obstacle is to start (as in the acoustic case) by considering a

point source problem. This approach is not considered here. Instead, in the next section, using scalar (Debye) potentials, we reduce the electromagnetic planar incidence scattering problem (exterior to a conical obstacle) to two scalar problems analogous to the acoustic planar incidence scattering problem. We then solve these scalar problems using techniques applied in §2.1 and we can check *a posteriori* that the “outgoing” conditions (2.2.4) are satisfied (this is discussed in Remark A.14).

A.1 Debye potentials

It is well known that an electromagnetic field can often be expressed in terms of two scalar functions. We seek the solution to (A.0.1) exterior to Ξ in the form

$$\begin{aligned}\mathbf{E}(\mathbf{x}) &= \text{curl curl } (V(\mathbf{x})\mathbf{x}) + ik \text{ curl } (W(\mathbf{x})\mathbf{x}), \\ \mathbf{H}(\mathbf{x}) &= \text{curl curl } (W(\mathbf{x})\mathbf{x}) - ik \text{ curl } (V(\mathbf{x})\mathbf{x}),\end{aligned}\tag{A.1.1}$$

where V and W are the so-called Debye potentials. In Lemmas A.2 and A.3 we describe the sufficient conditions that V and W should satisfy so that \mathbf{E} and \mathbf{H} defined in (A.1.1) satisfy the conditions of the electromagnetic scattering problem (A.0.1) and (A.0.2), cf. [69].

Lemma A.2. *If we define \mathbf{E} and \mathbf{H} by (A.1.1) for arbitrary $V, W \in C^3(\Omega)$ satisfying the scalar Helmholtz equation,*

$$(\Delta + k^2)V(\mathbf{x}) = 0, \quad (\Delta + k^2)W(\mathbf{x}) = 0, \quad \text{for } \mathbf{x} \in \mathbb{R}^3 \setminus \Xi,\tag{A.1.2}$$

then \mathbf{E} and \mathbf{H} will satisfy the Maxwell equations (A.0.1).

Proof Here we prove the first equation in (A.0.1) will hold, the proof for the second equation is analogous.

In order to calculate $\text{curl } \mathbf{E}(\mathbf{x})$ using (A.1.1) we first need to be able to calculate $\text{curl curl curl } (V(\mathbf{x})\mathbf{x})$. First note that for an arbitrary scalar function $w(\mathbf{x})$,

$$\text{curl } (w(\mathbf{x})\mathbf{x}) = \text{grad } (w(\mathbf{x})) \wedge \mathbf{x},\tag{A.1.3}$$

$$\text{and } \text{curl grad } (w(\mathbf{x})) = 0.\tag{A.1.4}$$

Therefore since,

$$\operatorname{curl} \operatorname{curl} (V(\mathbf{x})\mathbf{x}) = -\Delta(V(\mathbf{x})\mathbf{x}) + \operatorname{grad} \operatorname{div} (V(\mathbf{x})\mathbf{x}) \quad \text{and} \quad (\text{A.1.5})$$

$$\Delta(V(\mathbf{x})\mathbf{x}) = (\Delta V(\mathbf{x}))\mathbf{x} + 2\operatorname{grad} V(\mathbf{x}), \quad (\text{A.1.6})$$

it follows from (A.1.3) and (A.1.4) that,

$$\operatorname{curl} \operatorname{curl} \operatorname{curl} (V(\mathbf{x})\mathbf{x}) = -\operatorname{curl} ((\Delta V(\mathbf{x}))\mathbf{x}) = -\operatorname{grad} (\Delta V(\mathbf{x})) \wedge \mathbf{x}. \quad (\text{A.1.7})$$

Therefore if \mathbf{E} , \mathbf{H} are given by (A.1.1) and if V , W satisfy the scalar Helmholtz equation (A.1.2),

$$\begin{aligned} \operatorname{curl} \mathbf{E}(\mathbf{x}) &= \operatorname{curl} \operatorname{curl} \operatorname{curl} (V(\mathbf{x})\mathbf{x}) + ik \operatorname{curl} \operatorname{curl} (W(\mathbf{x})\mathbf{x}) \\ &= -\operatorname{grad} (\Delta V(\mathbf{x})) \wedge \mathbf{x} + ik \operatorname{curl} \operatorname{curl} (W(\mathbf{x})\mathbf{x}) \\ &= k^2 \operatorname{grad} (V(\mathbf{x})) \wedge \mathbf{x} + ik \operatorname{curl} \operatorname{curl} (W(\mathbf{x})\mathbf{x}) \\ &= ik(-ik \operatorname{curl} (V(\mathbf{x})\mathbf{x}) + \operatorname{curl} \operatorname{curl} (W(\mathbf{x})\mathbf{x})) = ik\mathbf{H}(\mathbf{x}). \end{aligned} \quad (\text{A.1.8})$$

□

The next result gives the sufficient conditions for V and W so that \mathbf{E} , \mathbf{H} given by (A.1.1) satisfy the perfectly conducting boundary conditions (A.0.2).

Lemma A.3. *If we define \mathbf{E} and \mathbf{H} by (A.1.1) for arbitrary V and $W \in C^2(\bar{\Omega})$ satisfying the Helmholtz equations (A.1.2) and the boundary conditions,*

$$V \Big|_{\partial\Xi} = 0, \quad \frac{\partial W}{\partial \mathbf{n}} \Big|_{\partial\Xi} = 0, \quad (\text{A.1.9})$$

on the surface, $\partial\Xi$, of an arbitrarily shaped cone, Ξ , then the boundary condition (A.0.2) will hold.

Proof First note that,

$$\begin{aligned} \operatorname{div} (V(\mathbf{x})\mathbf{x}) &= 3V(\mathbf{x}) + \operatorname{grad} V(\mathbf{x}) \cdot \mathbf{x} = 3V(\mathbf{x}) + r \left(\operatorname{grad} V(\mathbf{x}) \cdot \frac{\mathbf{x}}{r} \right) \\ &= 3V(\mathbf{x}) + r \frac{\partial V}{\partial r}(\mathbf{x}), \end{aligned}$$

and hence,

$$\operatorname{grad} \operatorname{div} (V(\mathbf{x})\mathbf{x}) = 3 \operatorname{grad} V(\mathbf{x}) + \operatorname{grad} \left(r \frac{\partial V}{\partial r}(\mathbf{x}) \right).$$

Therefore from (A.1.5) and (A.1.6)

$$\text{curl curl } (V(\mathbf{x})\mathbf{x}) = -(\Delta V(\mathbf{x}))\mathbf{x} + \text{grad } V(\mathbf{x}) + \text{grad} \left(r \frac{\partial V}{\partial r}(\mathbf{x}) \right). \quad (\text{A.1.10})$$

Note that from the boundary condition (A.1.9) and because Ξ is a cone, we have $\partial V/\partial r(\mathbf{x}) = 0$ for $\mathbf{x} \in \partial\Xi$. Also for $\mathbf{x} \in \partial\Xi$, $\Delta V(\mathbf{x}) = -k^2 V(\mathbf{x}) = 0$. Therefore from (A.1.10), (A.1.3) and (A.1.1)

$$\mathbf{E}(\mathbf{x}) \wedge \mathbf{n} = \text{grad } V(\mathbf{x}) \wedge \mathbf{n} + \text{grad} \left(r \frac{\partial V}{\partial r}(\mathbf{x}) \right) \wedge \mathbf{n} + ik(\text{grad } W(\mathbf{x}) \wedge \mathbf{x}) \wedge \mathbf{n}. \quad (\text{A.1.11})$$

Now for arbitrary vectors \mathbf{A} , \mathbf{B} and \mathbf{C} we have the following identity for the vector triple product

$$(\mathbf{B} \wedge \mathbf{C}) \wedge \mathbf{A} = (\mathbf{A} \cdot \mathbf{B})\mathbf{C} - (\mathbf{A} \cdot \mathbf{C})\mathbf{B}.$$

Using this, with $\mathbf{B} = \text{grad } W(\mathbf{x})$, $\mathbf{C} = \mathbf{x}$ and $\mathbf{A} = \mathbf{n}$, we get the following formula,

$$\begin{aligned} \mathbf{E}(\mathbf{x}) \wedge \mathbf{n} &= \text{grad } V(\mathbf{x}) \wedge \mathbf{n} + \text{grad} \left(r \frac{\partial V}{\partial r}(\mathbf{x}) \right) \wedge \mathbf{n} \\ &\quad - ik((\mathbf{n} \cdot \mathbf{x})\text{grad } W(\mathbf{x}) - (\mathbf{n} \cdot \text{grad } W(\mathbf{x}))\mathbf{x}). \end{aligned} \quad (\text{A.1.12})$$

We now consider each term on the right-hand side of (A.1.12). Firstly since $V(\mathbf{x}) = 0$ for all $\mathbf{x} \in \partial\Xi$, it follows that $\partial V(\mathbf{x})/\partial \mathbf{s}(\mathbf{x}) = 0$ where $\mathbf{s}(\mathbf{x})$ is any vector tangent to $\partial\Xi$ at \mathbf{x} . Hence, $\text{grad } V(\mathbf{x}) \cdot \mathbf{s}(\mathbf{x}) = 0$, and so $\text{grad } V(\mathbf{x})$ is normal to $\partial\Xi$. Therefore it follows that $\text{grad } V(\mathbf{x}) \wedge \mathbf{n} = 0$, i.e. the first term on the right-hand side of (A.1.12) vanishes. Similarly the second term vanishes since $r\partial V/\partial r \equiv 0$ on $\partial\Xi$. The third term on the right-hand side of (A.1.12) is clearly zero since for all $\mathbf{x} \in \partial\Xi$, $\mathbf{x} \cdot \mathbf{n} = 0$. Finally $\mathbf{n} \cdot \text{grad } W(\mathbf{x}) = \partial W(\mathbf{x})/\partial \mathbf{n} = 0$, from (A.1.9), so the fourth term on the right-hand side of (A.1.12) is zero. It therefore follows that $\mathbf{E}(\mathbf{x}) \wedge \mathbf{n} = 0$. \square

The problem of solving the planar incidence scattering problem (see Definition 2.16) now reduces to that of finding two scalar functions V and W which satisfy (A.1.2) and (A.1.9). To do this we write V and W in terms of the ‘‘incident part’’ and ‘‘scattered part’’,

$$V = V_{inc} + V_{sc}, \quad W = W_{inc} + W_{sc}. \quad (\text{A.1.13})$$

Now recall the strategy for finding analytic formulae for \mathbf{E} and \mathbf{H} from §2.2: First

we find solutions V_{inc} and W_{inc} of the Helmholtz equation with the property that

$$\begin{aligned}\mathbf{E}_{inc}(\mathbf{x}) &= \text{curl curl } (V_{inc}(\mathbf{x})\mathbf{x}) + ik \text{ curl } (W_{inc}(\mathbf{x})\mathbf{x}), \\ \mathbf{H}_{inc}(\mathbf{x}) &= \text{curl curl } (W_{inc}(\mathbf{x})\mathbf{x}) - ik \text{ curl } (V_{inc}(\mathbf{x})\mathbf{x}),\end{aligned}\tag{A.1.14}$$

where \mathbf{E}_{inc} and \mathbf{H}_{inc} are given by (2.2.6). Then we find the solutions to two scalar “acoustic” scattering problems (cf. §2.1) with the incident waves given by V_{inc} and W_{inc} , i.e. we use procedures developed in §2.1 to solve the scalar problems

$$(\Delta + k^2)V_{sc} = 0, \quad V_{sc}\Big|_{\partial\Xi} = -V_{inc}\Big|_{\partial\Xi},\tag{A.1.15}$$

$$(\Delta + k^2)W_{sc} = 0, \quad \frac{\partial W_{sc}}{\partial \mathbf{n}}\Big|_{\partial\Xi} = -\frac{\partial W_{inc}}{\partial \mathbf{n}}\Big|_{\partial\Xi}.\tag{A.1.16}$$

(V_{sc} and W_{sc} also have to satisfy appropriate “radiation”, “tip” and “edge” conditions, cf. §2.1.) From the solutions to (A.1.15) and (A.1.16) we have formulae for V and W from (A.1.13). These can then be substituted into (A.1.1) to get \mathbf{E} and \mathbf{H} .

A.2 Finding the Debye potentials

The purpose of this subsection is to find formulae for V and W as described at the end of the previous section. From Theorem A.4 we obtain expressions for V_{inc} and W_{inc} . This allows us to formulate a solution to (A.1.15) and (A.1.16) in Theorem A.6. Then the formulae for V and W are given in Corollary A.7.

Theorem A.4. *Consider \mathbf{E}_{inc} , \mathbf{H}_{inc} given by (2.2.6). These vector fields can be expressed in the form (A.1.14) where V_{inc} and W_{inc} are solutions to the Helmholtz equation given by (writing $\mathbf{x} = (r, \boldsymbol{\omega})$ and using the Cartesian coordinate system introduced in Notation A.1),*

$$\begin{aligned}\left\{ \begin{array}{l} V_{inc} \\ W_{inc} \end{array} \right\} (r, \boldsymbol{\omega}) \\ = (-ik)^{-1} \left(\frac{\pi}{2kr} \right)^{\frac{1}{2}} \sum_{n=1}^{\infty} i^n \frac{2n+1}{n(n+1)} J_{n+\frac{1}{2}}(kr) P_n^1(-\cos\theta) \left\{ \begin{array}{l} \sin\phi \\ \cos\phi \end{array} \right\}.\end{aligned}\tag{A.2.1}$$

Here $J_{n+1/2}(kr)$ are the Bessel functions of the first kind [1, pg. 358], P_n^1 are special Legendre functions of index n and order 1 [1, pg. 332]. Recall that θ and ϕ are the standard spherical coordinates which describe the direction $\boldsymbol{\omega}$ (see (A.0.4)). The result that V_{inc} and W_{inc} given by (A.2.1) satisfy (A.1.14)

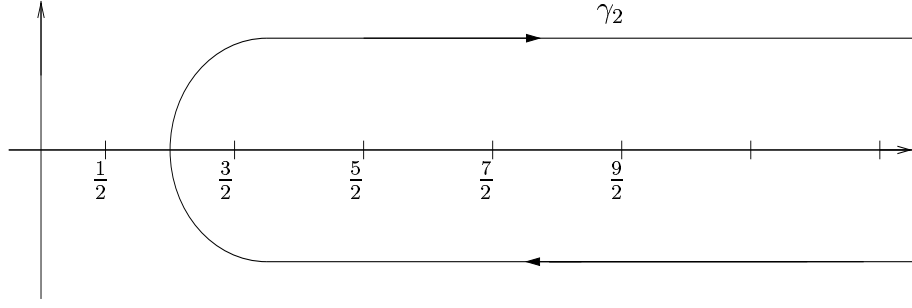


Figure A-2: Contour of integration γ_2

is proved by using a separation of variables type argument (see e.g. [74, §8.9]). The fact that V_{inc} and W_{inc} in (A.2.1) satisfy Helmholtz's equation follows by straightforward differentiation.

This series representation can be transformed into an integral over a contour γ_2 , using a procedure referred to as “Watson’s transformation”:

Theorem A.5. *The Debye potentials, V_{inc}, W_{inc} , corresponding to incident electromagnetic wave are given by the following formulae*

$$\begin{Bmatrix} V_{inc} \\ W_{inc} \end{Bmatrix} (r, \boldsymbol{\omega}) = -2 \left(\frac{2\pi}{k^3 r} \right)^{\frac{1}{2}} e^{i\pi/4} \int_{\gamma_2} \frac{\nu e^{-i\pi\nu/2}}{\nu^2 - 1/4} J_\nu(kr) \begin{Bmatrix} g_D^{inc} \\ g_N^{inc} \end{Bmatrix} (\boldsymbol{\omega}, \boldsymbol{\omega}_0, \nu) d\nu \quad (\text{A.2.2})$$

where (using the notational convention in Notation A.1),

$$\begin{Bmatrix} g_D^{inc} \\ g_N^{inc} \end{Bmatrix} (\boldsymbol{\omega}, \boldsymbol{\omega}_0, \nu) = \frac{P_{\nu-\frac{1}{2}}^1(-\cos\theta)}{-4 \cos \pi \nu} \begin{Bmatrix} \sin \phi \\ \cos \phi \end{Bmatrix}. \quad (\text{A.2.3})$$

and γ_2 is a contour in the complex plane which lies to the right of $1/2$ and bends around $n + 1/2$ for $n \in \mathbb{N}$ (see Fig. A-2).

Proof We give the proof for V_{inc} , the proof for W_{inc} is analogous. The poles of the integrand of (A.2.2) lying to the right of the contour γ_2 are $\nu = n + 1/2$, $n \in \mathbb{N}$. Applying Cauchy’s residue theorem it follows from Theorem 2.7 that,

$$\begin{aligned} & -2 \left(\frac{2\pi}{k^3 r} \right)^{\frac{1}{2}} e^{i\pi/4} \int_{\gamma_2} \frac{\nu}{\nu^2 - 1/4} J_\nu(kr) g_D^{inc}(\boldsymbol{\omega}, \boldsymbol{\omega}_0, \nu) e^{-i\pi\nu/2} d\nu \\ &= 4\pi i \left(\frac{2\pi}{k^3 r} \right)^{\frac{1}{2}} e^{i\pi/4} \sum_{n=1}^{\infty} \text{res} \left\{ \frac{\nu}{\nu^2 - 1/4} J_\nu(kr) g_D^{inc}(\boldsymbol{\omega}, \boldsymbol{\omega}_0, \nu) e^{-i\pi\nu/2}, n + 1/2 \right\}. \end{aligned} \quad (\text{A.2.4})$$

Using Taylor's theorem, it follows that, for ν in a neighbourhood of $n + 1/2$, where $n \in \mathbb{N}$,

$$\cos \pi \nu = -\pi(\nu - (n + 1/2)) \sin(\pi(n + 1/2)) + O((\nu - (n + 1/2))^2).$$

Hence, from (A.2.3)

$$\begin{aligned} \lim_{\nu \rightarrow n+1/2} (\nu - (n + 1/2)) g_D^{inc}(\boldsymbol{\omega}, \boldsymbol{\omega}_0, \nu) &= \frac{P_n^1(-\cos \theta)}{4\pi \sin(\pi(n + 1/2))} \sin \phi \\ &= (-1)^n \frac{P_n^1(-\cos \theta)}{4\pi} \sin \phi. \end{aligned}$$

Therefore, combining this with the fact that

$$\lim_{\nu \rightarrow n+1/2} \frac{\nu}{\nu^2 - 1/4} e^{-i\pi\nu/2} \rightarrow \frac{n + 1/2}{n(n + 1)} e^{-i\pi/4} (-i)^n,$$

it follows from (A.2.4) and (2.1.25) that,

$$\begin{aligned} &-2 \left(\frac{2\pi}{k^3 r} \right)^{\frac{1}{2}} e^{i\pi/4} \int_{\gamma_2} \frac{\nu}{\nu^2 - 1/4} J_\nu(kr) g_D^{inc}(\boldsymbol{\omega}, \boldsymbol{\omega}_0, \nu) e^{-i\pi\nu/2} d\nu \\ &= 4\pi i \left(\frac{2\pi}{k^3 r} \right)^{1/2} \sum_{n=1}^{\infty} i^n \frac{n + 1/2}{n(n + 1)} J_{n+1/2}(kr) \frac{P_n^1(-\cos \theta)}{4\pi} \sin \phi \\ &= (-ik)^{-1} \left(\frac{\pi}{2kr} \right)^{1/2} \sum_{n=1}^{\infty} i^n \frac{2n + 1}{n(n + 1)} J_{n+1/2}(kr) P_n^1(-\cos \theta) \sin \phi \\ &= V_{inc}(r, \boldsymbol{\omega}), \end{aligned}$$

and this completes the proof. \square

The representation (A.2.2) of the Debye potentials corresponding to the planar electromagnetic incident wave, motivates seeking the scattered potentials V_{sc} and W_{sc} in the form

$$\begin{Bmatrix} V_{sc} \\ W_{sc} \end{Bmatrix} (r, \boldsymbol{\omega}) = -2 \left(\frac{2\pi}{k^3 r} \right)^{\frac{1}{2}} e^{i\pi/4} \int_{\gamma_2} \frac{\nu e^{-i\pi\nu/2}}{\nu^2 - 1/4} J_\nu(kr) \begin{Bmatrix} g_D^{sc} \\ g_N^{sc} \end{Bmatrix} (\boldsymbol{\omega}, \boldsymbol{\omega}_0, \nu) d\nu \quad (\text{A.2.5})$$

where g_D^{sc} and g_N^{sc} are to be found. Care needs to be taken when defining γ_2 . As described above γ_2 must cross the real axis between $1/2$ and $3/2$. To be more precise we require (so that the radiation conditions (2.2.4) are satisfied which will be discussed in Remark A.14), for V_{sc} that γ_2 crosses the real axis at a point which lies to the left of the internal Dirichlet eigenvalues $\nu_{D,j}$, $j = 1, 2, \dots$, (see

Definition 2.4) so as to avoid any residue contributions. For W_{sc} , we require that γ_2 crosses the real axis to the left of the internal Neumann eigenvalues $\nu_{N,j}$, $j = 2, 3, \dots$, (recall that $\nu_{N,1} = 1/2$) see Fig. 2-5.

Now to find \mathbf{E} and \mathbf{H} we use the representation (A.2.5) to solve (A.1.15) and (A.1.16). The next result gives sufficient conditions for g_D^{sc} and g_N^{sc} so that the representation V_{sc} and W_{sc} given in (A.2.5) will satisfy (A.1.15) and (A.1.16).

Theorem A.6. *Suppose V_{sc} and W_{sc} are given by (A.2.5) where g_D^{sc} and g_N^{sc} satisfy,*

$$\left(\Delta^* + \nu^2 - \frac{1}{4}\right) \begin{Bmatrix} g_D^{sc} \\ g_N^{sc} \end{Bmatrix} (\boldsymbol{\omega}, \boldsymbol{\omega}_0, \nu) = 0, \quad \boldsymbol{\omega} \in M, \quad (\text{A.2.6})$$

$$g_D^{sc}|_{\ell} = -g_D^{inc}|_{\ell}, \quad \frac{\partial g_N^{sc}}{\partial \mathbf{m}}|_{\ell} = -\frac{\partial g_N^{inc}}{\partial \mathbf{m}}|_{\ell}, \quad (\text{A.2.7})$$

then V_{sc} and W_{sc} will satisfy (A.1.15) and (A.1.16) respectively. (Recall that M is the portion of the unit sphere exterior to Ξ and that ℓ is the boundary of M .)

Proof From (A.2.5) we can write

$$\begin{Bmatrix} V_{sc} \\ W_{sc} \end{Bmatrix} (r, \boldsymbol{\omega}) = -2 \left(\frac{(2\pi)^{1/2}}{k} \right) e^{i\pi/4} \int_{\gamma_2} \frac{\nu}{\nu^2 - 1/4} \begin{Bmatrix} w_D \\ w_N \end{Bmatrix} (r, \boldsymbol{\omega}, \boldsymbol{\omega}_0, \nu) e^{-i\pi\nu/2} d\nu,$$

where $w_B(r, \boldsymbol{\omega}, \boldsymbol{\omega}_0, \nu) := (kr)^{-1/2} J_\nu(kr) g_B^{sc}(\boldsymbol{\omega}, \boldsymbol{\omega}_0, \nu)$, $B = D$ or N . (Notice that the integral over γ_2 converges due to the fast decay of $J_\nu(kr)$ when $|\text{Im}(\nu) \leq C, \text{Re}(\nu) \rightarrow +\infty$.)

It follows that if w_B satisfies the scalar Helmholtz equation with respect to $(r, \boldsymbol{\omega})$ for $B = D$ or N and every $\nu \in \gamma_2$ then V_{sc} and W_{sc} will also satisfy the Helmholtz equation. To show that w_B satisfies the Helmholtz equation, we write the Laplace operator in $(r, \boldsymbol{\omega})$ variables as

$$\Delta = \frac{1}{r^2} \frac{\partial}{\partial r} \left(r^2 \frac{\partial}{\partial r} \right) + \frac{1}{r^2} \Delta^*, \quad (\text{A.2.8})$$

where Δ^* is the Laplace-Beltrami operator. We consider the radial part first,

$$\begin{aligned} \frac{\partial}{\partial r} \left(r^2 \frac{\partial w_B}{\partial r} \right) &= \left((kr)^{3/2} J_\nu''(kr) + (kr)^{1/2} J_\nu'(kr) - \frac{1}{4} (kr)^{-1/2} J_\nu(kr) \right) g_B^{sc}(\boldsymbol{\omega}, \boldsymbol{\omega}_0, \nu) \\ &= \left(\nu^2 - (kr)^2 - \frac{1}{4} \right) (kr)^{-1/2} J_\nu(kr) g_B^{sc}(\boldsymbol{\omega}, \boldsymbol{\omega}_0, \nu). \end{aligned} \quad (\text{A.2.9})$$

The previous line is a consequence of the fact that $J_\nu(kr)$ satisfies the Bessel

differential equation (e.g. [1, 9.1.1]):

$$(kr)^2 J_\nu''(kr) + (kr) J_\nu'(kr) + ((kr)^2 - \nu^2) J_\nu(kr) = 0.$$

Therefore it follows from (A.2.8), (A.2.9) and (A.2.6) that,

$$\begin{aligned} (\Delta + k^2) w_B(r, \boldsymbol{\omega}, \boldsymbol{\omega}_0, \nu) &= \frac{1}{r^2} \left(\nu^2 - (kr)^2 - \frac{1}{4} \right) (kr)^{-1/2} J_\nu(kr) g_B^{sc}(\boldsymbol{\omega}, \boldsymbol{\omega}_0, \nu) \\ &+ \frac{1}{r^2} (kr)^{-1/2} J_\nu(kr) \Delta^* g_B^{sc}(\boldsymbol{\omega}, \boldsymbol{\omega}_0, \nu) \\ &+ k^2 (kr)^{-1/2} J_\nu(kr) g_B^{sc}(\boldsymbol{\omega}, \boldsymbol{\omega}_0, \nu) \\ &= \frac{1}{r^2} (kr)^{-1/2} J_\nu(kr) \left(\Delta^* + \nu^2 - \frac{1}{4} \right) g_B^{sc}(\boldsymbol{\omega}, \boldsymbol{\omega}_0, \nu) = 0, \end{aligned}$$

for $B = D, N$. This shows that both V_{sc} and W_{sc} satisfy the Helmholtz equation. Moreover, if $\mathbf{x} \in \partial\Xi$ then it is clear that $\boldsymbol{\omega} \in \ell$. Also note that

$$\frac{\partial W_{sc}(\mathbf{x})}{\partial \mathbf{n}} = \frac{1}{r} \frac{\partial W_{sc}(\mathbf{x})}{\partial \mathbf{m}}$$

and hence an expression for $(\partial W_{sc} / \partial \mathbf{n})(\mathbf{x})$ is found by replacing $g_n^{sc}(\boldsymbol{\omega}, \boldsymbol{\omega}_0, \nu)$ in (A.2.5) by $r^{-1}(\partial g_N^{sc} / \partial \mathbf{m})(\boldsymbol{\omega}, \boldsymbol{\omega}_0, \nu)$ for $\mathbf{x} \in \partial\Xi$. Therefore it is a straightforward consequence of (A.2.7) and (A.2.2) that V_{sc} and W_{sc} defined by (A.2.5) satisfy the boundary conditions in (A.1.15) and (A.1.16). \square

This leads to the next result.

Corollary A.7. *Suppose the Debye potentials V and W are given by*

$$\begin{Bmatrix} V \\ W \end{Bmatrix} (r, \boldsymbol{\omega}) = -2 \left(\frac{2\pi}{k^3 r} \right)^{\frac{1}{2}} e^{i\pi/4} \int_{\gamma_2} \frac{\nu}{\nu^2 - 1/4} J_\nu(kr) \begin{Bmatrix} g_D \\ g_N \end{Bmatrix} (\boldsymbol{\omega}, \boldsymbol{\omega}_0, \nu) e^{-i\pi\nu/2} d\nu \quad (\text{A.2.10})$$

where $g_B = g_B^{inc} + g_B^{sc}$ for $B = D, N$. Then the electromagnetic fields, \mathbf{E} , \mathbf{H} , given by (2.1.15) satisfy the Maxwell equations (A.0.1) and the perfectly conducting boundary conditions (A.0.2).

Proof The result follows from (A.1.13), (A.2.2) and (A.2.5). \square

This result gives formulae for V and W via the solution to (A.2.6) and (A.2.7). To find expressions for V_{diff} and W_{diff} we follow the same procedure as in §2.1.2 and look at the behaviour of V and W as $k \rightarrow \infty$.

A.3 High frequency asymptotics

We are interested in the solution to our problem for high frequencies k . In fact we want the asymptotics of (A.2.10) as the dimensionless parameter $kr \rightarrow \infty$. For this, as with the acoustic case, it is convenient to use Sommerfeld's integral representation (2.1.41) of the Bessel function $J_\nu(kr)$ in (A.2.10):

$$J_\nu(kr) = \frac{1}{2\pi} \int_{\mathcal{W}} e^{-ikr \cos s + i\nu(\pi/2-s)} ds, \quad (\text{A.3.1})$$

where \mathcal{W} is the contour in Fig. 2-2. Now substituting (A.3.1) in (A.2.10) we get

$$\left\{ \begin{array}{c} V \\ W \end{array} \right\} (r, \boldsymbol{\omega}) = -2(2\pi k^3 r)^{-1/2} e^{i\pi/4} \int_{\mathcal{W}} e^{-ikr \cos s} \left\{ \begin{array}{c} \Gamma_D \\ \Gamma_N \end{array} \right\} (\boldsymbol{\omega}, \boldsymbol{\omega}_0, s) ds, \quad (\text{A.3.2})$$

where

$$\left\{ \begin{array}{c} \Gamma_D \\ \Gamma_N \end{array} \right\} (\boldsymbol{\omega}, \boldsymbol{\omega}_0, s) := \int_{\gamma_2} e^{-i\nu s} \left\{ \begin{array}{c} g_D \\ g_N \end{array} \right\} (\boldsymbol{\omega}, \boldsymbol{\omega}_0, \nu) \frac{\nu}{\nu^2 - 1/4} d\nu. \quad (\text{A.3.3})$$

Thus we are interested in the asymptotics of (A.3.2) as $kr \rightarrow \infty$. In a similar way as for the acoustic case we can replace the contour \mathcal{W} with \mathcal{W}' in Fig. 2-3 and the only possible non-negligible contribution to the asymptotics of the Debye potentials, V_{diff} and W_{diff} , associated with the diffracted wave are given by integration in a neighbourhood of stationary phase points, namely $s_0 = 0$ and $s_0 = \pi$. Using the "cut off" functions η_{s_0} defined in (2.1.45) we can isolate the contributions from the stationary points by writing, analogously to (2.1.46) in §2.1.2,

$$\begin{aligned} V(\mathbf{x}) &= V_0(\mathbf{x}) + V_\pi(\mathbf{x}) + V_{rem}(\mathbf{x}), \quad \text{and} \\ W(\mathbf{x}) &= W_0(\mathbf{x}) + W_\pi(\mathbf{x}) + W_{rem}(\mathbf{x}), \end{aligned}$$

where for $s_0 = 0$ or π , writing $\mathbf{x} = (r, \boldsymbol{\omega})$,

$$\left\{ \begin{array}{c} V_{s_0} \\ W_{s_0} \end{array} \right\} (r, \boldsymbol{\omega}) = -2(2\pi k^3 r)^{-1/2} e^{i\pi/4} \int_{\mathcal{W}'} e^{-ikr \cos s} \left\{ \begin{array}{c} \Gamma_D \\ \Gamma_N \end{array} \right\} (\boldsymbol{\omega}, \boldsymbol{\omega}_0, s) \eta_{s_0}(s) ds, \quad (\text{A.3.4})$$

and $V_{rem}(\mathbf{x})$ and $W_{rem}(\mathbf{x})$ are the Debye potentials which contain only the contributions to the asymptotics from non-stationary critical points which are exactly those associated with non-tip-diffracted electromagnetic waves.

To find the asymptotic expansions of V_{diff} and W_{diff} we investigate the asymptotics of $V_{s_0}(r, \boldsymbol{\omega})$ and $W_{s_0}(r, \boldsymbol{\omega})$ for $s_0 = 0$ and π . In Lemma A.13 we show that the contribution from the stationary point $s_0 = 0$ to the asymptotics of the diffracted wave is negligible. In order to do this we need to show that $\nabla_{\boldsymbol{\omega}} g_D^{sc}(\boldsymbol{\omega}, \boldsymbol{\omega}_0, 1/2) = \nabla_{\boldsymbol{\omega}} g_N(\boldsymbol{\omega}, \boldsymbol{\omega}_0, 1/2) \wedge \boldsymbol{\omega}$ which is the subject of Lemma A.12. Before we can do this we require the following two lemmas.

Lemma A.8. *Suppose $\boldsymbol{\omega} \in M$, and $\nu \neq \nu_{B,j}, j = 1, 2, \dots$, where $\nu_{B,j}$ are the eigenvalues associated with the eigenfunctions $\Phi_{B,j}$, see Definition 2.4. Then, adopting the Cartesian coordinate system in Notation A.1, g_D and g_N can be represented in the form,*

$$\begin{aligned} g_D(\boldsymbol{\omega}, \boldsymbol{\omega}_0, \nu) &= \sum_{j=1}^{\infty} (\nu^2 - \nu_j^2)^{-1} \Phi_{D,j}(\boldsymbol{\omega}) \{ \nabla_{\boldsymbol{\omega}'} \Phi_{D,j}(\boldsymbol{\omega}') |_{\boldsymbol{\omega}'=\boldsymbol{\omega}_0} \} \cdot \mathbf{e}_2, \\ g_N(\boldsymbol{\omega}, \boldsymbol{\omega}_0, \nu) &= \sum_{j=1}^{\infty} (\nu^2 - \nu_j^2)^{-1} \Phi_{N,j}(\boldsymbol{\omega}) \{ \nabla_{\boldsymbol{\omega}'} \Phi_{N,j}(\boldsymbol{\omega}') |_{\boldsymbol{\omega}'=\boldsymbol{\omega}_0} \} \cdot \mathbf{e}_1, \end{aligned} \quad (\text{A.3.5})$$

where the convergence holds in the distributional sense and $\nabla_{\boldsymbol{\omega}'}$ denotes the spherical gradient with respect to $\boldsymbol{\omega}'$ (see (3.1.3)).

Proof We give the proof for g_D only, the proof for g_N is analogous. In the same way as for Lemma 2.6 we seek $g_D(\boldsymbol{\omega}, \boldsymbol{\omega}_0, \nu)$ in the form of a spectral decomposition along the orthonormal eigenfunctions $\{\Phi_{D,j}\}$,

$$g_D(\boldsymbol{\omega}, \boldsymbol{\omega}_0, \nu) = \sum_{j=1}^{\infty} \mathcal{G}_j(\boldsymbol{\omega}_0, \nu) \Phi_{D,j}(\boldsymbol{\omega}). \quad (\text{A.3.6})$$

where $\mathcal{G}_j(\boldsymbol{\omega}_0, \nu)$ are to be found.

First recall the Green's function on the whole sphere, g_0 , given by (2.1.55),

$$g_0(\boldsymbol{\omega}, \boldsymbol{\omega}_0, \nu) = -\frac{1}{4 \cos(\pi\nu)} P_{\nu-\frac{1}{2}}(-\cos \theta(\boldsymbol{\omega}, \boldsymbol{\omega}_0)).$$

We claim that $g_D^{inc}(\boldsymbol{\omega}, \boldsymbol{\omega}_0, \nu) = \{ \nabla_{\boldsymbol{\omega}'} g_0(\boldsymbol{\omega}, \boldsymbol{\omega}', \nu) |_{\boldsymbol{\omega}'=\boldsymbol{\omega}_0} \} \cdot \mathbf{e}_2$ and we then use this to prove the result. To prove the claim recall $\nabla_{\boldsymbol{\omega}'}$ defined in (3.1.3). It follows that

$$\begin{aligned} \nabla_{\boldsymbol{\omega}'} g_0(\boldsymbol{\omega}, \boldsymbol{\omega}', \nu) |_{\boldsymbol{\omega}'=\boldsymbol{\omega}_0} &= -\frac{1}{4 \cos(\pi\nu)} \nabla_{\boldsymbol{\omega}'} P_{\nu-\frac{1}{2}}(-\cos \theta(\boldsymbol{\omega}, \boldsymbol{\omega}')) |_{\boldsymbol{\omega}'=\boldsymbol{\omega}_0} \\ &= \frac{1}{4 \cos(\pi\nu)} P'_{\nu-\frac{1}{2}}(-\cos \theta(\boldsymbol{\omega}, \boldsymbol{\omega}_0)) \nabla_{\boldsymbol{\omega}'} (\cos \theta(\boldsymbol{\omega}, \boldsymbol{\omega}')) |_{\boldsymbol{\omega}'=\boldsymbol{\omega}_0}. \end{aligned} \quad (\text{A.3.7})$$

Now recall from Notation 2.2 that $\cos \theta(\boldsymbol{\omega}, \boldsymbol{\omega}') = \boldsymbol{\omega} \cdot \boldsymbol{\omega}'$. Therefore using the fact

that $\nabla_{\omega'}(\omega \cdot \omega') = \omega - \omega'(\omega \cdot \omega')$ from (3.1.4), we have, from (A.3.7), that

$$\nabla_{\omega'} g_0(\omega, \omega_0, \nu)|_{\omega'=\omega_0} = \frac{1}{4 \cos(\pi\nu)} P'_{\nu-\frac{1}{2}}(-\cos \theta(\omega, \omega_0)) (\omega - \omega_0(\omega \cdot \omega_0)). \quad (\text{A.3.8})$$

In the Cartesian coordinate system introduced in Notation A.1, since $\mathbf{e}_2 \cdot \omega_0 = 0$ and $\theta(\omega, \omega') = \theta$, it follows from (A.3.8) that,

$$\begin{aligned} \{\nabla_{\omega'} g_0(\omega, \omega', \nu)|_{\omega'=\omega_0}\} \cdot \mathbf{e}_2 &= \frac{1}{4 \cos(\pi\nu)} P'_{\nu-\frac{1}{2}}(-\cos \theta) \omega \cdot \mathbf{e}_2 \\ &= \frac{1}{4 \cos(\pi\nu)} P'_{\nu-\frac{1}{2}}(-\cos \theta) \sin \theta \sin \phi. \end{aligned} \quad (\text{A.3.9})$$

Finally to prove the claim we use the identity [44, 8.752(1)]

$$P'_{\nu-1/2}(-\cos \theta) = -P_{\nu-1/2}^1(-\cos \theta) / \sin \theta.$$

Hence it follows from (A.3.9) that

$$\begin{aligned} \{\nabla_{\omega'} g_0(\omega, \omega', \nu)|_{\omega'=\omega_0}\} \cdot \mathbf{e}_2 &= -\frac{1}{4 \cos(\pi\nu)} P_{\nu-\frac{1}{2}}^1(-\cos \theta) \sin \phi \\ &= g_D^{inc}(\omega, \omega_0, \nu), \end{aligned} \quad (\text{A.3.10})$$

as required.

Now to complete the proof note that since $g_0(\omega, \omega_0, \nu)$ is the solution to (2.1.54) it follows that

$$\left(\Delta^* + \nu^2 - \frac{1}{4}\right) g_D^{inc}(\omega, \omega_0, \nu) = \{\nabla_{\omega'} \delta(\omega - \omega')|_{\omega'=\omega_0}\} \cdot \mathbf{e}_2,$$

and so by the definition of g_D and (A.2.6)

$$\begin{aligned} \left(\Delta^* + \nu^2 - \frac{1}{4}\right) g_D(\omega, \omega_0, \nu) &= \left(\Delta^* + \nu^2 - \frac{1}{4}\right) (g_D^{inc} + g_D^{sc})(\omega, \omega_0, \nu) \\ &= \left(\Delta^* + \nu^2 - \frac{1}{4}\right) g_D^{inc}(\omega, \omega_0, \nu) \\ &= \nabla_{\omega_0} \delta(\omega - \omega_0) \cdot \mathbf{e}_2. \end{aligned} \quad (\text{A.3.11})$$

Arguing in the same way as in Lemma 2.6 we can use the representation (A.3.6)

to write,

$$(\Delta^* + \nu^2 - 1/4)g_D(\boldsymbol{\omega}, \boldsymbol{\omega}_0, \nu) = \sum_{j=1}^{\infty} \mathcal{G}_j(\boldsymbol{\omega}_0, \nu)(\nu^2 - \nu_j^2)\Phi_{D,j}(\boldsymbol{\omega}). \quad (\text{A.3.12})$$

Also note from (2.1.20) that, in the distributional sense,

$$\begin{aligned} \{\nabla_{\boldsymbol{\omega}'}\delta(\boldsymbol{\omega} - \boldsymbol{\omega}')|_{\boldsymbol{\omega}'=\boldsymbol{\omega}_0}\} \cdot \mathbf{e}_2 &= \nabla_{\boldsymbol{\omega}'}\left(\sum_{j=1}^{\infty} \left\{\Phi_{D,j}(\boldsymbol{\omega})\Phi_{D,j}(\boldsymbol{\omega}')\right\}\Big|_{\boldsymbol{\omega}'=\boldsymbol{\omega}_0}\right) \cdot \mathbf{e}_2 \\ &= \sum_{j=1}^{\infty} \Phi_{D,j}(\boldsymbol{\omega})\{\nabla_{\boldsymbol{\omega}'}\Phi_{D,j}(\boldsymbol{\omega}')|_{\boldsymbol{\omega}'=\boldsymbol{\omega}_0}\} \cdot \mathbf{e}_2. \end{aligned} \quad (\text{A.3.13})$$

Therefore by comparing (A.3.13) and (A.3.12) the result follows from (A.3.11). \square

Remark A.9. Notice that $g_D(\boldsymbol{\omega}, \boldsymbol{\omega}_0, \nu)$ has positive poles at $\nu_{D,j}$ for $j = 1, 2, \dots$ and that $g_N(\boldsymbol{\omega}, \boldsymbol{\omega}_0, \nu)$ has poles at $\nu_{N,j}$ for $j = 2, 3, \dots$ but not at $\nu = \nu_{N,1} = 1/2$ since the orthonormal eigenvector, $\Phi_{N,1} = |M|^{-1/2}$ is constant and so there is no contribution from $j = 1$ to the sum in (A.3.5).

Also note that in the proof of Lemma A.8 we use the fact that (in the Cartesian coordinate system in Notation A.1)

$$g_D^{inc}(\boldsymbol{\omega}, \boldsymbol{\omega}_0, \nu) = \{\nabla_{\boldsymbol{\omega}'}g_0(\boldsymbol{\omega}, \boldsymbol{\omega}', \nu)|_{\boldsymbol{\omega}'=\boldsymbol{\omega}_0}\} \cdot \mathbf{e}_2, \quad (\text{A.3.14})$$

and analogously,

$$g_N^{inc}(\boldsymbol{\omega}, \boldsymbol{\omega}_0, \nu) = \{\nabla_{\boldsymbol{\omega}'}g_0(\boldsymbol{\omega}, \boldsymbol{\omega}', \nu)|_{\boldsymbol{\omega}'=\boldsymbol{\omega}_0}\} \cdot \mathbf{e}_1. \quad (\text{A.3.15})$$

It can be shown that this can be written equivalently (independently of the choice of Cartesian coordinate system) as

$$\begin{aligned} g_D^{inc}(\boldsymbol{\omega}, \boldsymbol{\omega}_0, \nu) &= \{\nabla_{\boldsymbol{\omega}'}g_0(\boldsymbol{\omega}, \boldsymbol{\omega}', \nu)|_{\boldsymbol{\omega}'=\boldsymbol{\omega}_0}\} \cdot \mathbf{E}^0, \\ g_N^{inc}(\boldsymbol{\omega}, \boldsymbol{\omega}_0, \nu) &= \{\nabla_{\boldsymbol{\omega}'}g_0(\boldsymbol{\omega}, \boldsymbol{\omega}', \nu)|_{\boldsymbol{\omega}'=\boldsymbol{\omega}_0}\} \cdot \mathbf{H}^0, \end{aligned}$$

where $\mathbf{E}^0, \mathbf{H}^0$ describe the polarisation of the incident wave, see (2.2.6). We use this representation of g_B^{inc} , $B = D, N$ in §2.2.

As stated above we aim to show that

$$\nabla_{\boldsymbol{\omega}}g_D^{sc}(\boldsymbol{\omega}, \boldsymbol{\omega}_0, 1/2) = \nabla_{\boldsymbol{\omega}}g_N^{sc}(\boldsymbol{\omega}, \boldsymbol{\omega}_0, 1/2) \wedge \boldsymbol{\omega}$$

in Lemma A.12. To prove this we need to evaluate the limit values of g_D and g_N as $\nu \rightarrow 1/2$. Lemma A.10 contains some related technical details which allow us to do this.

Lemma A.10. *For all $\boldsymbol{\omega} \in M$, the limit of g_B^{inc} and (defined by (A.2.3)) as $\nu \rightarrow 1/2$ exists for $B = D, N$. Moreover, (again adopting the Cartesian coordinate system in Notation A.1)*

$$\lim_{\nu \rightarrow 1/2} \left\{ \begin{array}{c} g_D^{inc} \\ g_N^{inc} \end{array} \right\} (\boldsymbol{\omega}, \boldsymbol{\omega}_0, \nu) = -\frac{1}{4\pi} \cot\left(\frac{\theta}{2}\right) \left\{ \begin{array}{c} \sin \phi \\ \cos \phi \end{array} \right\}. \quad (\text{A.3.16})$$

Proof We give the proof for g_D^{inc} only, the proof for g_N^{inc} is analogous. Recall from (A.3.10) that $g_D^{inc}(\boldsymbol{\omega}, \boldsymbol{\omega}_0, \nu) = \{\nabla_{\boldsymbol{\omega}'} g_0(\boldsymbol{\omega}, \boldsymbol{\omega}', \nu)|_{\boldsymbol{\omega}'=\boldsymbol{\omega}_0}\} \cdot \mathbf{e}_2$ where g_0 is the Green's function for the whole sphere S^2 given by (2.1.55). We will use this formula to prove the result but first since the representation (2.1.55) of $g_0(\boldsymbol{\omega}, \boldsymbol{\omega}_0, \nu)$ is undefined for $\nu = 1/2$ we need to find an alternative expression. Recall that g_0 satisfies

$$(\Delta^* + \nu^2 - 1/4)g_0(\boldsymbol{\omega}, \boldsymbol{\omega}_0, \nu) = \delta(\boldsymbol{\omega} - \boldsymbol{\omega}_0), \quad \boldsymbol{\omega} \in S^2. \quad (\text{A.3.17})$$

However, (A.3.17) has a singularity when $\nu \rightarrow 1/2$ since a solution for (A.3.17) is not defined for $\nu = 1/2$. This is because if $\Delta^* \psi = f$ on S^2 then it follows via Green's identity that $\int_{S^2} f(\boldsymbol{\omega}) dS(\boldsymbol{\omega}) = 0$ but $\int_{S^2} \delta(\boldsymbol{\omega} - \boldsymbol{\omega}_0) dS(\boldsymbol{\omega}) = 1$ so (A.3.17) is not solvable for $\nu = 1/2$. Consequently, instead of $g_0(\boldsymbol{\omega}, \boldsymbol{\omega}_0, \nu)$, we consider $\widehat{g}_0(\boldsymbol{\omega}, \boldsymbol{\omega}_0, \nu)$ the solution of

$$(\Delta^* + \nu^2 - 1/4)\widehat{g}_0(\boldsymbol{\omega}, \boldsymbol{\omega}_0, \nu) = \delta(\boldsymbol{\omega} - \boldsymbol{\omega}_0) - 1/4\pi, \quad \boldsymbol{\omega} \in S^2. \quad (\text{A.3.18})$$

The advantage of the equation (A.3.18) is that it is solvable for $\nu = 1/2$ (up to an arbitrary constant) since $\int_{S^2} \delta(\boldsymbol{\omega} - \boldsymbol{\omega}_0) - 1/4\pi dS(\boldsymbol{\omega}) = 0$. Also from (A.3.14) and (A.3.15) we see that

$$\begin{aligned} \lim_{\nu \rightarrow 1/2} g_D^{inc}(\boldsymbol{\omega}, \boldsymbol{\omega}_0, \nu) &= \lim_{\nu \rightarrow 1/2} \left\{ \nabla_{\boldsymbol{\omega}'} g_0(\boldsymbol{\omega}, \boldsymbol{\omega}', \nu)|_{\boldsymbol{\omega}'=\boldsymbol{\omega}_0} \right\} \cdot \mathbf{e}_2 \\ &= \lim_{\nu \rightarrow 1/2} \left\{ \nabla_{\boldsymbol{\omega}'} \widehat{g}_0(\boldsymbol{\omega}, \boldsymbol{\omega}', \nu)|_{\boldsymbol{\omega}'=\boldsymbol{\omega}_0} \right\} \cdot \mathbf{e}_2. \end{aligned} \quad (\text{A.3.19})$$

(The latter inequality follows e.g. by applying $\nabla_{\boldsymbol{\omega}'}$ to (A.3.17) and (A.3.18), with $\boldsymbol{\omega}_0$ replaced by $\boldsymbol{\omega}'$, and using uniqueness.) It follows that a formula for $\lim_{\nu \rightarrow 1/2} g_D^{inc}(\boldsymbol{\omega}, \boldsymbol{\omega}_0, \nu)$ can be recovered from the solution to (A.3.18) via (A.3.19).

First we show the limit on the right-hand side of (A.3.19) exists. To do

this we introduce the eigenvalues, $\nu_{0,j}^2$, and eigenfunctions, $\Phi_{0,j}$, of the operator $-\Delta^* + 1/4$ on the whole sphere S^2 . Clearly, $\nu_{0,1} = 1/2$, $\nu_{0,j} > 1/2$, for $j = 2, 3, \dots$ and $\Phi_{0,1} \equiv (4\pi)^{-1/2}$. Using similar techniques to those used in the proof of Lemma 2.6 we can write,

$$\begin{aligned}\widehat{g}_0(\boldsymbol{\omega}, \boldsymbol{\omega}_0, \nu) &= \sum_{j=1}^{\infty} (\nu^2 - \nu_{0,j}^2)^{-1} \Phi_{0,j}(\boldsymbol{\omega}) \Phi_{0,j}(\boldsymbol{\omega}_0) - (\nu^2 - 1/4)^{-1} \Phi_{0,1}(\boldsymbol{\omega}) \Phi_{0,1}(\boldsymbol{\omega}_0) \\ &= \sum_{j=2}^{\infty} (\nu^2 - \nu_{0,j}^2)^{-1} \Phi_{0,j}(\boldsymbol{\omega}) \Phi_{0,j}(\boldsymbol{\omega}_0).\end{aligned}$$

Hence the limit of $\nabla_{\boldsymbol{\omega}'} \widehat{g}_0(\boldsymbol{\omega}, \boldsymbol{\omega}', \nu)|_{\boldsymbol{\omega}'=\boldsymbol{\omega}_0}$ (and therefore $g_D^{inc}(\boldsymbol{\omega}, \boldsymbol{\omega}_0, \nu)$) exists as $\nu \rightarrow 1/2$, which we henceforth denote by $\nabla_{\boldsymbol{\omega}'} \widehat{g}_0(\boldsymbol{\omega}, \boldsymbol{\omega}', 1/2)|_{\boldsymbol{\omega}'=\boldsymbol{\omega}_0}$ (respectively $g_D^{inc}(\boldsymbol{\omega}, \boldsymbol{\omega}_0, 1/2)$).

To complete the proof we find a formula for the solution to (A.3.18) when $\nu = 1/2$. It can be shown, by direct differentiation, that for $\boldsymbol{\omega} \neq \boldsymbol{\omega}_0$, a solution to (A.3.18) with $\nu = 1/2$ is given by

$$\widehat{g}_0(\boldsymbol{\omega}, \boldsymbol{\omega}_0, 1/2) = \frac{1}{4\pi} \log(1 - \cos(\theta(\boldsymbol{\omega}, \boldsymbol{\omega}_0))). \quad (\text{A.3.20})$$

To show that this is a solution for all $\boldsymbol{\omega} \in S^2$ we show that $\Delta^* \widehat{g}_0(\boldsymbol{\omega}, \boldsymbol{\omega}_0, 1/2) = \delta(\boldsymbol{\omega} - \boldsymbol{\omega}_0) - 1/4\pi$ in the sense of distributions. Consider a test function $\psi \in C^\infty(S^2)$. By definition the action of the distribution $\Delta^* \widehat{g}_0(\boldsymbol{\omega}, \boldsymbol{\omega}_0, 1/2)$ on ψ satisfies (see e.g. [41]),

$$\begin{aligned}\langle \Delta^* \widehat{g}_0(\boldsymbol{\omega}, \boldsymbol{\omega}_0, 1/2), \psi(\boldsymbol{\omega}) \rangle &= \int_{S^2} \widehat{g}_0(\boldsymbol{\omega}, \boldsymbol{\omega}_0, 1/2) \Delta^* \psi(\boldsymbol{\omega}) dS(\boldsymbol{\omega}) \\ &= \lim_{\epsilon \rightarrow 0} \int_{S_\epsilon^2} \widehat{g}_0(\boldsymbol{\omega}, \boldsymbol{\omega}_0, 1/2) \Delta^* \psi(\boldsymbol{\omega}) dS(\boldsymbol{\omega}), \quad (\text{A.3.21})\end{aligned}$$

where $S_\epsilon^2 = \{\boldsymbol{\omega} \in S^2 : \theta(\boldsymbol{\omega}, \boldsymbol{\omega}_0) \geq \epsilon\}$. Applying Green's identity we have that for any $\epsilon \in (0, \pi)$,

$$\begin{aligned}\int_{S_\epsilon^2} \widehat{g}_0(\boldsymbol{\omega}, \boldsymbol{\omega}_0, 1/2) \Delta^* \psi(\boldsymbol{\omega}) dS(\boldsymbol{\omega}) &= \int_{S_\epsilon^2} \psi(\boldsymbol{\omega}) \Delta^* \widehat{g}_0(\boldsymbol{\omega}, \boldsymbol{\omega}_0, 1/2) dS(\boldsymbol{\omega}) \\ &\quad + \int_{\partial S_\epsilon^2} \left(\widehat{g}_0(\boldsymbol{\omega}, \boldsymbol{\omega}_0, 1/2) \frac{\partial \psi}{\partial \widehat{\mathbf{m}}}(\boldsymbol{\omega}) - \frac{\partial \widehat{g}_0}{\partial \widehat{\mathbf{m}}}(\boldsymbol{\omega}, \boldsymbol{\omega}_0, 1/2) \psi(\boldsymbol{\omega}) \right) d\boldsymbol{\omega}, \quad (\text{A.3.22})\end{aligned}$$

where $\widehat{\mathbf{m}}$ is the exterior normal to S_ϵ^2 at $\boldsymbol{\omega} \in \partial S_\epsilon^2$. It is clear from (A.3.18)

(with $\nu = 1/2$) that the first term on the right-hand side of (A.3.22) is equal to $-1/4\pi \int_{S_\epsilon^2} \psi(\boldsymbol{\omega}) dS(\boldsymbol{\omega})$. Now we consider the second and third terms on the right-hand side of (A.3.22). Note that $\partial\psi/\partial\widehat{\mathbf{m}}(\boldsymbol{\omega})$ is bounded and so it follows that,

$$\begin{aligned} \int_{\partial S_\epsilon^2} \widehat{g}_0(\boldsymbol{\omega}, \boldsymbol{\omega}_0, 1/2) \frac{\partial\psi}{\partial\widehat{\mathbf{m}}}(\boldsymbol{\omega}) d\boldsymbol{\omega} &= \frac{1}{4\pi} \log(1 - \cos(\epsilon)) \int_{\partial S_\epsilon^2} \frac{\partial\psi}{\partial\widehat{\mathbf{m}}}(\boldsymbol{\omega}) d\boldsymbol{\omega} \\ &= O(\epsilon |\log \epsilon|) \rightarrow 0 \text{ as } \epsilon \rightarrow 0, \end{aligned} \quad (\text{A.3.23})$$

since $\int_{\partial S_\epsilon^2} d\boldsymbol{\omega} = \sin(\epsilon) = O(\epsilon)$ and $1 - \cos(\theta) = O(\epsilon^2)$. Furthermore, in the Cartesian coordinate system introduced in Notation A.1 we can write $\partial/\partial\widehat{\mathbf{m}} = -\partial/\partial\theta|_{\theta=\epsilon}$. Using this and applying Taylor's theorem to ψ we have,

$$\begin{aligned} - \int_{\partial S_\epsilon^2} \frac{\partial\widehat{g}_0}{\partial\widehat{\mathbf{m}}}(\boldsymbol{\omega}, \boldsymbol{\omega}_0, 1/2) \psi(\boldsymbol{\omega}) d\boldsymbol{\omega} &= \frac{1}{4\pi} \frac{\sin(\epsilon)}{1 - \cos(\epsilon)} \int_{\partial S_\epsilon^2} \psi(\boldsymbol{\omega}) d\boldsymbol{\omega} \\ &= \psi(\boldsymbol{\omega}_0) + O(\epsilon) \rightarrow \psi(\boldsymbol{\omega}_0) \text{ as } \epsilon \rightarrow 0. \end{aligned} \quad (\text{A.3.24})$$

Therefore combining (A.3.22), (A.3.23) and (A.3.24) it follows from (A.3.21) that

$$\begin{aligned} \langle \Delta^* \widehat{g}_0(\boldsymbol{\omega}, \boldsymbol{\omega}_0, 1/2), \psi(\boldsymbol{\omega}) \rangle &= -1/4\pi \int_{S_\epsilon^2} \psi(\boldsymbol{\omega}) dS\boldsymbol{\omega} + \psi(\boldsymbol{\omega}_0) \\ &= \langle \delta(\boldsymbol{\omega} - \boldsymbol{\omega}_0) - 1/4\pi, \psi(\boldsymbol{\omega}) \rangle, \end{aligned}$$

for any $\psi \in C^\infty(S^2)$ and so \widehat{g} defined in (A.3.20) gives the solution to (A.3.18) in the sense of distributions.

Now it follows from (A.3.19) that,

$$\begin{aligned} \lim_{\nu \rightarrow 1/2} g_D^{inc}(\boldsymbol{\omega}, \boldsymbol{\omega}_0, \nu) &= \{ \nabla_{\boldsymbol{\omega}'} \widehat{g}_0(\boldsymbol{\omega}, \boldsymbol{\omega}', 1/2) |_{\boldsymbol{\omega}'=\boldsymbol{\omega}_0} \} \cdot \mathbf{e}_2 \\ &= \frac{1}{4\pi} \{ \nabla_{\boldsymbol{\omega}'} \log(1 - \cos \theta(\boldsymbol{\omega}, \boldsymbol{\omega}')) |_{\boldsymbol{\omega}'=\boldsymbol{\omega}_0} \} \cdot \mathbf{e}_2 \\ &= \frac{\{ \nabla_{\boldsymbol{\omega}'} (1 - \cos \theta(\boldsymbol{\omega}, \boldsymbol{\omega}')) |_{\boldsymbol{\omega}'=\boldsymbol{\omega}_0} \} \cdot \mathbf{e}_2}{4\pi(1 - \cos(\theta(\boldsymbol{\omega}, \boldsymbol{\omega}_0)))}. \end{aligned} \quad (\text{A.3.25})$$

Recalling from Notation 2.2 that $\cos \theta(\boldsymbol{\omega}, \boldsymbol{\omega}') = \boldsymbol{\omega} \cdot \boldsymbol{\omega}'$ and using (3.1.4) we have

$$\begin{aligned} \{ \nabla_{\boldsymbol{\omega}'} (1 - \cos \theta(\boldsymbol{\omega}, \boldsymbol{\omega}')) |_{\boldsymbol{\omega}'=\boldsymbol{\omega}_0} \} \cdot \mathbf{e}_2 &= - \{ \nabla_{\boldsymbol{\omega}'} ((\boldsymbol{\omega} \cdot \boldsymbol{\omega}') |_{\boldsymbol{\omega}'=\boldsymbol{\omega}_0}) \} \cdot \mathbf{e}_2 \\ &= -(\boldsymbol{\omega} - \boldsymbol{\omega}_0(\boldsymbol{\omega} \cdot \boldsymbol{\omega}_0)) \cdot \mathbf{e}_2. \end{aligned} \quad (\text{A.3.26})$$

Therefore by representing $\boldsymbol{\omega}$ in the form (A.0.4) it follows from (A.3.25) and

(A.3.26) that

$$\lim_{\nu \rightarrow 1/2} g_D^{inc}(\boldsymbol{\omega}, \boldsymbol{\omega}_0, \nu) = -\frac{\sin \theta(\boldsymbol{\omega}, \boldsymbol{\omega}_0)}{4\pi(1 - \cos(\theta(\boldsymbol{\omega}, \boldsymbol{\omega}_0)))} \sin \phi = -\frac{1}{4\pi} \cot(\theta(\boldsymbol{\omega}, \boldsymbol{\omega}_0)/2) \sin \phi,$$

and the result follows from the fact $\theta = \theta(\boldsymbol{\omega}, \boldsymbol{\omega}_0)$ in the coordinate system in Notation A.1. \square

Remark A.11. In the practical evaluation of the diffraction coefficients it is often convenient to deform the contour γ_2 , for example onto the imaginary axis. This is discussed in §6.1.2. It is shown there that in the course of such a deformation of the contour a residue contribution at $\nu = 1/2$ for integrals similar to (A.3.3) need to be computed. Therefore some of the details in the proof of Lemma A.10 are of use in §6.1.2.

Lemma A.12. For all $\boldsymbol{\omega} \in M$,

$$\nabla_{\boldsymbol{\omega}} g_D^{sc}(\boldsymbol{\omega}, \boldsymbol{\omega}_0, 1/2) = \nabla_{\boldsymbol{\omega}} g_N^{sc}(\boldsymbol{\omega}, \boldsymbol{\omega}_0, 1/2) \wedge \boldsymbol{\omega}. \quad (\text{A.3.27})$$

Proof The proof follows a sketched proof for this result given in [69, pg. 685]. Define $S : M \rightarrow \mathbb{R}^2$ by the stereographic projection of M onto the plane tangent to S^2 at $-\boldsymbol{\omega}_0$ (and then shifted to the plane $x_3 = 0$) given by (adopting the Cartesian coordinate system in Notation A.1),

$$S(\boldsymbol{\omega}) = 2 \cot(\theta/2)(\cos \phi, \sin \phi). \quad (\text{A.3.28})$$

We introduce the polar coordinates r, ψ to represent a point $\mathbf{x} \in \mathbb{R}^2$. We can define the action of S by

$$\boldsymbol{\omega} = (\theta, \phi) \mapsto (2 \cot(\theta/2), \phi), \quad (\text{A.3.29})$$

in polar coordinates. Similarly we can define the action of S^{-1} by

$$\mathbf{x} = (r, \psi) \mapsto (2 \cot^{-1}(r/2), \psi), \quad (\text{A.3.30})$$

is spherical coordinates.

A stereographic projection is known to be a *conformal mapping*, hence the following useful properties of S follow. Firstly the mapping S preserves angles, i.e. two geodesic curves on S^2 meeting at an angle of α are mapped by S onto two curves in \mathbb{R}^2 meeting at an angle of α also. Secondly, if $v(\boldsymbol{\omega})$ is a harmonic function on M then $\tilde{v}(\mathbf{x}) := v(S^{-1}(\mathbf{x}))$ is harmonic on $S(M)$.

We define $\tilde{g}_B^{sc}(\mathbf{x}) := g_B^{sc}(S^{-1}(\mathbf{x}), \boldsymbol{\omega}_0, 1/2)$ for $B = D, N$ and $\mathbf{x} \in S(M) \subset \mathbb{R}^2$. (Hence, since $\Delta^* g_B^{sc}(\boldsymbol{\omega}) = 0$, for $\boldsymbol{\omega} \in M$ it follows that $\Delta \tilde{g}_B^{sc}(\mathbf{x}) = 0$, for $\mathbf{x} \in S(M)$.) Let $\mathbf{x} = (x_1, x_2)$ and consider $z = x_1 + ix_2$. Define $\tilde{g}^{sc}(z) = \tilde{g}^{sc}(x_1, x_2) = \tilde{g}_D^{sc}(\mathbf{x}) - i\tilde{g}_N^{sc}(\mathbf{x})$. We claim that $\tilde{g}^{sc}(z)$ is analytic. This is equivalent to $\tilde{g}_D^{sc}(\mathbf{x})$ and $\tilde{g}_N^{sc}(\mathbf{x})$ satisfying the Cauchy-Riemann equations

$$\frac{\partial \tilde{g}_D^{sc}}{\partial x_1}(\mathbf{x}) = -\frac{\partial \tilde{g}_N^{sc}}{\partial x_2}(\mathbf{x}), \quad \frac{\partial \tilde{g}_D^{sc}}{\partial x_2}(\mathbf{x}) = \frac{\partial \tilde{g}_N^{sc}}{\partial x_1}(\mathbf{x}). \quad (\text{A.3.31})$$

We can use this and the properties of the conformal mapping S to prove the result.

To prove (A.3.31) consider first $\tilde{g}^{inc}(z) = \tilde{g}_D^{inc}(\mathbf{x}) - i\tilde{g}_N^{inc}(\mathbf{x})$, where \tilde{g}_B^{inc} , $B = D, N$ are defined in a similar way to \tilde{g}_B^{sc} , $\tilde{g}_B^{inc}(\mathbf{x}) := g_B^{inc}(S^{-1}(\mathbf{x}), \boldsymbol{\omega}_0, 1/2)$. We have from Lemma A.10 and (A.3.30) that

$$\begin{Bmatrix} \tilde{g}_D^{inc} \\ \tilde{g}_N^{inc} \end{Bmatrix}(\mathbf{x}) = -\frac{r}{8\pi} \begin{Bmatrix} \sin \psi \\ \cos \psi \end{Bmatrix}.$$

Hence $\tilde{g}^{inc}(z) = iz/8\pi$ which is certainly an analytic function.

Note that, from the boundary conditions (A.2.7) and using the fact that S is a conformal mapping, for $\mathbf{x} \in S(\ell)$

$$\tilde{g}_D^{sc}(\mathbf{x}) = -\tilde{g}_D^{inc}(\mathbf{x}) \quad \text{and} \quad \frac{\partial \tilde{g}_N^{sc}}{\partial \tilde{\mathbf{n}}}(\mathbf{x}) = -\frac{\partial \tilde{g}_N^{inc}}{\partial \tilde{\mathbf{n}}}(\mathbf{x}) \quad (\text{A.3.32})$$

where $\tilde{\mathbf{n}}$ is the exterior normal to $S(M) \subset \mathbb{R}^2$. It follows from complex analysis that every harmonic function in \mathbb{R}^2 is the real part of some analytic function on \mathbb{C} . Hence there exists a harmonic function $w(\mathbf{x})$ such that $\tilde{g}_D^{sc}(\mathbf{x}) + iw(\mathbf{x})$ is analytic. Moreover, it follows that \tilde{g}_D^{sc} and $w(\mathbf{x})$ satisfy the Cauchy-Riemann equations (A.3.31) with \tilde{g}_N^{sc} replaced by $-w$. Hence we have for $\mathbf{x} \in S(\ell)$,

$$\begin{aligned} \frac{\partial w}{\partial \tilde{\mathbf{n}}}(\mathbf{x}) &= \nabla w(\mathbf{x}) \cdot \tilde{\mathbf{n}} = \left(-\frac{\partial \tilde{g}_D^{sc}}{\partial x_2}(\mathbf{x}), \frac{\partial \tilde{g}_D^{sc}}{\partial x_1}(\mathbf{x}) \right) \cdot \tilde{\mathbf{n}} = -\left(\frac{\partial \tilde{g}_D^{sc}}{\partial x_1}(\mathbf{x}), \frac{\partial \tilde{g}_D^{sc}}{\partial x_2}(\mathbf{x}) \right) \cdot \tilde{\mathbf{t}} \\ &= -\frac{\partial \tilde{g}_D^{sc}}{\partial \tilde{\mathbf{t}}}(\mathbf{x}), \end{aligned} \quad (\text{A.3.33})$$

where $\tilde{\mathbf{t}}$ is a tangent to $S(\ell)$ at \mathbf{x} . From (A.3.32), it follows that \tilde{g}_D^{sc} coincides with $-\tilde{g}_D^{inc}$ on $S(\ell)$, hence tangential derivatives of \tilde{g}_D^{sc} and $-\tilde{g}_D^{inc}$ will also be equal. Therefore using the Cauchy-Riemann equations for the ‘‘incident parts’’

(replacing the superscripts sc in (A.3.31) by inc) and (A.3.33),

$$\begin{aligned}\frac{\partial w}{\partial \tilde{\mathbf{n}}}(\mathbf{x}) &= \frac{\partial \tilde{g}_D^{inc}}{\partial \tilde{\mathbf{t}}}(\mathbf{x}) = \left(\frac{\partial \tilde{g}_D^{inc}}{\partial x_1}(\mathbf{x}), \frac{\partial \tilde{g}_D^{inc}}{\partial x_2}(\mathbf{x}) \right) \cdot \tilde{\mathbf{t}} = \left(\frac{\partial \tilde{g}_D^{inc}}{\partial x_2}(\mathbf{x}), -\frac{\partial \tilde{g}_D^{inc}}{\partial x_1}(\mathbf{x}) \right) \cdot \tilde{\mathbf{n}} \\ &= \nabla \tilde{g}_N^{inc}(\mathbf{x}) \cdot \tilde{\mathbf{n}} = \frac{\partial \tilde{g}_N^{inc}}{\partial \tilde{\mathbf{n}}}(\mathbf{x}).\end{aligned}$$

Thus, $-w(\mathbf{x})$ is harmonic on $S(M)$ and satisfies the Neumann boundary conditions in (A.3.32). Since there is a unique solution to the Neumann problem (up to a constant) it follows that $\tilde{g}_N^{sc}(\mathbf{x}) = -w(\mathbf{x}) + C$, hence

$$\tilde{g}^{sc}(z) = \tilde{g}_D^{sc}(\mathbf{x}) - i\tilde{g}_N^{sc}(\mathbf{x}) = \tilde{g}_D^{sc}(\mathbf{x}) + iw(\mathbf{x}) - iC$$

is analytic. This proves the claim that \tilde{g}^{sc} is analytic.

Now using the Cauchy-Riemann equations (A.3.31),

$$\nabla \tilde{g}_D^{sc}(\mathbf{x}) = \left(-\frac{\partial \tilde{g}_N^{sc}}{\partial x_2}(\mathbf{x}), \frac{\partial \tilde{g}_N^{sc}}{\partial x_1}(\mathbf{x}) \right). \quad (\text{A.3.34})$$

Notice that interpreting $\nabla \tilde{g}_B^{sc}(\mathbf{x})$, $B = D, N$ as a $3D$ rather than $2D$ vector

$$\nabla \tilde{g}_B^{sc}(\mathbf{x}) = \left(\frac{\partial \tilde{g}_B^{sc}}{\partial x_1}(\mathbf{x}), \frac{\partial \tilde{g}_B^{sc}}{\partial x_2}(\mathbf{x}), 0 \right),$$

allows us to write (A.3.34) as

$$\nabla \tilde{g}_D^{sc}(\mathbf{x}) = \nabla \tilde{g}_N^{sc}(\mathbf{x}) \wedge (-\boldsymbol{\omega}_0), \quad (\text{A.3.35})$$

which is of a similar form to the result (A.3.27). To complete the proof we now show that (A.3.35) implies (A.3.27). To do this note that for an arbitrary function v defined on \mathbb{R}^2 we can write $\nabla v(\mathbf{x})$ in the polar coordinates (r, ψ) as,

$$\nabla v(\mathbf{x}) = \mathbf{e}_r \frac{\partial v(\mathbf{x})}{\partial r} + \mathbf{e}_\psi \frac{1}{r} \frac{\partial v(\mathbf{x})}{\partial \psi}.$$

By substituting this into (A.3.35) and using the fact that $\mathbf{e}_r \wedge (-\boldsymbol{\omega}_0) = \mathbf{e}_\psi$ and $\mathbf{e}_\psi \wedge (-\boldsymbol{\omega}_0) = -\mathbf{e}_r$, it follows that

$$\frac{\partial \tilde{g}_D^{sc}(\mathbf{x})}{\partial r} = -\frac{1}{r} \frac{\partial \tilde{g}_N^{sc}(\mathbf{x})}{\partial \psi} \quad (\text{A.3.36})$$

$$\text{and } \frac{\partial \tilde{g}_N^{sc}(\mathbf{x})}{\partial r} = \frac{1}{r} \frac{\partial \tilde{g}_D^{sc}(\mathbf{x})}{\partial \psi}. \quad (\text{A.3.37})$$

Now using the chain rule and recalling (A.3.30) we have

$$\begin{aligned} \frac{\partial \tilde{g}_B^{sc}(\mathbf{x})}{\partial r} &= \frac{\partial \theta}{\partial r} \frac{\partial g_B^{sc}(\boldsymbol{\omega}, \boldsymbol{\omega}_0, \nu)}{\partial \theta} = -\frac{1}{1 + (r/2)^2} \frac{\partial g_B^{sc}(\boldsymbol{\omega}, \boldsymbol{\omega}_0, \nu)}{\partial \theta} \\ \text{and } \frac{\partial \tilde{g}_B^{sc}(\mathbf{x})}{\partial \psi} &= \frac{\partial g_B^{sc}(\boldsymbol{\omega}, \boldsymbol{\omega}_0, \nu)}{\partial \phi}. \end{aligned}$$

Hence a straightforward calculation shows that (A.3.36) and (A.3.37) together with (A.3.30) imply,

$$\begin{aligned} \frac{\partial g_D^{sc}(\boldsymbol{\omega}, \boldsymbol{\omega}_0, \nu)}{\partial \theta} &= \frac{1}{\sin \theta} \frac{\partial g_N^{sc}(\boldsymbol{\omega}, \boldsymbol{\omega}_0, \nu)}{\partial \phi} \\ \text{and } \frac{\partial g_N^{sc}(\boldsymbol{\omega}, \boldsymbol{\omega}_0, \nu)}{\partial \theta} &= -\frac{1}{\sin \theta} \frac{\partial g_D^{sc}(\boldsymbol{\omega}, \boldsymbol{\omega}_0, \nu)}{\partial \phi}. \end{aligned} \quad (\text{A.3.38})$$

Using this, the result (A.3.27) follows from (3.1.3) and the fact that $\mathbf{e}_\theta \wedge \boldsymbol{\omega} = -\mathbf{e}_\phi$ and $\mathbf{e}_\phi \wedge \boldsymbol{\omega} = \mathbf{e}_\theta$. \square

We use Lemma A.12 in Lemma A.13 to show that the combined contribution from the stationary point $s_0 = 0$, i.e. the contribution from V_0 and W_0 defined in (A.3.4), to the electromagnetic field \mathbf{E} , \mathbf{H} is negligible. First we define the contribution to the electric field and the magnetic field from a stationary point s_0 by \mathbf{E}_{s_0} and \mathbf{H}_{s_0} respectively, i.e.

$$\begin{aligned} \mathbf{E}_{s_0}(\mathbf{x}) &= \text{curl curl } (V_{s_0}(\mathbf{x})\mathbf{x}) + ik \text{ curl } (W_{s_0}(\mathbf{x})\mathbf{x}), \\ \mathbf{H}_{s_0}(\mathbf{x}) &= \text{curl curl } (W_{s_0}(\mathbf{x})\mathbf{x}) - ik \text{ curl } (V_{s_0}(\mathbf{x})\mathbf{x}). \end{aligned} \quad (\text{A.3.39})$$

Lemma A.13. *Suppose that $\boldsymbol{\omega} \neq \boldsymbol{\omega}_0$ then the contribution from the stationary point $s_0 = 0$ to the asymptotics of the electromagnetic field, $\mathbf{E}(r, \boldsymbol{\omega})$, $\mathbf{H}(r, \boldsymbol{\omega})$, is $O((kr)^{-2})$, i.e. for all $\mathbf{x} \in \mathbb{R}^3 \setminus \Xi$, $\mathbf{E}_0(\mathbf{x}) = O((kr)^{-2})$ and $\mathbf{H}_0(\mathbf{x}) = O((kr)^{-2})$ as $kr \rightarrow \infty$.*

Proof We prove this result for the electric field only, the proof for the magnetic field is analogous. The first thing we need to do is apply the stationary phase technique to calculate the asymptotic expansion of V_{s_0} and W_{s_0} (see e.g. [15, §2.7]). It follows that

$$\left\{ \begin{array}{c} V_0 \\ W_0 \end{array} \right\} (r, \boldsymbol{\omega}) = -2i \frac{e^{-ikr}}{k^2 r} \left\{ \begin{array}{c} \Gamma_D \\ \Gamma_N \end{array} \right\} (\boldsymbol{\omega}, \boldsymbol{\omega}_0, 0) + O(k^{-1}(kr)^{-2}), \quad \text{as } kr \rightarrow \infty.$$

Now we substitute these representations of V_0 and W_0 into (A.3.39). Using

(A.1.5), (A.1.6) and (A.1.3) we get, after some straightforward calculus,

$$\begin{aligned} \operatorname{curl} \operatorname{curl} (V_0(\mathbf{x})\mathbf{x}) &= -2 \frac{e^{-ikr}}{kr} \nabla_{\boldsymbol{\omega}} \Gamma_D(\boldsymbol{\omega}, \boldsymbol{\omega}_0, 0) + O((kr)^{-2}), \quad \text{and} \\ ik \operatorname{curl} (W_0(\mathbf{x})\mathbf{x}) &= 2 \frac{e^{-ikr}}{kr} \nabla_{\boldsymbol{\omega}} \Gamma_N(\boldsymbol{\omega}, \boldsymbol{\omega}_0, 0) \wedge \boldsymbol{\omega} + O((kr)^{-2}) \quad \text{as } kr \rightarrow \infty. \end{aligned}$$

Therefore substituting this into (A.3.39) with $s_0 = 0$ and writing $\mathbf{x} = (r, \boldsymbol{\omega})$,

$$\mathbf{E}_0(r, \boldsymbol{\omega}) = -2 \frac{e^{-ikr}}{kr} (\nabla_{\boldsymbol{\omega}} \Gamma_D(\boldsymbol{\omega}, \boldsymbol{\omega}_0, 0) - \nabla_{\boldsymbol{\omega}} \Gamma_N(\boldsymbol{\omega}, \boldsymbol{\omega}_0, 0) \wedge \boldsymbol{\omega}) + O((kr)^{-2}), \quad (\text{A.3.40})$$

as $kr \rightarrow \infty$. All that remains to complete the proof is to show that

$$\nabla_{\boldsymbol{\omega}} \Gamma_D(\boldsymbol{\omega}, \boldsymbol{\omega}_0, 0) - \nabla_{\boldsymbol{\omega}} \Gamma_N(\boldsymbol{\omega}, \boldsymbol{\omega}_0, 0) \wedge \boldsymbol{\omega} = 0 \quad \text{for } \boldsymbol{\omega} \neq \boldsymbol{\omega}_0.$$

To do this we formally apply Cauchy's residue theorem to the integral representation of Γ_B , $B = D, N$ in (A.3.3). We have using Theorem 2.7 that for $B = D, N$,

$$\begin{aligned} \Gamma_B(\boldsymbol{\omega}, \boldsymbol{\omega}_0, 0) &= \int_{\gamma_2} g_B^{sc}(\boldsymbol{\omega}, \boldsymbol{\omega}_0, \nu) \frac{\nu}{\nu^2 - 1/4} d\nu \\ &= -2\pi i \sum_{j=1}^{\infty} \operatorname{res} \left(g_B^{sc}(\boldsymbol{\omega}, \boldsymbol{\omega}_0, \nu) \frac{\nu}{\nu^2 - 1/4}, \nu_{B,j} \right). \quad (\text{A.3.41}) \end{aligned}$$

It follows from (2.1.25) and Lemma A.8 that for $j = 1, 2, \dots$,

$$\begin{aligned} \operatorname{res} \left(g_D^{sc}(\boldsymbol{\omega}, \boldsymbol{\omega}_0, \nu) \frac{\nu}{\nu^2 - 1/4}, \nu_{D,j} \right) &= \frac{1}{2(\nu_{D,j}^2 - 1/4)} \Phi_{D,j}(\boldsymbol{\omega}) \nabla_{\boldsymbol{\omega}_0} \Phi_{D,j}(\boldsymbol{\omega}_0) \cdot \mathbf{e}_2, \\ \operatorname{res} \left(g_N^{sc}(\boldsymbol{\omega}, \boldsymbol{\omega}_0, \nu) \frac{\nu}{\nu^2 - 1/4}, \nu_{N,j} \right) &= \frac{1}{2(\nu_{N,j}^2 - 1/4)} \Phi_{N,j}(\boldsymbol{\omega}) \nabla_{\boldsymbol{\omega}_0} \Phi_{N,j}(\boldsymbol{\omega}_0) \cdot \mathbf{e}_1, \end{aligned}$$

therefore, applying Lemma A.8 again and using (A.3.41), we get,

$$\begin{aligned} \Gamma_D(\boldsymbol{\omega}, \boldsymbol{\omega}_0, 0) &= \pi i \sum_{j=1}^{\infty} \frac{1}{1/4 - \nu_{D,j}^2} \Phi_{D,j}(\boldsymbol{\omega}) \nabla_{\boldsymbol{\omega}_0} \Phi_{D,j}(\boldsymbol{\omega}_0) \cdot \mathbf{e}_2 \\ &= \pi i g_D(\boldsymbol{\omega}, \boldsymbol{\omega}_0, 1/2), \\ \Gamma_N(\boldsymbol{\omega}, \boldsymbol{\omega}_0, 0) &= \pi i \sum_{j=1}^{\infty} \frac{1}{1/4 - \nu_{N,j}^2} \Phi_{N,j}(\boldsymbol{\omega}) \nabla_{\boldsymbol{\omega}_0} \Phi_{N,j}(\boldsymbol{\omega}_0) \cdot \mathbf{e}_1 \\ &= \pi i g_N(\boldsymbol{\omega}, \boldsymbol{\omega}_0, 1/2). \end{aligned}$$

Hence from Lemma A.12 it follows that,

$$\begin{aligned} \nabla_{\boldsymbol{\omega}} \Gamma_D(\boldsymbol{\omega}, \boldsymbol{\omega}_0, 0) - \nabla_{\boldsymbol{\omega}} \Gamma_N(\boldsymbol{\omega}, \boldsymbol{\omega}_0, 0) \wedge \boldsymbol{\omega} \\ = \pi i (\nabla_{\boldsymbol{\omega}} g_D(\boldsymbol{\omega}, \boldsymbol{\omega}_0, 1/2) - \nabla_{\boldsymbol{\omega}} g_D(\boldsymbol{\omega}, \boldsymbol{\omega}_0, 1/2) \wedge \boldsymbol{\omega}) = 0, \end{aligned}$$

thus the result follows from (A.3.40). \square

Remark A.14. Lemma A.13 establishes that the contribution from the stationary phase point $s_0 = 0$ to the principal term in the asymptotics of \mathbf{E}_0 and \mathbf{H}_0 vanishes. Therefore there are no $O(\exp(-ikr)/kr)$ terms contributing to the asymptotics of the scattered field \mathbf{E}_{sc} , \mathbf{H}_{sc} . This corresponds physically to the absence of “in going” waves and, in a sense, justifies *a posteriori* the radiation conditions.

Thus the contributions to the diffracted wave must come from $V_\pi(r, \boldsymbol{\omega})$ and $W_\pi(r, \boldsymbol{\omega})$. (In analogy with the acoustic case the diffracted wave is undefined for directions which correspond with singularities occurring at $s = \pi$, namely the singular directions, see Definition 2.13.) Therefore we get the next result.

Corollary A.15. *For all nonsingular directions $\boldsymbol{\omega} \in S^2$, the Debye potentials V_{diff} , W_{diff} corresponding to the electromagnetic field diffracted by the conical point (see (2.2.14)) take the form,*

$$\left\{ \begin{array}{c} V_{diff} \\ W_{diff} \end{array} \right\} (r, \boldsymbol{\omega}) = 2\pi i \frac{e^{ikr}}{k^2 r} \left\{ \begin{array}{c} f_D \\ f_N \end{array} \right\} (\boldsymbol{\omega}, \boldsymbol{\omega}_0) + O(k^{-1}(kr)^{-2}), \quad \text{as } kr \rightarrow \infty, \quad (\text{A.3.42})$$

where for $B = D$ or N , $f_B(\boldsymbol{\omega}, \boldsymbol{\omega}_0) := i/\pi \Gamma_B(\boldsymbol{\omega}, \boldsymbol{\omega}_0, \pi)$.

Proof Applying the stationary phase technique to V_π and W_π we get [15]

$$\left\{ \begin{array}{c} V_{diff} \\ W_{diff} \end{array} \right\} (r, \boldsymbol{\omega}) = \left\{ \begin{array}{c} V_\pi \\ W_\pi \end{array} \right\} (r, \boldsymbol{\omega}) = -2 \frac{e^{ikr}}{k^2 r} \left\{ \begin{array}{c} \Gamma_D \\ \Gamma_N \end{array} \right\} (\boldsymbol{\omega}, \boldsymbol{\omega}_0) + O(k^{-1}(kr)^{-2}),$$

as $kr \rightarrow \infty$. Hence the result. \square

Our final result in this appendix gives the formula (2.2.19) given in §2.2 for the high-frequency asymptotics of a wave diffracted by the vertex of a cone, see e.g. [69], [12].

Lemma A.16. *For $\mathbf{x} \in \mathbb{R}^3 \setminus \Xi$, such that $\boldsymbol{\omega} = |\mathbf{x}|$ is not a singular direction*

$$\left\{ \begin{array}{c} \mathbf{E}_{diff} \\ \mathbf{H}_{diff} \end{array} \right\} (\mathbf{x}) = 2\pi \frac{e^{ikr}}{kr} \left\{ \begin{array}{c} \mathcal{E}(\boldsymbol{\omega}, \boldsymbol{\omega}_0) \\ \mathcal{H}(\boldsymbol{\omega}, \boldsymbol{\omega}_0) \end{array} \right\} + O((kr)^{-2}), \quad \text{as } kr \rightarrow \infty, \quad (\text{A.3.43})$$

where

$$\begin{aligned}\mathcal{E}(\boldsymbol{\omega}, \boldsymbol{\omega}_0) &= -\nabla_{\boldsymbol{\omega}} f_D(\boldsymbol{\omega}, \boldsymbol{\omega}_0) - \nabla_{\boldsymbol{\omega}} f_N(\boldsymbol{\omega}, \boldsymbol{\omega}_0) \wedge \boldsymbol{\omega}, \\ \mathcal{H}(\boldsymbol{\omega}, \boldsymbol{\omega}_0) &= -\nabla_{\boldsymbol{\omega}} f_N(\boldsymbol{\omega}, \boldsymbol{\omega}_0) + \nabla_{\boldsymbol{\omega}} f_D(\boldsymbol{\omega}, \boldsymbol{\omega}_0) \wedge \boldsymbol{\omega}.\end{aligned}\tag{A.3.44}$$

Proof We give the proof for \mathbf{E}_{diff} , the proof for \mathbf{H}_{diff} is analogous. It follows from (A.3.42), (A.1.5), (A.1.6), (A.1.3) and some elementary calculus that,

$$\begin{aligned}\text{curl curl } (V_{diff}(\mathbf{x})\mathbf{x}) &= -2\pi \frac{e^{ikr}}{kr} \nabla_{\boldsymbol{\omega}} f_D(\boldsymbol{\omega}, \boldsymbol{\omega}_0) + O((kr)^{-2}), \quad \text{and} \\ ik \text{ curl } (W_{diff}(\mathbf{x})\mathbf{x}) &= -2\pi \frac{e^{ikr}}{kr} \nabla_{\boldsymbol{\omega}} f_N(\boldsymbol{\omega}, \boldsymbol{\omega}_0) \wedge \boldsymbol{\omega} + O((kr)^{-2}) \quad \text{as } kr \rightarrow \infty.\end{aligned}$$

Therefore the result follows from (A.3.39) and (A.3.42). \square

It follows from Lemma A.16 that the key to calculating the diffraction coefficients is the computation of the scalar potentials $f_B(\boldsymbol{\omega}, \boldsymbol{\omega}_0)$, $B = D, N$ given by (using (A.3.3))

$$f_B(\boldsymbol{\omega}, \boldsymbol{\omega}_0) = \frac{i}{\pi} \Gamma_B(\boldsymbol{\omega}, \boldsymbol{\omega}_0, \pi) = \frac{i}{\pi} \int_{\gamma_2} e^{-i\nu\pi} g_B(\boldsymbol{\omega}, \boldsymbol{\omega}_0, \nu) \frac{\nu}{\nu^2 - 1/4} d\nu \quad \text{for } B = D, N,$$

(holding in the distributional sense) which are analogous to the acoustic diffraction coefficient $f(\boldsymbol{\omega}, \boldsymbol{\omega}_0)$ cf. (2.1.56). In the same way as with the acoustic case by writing $g_B(\boldsymbol{\omega}, \boldsymbol{\omega}_0, \nu) = g_B^{sc}(\boldsymbol{\omega}, \boldsymbol{\omega}_0, \nu) + g_B^{inc}(\boldsymbol{\omega}, \boldsymbol{\omega}_0, \nu)$ the formulae for $f_B(\boldsymbol{\omega}, \boldsymbol{\omega}_0)$ become,

$$f_B(\boldsymbol{\omega}, \boldsymbol{\omega}_0) = \frac{i}{\pi} \int_{\gamma_2} e^{-i\nu\pi} g_B^{sc}(\boldsymbol{\omega}, \boldsymbol{\omega}_0, \nu) \frac{\nu}{\nu^2 - 1/4} d\nu \quad \text{for } B = D, N,\tag{A.3.45}$$

since, in analogy with the acoustic case, the combined contribution of

$$\frac{i}{\pi} \int_{\gamma_2} e^{-i\nu\pi} g_B^{inc}(\boldsymbol{\omega}, \boldsymbol{\omega}_0, \nu) \frac{\nu}{\nu^2 - 1/4} d\nu$$

to the electromagnetic diffraction coefficients can be shown to be zero.

Bibliography

- [1] M. Abramowitz and I.E. Stegun. *Handbook of Mathematical Functions*. Dover Publications, New York, 1965.
- [2] Y.A. Antipov. Diffraction of a plane wave by a circular cone with an impedance boundary condition. *SIAM J. Appl. Math.*, 62:1122–1152, 2002.
- [3] K.E. Atkinson. *An Introduction to Numerical Analysis*. John Wiley & Sons, New York, 1989.
- [4] K.E. Atkinson. *The Numerical Solution of Integral Equations of the Second Kind*. Cambridge University Press, Cambridge, 1997.
- [5] K.E. Atkinson and F. de Hoog. The numerical solution of Laplace’s equation on a wedge. *IMA J. Num. Anal.*, 4:19–41, 1984.
- [6] V.M. Babič and V.S. Buldryev. *Short-Wave-Length Diffraction Theory*. Springer-Verlag, Berlin, 1991.
- [7] V.M. Babich. Rigorous justification of the shortwave approximation in the three-dimensional case. *J. Sov. Math.*, 6:488–509, 1976.
- [8] V.M. Babich, D.B. Dement’ev, and B.A. Samokish. On the diffraction of high-frequency waves by a cone of arbitrary shape. *Wave Motion*, 21:203–207, 1995.
- [9] V.M. Babich, D.B. Dement’ev, B.A. Samokish, and V.P. Smyshlyaev. On evaluation of the diffraction coefficients for arbitrary ”nonsingular” directions of a smooth convex cone. *SIAM J. Appl. Math.*, 60:536–573, 2000.
- [10] V.M. Babich, D.B. Dement’ev, B.A. Samokish, and V.P. Smyshlyaev. Scattering of a high-frequency wave by the vertex of an arbitrary cone (singular directions). *Journal of Mathematical Sciences*, 111(4):3623–3631, 2002.

- [11] V.M. Babich and V.V. Kamotskii. Computation of the scattering amplitude of a wave diffracted by the vertex of a cone of arbitrary shape. *Journal of Mathematical Sciences*, 108(5):635–641, 2002.
- [12] V.M. Babich, V.P. Smyshlyaev, D.B. Dement'ev, and B.A. Samokish. Numerical calculation of the diffraction coefficients for an arbitrarily shaped perfectly conducting cone. *IEEE Trans. Antennas & Propagation*, 44:740–747, 1996.
- [13] J.M.L. Bernard. Méthode analytique et transformées fonctionnelles pour la diffraction d'ondes par une singularité conique. Rapport CEA-R-5764 Editions Dist/Salsay 1997.
- [14] J.M.L. Bernard and M.A. Lyalinov. Electromagnetic scattering by an impedance cone. *J. Mech. Appl. Math. (to appear)*, 2003.
- [15] N. Bleistein. *Mathematical Methods for Wave Phenomena*. Academic Press, New York, 1984.
- [16] V.A. Borovikov. *Diffraction by Polygons and Polyhedrons*. Nauka, Moscow, 1966.
- [17] V.A. Borovikov and B. Ye. Kinber. *Geometrical Theory of Diffraction*. IEE, London, 1994.
- [18] J.J. Bowman, T.B.A. Senior, and P.L.E. Uslenghi. *Electromagnetic and Acoustic Scattering by Simple Shapes*. North-Holland, Amsterdam, 1969. Revised 1987.
- [19] J.C. Burkill and H. Burkill. *A Second Course of Mathematical Analysis*. Cambridge University Press, Cambridge, 1970.
- [20] V.S. Buslaev. Potential theory and geometrical optics. *J. Sov. Math.*, 2:204–209, 1974.
- [21] G.A. Chandler and I.G. Graham. Uniform convergence of Galerkin solutions to non-compact integral operator equations. *IMA J. Numer. Analysis*, 7:327–334, 1987.
- [22] G.A. Chandler and I.G. Graham. Product integration-collocation methods for noncompact integral operator equations. *Math. Comp.*, 50:125–138, 1988.

- [23] J. Cheeger and I.M. Taylor. On the diffraction of waves by conical singularities I and II. *Comm. Pure Appl. Math.*, 35:275–331,487–529, 1982.
- [24] K. Chen and S. Amini. Numerical analysis of boundary integral solution of the Helmholtz equation in domains with non-smooth boundaries. *IMA J. Num. Anal.*, 13:43–68, 1993.
- [25] D. Colton and R. Kress. *Integral Equation Methods in Scattering Theory*. Wiley, New York, 1983.
- [26] D. Colton and R. Kress. *Inverse Acoustic and Electromagnetic Scattering Theory*. Springer-Verlag, New York, 1992.
- [27] M. Costabel and E.P. Stephan. Boundary integral equations for mixed boundary value problems in polygonal domains and Galerkin approximation. In *Mathematical Models and Methods in Mechanics*, volume 15, pages 175–251. Banach Centre Publications, PWN, Warsaw, 1985.
- [28] P.J. Davis and P. Rabinowitz. *Methods of Numerical Integration*. Academic Press, New York, 1975.
- [29] D.B. Dement'ev, B.A. Samokish, and V.M. Babich. Computation of the Legendre function. Unpublished manuscript, 2000.
- [30] J.A. DeSanto. *Scalar Wave Theory*. Springer-Verlag, Berlin, 1992.
- [31] R. Duduchava. The Green formula and layer potentials. *Integral Equations and Operator Theory*, 41:127–178, 2001.
- [32] R. Duduchava. Boundary value problems on a smooth surface with smooth boundary. *Universität Stuttgart, Preprint 2002-5*, pages 1–19, 2002.
- [33] N. Dunford and J.T. Schwartz. *Linear Operators Pt.1*. Interscience Publishers, Inc., New York, 1967.
- [34] J. Elschner. On spline approximation for a class of integral equations. I: Galerkin and Collocation methods with piecewise polynomials. *Math. Methods Appl. Sci.*, 10:543–559, 1988.
- [35] J. Elschner. On spline collocation for convolution equations. *Integral Equations and Oper. Theory*, 12:486–510, 1989.
- [36] J. Elschner. On spline approximation for a class of non-compact integral operators. *Math. Nachr.*, 146:271–321, 1990.

- [37] J. Elschner. The $h - p$ -version of spline approximation methods for Mellin convolution equations. *J. Integral Equations and Appl.*, 5(1):47–73, 1993.
- [38] J. Elschner and I.G. Graham. Numerical methods for integral equations of Mellin type. *J. Comp. Appl. Math.*, 125:423–437, 2000.
- [39] G. Friedlander and M. Joshi. *Introduction to the Theory of Distributions*. Cambridge University Press, Cambridge, 1998.
- [40] A. Friedman. *Foundations of Modern Analysis*. Dover Publications, Inc., New York, 1970.
- [41] I.M. Gel'fand and G.E. Shilov. *Generalised Functions V.1 : Properties and Operations*. Academic Press, New York, 1964.
- [42] I.M. Gel'fand and G.E. Shilov. *Generalised Functions V.3 : Theory of Differential Equations*. Academic Press, New York, 1964.
- [43] P. Gerard and G. Lebeau. Diffusion d'une onde par un coin. *J. Amer. Math. Soc.*, 6(2):341–424, 1993.
- [44] I.S. Gradshteyn and I.M. Ryzhik. *Tables of Integrals, Series and Products, 4th ed.* Academic Press, Orlando, 1980.
- [45] I.G. Graham and G.A. Chandler. High-order methods for linear functionals of solutions of second kind integral equations. *SIAM J. Numer. Anal.*, 25(5):1118–1137, 1988.
- [46] I.G. Graham, W. Hackbusch, and S.A. Sauter. Discrete boundary element methods on general meshes in 3D. *Numer. Math.*, 86(1):103–137, 2000.
- [47] I.G. Graham and I.H. Sloan. On the compactness of certain integral operators. *J. Math. Anal. Appl.*, 68(2):580–594, 1979.
- [48] R. Grimshaw. High-frequency scattering by finite convex regions. *Comm. Pure Appl. Math.*, 19:167–193, 1966.
- [49] B.Q. Guo and I. Babuška. The $h - p$ version of the finite element method. Part 1: The basic approximation results, Part 2: General results and applications. *Comput. Mech.*, 1:21–41, 203–226, 1997.
- [50] W. Hackbusch. *Integral Equations : Theory and Numerical Treatment*. Birkhäuser, Basel, 1995.

- [51] R.C. Hansen. *Geometric Theory of Diffraction edited by Robert C. Hansen prepared under the sponsorship of the IEEE Antennas and Propagation Society*. IEEE, New York, 1981.
- [52] E.W. Hobson. *The Theory of Spherical and Ellipsoidal Harmonics*. Cambridge University Press, Cambridge, 1931.
- [53] L. Hormander. *The Analysis of Linear Partial Differential Operators*, volume 3: Pseudo-differential Operators. Springer-Verlag, Berlin, 1985.
- [54] G.L. James. *Geometrical Theory of Diffraction for Electromagnetic Waves*. IEE, London, 1976.
- [55] D.S. Jones. *The Theory of Electromagnetism*. Pergamon Press, Oxford, 1964.
- [56] D.S. Jones. Scattering by a cone. *Quart. J. Mech. Appl. Math.*, 50:499–523, 1997.
- [57] V.V. Kamotskii. Calculation of some integrals describing wave fields. *Journal of Mathematical Sciences*, 108(5):665–673, 2002.
- [58] L.V. Kantorovich and G.P. Akilov. *Functional Analysis*. Pergamon, Oxford, 1982.
- [59] J.B. Keller. Diffraction by a convex cylinder. *IRE Trans. Ant. Prop.*, 4:312–321, 1956.
- [60] J.B. Keller. The geometrical theory of diffraction. *J. Opt. Soc. Amer.*, 52:116–130, 1962.
- [61] O.V. Klyubina. Diffraction of plane waves on bodies of different types. *Journal of Mathematical Sciences*, 111(4):3708–3716, 2002.
- [62] L. Krauss and L.M. Levine. Diffraction by an elliptic cone. *Comm. Pure Appl. Math.*, 14:49–68, 1961.
- [63] O.A. Ladyzhenskaya. *The Boundary Value Problems of Mathematical Physics*. Springer-Verlag, Berlin, 1985.
- [64] L. Lebeau. Propagation des ondes dans les variétés à coins. *Ann. scient. Éc. Norm. Sup.*, 30:429–497, 1997.

- [65] H.A. Priestly. *Introduction to Complex Analysis*. Clarendon Press, Oxford, 1999.
- [66] S.A. Sauter and C. Schwab. Quadrature for hp-Galerkin BEM in \mathbb{R}^3 . *Num. Math.*, 78:211–258, 1997.
- [67] V.P. Smyshlyaev. On the diffraction of waves by cones at high frequencies. *LOMI preprint E-9-89, Leningrad*, 1989.
- [68] V.P. Smyshlyaev. Diffraction by conical surfaces at high frequencies. *Wave Motion*, 12:329–339, 1990.
- [69] V.P. Smyshlyaev. The high-frequency diffraction of electromagnetic waves by cones of arbitrary cross-sections. *SIAM J. Appl. Math.*, 53:670–688, 1993.
- [70] V.P. Smyshlyaev, V.M. Babich, D.B. Dement'ev, and B.A. Samokish. Diffraction of electromagnetic creeping waves by conical points. In *IUTAM Symposium in Diffraction and Scattering in Fluid Mechanics and Elasticity, Proceedings*. Kluwer, London, 2002.
- [71] A. Sommerfeld. Mathematische Theorie der Diffraction. *Math. Ann.*, 47:317–374, 1896.
- [72] A. Sommerfeld. *Optics*. Academic Press, New York, 1964.
- [73] M.E. Taylor. *Partial Differential Equations I*. Springer-Verlag, New York, 1996.
- [74] J. Van Bladel. *Electromagnetic fields*. McGraw-Hill, New York, 1964. revised printing, Hemisphere, New York, London, 1985.